Breakage of water-in-oil emulsions using membranes as a coalescing aid

Platt, Samantha Helen

Award date:
1999

Awarding institution:
University of Bath

BREAKAGE OF WATER-IN-OIL EMULSIONS USING MEMBRANES AS A COALESCING AID

Submitted by Samantha Helen Platt
for the degree of PhD
of the University of Bath
1999

COPYRIGHT

S. H. Platt

ProQuest LLC
789 East Eisenhower Parkway
P.O. Box 1346
Ann Arbor, MI 48106-1346

This thesis is dedicated to my Mother

Acknowledgements

I am greatly indebted to my supervisors for their patience and support. I must especially mention Dr Julian Chaudhuri and Dr Tom Arnot. The entire responsibility for the content and expression of this thesis is however mine.

My thanks also go to my industrial supervisor Dr Keith Carpenter and Nick Dickins of Zeneca Specialties. I would also like to thank Professor John Howell and Dr Robert Field at the University of Bath.

I would also like to thank Zeneca Specialties and EPSRC for funding this work.

I would also like to thank my friends in the Technical University of Lappeenranta. I would especially like to thank Marianne Nystrom for the excellent advice I was fortunate in receiving and for the opportunity to carry out some of my experiments at the above institute. Many thanks also go to NORFA for the financial support of my trips to Finland.

Finally, I would like to thank my family and friends for all their support when I needed it most

To my brother Royston, thank you for the financial support.

To my sister Katie and Goddaughters Laura and Sarah.

To Susan and Matthew for proof reading my thesis and to Lena for the constant stream of e-mail over the last year.

To my mother thank you for the encouragement which has sustained me during its preparation.

ABSTRACT

Emulsions of the type used in emulsion liquid membrane systems are highly stable and need to be broken to recover the internal phase products. The majority of emulsion breakage techniques available could not be used because they were designed for dilute systems. This work investigated the breakage of water-in-dodecane emulsions (stabilised with Paranox 100) by microfiltration using membranes (Supor, Nylaflo, Versapor and HTTuffryn). The emulsions used contained the surfactant (up to 2 w/w %) which was added to a dodecane phase, and had a stability similar to that used in liquid membrane emulsions. The microfiltration of a 100 ml of water-in-dodecane (phase ratio: 20:80 to 50:50 and stabilised with Paranox 100) emulsion was carried out at a constant flux (13 l/h/m^2 and 26 l/h/m^2). The results showed that the type of membrane, membrane structure, pore size and emulsion composition (surfactant concentration, droplet size and distribution, homogenisation speed) influenced the breakage and pressure drop. The initial and final steps of filtration were analysed in terms of breakthrough pressure and formation of a cake. In the initial steps only dodecane permeated through the membrane and the water droplets were retained by the membrane. Under pressure the droplets deformed, broke and wet the membrane surface. Pressure continued to increase, so that the flowrate remained constant, until the breakthrough of the water phase was reached. During the final steps, where cake filtration dominated both phases permeated through the membrane at almost the same ratio as that in the original emulsion (50:50). The permeation of both phases only occurred for three of the membranes used. However, in the case of the other membranes only dodecane permeated through until the maximum pressure of the system was reached but in all cases the water droplets on the membrane surface were partly broken (indicated by the dye tests). The breakthrough of both phases only occurred if the pressure across the membrane was sufficient for the breakthrough of water in the presence of dodecane for the type of membrane used (membrane structure, pore size). The emulsion breakage mechanism proposed here was a combination of rupture of the surfactant layer surrounding the droplets on the membrane surface followed by squeezing of the partly broken droplets into the pores. On depletion of the continuous phase the droplets become tightly packed so that they deformed and finally the protective surfactant layer ruptured. The partly broken emulsion droplets were then squeezed into the membrane pores where any remaining surfactant was removed and the two phases collected in the permeate were completely separated with the surfactant concentration in the dodecane phase being similar to that in the feed emulsion. A comparison between D.C electrostatic coalescence and membrane filtration for emulsion breakage was made. It was found that emulsions stabilised with Paranox 100 at concentrations 0.5-2 w/w % and phase ratios 20:80-50:50 were not demulsified using D.C electrostatic coalescence. All emulsions were broken by filtration using a hydrophilic membrane.

Table of Contents

CHAPTER 3: EMULSION BREAKAGE USING HYDROPHILIC MEMBRANES AS A COALESCING AID.....29

CHAPTER 4: COMPARISON OF EXPERIMENTAL RESULTS AND CONSTANT FLUX EQUATIONS TO PREDICT THE MECHANISM OF BREAKAGE 94

Nomenclature

a	Side of a dodecahedron	m
A	Membrane area	m^2
B	Breakdown ratio	-
C	Volume of deposit per unit volume of filtered suspension	-
c_{et}	Concentration of nickel at time, t	$moll^{-1}$
c_{io}	Initial concentration of nickel	$moll^{-1}$
c_{Ed}	Concentration of EDTA solution	$moll^{-1}$
c_z	Concentration of zinc solution	$moll^{-1}$
d	Droplet diameter	m
d_a	Thickness of the insulation	m
d_b	Thickness of the continuous phase	m
d_s	Droplet separation	m
d_p	Droplet equivalent diameter	m
e	Voidage	-
E	Electric field strength	Vm^{-1}
F	Attractive force between the droplets causing coalescence	N
f_m	Optimum frequency	Hz
Δh_e	Height of the sedimentation	m
Δh_w	Height of the sedimented droplets	m
H_A	Height of the aqueous phase	m
H_E	Height of the emulsion phase	m
H_O	Height of the oil phase	m
k	number of experimental points	-
k_c	Electrical conductivity of the external phase	Sm^{-1}
k_a	Electrical conductivity of the insulation	Sm^{-1}
k_b	Electrical conductivity of the continuous phase	Sm^{-1}
K	Constant	-
K_c	Cake filtration constant	bar $minm^{-6}$

L	Pore length	m
m	Mass ratio of wet to dry cake (=W/W_D)	-
M	Mass of cake per unit membrane area (=W/A)	kgm^{-2}
N	Number of membrane pores	-
Q	Volumetric flowrate (=V/t)	m^3min^{-1}
Q_0	Initial volumetric flowrate ($Q=Q_0$)	m^3min^{-1}
r	Free pore radius	m
r_{Dr}	Droplet radius	m
r_0	Initial pore radius	m
ΔP	Pressure drop	bar
ΔP_0	Initial pressure drop	bar
ΔP_{ca}	Capillary pressure	bar
P_A	Applied pressure	bar
P_I	Internal droplet pressure	bar
R	Universal gas constant (0.082)	dm^3 atm mol^{-1} K^{-1}
R_m	Resistance of the membrane	m^{-1}
R^2	Coefficient of linear regression	-
R*	Critical radius	m
S_0	Initial pore surface (=εA)	m^2
S	Free pore surface	m^2
S_A	Volume specific surface area	m^{-1}
s	Mass fraction of solids in the slurry	-
s_v	Volume fraction of solids in the slurry	-
t	Time	min
T	Absolute temperature	K
V	Volumetric flowrate (feed or filtrate)	m^3
V_{dr}	Volume of drop	m^3
Ve	External phase volume	ml
V_F	Volume of filtrate	m^3
Vi	Internal phase volume	ml
V_{Ed}	Volume of EDTA solution	ml

V_p	Patial molar volume of the solvent	dm^3mol^{-1}
V_Z	Volume of Zinc solution	ml
V*	Slurry volume	m^3
W	Mass of wet cake	kg
W_D	Mass of dry cake	kg
x	Mol fraction	-
yi	Ith experimental point	bar
yi*	Theoretical value	bar
yi^m	Mean value	bar

Greek symbols

α	Specific cake resistance	m/kg
ε	Permittivity of free space	Fm^{-1}
ε_m	Membrane porosity	-
ε_0	Initial membrane porosity	-
ε_b	Permittivity of the continuous phase	Fm^{-1}
ε_s	Permittivity of the insulation	Fm^{-1}
ϕ	Correction factor	-
φ	phase ratio	-
γ	Interfacial tension	N/m
γ_s	Slurry density	kg/m^3
γ_0	dispersed phase density	kg/m^3
γ_c	Cake density	kg/m^3
μ	Viscosity of the filtrate	bar min
π	Applied osmotic pressure	bar
$\Delta\pi$	Osmotic pressure of aqueous phase	atm
π_i	Droplet internal osmotic pressure	bar
π_0	Laplace pressure	bar
π_i*	Critical disjoining pressure	bar
π*	Critical osmotic pressure	bar

θ	Contact angle	degrees
ρ_f	Filtrate density	kg/m^3
σ	Clogging coefficient	m^{-1}
τ_b	Relaxation time of the continuous phase	min
ψ	Shape factor	-

Subscripts/ superscripts

0	Initial value
A	Area
a	Insulation
b	Continuous phase
c	Cake
ca	Cappillary
D	Dry
Dr	Drop
e	External
Ed	EDTA
F	Filtrate
i	Internal
m	Membrane
p	Equivalent
s	Separation
t	Time
V	Volume
Z	Zinc
*	Critical

Chapter 1

Liquid Membrane Emulsion Breakage Techniques

1.1 Introduction

Demulsification of an emulsion is unavoidable if the internal phase is to be recovered and the membrane reused. There are three principle approaches: chemical; electrical and physical treatment. The economics of emulsion breakage determines which methods and to what degree each method is used to achieve the goals. As well as the economics there are other limitations that decide which method is used. Both filtration (micro and ultra) and electrostatic coalescence have been successfully used for the breakage of emulsions. However, the emulsions used were either of low internal phase or the surfactant used possessed low mechanical properties.

Mechanisms of breakage have been proposed by many authors. The possibilities have varied from (1) phase inversion of the emulsion in the filtration module depleting of the external phase to (2) deforming of the internal phase droplet so that it entered the narrow pores of the membrane where the surfactant film was removed due to confined flow. Both of these proposed mechanisms depended on the operating conditions used and it was concluded that more work was needed to understand the underlying mechanisms.

The aim of this work is to determine if stable liquid membrane emulsions, where surfactant forms a strong protective barrier around the emulsion droplets and the phase ratio is high (water/oil is 50/50), can be broken using dead-end microfiltration and if so find out the mechanism of breakage.

The thesis is divided into 7 chapters, references and appendix. This Chapter includes a breakdown of all the proceeding chapters and an overview of the subject areas covered in this work. These include: emulsion technology and methods of breaking

water-in-oil emulsions. Where appropriate, references to specific literature reviews are cited in the relevant chapter.

Chapter 2 describes the general materials and methods used, with the problems associated with some of the experimental filtration runs. Only materials and methods that were generally used are outlined in this chapter. The materials and methods specific to an area of research are presented in the appropriate chapter.

Chapters 3, 4 and 5 have the following structure:

* Literature survey of the area investigated;
* The theory to the area studied;
* Materials and methods specific to the area studied;
* Analysis of experimental data;
* Comparison of experimental data with the published work;

The division between Chapter 3 and 4 is that raw data is presented in Chapter 3 and the mechanism for emulsion breakage is proposed in Chapter 4.

Chapter 5 looks at the comparison between emulsion breakage by membrane filtration and that by electrostatic coalescence. Chapter 6 summarises the main points to be drawn from the work and outlines the future work. The Appendix shows raw experimental data and sample calculations.

1.2 Emulsion technology

This section introduces the technology of liquid membranes, the formation of emulsion liquid membranes and examples of the fields in which liquid membranes have been applied.

1.2.1 Emulsion liquid membranes

A liquid membrane is an insoluble liquid (oil phase), which is selective for a solute separating two water phases, a feed phase which contains the desired solute and a stripping phase into which the solute is extracted (Figure 1.1). Emulsion liquid membranes are prepared by forming an emulsion (Figure 1.2) between the membrane phase (oil phase) and the stripping phase (water phase). The emulsion is then dispersed in an external water phase containing the chemicals to be extracted by agitation (Figure 1.3). After extraction the emulsion has to be broken (section 1.3) to recover the internal reagent phase which contains the extracted species. The oil phase from the broken emulsion is recycled.

1.2.1.1 Emulsion formation

The water phase (stripping phase) is dispersed within an oil phase (membrane) using an homogeniser. The oil forms a non-porous film around the water droplets. The emulsion formed is stabilised by a surfactant to ensure adequate stability. The water droplets are usually between 0.5-10 μm [Draxler and Marr, 1986] to provide good emulsion stability

1.2.1.2 Membrane solvent

The membrane phase must not be miscible with either the internal or external phase [Ho and Li, 1983]. Draxler and Marr (1986) reported that aliphatic diluents were generally preferred as the membrane solvent because of their lower solubility in water. Other factors that should be considered when choosing a suitable solvent are: the solvent should be compatible with other membrane components (eg surfactant) and the oil viscosity should be kept as low as possible to maximise the diffusivity of the solute through the membrane phase. By reducing the viscosity of the membrane phase the membrane instability is increased. Solvents used are cyclohexane [Scheper et al, 1987] , kersosene [Scheper et al, 1987], paraffin [Scheper et al, 1987], S100N

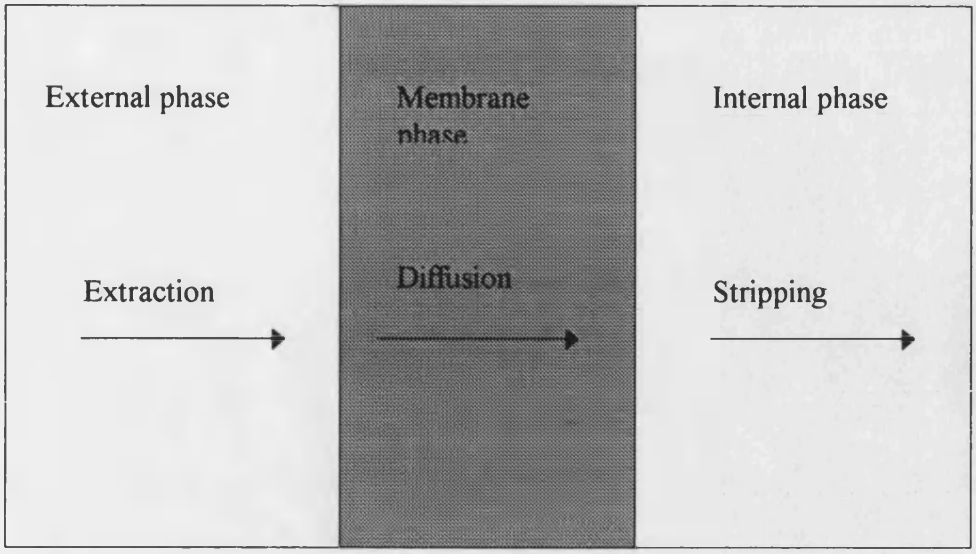

Figure 1.1 Principle of liquid membrane extraction

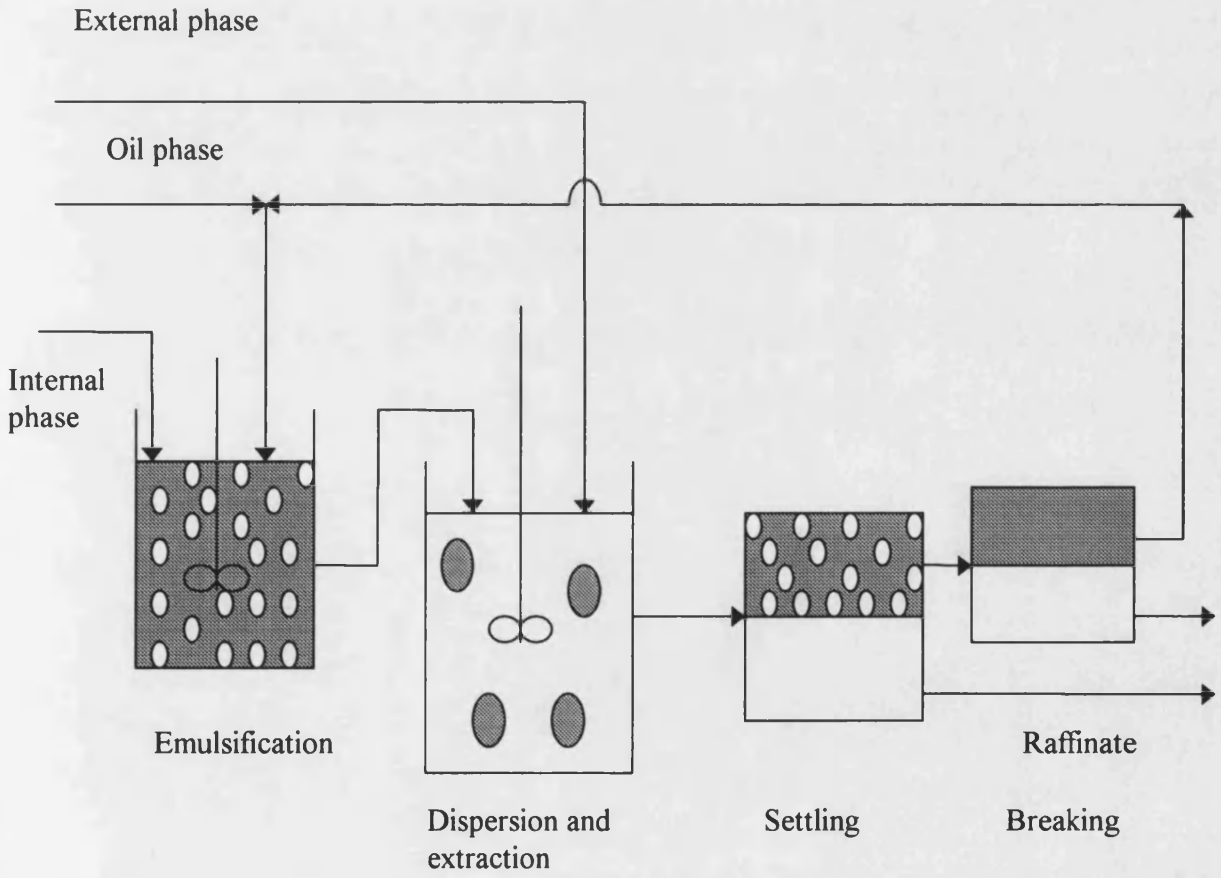

Figure1.2 The formation and use of emulsion liquid membranes.

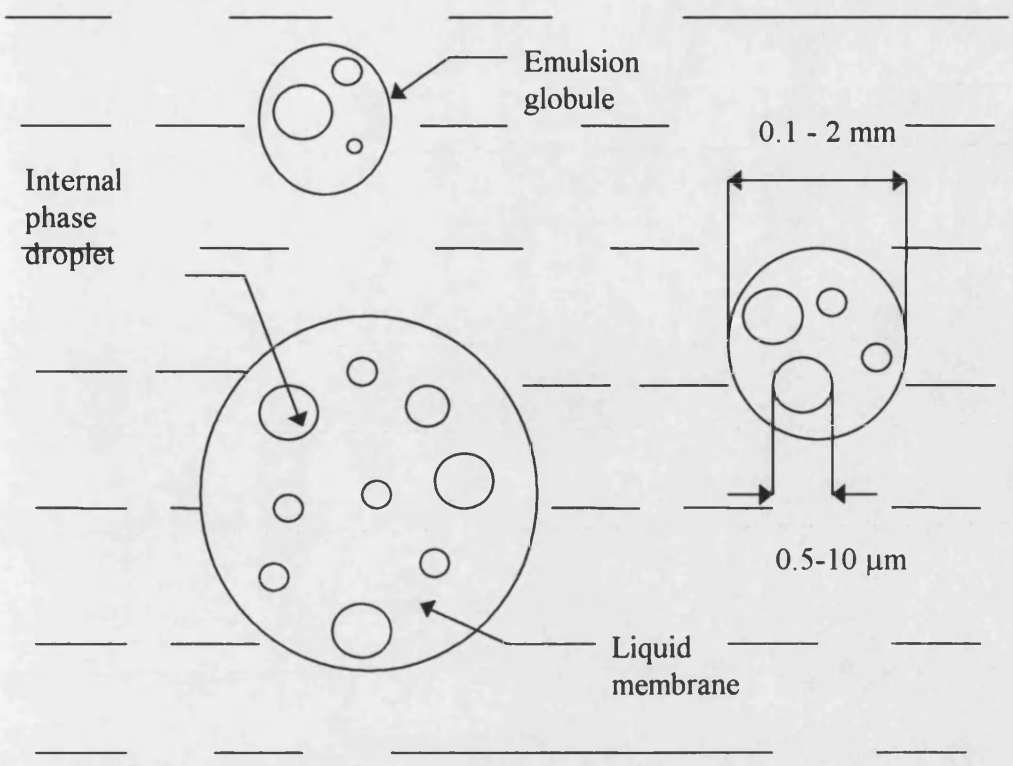

Figure 1.3 Emulsion liquid membrane configuration.

(a high molecular weight isoparaffin) [Thein et al, 1986 and 1988] and shellsol (a paraffin containing xylene) [Boey et al, 1987].

1.2.1.3 Surfactants

The surfactant is the most important component in emulsion liquid membrane processes, as it determines the stability and influences water transport. When choosing a suitable surfactant for emulsification the following should be taken into consideration: (1) Surfactant should be a good emulsifying agent (eg. Span 80, ECA 4360) [Draxler and Marr, 1986], (2) surfactant should not be a water molecule carrier. If the surfactant is a carrier for water molecules (eg. Span 80) [Draxler and Marr, 1986] it will favour swelling of the emulsion by osmosis. (3) The surfactant should have a low solubility in the aqueous phase (eg. ECA 4360) [Draxler and Marr, 1986].

In order to stabilise a water -in- oil emulsion a surfactant (e.g. Paranox 100, Span 80) [Thien et al, 1986 and 1988, Pickering and Chaudhuri, 1997 and Hano et al, 1994] is added to the oil phase. Depending on the surfactant concentration and dispersion conditions the emulsion droplet diameter will be micron sized (0.5-10 μm) [Draxler and Marr, 1986]. By increasing the surfactant concentration (0.1-5 w/w %) and mechanical energy it is possible to produce an emulsion with very high stability. However this is not favourable for breaking the emulsion to recover the internal phase. A compromise needs to be found between sufficient stability of the emulsion and easy breakage [Draxler et al, 1988]

The droplets in an emulsion are in constant motion and therefore there are frequent collisions between them. If on collision the surfactant film at the interface ruptures the two droplets will coalesce to form a larger droplet. If this continues the dispersed phase will separate from the continuous phase. Therefore the mechanical strength of the interfacial film (protective surfactant layer) is one of the main factors determining the stability of the emulsion. For maximum mechanical stability the adsorbed

surfactants at the interface should be condensed, with strong lateral intermolecular forces and should exhibit high film elasticity [Rosen, 1989]

1.2.1.4 Size distribution of droplets

The droplet size distribution influences the rate of coalescence (stability) of the droplets. Larger droplets have less interfacial surface per unit volume than smaller droplets and therefore larger droplets are more stable than smaller droplets and tend to grow at the expense of the smaller ones. This process will eventually result in emulsion breakage. An emulsion with a fairly uniform size distribution is therefore more stable than one with the same average droplet size having a wider distribution of sizes [Rosen, 1989].

1.2.2 Formation of stable water-in-oil emulsions

Marr and Kopp (1982) identified the following guidelines for the formation of a stable water in oil emulsion liquid membrane: (1) the organic phase soluble surfactant requires to be 0.1 -5 w/w %; (2) the organic phase viscosity is required to be between 30-1000 mPas; (3) the volume of the internal phase / membrane phase 0.2-2; (4) volume ratios of the stripping phase to external feed phase is 0.05 -0.2 and (5) the volume ratio of feed phase to emulsion phase is 1-40, surfactant hydrophile-lipophile balance value 6-8.

1.2.3 Transfer process

The transfer process is as follows (Figure 1.1):

* The solute in the feed phase diffuses to the interface (feed phase and membrane phase).
* The solute then dissolves in the membrane phase and diffuses across it, either as a free solute or in a complexed form.

* The solute then reaches the membrane / stripping phase interface where it passes across into the stripping phase by either partition or chemical reaction.
* The solute is prevented from transporting back to the feed phase by alteration of its solubility in the oil phase. This is usually achieved by ionizing the solute so that it is insoluble in the organic solvent by the presence of a charge.

1.2.4 Applications

The liquid membrane technique was developed by Li (1968). Many applications of this technique have been studied, especially in waste water treatment [Li and shirer, 1972 and Terry et al, 1982], hydrometallurgy [Izatt et al, 1983; Parkinson et al, 1983; Fuller and Li, 1984 and Draxler and Marr, 1986] and biological processes [Armstrong and Li, 1988; Dahuron and Cussler, 1988; May and Li, 1972 and Mohan and Li, 1975].

In waste water treatment using emulsion liquid membranes Li and Shirer, 1972 focused on the removal of phenol. Here the external phase is of importance by reducing the phenol concentration in it. Once the required concentration is reached the emulsion is separated from the treated water and disposed (incineration) of or broken to recover only the membrane phase for reuse. Therefore, a cheap emulsion breakage method is required. Also Terry et al (1982) studied the removal of phenolic compounds such as phenol and cresols and acetic acid from waste water.

In the field of hydrometallurgy there have been several reports of the use of liquid membranes. These reports involve the extraction of the following metals: strontium, lead and lithium [Izatt et al, 1983]; chromium and zinc was studied by Fuller and Li (1984); uranium [Parkinson et al, 1983]; Draxler and Marr (1986) reported the extraction of zinc, copper and nickel using emulsion liquid membranes. They report the construction of a large-scale plant in Austria for the recovery of zinc.

Draxler et al, 1988 have given a detailed review of the application of emulsion liquid membranes for the separation of metal ions from waste water streams. This review

looks at pilot plant and large-scale plant recovery of zinc from viscose waste. They reported that the choice surfactant (up to the present) was only chosen according to its ability to stabilise the emulsion and there were many other factors that should be considered when choosing a suitable surfactant. Which included mass transfer resistance, capability of transporting water, decomposition of extractant and resistance to bacteria.

other areas where emulsion liquid membranes have been used include the following extraction of acetic acid [Terry et al, 1982], citric acid [Boey et al, 1987], phenylalanine [Thien et al, 1986 and 1988], protein recovery [Armstrong and Li, 1988 and Dahuron and Cussler, 1988], imobilisation of enzymes [May and Li, 1972 and Mohan and Li, 1975].

1.2.5 Advantages and disadvantages of emulsion liquid membranes

The main advantage of emulsion liquid membranes is that they have very fast transfer rates due to the formation of small droplets hence the high surface area (1000- 3000 m^2 m^{-3}) [Marr and Kopp, 1982] of the emulsion. The solute can be separated and concentrated in one step by making the stripping phase volume smaller than that of the feed

Three disadvantages are membrane stability and swelling, and difficulty in breaking the (loaded) emulsion. During extraction some of the solute in the internal phase can leak back into the external phase taking with it the internal phase reagent which can transform the solute into a non-extractable form. This is a stability problem that comes from trying to form an emulsion that is designed to be stable under process conditions but easy to break to recover the extracted solute. Due to osmotic pressure differences water can be transported from the feed phase to the stripping phase. This results in swelling of the emulsion and dilution of the stripping phase contents. This can be reduced by the selection of an appropriate surfactant (section 1.2.1.3). At the end of the extraction, the emulsion is separated from the external water phase and broken to recover the internal phase products. Due to the fact the emulsions are

designed to be stable under the extraction process conditions it is often found that breakage of these emulsions is very difficult.

1.2.6 Emulsion stability

The phenomenon of emulsion instability in emulsion liquid membranes has been attributed to emulsion swelling (water transport across the membrane resulting in a decrease in the phase ratio). Any increase in the internal phase volume will affect the droplet size distribution of the dispersed phase. This will result in the interfacial film of the surfactant molecules having to expand over more and more droplets so that the density and compaction of the surfactant decreases. The surfactant will no longer act as a barrier against coalescence and emulsion breakage will occur [Abou-Nemeh and van Peterghem, 1992]. Other factors which affect the stability are temperature, ionic strength, pH of the feed and pH of the internal phase, concentration of the surfactant. Ho and Li (1983) reported that the initial leakage of the internal phase after the emulsion was added to the external phase was due to lack of ideal encapsulation of the internal phase.

Due to the above disadvantages experimental studies on the stability of liquid membranes have been performed by Davis and Burbage (1977) freeze-etching electron-microscopy technique; Kita et al (1977) and Matsumoto and Kohda (1980) viscometric method; Shere and Cheung, 1987 using pH change; Florence and Whitehill, 1981 microscopic techniques; Abou-Nemeh and van Petergham, 1992 tracer technique.

1.3 Methods of breaking emulsions

Demulsification of an emulsion is unavoidable if the internal phase is to be recovered. There are three main approaches (1) applying chemicals (eg. demulsifiers), (2) applying electrical fields to promote coalescence (eg. electrostatic coalescence) and (3) physical treatment (eg. centrifugation, flotation, heating, high shear, membrane filtration). The economics of emulsion breakage determines which method is used to

achieve the goals. As well as the economics there are other limitations which decide which method is used. This section describes the breakage methods available along with their limitations.

1.3.1 Chemical demulsification

Addition of chemicals generally provide quick cost-effective results. The success of using chemicals depends on (1) an adequate quantity of the right chemical must enter the emulsion, (2) thorough mixing of the chemical in the emulsion must occur, (3) adequate heat must be added if required, in order to break the emulsion completely and (4) there must be sufficient residence time in the testing vessel to allow for the droplets to settle. The advantages of this method are the low costs of implementing or changing the demulsifier [Grace, 1992]. The disadvantage of this method is the chemicals can change the properties of the oil phase (for a water-in-oil emulsion) so that it cannot be reused. This is not a suitable method for breaking liquid membrane emulsions.

1.3.2 Physical demulsification

1.3.2.1 Packed beds

Few studies have been conducted on the breakage of liquid membrane emulsions using packed beds. Packed beds are considered to be economical and easily adaptable to industrial applications. Lee and Han (1993) used packed beds to break water -in-kerosene emulsions (50 (vol) % internal phase) stabilised with 1-3 (vol) % Span 80. Breakage of up to 95 % was possible at surfactant concentration of 1% and up to 80 % at surfactant concentration 3 %.

The presence of surfactants usually cause a decrease in the coalescence rate and therefore the applicability of this technique depends on surfactant type and concentration [Hlavacek, 1994].

1.3.2.2 Heat treatment

Heat treatment of emulsions is a very effective method of emulsion breakage because it reduces the viscosity and the density of the oil phase (for water-in-oil emulsion). Increasing the temperature also increases the solubility of the surfactants in both the oil and water phases and this leads to weakening of the interfacial film. The disadvantages of using heat alone is the slow demulsification rate. Heat treatment is usually used in conjunction with other techniques [Larson et al, 1994].

1.3.2.3 Centrifugation and high shear

Centrifugation of very stable emulsions (eg. through a centrifugal pump) does not completely break the emulsion. Centrifugation is usually carried out as a first step, followed be pumping the half broken emulsion through a high shear device. Li (1978) used centrifugation as a first step to remove a portion of the continuous phase. This was followed by adding a liquid miscible with the dispersed phase and a mechanical shearing stress was applied to rupture the surfactant layer so coalescence of the droplets resulted. He reported that an emulsion with a continuous to dispersed phase of 2:1 was centrifuged at 4000 rpm for 30 minutes to remove 90 % of the continuous phase. The remaining emulsion was a viscous gel which was subjected to high shear.

Kato and Kawasaki (1987) and Kato and Kawasaki (1988) found that emulsions could be broken when subjected to high shear. Kato and Kawasaki (1987) reported for a batch process that a yield of 80 % could be reached. Later Kato and Kawasaki (1987) reported for a continuous mechanical demulsification process a yield of 95 % was reached in 0.063 seconds using an agitation speed of 20,000 rpm.

1.3.2.4 Gravity settlers

The oil industry use gravity settlers for emulsions with a droplet size ranging between 20μm and 100 μm. The separation of oil from water is governed by the sedimenting velocity of the water droplet (for a water-in-oil emulsion), Stokes law applies

[Delaine, 1985]. The velocity is proportional to the density difference between the two fluids and to the square of the droplet radius and inversely proportional to the viscosity. The droplets are slow to sediment and usually other methods are used along with the gravity settlers to promote coalescence. These methods include the addition of chemical demulsifiers, increases in temperature and the introduction of surfaces (parallel or inclined) to reduce the distance droplets need to settle. All of these additional methods help to increase the coalescence rate. Highly stable emulsions used in emulsion liquid membrane systems have droplet sizes in the range of a few microns so coalescence would be very slow. The added advantages of demulsifiers would not be an option for reasons stated above (section 1.3.1) and the option of the other advantages would still mean breakage was very slow. The only way gravity settlers could be improved to be used to break liquid membrane emulsions is to apply an electric field (electrostatic coalescence, section 1.3.3) [Bailes, 1992].

1.3.2.5 Coalescers

Coalescers have been used for the breakage of secondary dispersions (droplet size < 10 μm) which are stabilised by surfactants [Jeater et al, 1979]. The coalescer usually consists of a fibre coalescing cartridge; [Toms, 1987; Delaine, 1985 and Bevis and Cobhass, 1992].

Coalescers are basically filtration systems using material designed to provide a surface on which the droplets collect and coalesce into larger droplets for separation. The small pore size used to create the semi-permeable surface require the flow to be free from solids to prevent the pores becoming blocked. The coalescer can be a metal gauge of fine mesh, ceramic or polymer based. It usually comes in the form of a cartridge in which the flow passes from one side of the cartridge to the other. during passage the droplets are retained on the surface of the cartridge to collect and coalesce with other droplets [Delaine., 1985].

The disadvantages of this method are dirt build up among the fibres limits the lifetime of the cartridges and the presence of surfactants reduces droplet coalescence [Bevis

and Cobham, 1992]. Droplet coalescence, using coalescers where surfactants are present, can be increased by adding chemical agents. However, for reasons pointed out in section 1.3.1 the addition of chemicals is not an option.

An improvement on coalescers is microfiltration or ultrafiltration using synthetic membranes (section 1.3.4).

1.3.3 Electrostatic Coalescence

Emulsion breakage by application of high voltage electricfields has proved to be the most efficient means of recovering the internal phase from the liquid membrane emulsion [Hsu and Li, 1985, Draxler and Marr, 1986, Draxler et al, 1988 and Kataoka and Nishiki, 1990].

Electrostatic coalescence is a method used to break emulsions (water-in-oil). The oil industry has used this technique to separate brine emulsified in crude oil. This form of demulsification is a physical process which makes recycle of the oil phase possible it is very suitable method for breaking liquid membrane emulsions. However, the electrostatic coalescers used for crude oil dewatering cannot be directly used for breaking water -in-oil emulsions (used in emulsion liquid membrane systems) for the following reasons.

* Emulsion liquid membranes contain much more water up to 50 (vol) % to about 5 (vol) % for crude oil systems.

* Emulsion liquid membranes contain high concentrations of surfactant.

* The oil phase needs to be preserved for re-emulsification

For the above reasons the electrostatic coalescers used for breakage of liquid membrane emulsions are especially designed for this purpose.

The application of high voltage electrostatic fields in the separation of water-in- oil emulsions can be classified in terms of the mechanisms which predominate in the system (Chapter 5). This is dependent upon the nature of the electrostatic field. The three main field types are AC, is used in the breakage of crude oil emulsions in production and refining; DC, is used for resolving emulsions with low water content (at high water content short circuiting can occur by the droplets forming chains between the electrodes) and pulsed DC with insulated electrodes, is being used for the breakage of emulsions with high water content (very useful for the breakage of emulsion liquid membranes) [Taylor, 1996].

Chapter 5 discusses in detail pulsed D.C electrostatic coalescence for the breakage of stable water-in-oil emulsions.

1.3.4 Membrane filtration

The majority of emulsion breakage using membranes in the literature looks at oil-in-water emulsions using hydrophilic ultrafiltration / microfiltration. Bhattacharyya et al (1979) used ultrafiltration to treat oil-detergent-water systems containing 500 mg/l of oil. Kirjasoff et al (1980) applied ultrafiltration to treat waste water streams (from the production of adhesives and sealants) which contained 0.3053 % oil and 0.758 % solids. Ultrafiltration removed 90-98 (volume) % of the waste. Kutowy et al (1981) used hydrophilic membranes (cellulose acetate) to treat oily water that contained 5-35 % oil. Lee et al (1984) and Lipp et al (1988) used ultrafiltration membranes to remove soluble oils. Break oil-in-water emulsions of oil concentrations 0.5 to 10 vol %. Lee et al (1984) investigated emulsions with oil contents of 1-5 vol % and surfactant concentrations 0.2-1 vol % using hydrophilic membranes (Iris 3042) and Lipp et al (1988) studied emulsions with oil contents of 0.5-10 volume % using hydrophilic membranes (Iris 3038, regenerated cellulosed and polysulfone). Vigo et al (1985) investigated the ultrafiltration of freshly prepared emulsions of cutting oils with up to 40 volume % of oil. Farnard et al (1985) looked at the ultrafiltration of untreated wellhead bitumen/water/mineral emulsions. Bhave and Fleming (1988) used microporous alumina membranes for the removal of oily contaminants from process

waste waters. Two types of emulsion were used where one contained 80-120 mg/l of lube oil and the other 200-700 mg/l of vegetable oil. The permeate was found to contain 3-5 mg/l of oil and grease. This was a 90 % reduction in the original volume. Scott et al (1992) looked at emulsions with an oil content of 40 % using three types of cellulose membranes. Zaidi et al (1992) used ceramic and hydrophilic membranes to remove oil from oil field brines. Scott et al (1994) investigated microfiltration of tridecanol -in- water emulsions using hydrophilic membranes (nylon, polysulphone and a mixture of cellulose nitrate and tri-acetate). Jueng and Jiang (1994) studied ultrafiltration to separate water-in-oil emulsions from the external water phase. Koltuniewicz et al (1995) looked at microfiltration of dilute dodecane-in-water emulsions. The dodecane concentration was 1000 ppm and no surfactant was used to stabilise the droplets. The above membrane techniques are based on separation due to size exclusion and in all cases the permeating phase was water.

Separation of dilute oil-in-water emulsions using hydrophobic microfiltration was shown by Hlavacek (1995); Daiminger et al (1995) and Sun et al (1998). This was not filtration where one phase is retained by the membrane. Here the whole emulsion passed through the membrane since the presence of surfactants in the emulsion allowed wetting of the membrane by both phases. The droplets being deformable could squeeze into the pores if the pressure applied was sufficient to exceed the capillary pressure. Hlavacek showed that dilute emulsions of oil concentration 2.8-3.2 vol % could be broken using microfiltration membranes as a coalescing aid. Separation was 60 % for a polypropylene (hydrophobic) membrane. Daiminger (1995) successfully demulsified isododecane-in-water emulsions where the internal phase was 2.5 vol % and surfactant concentration was 0.1 $Kmolm^{-3}$. Sun et al (1998) investigated the demulsification of water-in-oil emulsions using a porous glass membrane. The water content was 10-50 volume % and the surfactant used was Span 80.

All of the emulsion breakage using membrane technology discussed so far as looked at mainly dilute systems of low surfactant concentration. The following work covers concentrated emulsions where separation is due to preferential wetting. Tirmizi et al

(1996) looked at water-in-tetradecane breakage using hydrophobic membranes. They experimented with emulsions of no surfactant to high surfactant (ECA 5025) concentrations with various phase ratios. The lower surfactant concentrations (< $0.5kgm^{-3}$) resulted in complete phase inversion during depletion of the external phase. At surfactant concentrations between $0.5kgm^{-3}$ - $2kgm^{-3}$ phase inversion was not complete and demulsification was carried out using a hydrophilic and hydrophobic membrane in series. However, at high surfactant concentrations (> $2kgm^{-3}$) there was no phase in version (gel like emulsion on surface) and demulsification was carried out using electrostatic coalescence followed by membranes as a final polishing step.

1.4 Experimental objectives

This chapter has shown that membrane filtration has great potential to be used as a breakage technique for liquid membrane emulsions. These emulsions have a high water content (up to 50 vol %) and high surfactant concentration 1-5 w/w % which is usually of high mechanical stability. Most of the cited literature reported successful breakage at high water content but in these cases the surfactant concentration was low or its mechanical properties were weak. In the case where the surfactant concentration was high the water content was low. The only reported membrane breakage study where both the surfactant concentration (also strong mechanical properties) and water content were high resulted in the emulsions being destroyed by using an electrostaic coalescer where membranes were only used as a final polishing step. The objectives of this study are to use hydrophilic membranes to break emulsions of high water content and high surfactant concentration where the surfactant possesses strong mechanical properties, and in particular to determine the mechanism of emulsion breakage using membranes. Finally, the breakage results from the filtration experiments will be compared with the breakage results from D.C electrostatic coalescence which up to now is considered the best technique to break liquid membrane emulsions.

Chapter 2

General Materials and Methods

2.1 Materials

Dodecane (99 %) was obtained from BDH Laboratory Supplies (Poole, England). Paranox 100 was obtained from Exxon Chemicals (Southampton, England). Nickel II nitrate was purchased from Fluka (Gillingham, Dorset, England). The membranes (Table 2.1) were obtained from Gelman Sciences (Northampton, England).

2.2 Methods

2.2.1 Emulsification

2.2.1.1 Description of surfactant

By introducing a surfactant that is soluble in one phase more than the other does not guarantee the formation of a water-in-oil emulsion. In the case of Paranox 100 which is a hydrophobic agent (Fig 2.1) there is a strong tendency for a water-in-oil emulsion to be formed but only if all other conditions are favourable (see below) [Sutheim, 1947]. With a phase volume ratio of 50:50 there is no preference to form either oil-in-water or water-in-oil emulsions. The type formed depends upon the surfactant present, the chemical properties of the constituents and the order of incorporation. Usually the phase in excess tends to become the external phase. Therefore if the internal phase is gradually added to the external phase the latter will always be in excess and the stability conditions will be favourable. If the internal phase is added too quickly it could become locally in excess and if other conditions are not favourable, an emulsion of oil-in-water could be formed. By incorporating the above conditions into the method used for emulsification will provide assurance that a water-in-oil emulsion is produced.

Table. 2.1 Membrane characteristics (Gelman Science)

Name	Membrane thickness (μm)	Membrane porosity %	Pore size studied (μm)	Material
Supor	150	70-80	0.2, 0.45 and 0.1	udel polysulfone
Nylaflo	125	70-80	0.2	nylon 6-6
HTtuffryn	165	70-80	0.2	poly(arylenesulfone ether)
Versapor	125	70-80	0.2	polyvinylchloride and polyacrylonitrile

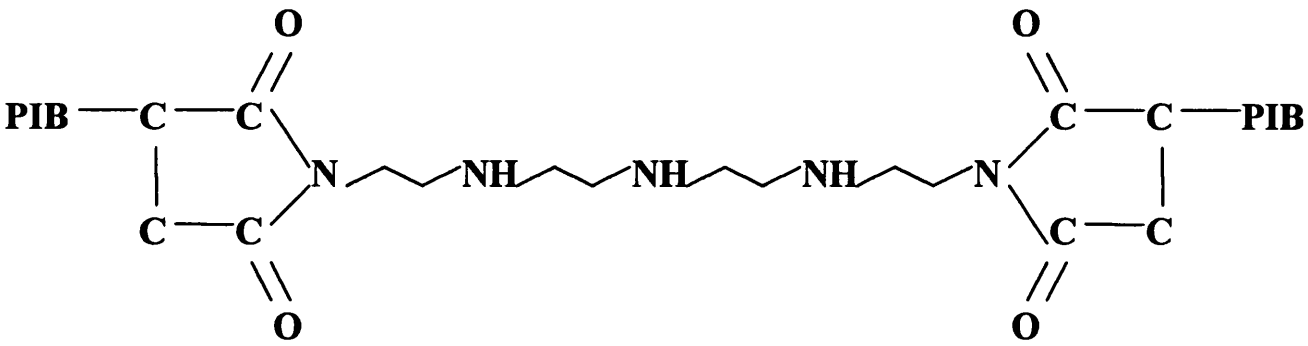

Fig. 2.1. Schematic of the surfactant, Paranox 100 (polyisobutylene bissuccinimide)

2.2.1.2 Operation

The emulsion comprised an organic phase (liquid membrane) and an aqueous phase (internal) in a 50:50 or 20:80 volumetric ratio (Table. 2.2). The membrane phase consisted of dodecane and varying surfactant concentrations (0.5-2 w/w %). The aqueous phase was distilled water and additionally for electrostatic coalescence Nickel(ii)-nitrate was added to a final concentration of 0.05 M to increase the dielectric constant to a value much greater than the oil phase. Both phases were used at room temperature and the temperature was recorded before and after emulsification. Emulsification was carried out using homogenisation (IKA-Ultra-Turrax T25). The internal phase was added dropwise into the continuous phase using a 50 ml burette (Borosilicate, BS 846) over a period of 3 minutes using a mixing speed of 8000 rpm.

Mixing was continued for a further 10 minutes (residence time) at either 8000 or 9500 rpm to promote a stable emulsion.

2.2.1.2 Emulsification problems

Temperature increase

After emulsification the temperature was recorded and compared with the initial value. When the homogeniser speed was kept at 8000 rpm for the mixing period the temperature after homogenisation was 25^0C. When the mixing period was homogenised at the higher speed of 9500 rpm the temperature after homogenisation was between 29-36.5 ^{0}C. At the higher speed the resulting emulsion was still stable which was shown by the stability tests (Chapter 3). It was therefore not deemed necessary for emulsification to take place in an ice bath. When the temperature rises, due to the heat produced from the homogeniser probe, the emulsion can sometimes become unstable because the temperature is close to the phase inversion temperature of the surfactant.

Table. 2.2: The emulsion composition and conditions for homogenisation and breakage

Emulsion phase volume ratio A: O	Surfactant concentration (w/w %)	Homogeniser residence		Breakage method
		speed (rpm)	time (min)	coalescer or filtration
50:50	1	9500	10	both
50:50	1	8000	10	both
50:50	2	9500	10	filtration
20:80	0.5	9500	10	both
50:50	0.5	9500	10	coalescer

Surfactant dispersion

The surfactant (Paranox 100) was added to the dodecane prior to emulsification and was left to stand for up to 8 hours. If the surfactant was not given sufficient time to dissolve in the dodecane phase the resulting emulsion was unstable.

Correct homogenisation procedure

The homoginiser rotor shaft works like a centrifugal pump (lower pressure on the inside of the shaft) such that a vacuum is set-up. Only liquid in close proximity to the shaft will be drawn in and therefore if the mixing vessel is very wide the liquid in the outer boundaries will not be fully homogenised and the resulting emulsion will be of a wide droplet size distribution. To avoid this the depth of the feed vessel should be 1.5 times the diameter (operators manual). Also the homogeniser should be run slightly off centre to avoid forming a vortex and 40 mm (operators manual) from the bottom of the mixing vessel to allow for adequate circulation of the emulsion.

2.2.2 Design and development of a dead-end membrane rig

This section describes in detail the equipment used in the membrane filtration rig. It also includes all the measuring equipment and its accuracy.

2.2.2.1 Details of the experimental apparatus

A flow diagram of the dead-end rig used for emulsion breakage is shown in Figure 2.2 and the components used in the construction are listed in Table 2.3. The rig consists of a 150 ml glass feed vessel, a pressure transducer (0-7 bar), membrane module and two pressure gauges 0-7 bar on the feed line and 0-2 bar on the permeate line. The membrane module (Figure 2.3) was made of stainless steel (dead volume 6.5 ml) and was purchased from Sartorius. The membranes were 4.2 cm in diameter giving a surface area of 13.86 cm^2 and a rubber gasket was used to provide an air-tight contact

between the membrane and membrane support. The emulsion flows perpendicular to the membrane, typical of dead-end filtration.

There were problems in preventing the membranes (Table 2.1) from creasing and folding during operation. The reason for this was that microfiltration membranes are soft and thin and at low pressures (start-up) the membranes can lift off the membrane support. Attempts were made to reduce this affect by changing the membrane installation. The membrane was stretched tightly as possible over the permeate section of the membrane module. This change reduced the creasing problem but did not eliminate it.

2.2.2.2 Measurement and control

The permeate was collected in 1.5 ml calibrated vessels. The flowrates (0.3×10^{-6} m^3/min, 0.6×10^{-6} m^3/min and 1×10^{-6} m^3/min) in the system were so small there was no suitable flowmeter available to use. By dividing the flowrate by the membrane area flux was calculated. The pump used was a high precision HPLC pump (Table 2.3) and the flowrates remained constant within the pressure range (0-6 bar) used in the experiments. This was checked by monitoring the feed rate via a balance and as the system was run at constant flowrate the permeate collected in the vessels was checked for the correct volume delivered.

A thermometer in the feed and the permeate was used to determine if there was any change in temperature due to the pump or flow through the pipe lines. All experiments were conducted at room temperature (23 ± 0.5^0 C) and the difference between the feed and permeate temperature was within $\pm 0.5^0$C. In all experiments reported temperature was manually controlled. A heated jacket was used to keep the feed at $23\ ^0$ C by placing the attached temperature probe in a water bath equipped with a heating element

The pressure on the feed side was measured by a pressure transducer (Table 2.3) with an accuracy of ± 0.1 psi. The permeate pressure was at atmospheric pressure and was monitored by a pressure gauge (0-2 bar).

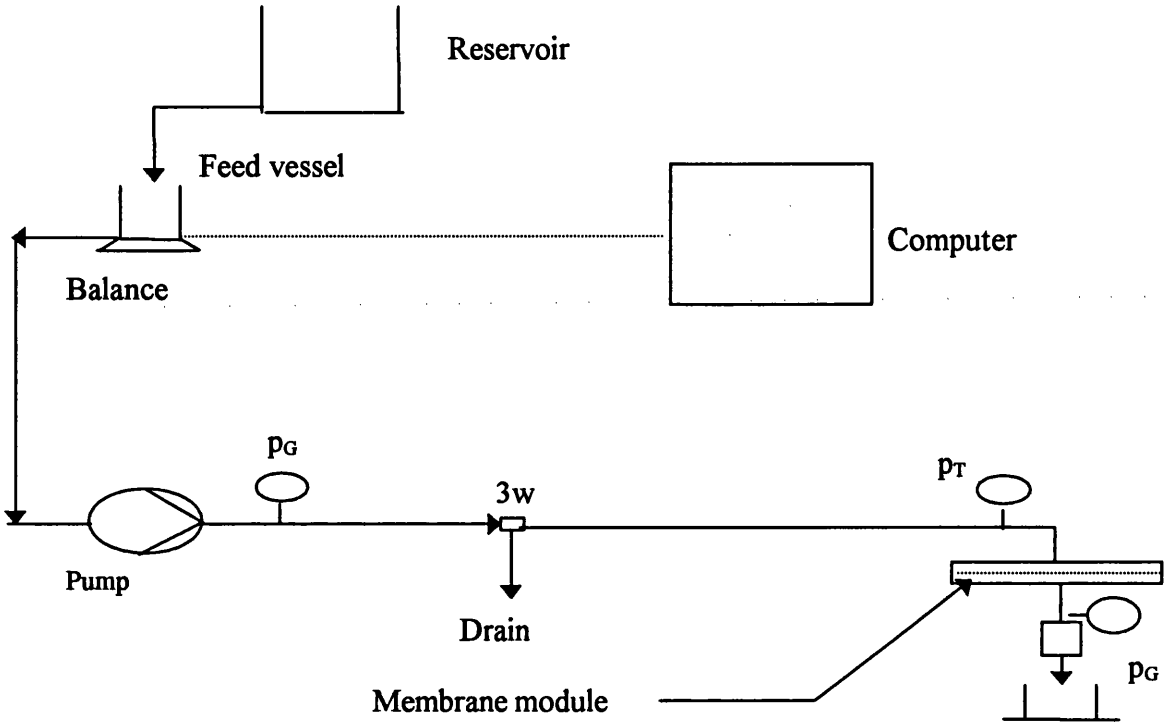

Fig. 2.2. Dead-end microfiltration unit used for the breakage of emulsions (P_G - pressure gauge, P_T -pressure transducer, 3w -three way valve).

Table 2.3 Components of a dead-end filtration rig

Component	Make and Model
Feed pump	Waters HPLC pump (510)
Pressure transducer	RS Components (PDCR 800)
Feed balance	Mettler (digital balance to 2 decimal places)

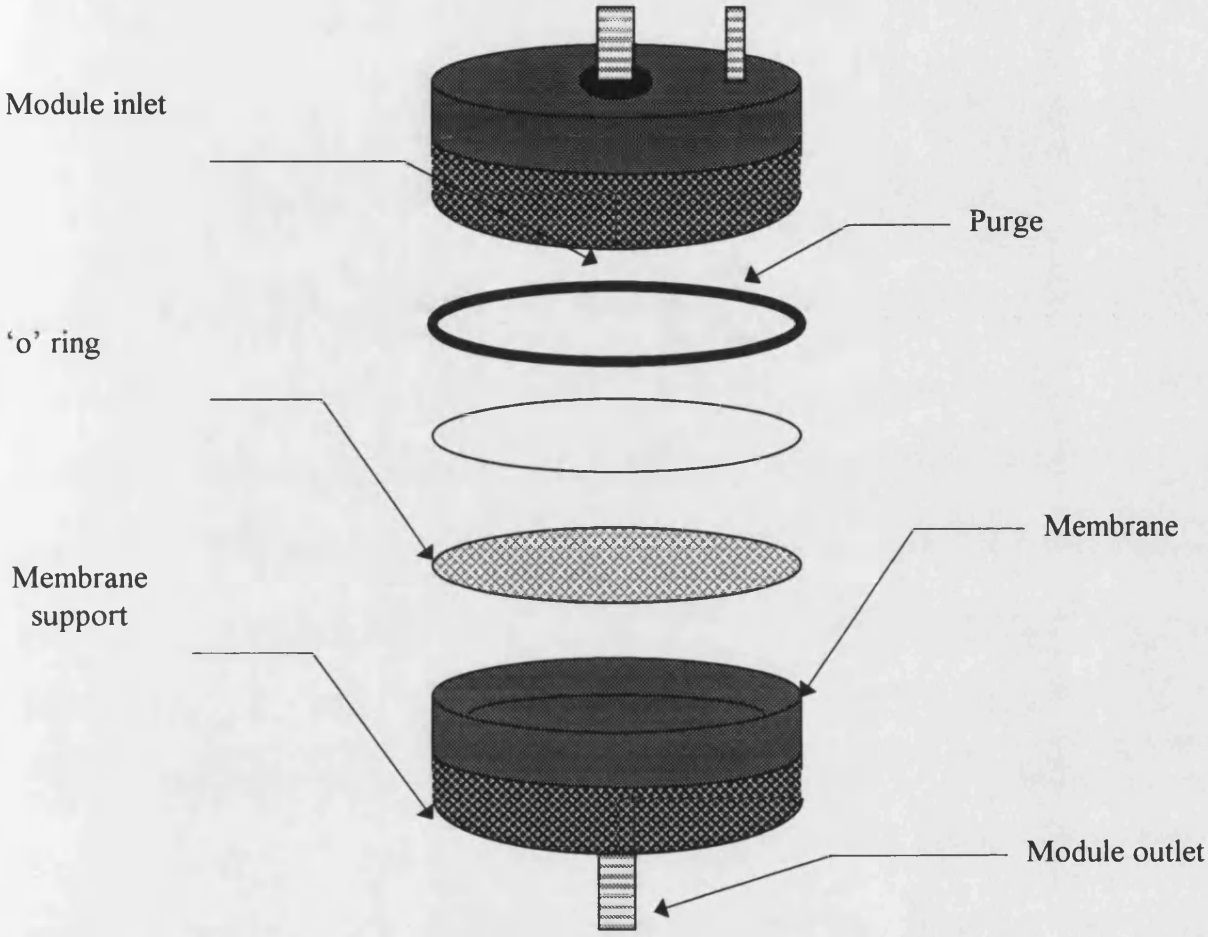

Fig 2.3 Schematic of the membrane module used in the emulsion breakage experiments by filtration

To avoid any affects of swelling of the pipelines due to the solvents and surfactant used all process lines and fittings were made of stainless steel.

All data collected during each run was sent to a computer where it could be suitably processed.

2.2.2.3 Equipment start-up, operation and system cleaning

The HPLC pump was primed according to the operators manual and dodecane was run from the feed tank through to the module. A new membrane was used for each experiment and in order to assure complete wetting of the membrane, dodecane was run through the membrane until a steady flux was obtained.

Once the membrane was completely wet the dodecane feed vessel was switched for the emulsion feed vessel and the pump was primed with the new feed. During operation air incorporation was avoided in the pipe lines and the module, by filling the module at 45 ° to its operating position. Air was then easily removed through the purge stream during initial start-up of the module. The effect of the flowrate was investigated at 0.3 $\times 10^{-6}$ and 0.6 $\times 10^{-6}$ $m^3 min^{-1}$ for all membranes and emulsions. All runs were performed at room temperature (23^0C) and the runs varied between 6 and 80 minutes, depending on the pressure increase (maximum pressure of the system was 6 bar).

Permeate samples were collected every 2 minutes but the first sample was not collected at time t=0. As outlined above the module was filled with emulsion prior to operation but the permeate line was empty and therefore a hold-up volume (3.3×10^{-6} m^3) had to be overcome before any permeate was collected. At flowrate 0.3 $\times 10^{-6}$ m^3/min the hold-up time was 11 minutes, at flowrate 0.6 $\times 10^{-6}$ m^3/min the hold-up time was 5.5 minutes and at flowrate 1 $\times 10^{-6}$ m^3/min the hold-up time was 3.3 min.

This lag period resulted in the samples collected at t=0 being unknown. The permeate data plotted in Chapters 3 and 5 are started at the end of the lag period and not from t=0 for reasons outlined above.

At the completion of each run on the emulsion the rig was flushed with acetone at room temperature (23°C) for at least 10 minutes. This was followed by air being blown through the system to remove any remaining emulsion. Again the system was flushed with acetone until the line was free of emulsion. Finally, the acetone was removed by the addition of air. Acetone was used to clean the system as it was miscible with both water and dodecane. Other cleaning fluids (eg, methanol and ethanol) tested were found to be only miscible with either water or dodecane and therefore formed another emulsion with the immiscible liquid. The acetone proved to fairly easy to remove from the system but it was important to remove all of it. Even a small trace of the acetone remaining in the system caused problems during operation. The membranes were found to turn yellow and became brittle if any acetone came into contact with them. To check that all the acetone was removed a red dye was added to the acetone so that it could be distinguished from the doecane. when the dodecane was flushed through the system after cleaning the presence of any remaining acetone was detected and easily cleaned away. Once the dodecane ran clear normal operation was applied as outlined above.

2.3 Analytical methods

2.3.1 Quantification of breakage

The percentage rate of demulsification could not be determined by mass balance (equation 2.1) because V_E was made up of the volume that had passed through the membrane at time, t and of part of the emulsion in the module (dead volume). The module held a volume of 6.5 ml. At the end of the process part of the volume was unaffected emulsion feed (not part of V_E) and the rest was a cake of dodecane and water. It was uncertain what proportion of this emulsion could be included in Equation 2.1. If the process had been run for sufficient time the influence of the hold-

up volume would have been negligible (< 10 %). However for all the breakage experiments the run times fell short of the time required for minimum error due to the maximum pressure of the system being reached. The calculated errors were > 25 %.

$$\text{Percentage demulsification} = \frac{V_W}{V_E \varphi} \qquad ..(2.1)$$

Where V_E is the volume of the emulsion in the demulsification vicinity (ml), V_W is the volume of water in the permeate and φ is the phase ratio of the emulsion.

By measuring the water content in the permeate at 2 minute intervals and representing it as a percentage of the total permeate at time, t allows the permeate water content to be compared with the original emulsion water content at 2 minute intervals.

2.3.2 Statistical Methods

For each emulsion breakage experiment 3 repeat experiments were carried out under the same conditions and the average of the three runs was recorded in Chapters 3 and 4. Appendix 1 shows the average data compared to the maximum and minimum data with the maximum error recorded.

Chapter 3

Emulsion Breakage Using Hydrophilic Membranes as a Coalescing Aid

3.1 Introduction

Emulsion liquid membranes are used to concentrate a solute. Extraction of the solute from a water feed phase, occurs across an oil liquid film and into a water-based recovery phase. The oil phase and water recovery phase are emulsified with the aid of surfactant into a stable water-in-oil emulsion. The emulsion offers the advantage of a very high surface area which leads to fast mass transfer. The recovery of the high value products is achieved by first separating the emulsion from the external water feed phase followed by breaking the emulsion [Draxler et al, 1986].

The aim of this work was to break stable water-in-oil emulsions stabilised by the surfactant, Paranox 100. The emulsions used were designed to be of stability similar to what would be used in an emulsion liquid membrane system. This chapter deals with testing the emulsions used in this study for stability. This is followed by the filtration results for emulsion breakage using dead-end filtration at a constant feedrate. During the investigation several parameters were varied some of which include: emulsion composition, membrane material, membrane pore size, and flowrate. Finally, in this chapter, the results are reported for the measurements of the physical properties of the emulsions used in this study. These measurements include, viscosity of the emulsions, surface and interfacial tension of the emulsions and the dodecane in the permeate, density and water content of the dodecane phase in the permeate.

In Chapter 4 the mechanism of emulsion breakage is described using the results reported in this chapter. Finally in Chapter 5 the emulsion breakage by filtration in Chapter 3 is compared with the emulsion breakage by electrostatic coalescence.

3.2 Theoretical considerations

3.2.1 Emulsion stability (tracer technique)

The principle of the tracer technique relies on determining the concentration of a tracer (originally in the internal phase) in the feed as a result of internal phase leakage. The tracer technique provides simplicity and good accuracy and the following conditions should be satisfied: (1) The tracer should be chemically inert in the presence of the carrier used, (2) Water transport from the external phase to the internal phase must be negligible. If not the tracer will be diluted. Choosing a good surfactant usually prevents water transport, (3) internal phase encapsulation.

3.2.1.1 Measurement of nickel by EDTA back titration

This technique was used to determine the concentration of the tracer (nickel II nitrate) in the feed phase. By using a back titration method, a known excess of ethylenediaminetetraacetic acid (EDTA) is allowed to react with an unknown amount of nickel II nitrate. At the end of the reaction, the amount of EDTA that remained was found by titration with zinc solution. A simple calculation (see below) gives the amount of EDTA used and the amount of nickel II nitrate that had reacted.

EDTA has the structure

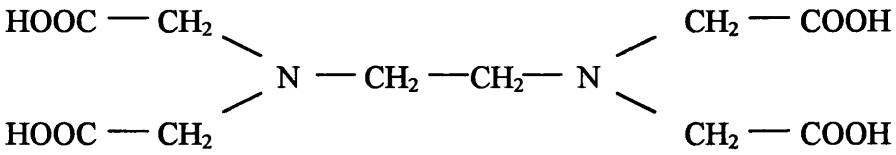

The molecule has six potential sites for bonding a metal ion, the four carboxyl groups and the two amino groups (unshared pair of electrons). Hence EDTA is a hexadentrate ligand and the various EDTA species are often abbreviated H_4Y, H_3Y^-,

H_2Y^{2-}, HY^{3-} and Y^{4-}. EDTA combines with metal ions in a 1:1 ratio regardless of the charge on the cation.

The two reactions which take place are:

$$Ni^{2+} + Y^{4-} \rightarrow NiY^{2-} \quad ...(3.1)$$

$$Zn^{2+} + Y^{4-} \rightarrow ZnY^{2-} \quad ...(3.2)$$

millimoles of EDTA taken is :

$$c_{Ed} \times V_{Ed} = \text{mmol of EDTA} \quad ....(3.3)$$

Where: c_{Ed} is the molarity of the EDTA solution and V_{Ed} is the volume of EDTA added.

millimoles of unreacted EDTA:

$$c_Z \times V_Z = \text{mmol of EDTA} \quad ...(3.4)$$

combining equations 3.3 and 3.4 gives the number of moles of reacted EDTA:

$$(c_{Ed} \times V_{Ed}) - (c_Z \times V_Z) = \text{millimoles of EDTA} \quad ... (3.5)$$

Where: c_Z is the molarity of the zinc solution and V_Z is the volume of zinc solution added.

The moles of reacted EDTA=moles of reacted nickel II nitrate (tracer). This is converted in to a concentration which substituted into equation 3.7 to determine the breakdown ratio. An example calculation of the concentration of nickel II nitrate in the external phase is set out in Appendix 2.

3.2.1.2 Emulsion breakage model

The extent of emulsion breakage on dispersion into a feed phase is represented by the breakdown ratio, B, which is defined as the ratio of the amount of tracer found in the external phase after a dispersion time, t to the amount of tracer initially present in the internal phase [Abou-Nemah and Petegem, 1992]:

$$B = \frac{V_e C_{et}}{V_i C_{i0}} \qquad ...(3.6)$$

Thus, percentage breakdown is given by

$$B\% = \frac{V_e C_{et}}{V_i C_{i0}} 100\% \qquad ...(3.7)$$

Where Ve is the external phase volume, V_i is the internal phase volume, C_{et} is the concentration of nickel at time, t and C_{io} is the initial concentration of nickel in the internal phase before dispersion.

Equation 3.7 does not give the true amount of emulsion breakage which occurs. The true amount is as follows:

$$B = \frac{(V_e + V_{bt})C_{et}}{V_i C_{i0}} \qquad ...(3.8)$$

Where V_{bt} is the volume of the internal phase now dispersed in the external phase at time, t. However, since V_{bt} is difficult to measure and at low breakage is negligible, the breakdown ratio in equation 3.7 is used to indicate the amount of emulsion breakage.

No account was made for emulsion swelling in the above equations. It was assumed to be negligible due to the surfactant not being a water carrier. An example of a percentage breakdown calculation is set out in Appendix 2.

3.2.1.3 Calculation of osmotic pressure

Water transport through the membrane phase is unfavourable since it results in the concentrated inner phase being diluted again. If there is an osmotic pressure difference across the membrane then water transport will be in the direction of higher osmotic pressure. However, if the surfactant used is not a water carrier then the osmotic pressure difference will not be important.

The osmotic pressure of the aqueous phase is calculated using the Vant' Hoff equation [Cussler, 1986].

$$\Delta\pi = -\frac{RT}{V_p}\ln(1-x) \qquad ..(3.9)$$

Where $\Delta\pi$ is the osmotic pressure (atm), R is the universal gas constant (0.082 dm^3 atm mol^{-1} K^{-1}), T is the absolute temperature, x is the mol fraction and V is the partial molar volume of the solvent (0.018 dm^3 mol^{-1} for water). An example of an osmotic pressure calculation is set out in Appendix 2.

3.2.4 Measurement of surface and interfacial tension

The accumulation of surfactant at the interface between the external phase and air (surface tension) or the external phase and internal phase (interfacial tension) results in the decrease of the interfacial or surface tension. The formation of an emulsion involves the break up of the internal phase. This is brought about by supplying mechanical (emulsifying machines) or chemical (surfactants) energy. Mechanical energy alone can only be used for emulsions with an internal phase of < 0.1 vol %. At higher concentrations the droplets will coalesce when the mechanical energy source is

removed [Kirk-Othmer, 1994]. By adding surfactants less mechanical energy is required and they form a protective film at the interface so the droplets do not coalesce when they collide. If sufficient surfactant is available to protect all the droplets and form micelles in the continuous phase a limiting surface tension will exist where increasing the surfactant concentration will not change this value. Also the surface tension of the emulsion will be similar to the limiting surface tension of the surfactant (Paranox 100) in the external phase (dodecane) before emulsification.

There are several ways of measuring surface tension and interfacial tension. The choice of method is influenced by the following factors: efficient temperature control and a high degree of cleanliness are of great importance .The drop volume method was chosen because it could be used for both surface and interfacial tension [Shaw, 1980].

Drops of liquid detach slowly from the tip of a vertically mounted narrow tube and their volume is measured. At the point of detachment Equation 3.10 applies

$$\gamma = \frac{\phi V \rho g}{2\pi r} \qquad \text{.....(3.10)}$$

Where V is the volume of the drop, ρ is the density of the liquid, r is the radius of the tip and ϕ is the correction factor.

Fig 3.1 shows the four stages of droplet formation. After reaching a certain degree of elongation (Figure 3.1a-3.1c) the growth process becomes irreversible and a droplet finally separates from the liquid (Figure 3.1d). The liquid that breaks away may form one or two smaller droplets, while the rest remains at the orifice. This is the reason

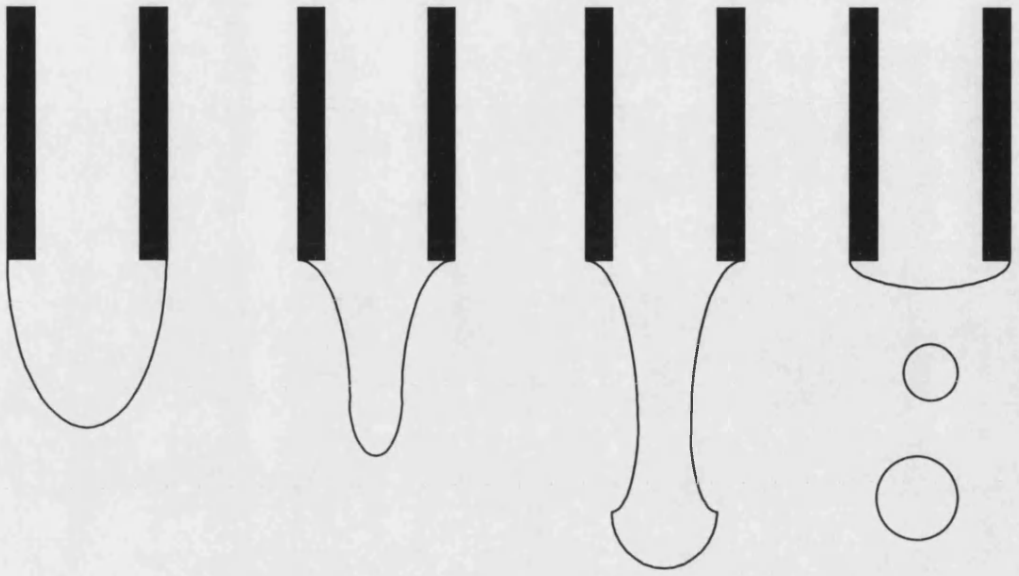

(a) (b) (c) (d)

Fig 3.1 Stages in the formation of a droplet

the correction factor is required. ϕ depends on the ratio $\frac{r}{V^{1/3}}$. Values of ϕ have been determined by Harkins and Brown [Shaw, 1980] and it can be seen that the values $\frac{r}{V^{1/3}}$ between 0.6 and 1.2 are preferable (Fig 3.2).

A tip that has been carefully ground smooth and used with a micrometer syringe burette will give a good a good drop-volume apparatus. The tip of the tube must be completely wetted and the last 10 % of the drop should be formed very slowly (~ 1 min). An example of a surface and interfacial tension calculation is set out in Appendix 2.

Stability tests using the tracer technique were carried out on all the emulsions used in the emulsion breakage experiments by microfiltration (section 3.4.5). The surface tension of the emulsions, the external phase and the dodecane phase of the permeate were measured and the results are presented in section 3.4.4.3. Also the interfacial tension of the external (dodecane) phase and internal (water) phase was measured. These results are also recorded in section 3.4.4.3.

3.3 Materials and Methods

3.3.1 Materials

Dodecane (99 %) was obtained from BDH Laboratory Supplies (Poole, England). Paranox 100 was obtained from Exxon Chemicals (Southhampton, England). Nickel II nitrate was purchased from Fluka (Gillingham, Dorset, England).

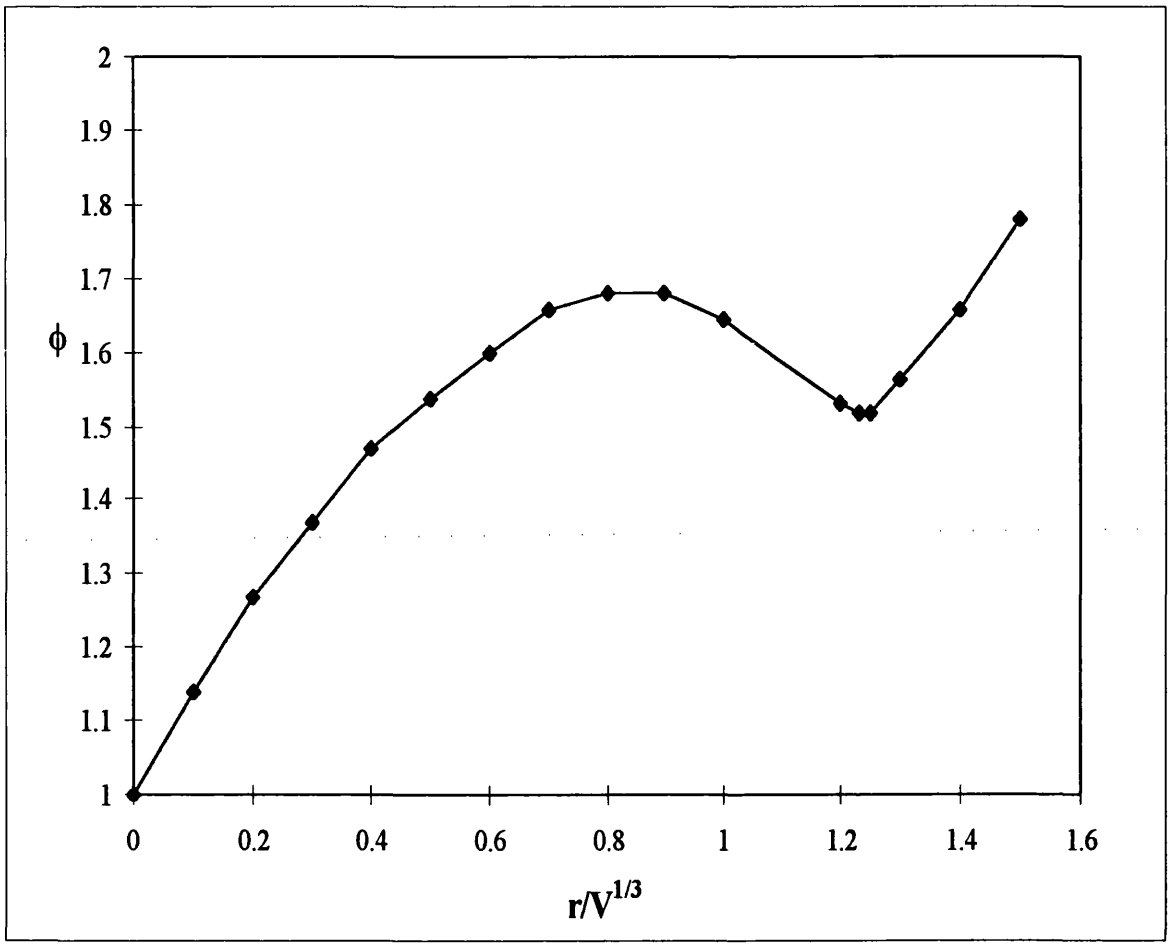

Figure 3.2 Standard graph of the correction factor for the drop volume method (ϕ) versus $r/V^{1/3}$

3.3.2 Methods

3.3.2.1 Emulsification

The method of emulsification was described in Chapter 2. The emulsion composition and experimental conditions used are summarised in Table 3.1

3.3.2.2 Preliminary breakage experiments

The equipment shown in Fig. 3.3 consists of a 50ml disposable plastic syringe and a membrane module made of stainless steel (dead volume 6.5 ml) and was purchased from Sartorius. This is then placed in a syringe press where the syringe plunger is attached to the cross head (A) and the membrane module is attached to the support (B), this arrangement reduced unsteady flow. The membranes were 4.2 cm in diameter giving a surface area of 13.86 cm^2. The emulsion flows perpendicular to the membrane, typical of dead-end filtration.

Operation

The emulsion was loaded in a disposable syringe which was then depressed at a fixed feed rate. Flowrates of 0.66 ml/min, 1.32 ml/min and 3.3 ml/min were tested. The emulsion used was a 50:50 water-in-dodecane (1 w/w % Paranox 100) emulsion. The system was run at room temperature and fresh emulsions and membranes were used for each run. The permeate was collected in a beaker and no pressure was recorded.

3.3.2.3 Membrane Module and Operation

The membrane module operation was outlined in Chapter 2. The runs where water was detected in the permeate were usually operated until either the maximum pressure (6 bar) of the system was reached or for approx 25 minutes at 0.6 $\times 10^{-6}$ $m^3 min^{-1}$ or between 39-64 minutes at 0.3 $\times 10^{-6}$ $m^3 min^{-1}$. Where no water was detected in the

Table 3.1 Summary of emulsion composition and emulsification conditions.

Emulsion phase volume ratio aqueous: organic	Surfactant concentration (w/w %)	Homogeniser		Homogeniser	
		speed (rpm)	Internal phase addition time (min)	speed (rpm)	residence time (min)
50:50	1	8000	3	9500	10
50:50	1	8000	3	8000	10
50:50	2	8000	3	9500	10
20:80	0.5	8000	3	9500	10

permeate the runs were operated until the maximum pressure (6 bar) of the system was reached.

3.3.2.4 Emulsion stability tests

Emulsion liquid membrane systems were designed so that there was maximum metal extraction and minimum emulsion instability. It is desirable to have some instability to avoid difficulties during demulsification (may have problems finding an emulsion breakage technique if the emulsion is too stable). A membrane leakage of about 1-2 % is allowable for a practical process [Draxler and Marr, 1986]. To determine the extent of internal phase leakage the internal tracer technique is applied.

Method

The emulsion (50 ml) was dispersed in an aqueous (100 ml) external phase (external phase was double the emulsion phase) in a 200 ml glass beaker with the aid of a teflon stirring bar (length: 3 cm) , at a speed just sufficient to disperse the emulsion uniformly into small drops. A relatively high stirring speed is required to in order to create a large interfacial area for mass transfer. However, the higher the stirring speed the greater the shear energy and this will increase the chances of entrainment of the external aqueous phase and lead to swelling. At the applied speed (170 rpm) the emulsion dispersed in to droplets of diameter of about 1-2 mm which was sufficient to create a large surface area for mass transfer.

Samples (containing both emulsion and external water) of approximately 15 ml were removed at 15 minute intervals over a period of 1 hour. After each sample was taken the temperature of the system was recorded. Exactly 5ml of the aqueous phase was removed from each sample and diluted 10 fold. The aqueous phase was then examined for nickel content using EDTA back titration.

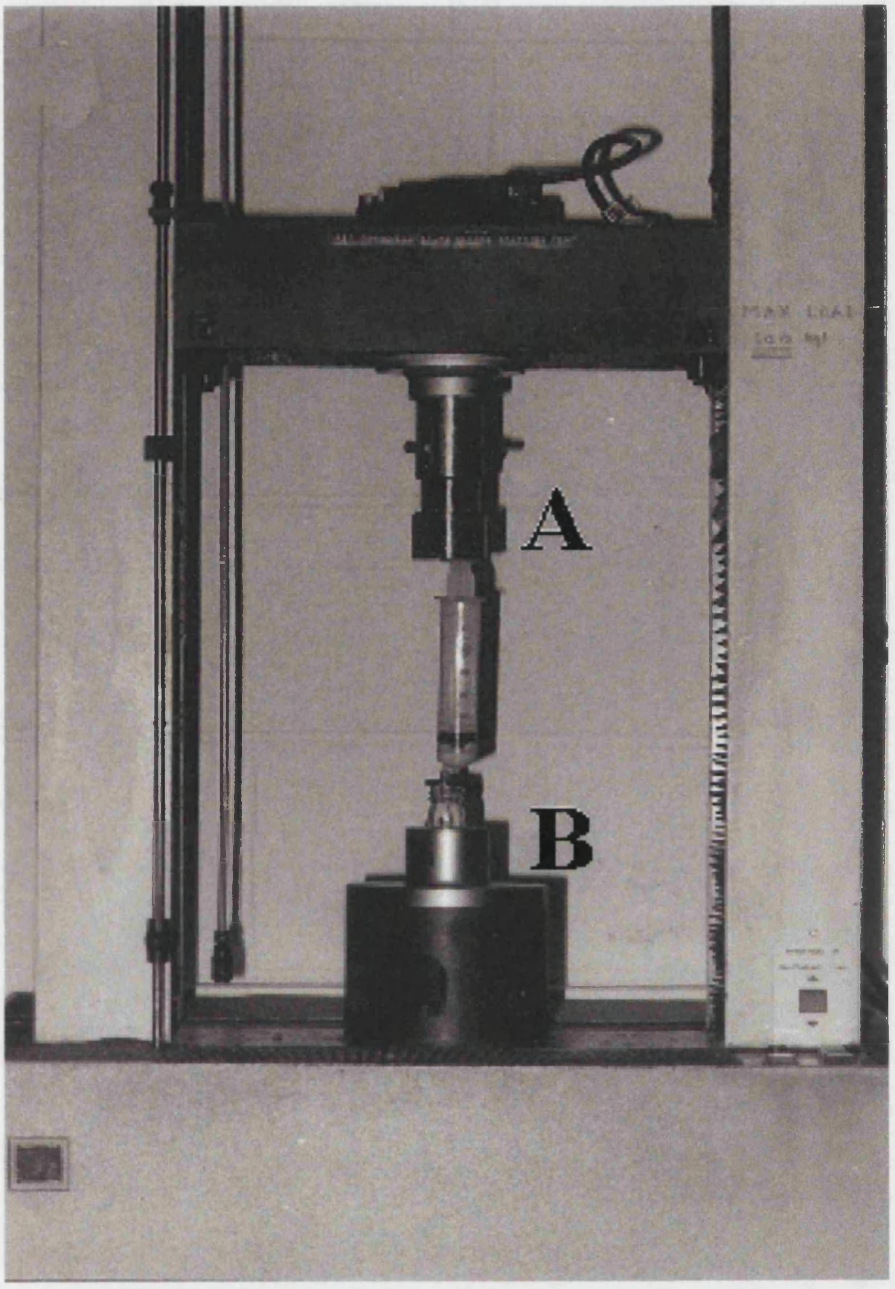

Fig 3.3 Preliminary emulsion breakage equipment

3.3.3 Analytical Methods

3.3.3.1 Viscosity measurements

Viscosity measurements were carried out using a Haake VT550 (concentric tubes). The equipment consists of a spindle and sample chamber. Temperature was kept constant via a thermosel system (special cylinder and spindle) with a thermocontainer and a digital proportional controller. The system was digital and records temperature, viscosity and shear rate.

Operation

Samples of 30 ml were put in the container and temperature was set at 24 °C. The shear rate was increased from 0-720 $s^{-1}$and then held at 720 s^{-1}. This was followed by decreasing the shear rate from 720-1.2 s^{-1}. The recorded viscosity was plotted against shear rate to determine if the behaviour was Newtonian or non-Newtonian. Newtonian fluids at a fixed temperature will remain constant over a range of shear rates. However, emulsions of high internal phase are often pseudoplastic (non-Newtonian).

3.3.3.2 Emulsion droplet size and size distribution

This is a visual technique that allows for the droplets to be looked at directly. It shows the shape of the particles and how well dispersed the sample is. One advantage of this method is it is relatively cheap. The main disadvantage is that 1g of 6.8 μm droplets (density 0.826 gcm^{-3}) contains $7.4x10^{9}$ droplets. All of these cannot be measured by microscopy, only a few droplets are examined so there is a danger of unrepresentative sampling.

The emulsion was placed on a flat slide by pipette and great care was taken in placing the cover slide to avoid squashing the droplets. Pictures were taken of different

sections of the slide to get a fair distribution of the droplet size. At least 300 droplets are required for an accurate statistical measurement of size distribution.

3.3.3.3 EDTA titration (back titration)

EDTA back titrations were used to measure the concentration of the tracer in the external water phase to determine if there was leakage from the internal water phase to the external water phase during agitation. The concentration was then represented as a breakage percentage using equation 3.7.

Titration of the nickel solutions were performed as follows. Each 50 ml sample was neutralised by adding 3 M NaOH with phenolphthalein as an indicator to bring about the appearance of a red colour, avoiding excess NaOH. Finally 6M HCl was added to remove the red base colour. Next 25 ml of standard 0.01 M EDTA was added to the sample followed by 5 drops of 9 M HCl, 1g of Hexamine and four drops of xylenol orange indicator solution. The hexamine buffers the solution at pH 5.5 ($\pm$ 0.1). If the solution turned red it was warmed and a further 10 ml EDTA was added. Finally, the solution was back-titrated with standard 0.01 M zinc solution until the indicator changed from yellow to red.

3.3.3.4 Density measurements

The density of the emulsions were measured so that these values could be used in Chapter 4 for the cake filtration models and in Equation 3.10 to calculate the surface tension. The density of the water (internal) phase and dodecane (external) phase were measured to calculate using Equation 3.10 the surface and interfacial tension. Also the density of the dodecane phase with surfactant concentrations between 0.5 - 2 w/w % was measured to determine if the surfactant concentration affected the density and used in Equation 3.10 to calculate the surface and interfacial tension.

A hand-held density meter (DMA 35, Paar Scientific, London) was used. This instrument does not require manipulations of balances, laboratory vessels or

thermometers. This device is excellent for samples that contain particles (or droplets). The sample to be measured (approximately 2 ml) was introduced into a hollow u-shaped oscillator made of borosilicate glass. It was important to ensure no air bubbles were introduced in the measuring cell. When the temperature equilibrium was reached the instrument showed the density of the sample at the measuring temperature.

3.3.3.5 Surface tension measurements

The surface tension of the dodecane and Paranox 100 was measured before emulsification and in the permeate. Also the surface tension of all emulsions were measured. The method used was the drop volume method.

Fig 3.4 shows the equipment used. It consists of a micrometer screw, which was used to form a series of droplets at a slow rate at the tip of a syringe needle of diameter 0.88 mm. The tip was ground absolutely flat. The syringe and its plunger were designed so that one revolution of the micrometer head, which advanced the plunger by 0.5 mm, delivered a volume of 10 μl.

The assembled syringe was mounted vertically on a vibration free surface. It was filled with the sample. The micrometer was then locked and the needle washed and dried (using acetone). The needle was then held in the air and the micrometer reading was recorded. The micrometer was then turned to depress the plunger and for a droplet at the tip of the needle. As the droplet got larger the rate of turning the micrometer was reduced. The micrometer reading when the droplet fell was recorded and taken to be the initial value. The procedure was repeated but the rotation of the micrometer was made very slowly once the reading had reached 90 % of the obtained initial value. Further replicate measurements were made until consistent results were obtained. The readings obtained were for the turns of the micrometer. The relationship between the micrometer reading (M) and the volume delivered is 20M=volume (μl). This value was substituted in to Equation 3.10 to determine the surface or interfacial tension.

3.3.3.6 Dye tests

Not all of the emulsion breakage experiments resulted in the passage of water and dodecane through the membranes. However, in the case of the membranes where only dodecane permeated through it was established that the emulsion was partially demulsified on the membrane surface. This was clarified by adding a water soluble dye to the emulsion directly above the membrane (cake). If the dye dispersed (bright blue colour observed) the droplets were no longer surrounded by the surfactant. If the droplets were still surrounded by a protective surfactant layer the water was not detected and the dye remained in the form of solid black crystals.

Methanol blue is a water soluble dye. It does not disperse in non polar solvents, it remains in black particles. In a polar solvent it disperses to give a bright blue colour. The emulsion where water droplets are surrounded by surfactant the addition of this dye will show no dispersion. In order to determine if the cake contained coalesced droplets and therefore emulsion breakage on the surface of the membrane the dye was introduced in to the cake (emulsion directly above the membrane).

3.3.3.7 Emulsion breakage by filtration

By measuring the water content in the permeate at 2 minute intervals and representing it as a percentage of the total permeate at time, t allows the permeate water content to be compared with the original emulsion water content at 2 minute intervals.

3.3.3.8 Water content in the permeate dodecane

Dodecane in the permeate samples was analysed for water content by means of a Coulometer (Mettler Model DL37 KF). Fig 3.5 shows the equipment used. It consists of an inner burette where 5 ml of catholyte was placed and a titration cell where 100 ml of anolyte was poured. The titration cell as a syringe inlet port where the samples are injected and sits in a titration cell holder attached to a keypad.

A pretitration was carried out on the KF Coulometer until the system was stable. This was followed by a titration. The sample was injected using a syringe through the septum (sample must be injected in 1 minute). The titration after the sample was injected started automatically. When the titration was finished the sample weight (in grams) was entered and the result was displayed and printed out. The display should show stable and then a second titration can be performed. The water content of the sample was given in ppm.

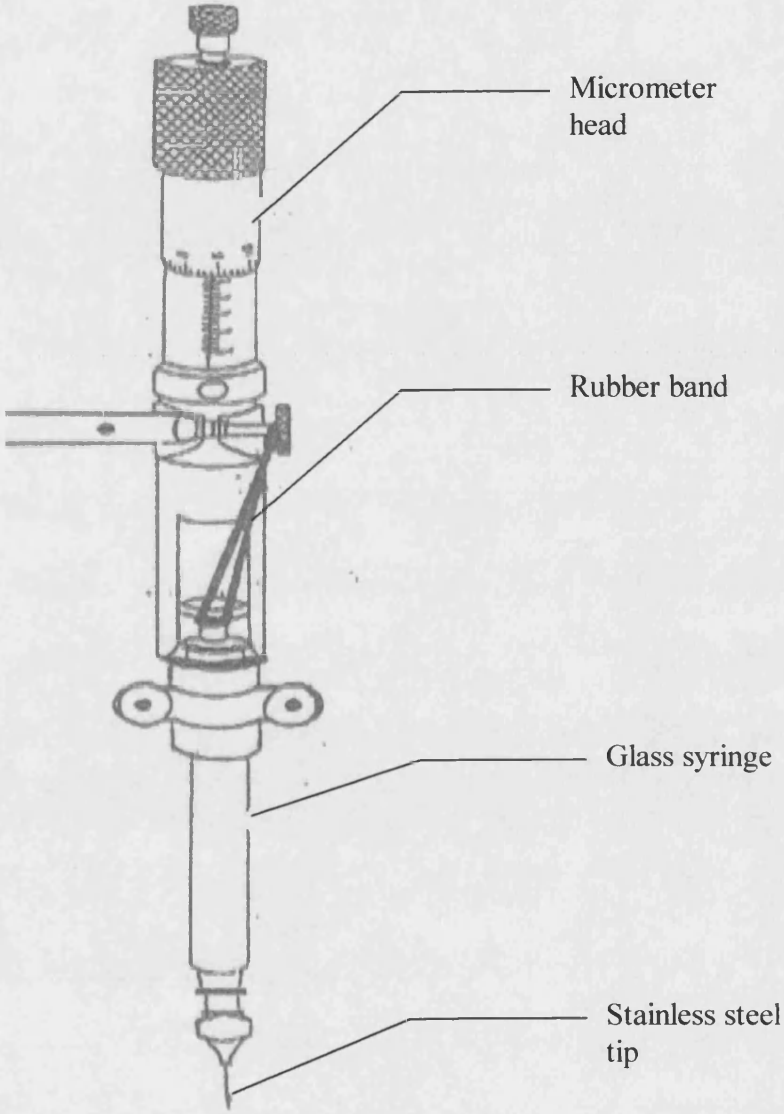

Fig 3.4 Diagram of the Agla micrometer syringe for the measurement of surface and interfacial tension

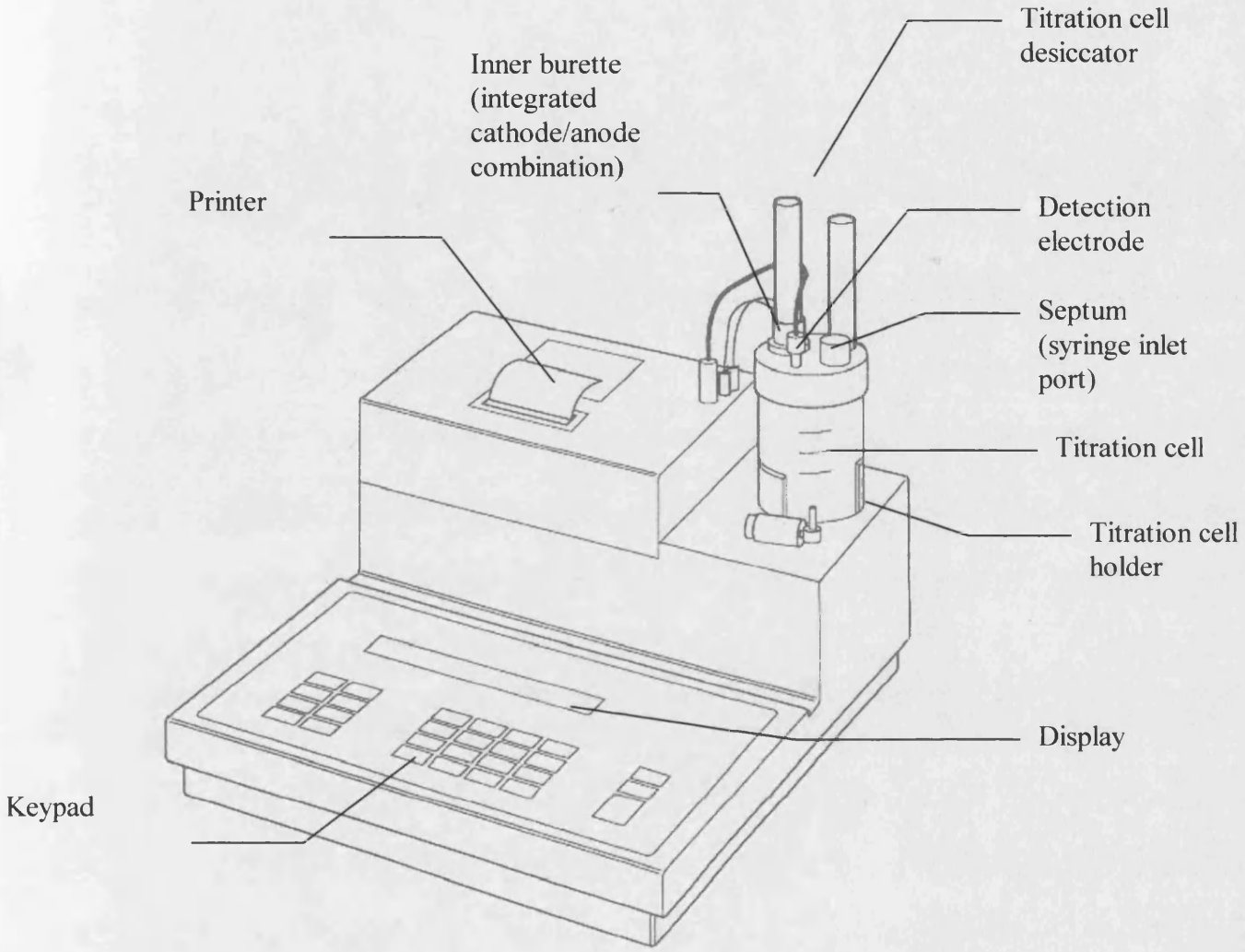

Fig 3.5 Diagram of a KF Coulometer used for measuring water content.

3.4 Results

3.4.1 Preliminary breakage

Fig 3.6 shows the permeate stream (settled for 5 minutes) for a Supor 200 membrane at fluxes (a) 28.6 l/h/m^2, (b) 57.1 l/h/m^2 and (c) 142.8 l/h/m^2. Breakage occurred at fluxes 57.1 l/h/m^2 and 142.8 l/h/m^2 and the permeate consisted of three phases a upper phase of dodecane, a lower phase of water and a phase in the middle of the emulsion. At a constant flux of 28.6 l/h/m^2 only two phases existed in the permeate. An upper phase of dodecane and a lower phase of water. The water phase in the permeate for all three fluxes was hazy.

3.4.2 Membrane Filtration

The breakage experiments were carried out in dead-end where the flux was kept constant (26 l/h/m^2 and 13 l/h/m^2). The pressure and volume of filtrate was recorded. Filtration results at fluxes 26 l/h/m^2 and 13 l/h/m^2 are represented in Figures 3.7 and 3.8 respectively. At constant flux, 26 l/h/m^2 between 7.2 $\times 10^{-6}$ m^3 and 15 $\times 10^{-6}$ m^3 of solution was passed through the membrane. The filtration was stopped at approximately 6 bar (maximum pressure of the system) for membranes Nylaflo and HTTuffryn and 5 bar for the Supor 200 membrane. The pressure of 5 bar was reached for much less volume of filtrate with a Nylaflo membrane than with a HTTuffryn or Supor 200 membrane (Figure 3.7). For membranes Supor 200 and HTTuffryn both water and dodecane was collected in the permeate. In the case of the Nylaflo membrane only dodecane was collected in the permeate.

At a flux of 13 l/h/m^2 between 9.9 $\times 10^{-6}$ m^3 and 19.2$\times 10^{-6}$ m^3 of solution was passed through the membrane. The filtration was stopped at approximately 6 bar (maximum pressure of the system) for the Nylaflo membrane, 3 bar for the HTTuffryn membrane and 5 bar for the Supor 200 membrane. A pressure of 3 bar was reached

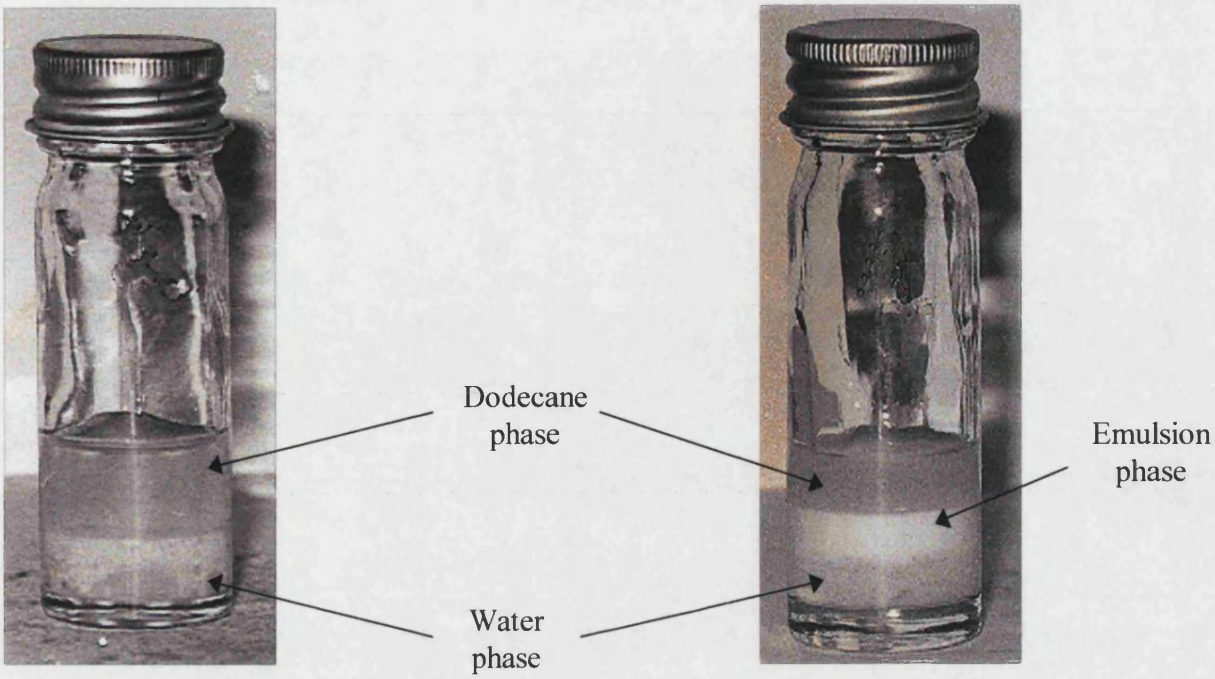

(a) (b)

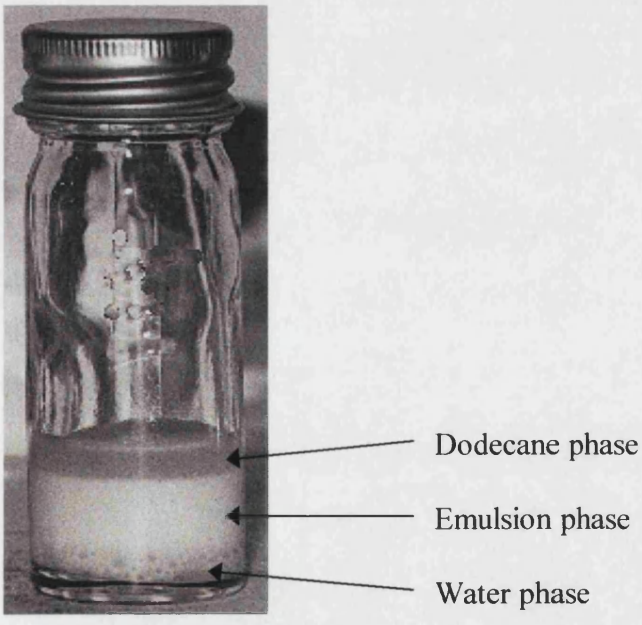

(c)

Fig 3.6 Emulsion breakage through a hydrophilic membrane of pore diameter 0.2 μm at fluxes: (a) 28.6 l/h/m^2, (b) 57.1 l/h/m^2 and (c) 142.8 l/h/m^2.

for much less volume of filtrate with the Nylaflo membrane than with the HTTuffryn or Supor 200 membrane (Figure 3.8). In all cases both water and dodecane was collected in the permeate. All the results showed that the pressure increased linearly with respects to the filtrate volume with an abrupt change in the slope (decrease in the slope).

The results represented in Figure 3.9 are at fluxes 26 l/h/m^{2}and 13 l/h/m^2. Between 3.9 $\times 10^{-6}$ m^3 and 4.2$\times 10^{-6}$ m^3 of solution was passed through the membrane. The filtration was stopped at approximately 6 bar (maximum pressure of the system). The maximum pressure was reached for the same volume of filtrate (4.2$\times 10^{-6}$ m^3) for membranes Supor 450 and Supor 100 at either flux. The Versapor membrane reached the maximum pressure of the system at a slightly lower volume of filtrate passing through the membrane. In all cases no water was detected in the permeate . In fact in almost all cases no permeate was collected due to the hold-up volume of the permeate line (3.3 ml).

Figure 3.10 shows the results, which is a combination of the Supor membranes from Figures 3.7, 3.8 and 3.9, to determine the effect of pore size (0.1 μm, 0.2 μm and 0.45 μm) on emulsion breakage. The results represented in Figure 3.10 are at fluxes 26 l/h/m^2 and 13 l/h/m^2. Between 4.2 $\times 10^{-6}$ m^3 and 19.2$\times 10^{-6}$ m^3 of solution was passed through the membrane. The filtration was stopped at approximately 6 bar (maximum pressure of the system) for membranes Supor 100 and Supor 450 and 5 bar for Supor 200. The pressure of 6 bar was reached for the same volume of filtrate (4.2$\times 10^{-6}$ m^3) for membranes Supor 450 and Supor 100 at either flux. The pressure of 5 bar was reached for a much lower volume of filtrate. for membranes Supor 100 and Supor 450 than membrane Supor 100. Similar amounts of water were collected in the permeate for membrane Supor 200 at fluxes 26 l/h/m^2 (51 %) ^{and} 13 l/h/m^2 (44 %). All of the results represented in Figure 3.10 show the pressure increasing linearly with the volume of solution through the membrane this is typical of cake filtration. However,

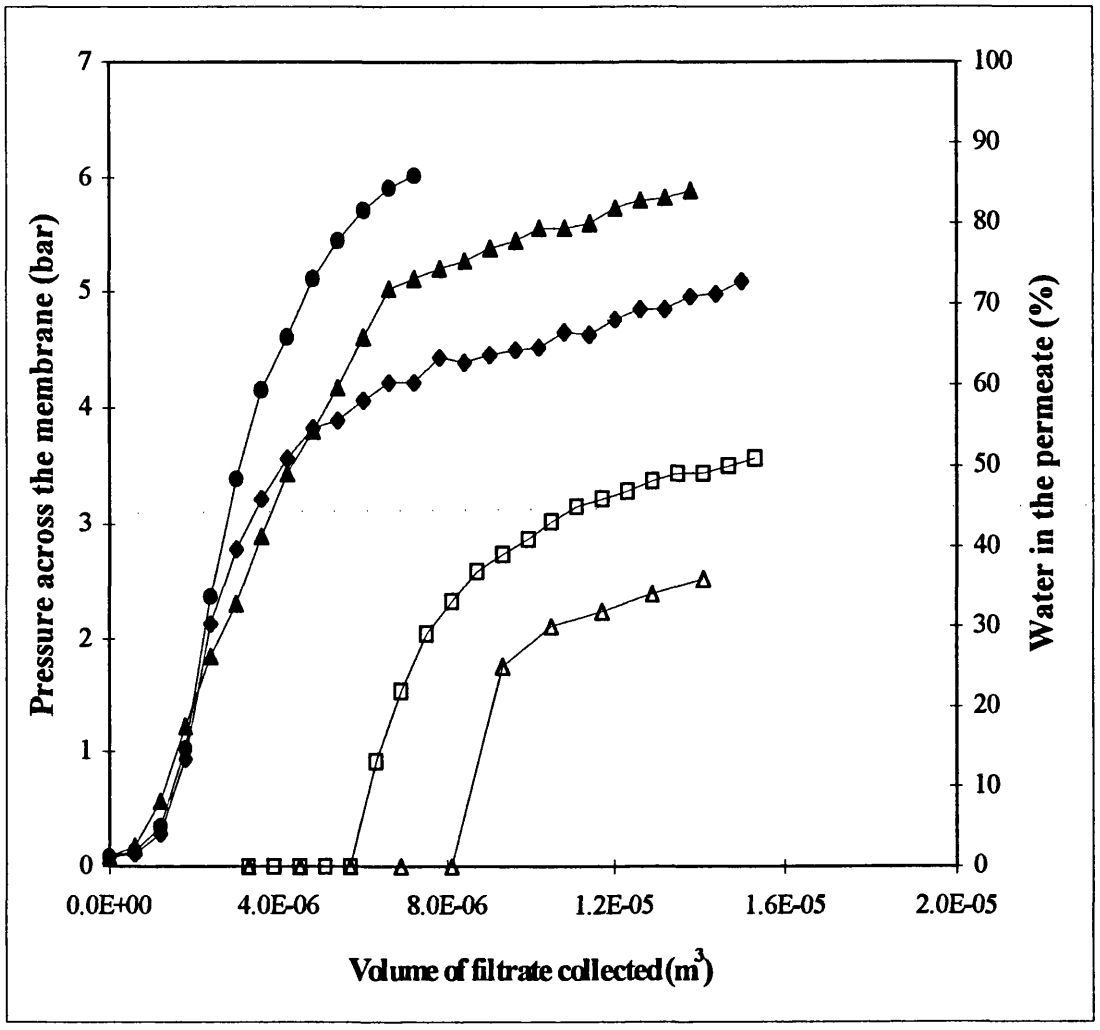

Figure 3.7 Variation in pressure drop and water collected in the permeate in microfiltration of 50:50 water-in-dodecane (1 % Paranox 100) emulsion at a flux of 26 l/h/m^2 for different membrane types. Pressure drop : -▲-HTTuffryn,-◆- Supor 200, - • - Nylaflo. Water collected in the permeate: -Δ- HTTuffryn, -□- Supor 200.

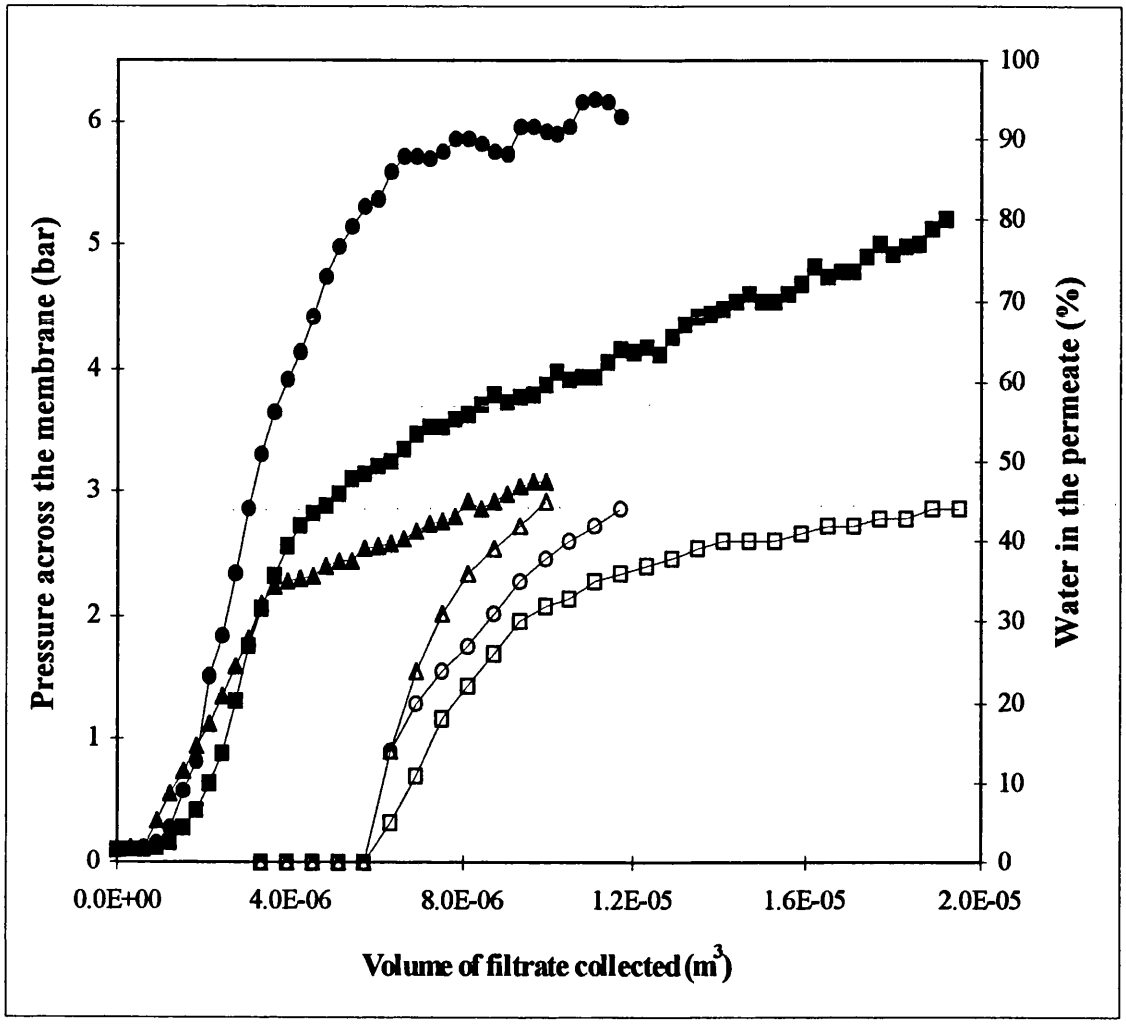

Figure 3.8 Variation in pressure drop and water collected in the permeate in microfiltration of 50:50 water-in-dodecane (1 % Paranox 100) emulsion at a flux of 13 l/h/m^2 for different membrane types. Pressure drop : -▲-HTTuffryn,-■- Supor 200, -●- Nylaflo. Water collected in the permeate: -Δ- HTTuffryn, -□- Supor 200, -O- Nylaflo.

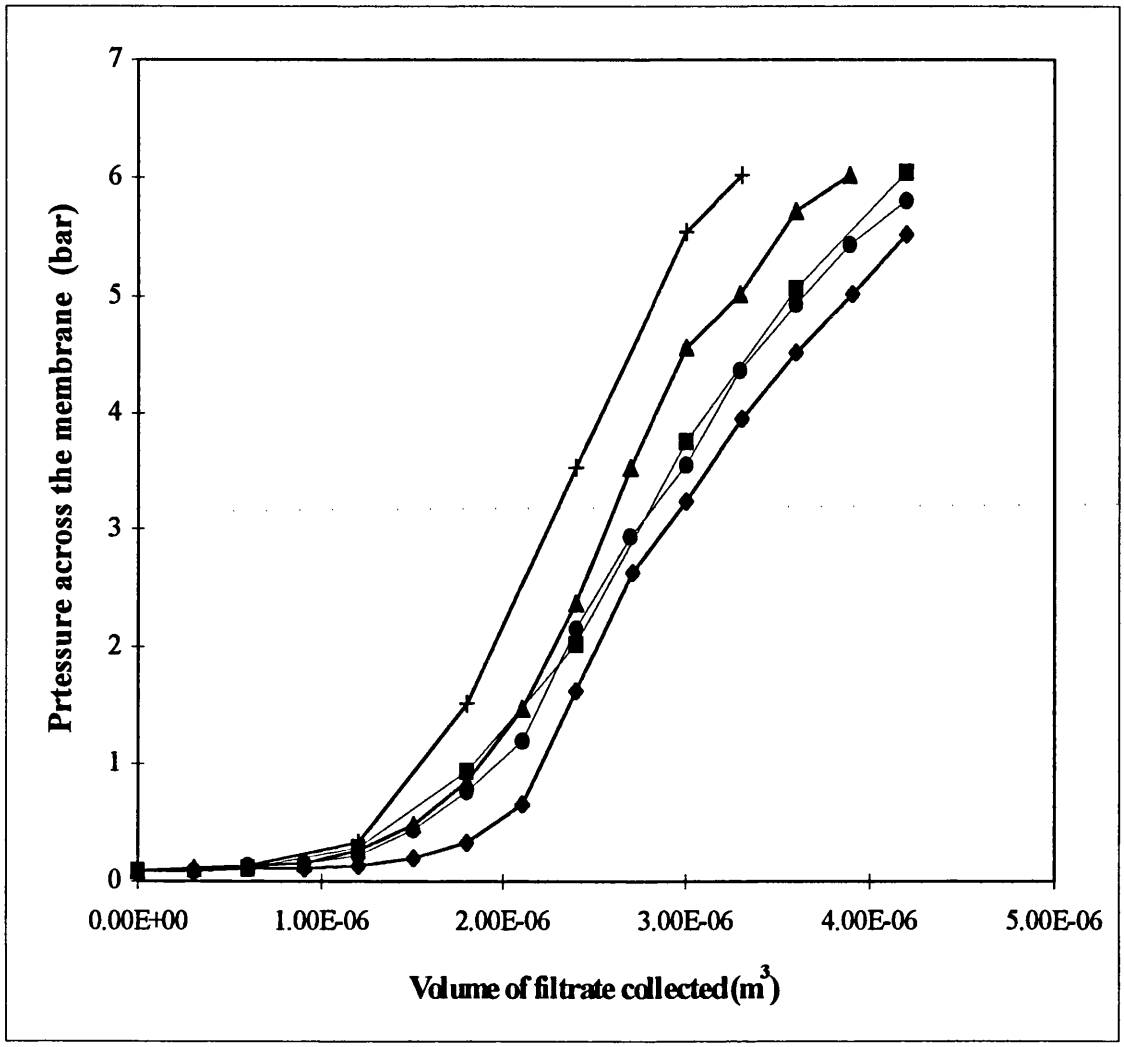

Figure 3.9 Variation in pressure drop in microfiltration of 50:50 water-in-dodecane (1 % Paranox 100) emulsion for different membrane types at a flux of 13 l/h/m^2: -◆- Supor 100, -●- Supor 450, -▲- Versapor at a flux of of 26 l/h/m^2: -■- Supor 450, -×- Versapor.

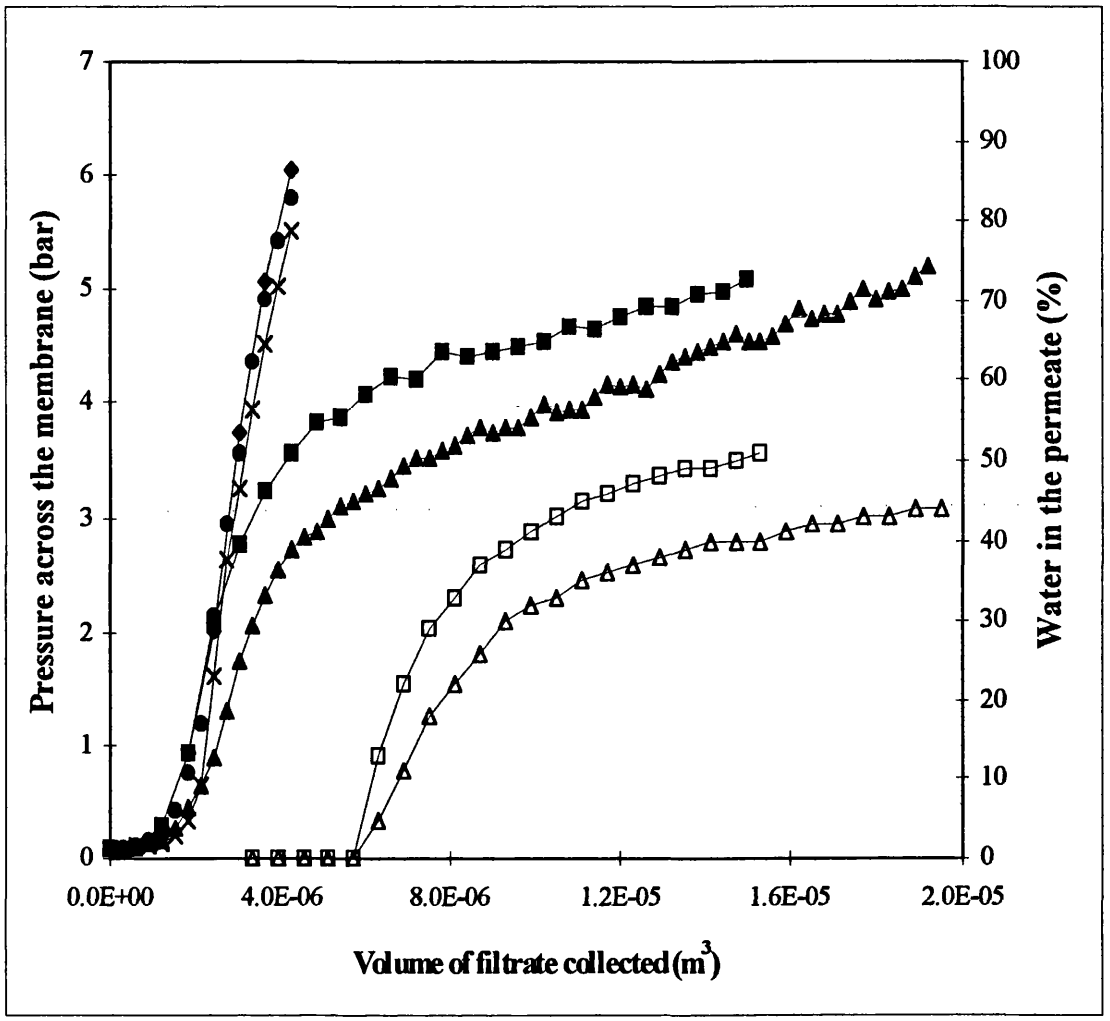

Figure 3.10 Variation in pressure drop and water collected in the permeate in microfiltration of 50:50 water-in-dodecane (1 % Paranox 100) for different membrane pore sizes. At a flux of 13 l/h/m^2, Pressure drop : -▲- Supor 200, -x- Supor 100, -●- Supor 450. Water collected in the permeate: -Δ- Supor 200. At a flux of 26 l/h/m^2, Pressure drop : -■- Supor 200, -◆- Supor 450. Water collected in the permeate: -□- Supor 200.

in the case of the Supor 200 membrane there are two linear sections. This result is consistent with the consecutive lay-down of two cakes. It can be surmised that the second cake where there is a decrease in the slope is the result of a change in the ratio of water/dodecane passing through the membrane. This will be discussed further in Chapter 4.

Filtration results for Supor 200 membrane at various fluxes are represented in Figure 3.11. Between 11×10^{-6} m^3 and 19.2×10^{-6} m^3 of solution was passed through the membrane. The filtration was stopped at approximately 5 bar. The maximum pressure was reached for much less volume of filtrate at a flux of 43.3 l/h/m^2 than at fluxes 26 l//m^2 and 13 l/h/m^2. The water collected in the permeate at the two lower fluxes was similar, 51 % and 44 % at fluxes 26 l//m^2 and 13 l/h/m^2 respectively. At the higher flux of 43.3 l/h/m^2 the water detected was much lower 35 %. All of the results represented in Figure 3.11 show the pressure increasing linearly with the volume of solution through the membrane with an abrupt change in the slope occurring at the transition from the first cake to the second cake. This transition resulted in a decrease in the slope. This will be discussed further in Chapter 4.

The behaviour of emulsion breakage also varied when the emulsion composition was changed. Figure 3.12 represents the results where the surfactant concentration was varied between 1 w/w % and 2 w/w % at fluxes 26 l/h/m^2 and 13 l/h/m^2. The filtration for the 2 w/w % Paranox 100 emulsion was stopped at 6 bar (maximum pressure of the system) at both fluxes and 5 bar for the 1w/w % Paranox 100 emulsion at both flowrates. The pressure of 5 bar was reached for much less volume of filtrate for the emulsion emulsified with 2 w/w % Paranox 100 than the emulsion containing 1 w/w % Paranox 100. The water percentage in the permeate at the end of filtration for the 1 w/w % Paranox 100 emulsion was 51 % and 44 % at fluxes 26 l/h/m^2 and 13 l/h/m^2 respectively. For the 2 w/w % Paranox 100 emulsion the water percentage at the end of filtration was 20 % at both flowrates.

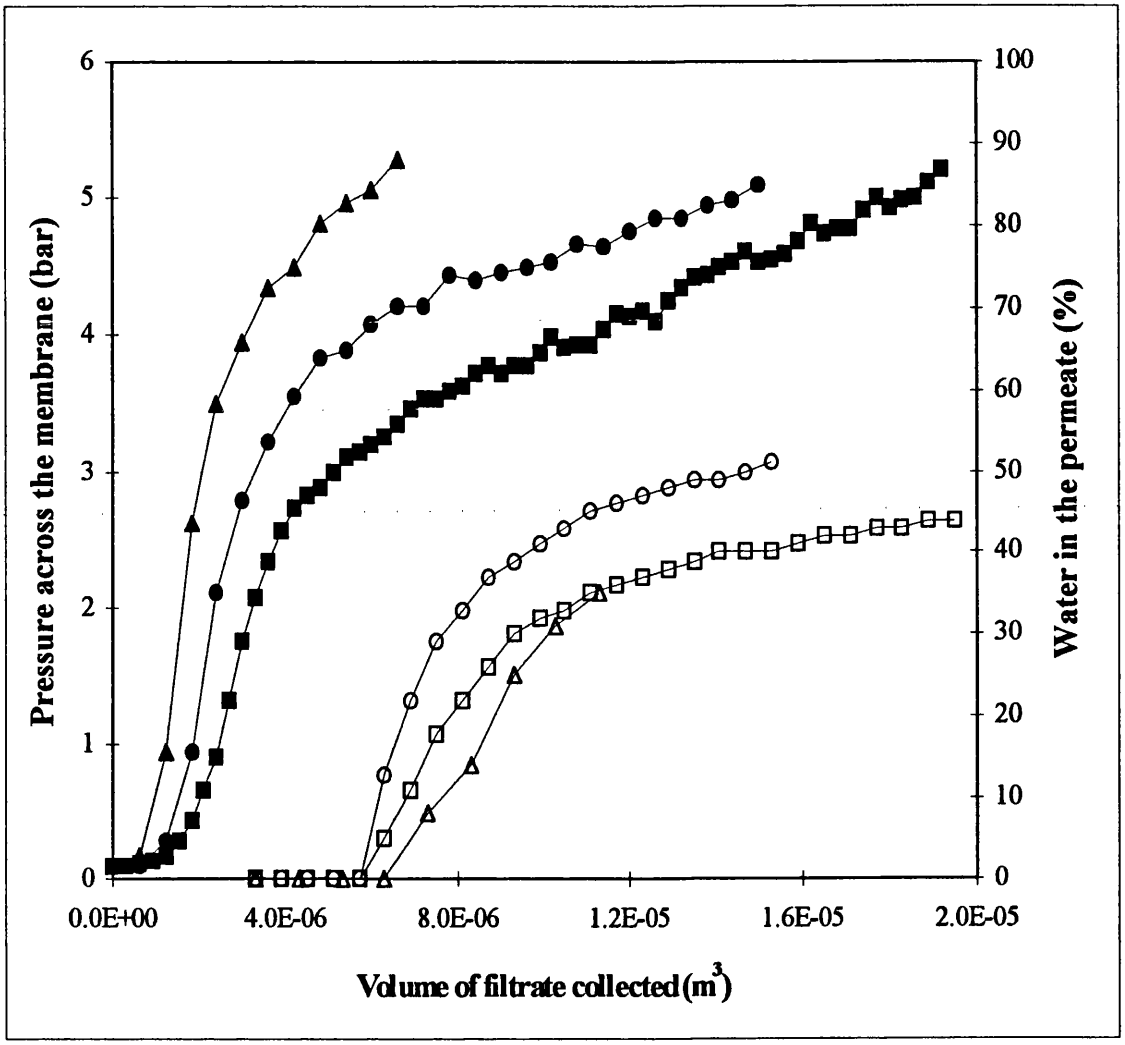

Figure 3.11 Variation in pressure drop and water collected in the permeate in microfiltration of 50:50 water-in-dodecane (1 % Paranox 100) emulsion using Supor 200 membrane at different fluxes. Pressure drop : -■- 13 l/h/m^2, -●- 26 l/h/m^2, -▲- 43.3 l/h/m^2. Water collected in the permeate: -□- 13 l/h/m^2, -O- 26 l/h/m^2, -Δ- 43.3 l/h/m^2.

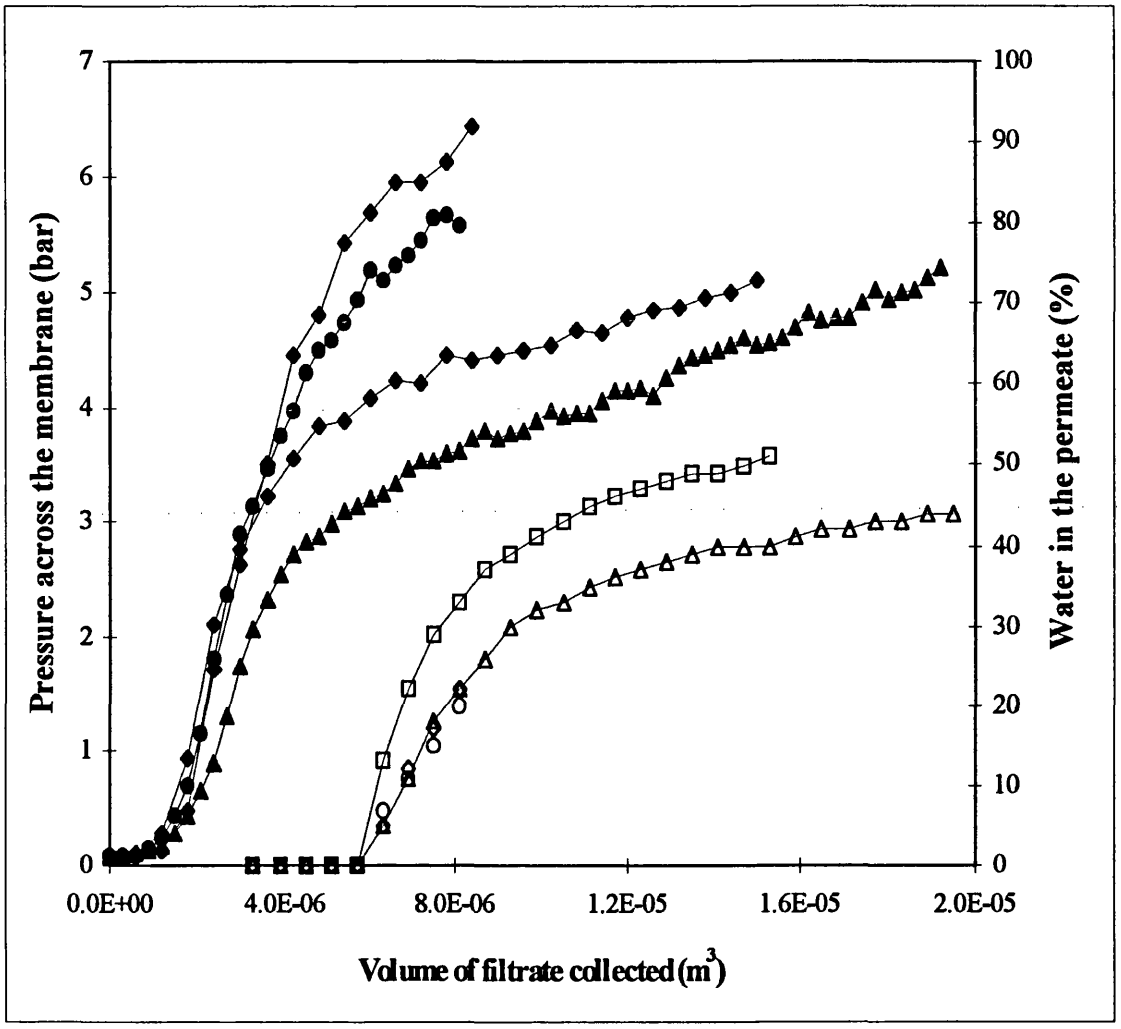

Figure 3.12 Variation in pressure drop and water collected in the permeate in microfiltration of 50:50 water-in-dodecane emulsion using Supor 200 membrane at different flowrates and different surfactant concentrations. For a flux of 13 l/h/m^2. Pressure drop : -●- 2 w/w % Paranox 100, -▲- 1 w/w % Paranox 100. Water collected in the permeate: -O- 2 w/w % Paranox 100, -Δ- 1 w/w % Paranox 100. For a flux of 26 l/h/m^2. Pressure drop : -◆- 2 w/w % Paranox 100, -■- 1 w/w % Paranox 100. Water collected in the permeate: -+- 2 w/w % Paranox 100, -□- 1 w/w % Paranox 100.

When the homogenisation conditions were varied (mixing speed 8000 rpm for 10 minutes or 9500 rpm for 10 minutes) the pressure results at a flux of 13 l/h/m^2 were of the type represented in Figure 3.13. The filtration was stopped at 5 bar for the emulsion homogenised at 9500 rpm and 3.6 bar for the emulsion homogenised at 8000 rpm as these were the pressures at which the mechanism was fully established for each emulsion used. The pressure of 3.6 bar was reached for a much lower volume of filtrate for the emulsion homogenised at 9500 rpm than the emulsion homogenised at 8000 rpm. Again the pressure increased linearly with an abrupt change in the slope occurring at the transition from the first cake to the second cake. This transition resulted in a decrease in the slope (this is discussed further in Chapter 4).

Figure 3.14 shows the results for a 20:80 water-in-dodecane (0.5 w/w % Paranox 100) emulsion. Initially the pressure increased linearly until the pressure reached about 1.1 bar and then there was a gradual decrease in the pressure to 0.6 bar where the pressure remained virtually constant.

3.4.3 Dye tests

Table 3.2 shows the dye test results carried out on the concentrated emulsions in the module after filtration. In almost all cases the emulsion was demulsified in the module. The only emulsion where there was no droplet coalescence was the 20:80 water-in-dodecane (0.5 w/w % Paranox 100) emulsion. The dye did not disperse through the concentrated emulsion it remained as solid black particles.

3.4.4 Physical properties

Several physical properties of the feed emulsion and permeate were measured, the results are reported below:

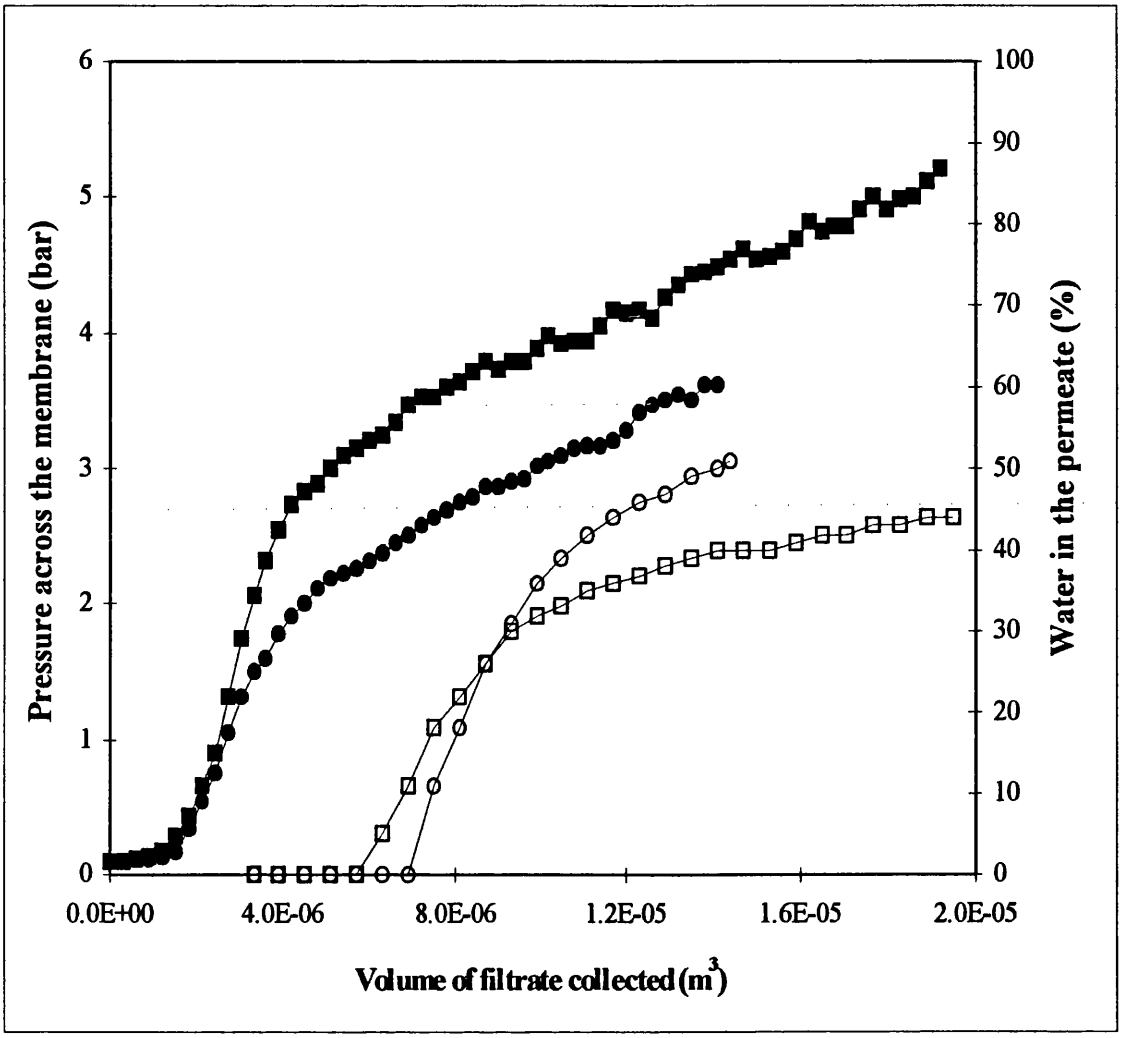

Figure 3.13 Variation in pressure drop and water collected in the permeate in microfiltration of 50:50 water-in-dodecane (1 % Paranox 100) emulsion at a flux of 13 l/h/m^2 for different homogeniser mixing speeds : -■- 9500 rpm, -●- 8000 rpm. Water collected in the permeate: -□- 9500 rpm, -O- 8000 rpm.

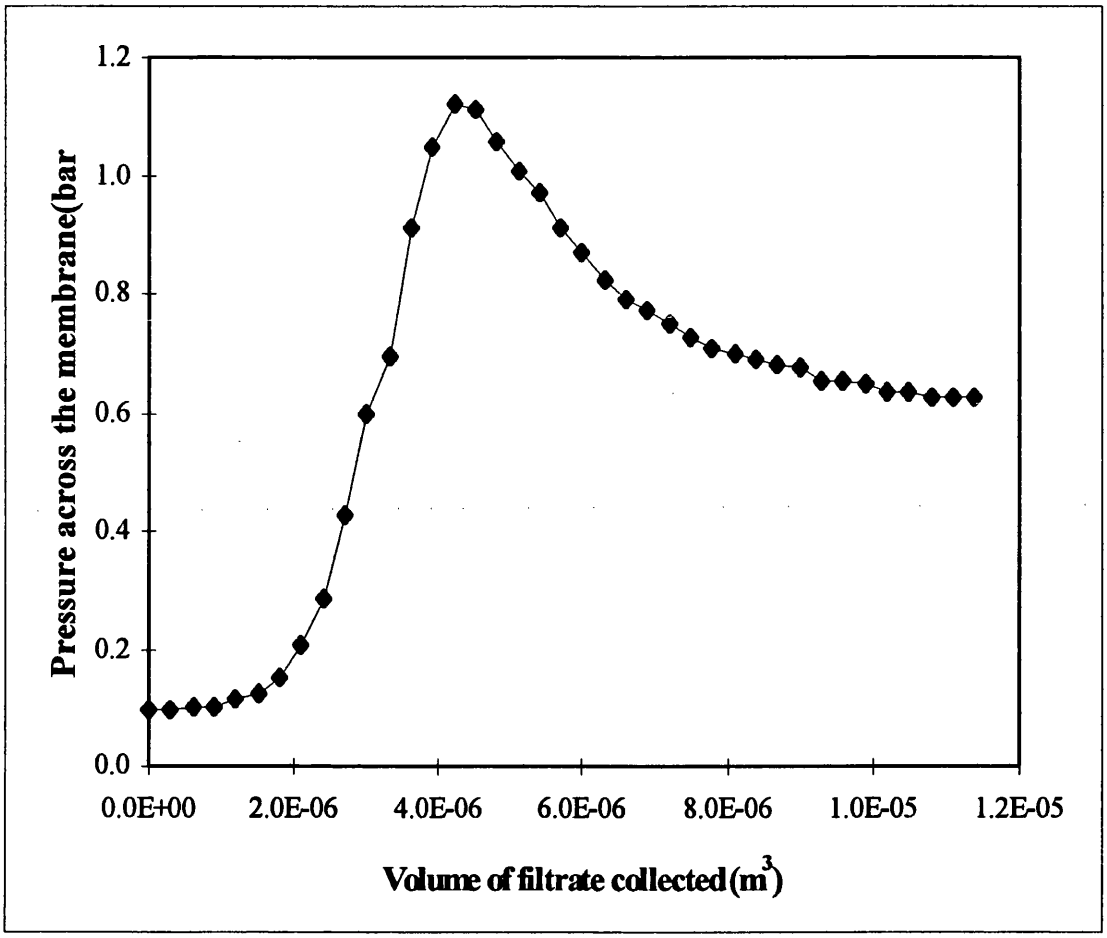

Figure 3.14 Variation in pressure drop in microfiltration of 20:80 water-in-dodecane (0.5 % Paranox 100) emulsion at a flux of 13 l/h/m^2.

Table 3.2 Dye test results for the concentrated emulsion in the membrane module at the end of filtration.

Membrane/pore size (μm)	Flux ($l/h/m^2$)	Emulsion (composition)	Results
Supor 0.2	13 and 26	50:50 water-in-dodecane (1% Paranox 100)	dye dispersed throughout the cake
	13	50:50 water-in-dodecane (1% Paranox 100) "homogeniser kept at 8000 rpm"	dye dispersed throughout the cake
	13 and 26	50:50 water-in-dodecane (2% Paranox 100)	dye dispersed throughout the cake
	13	20:80 water-in-dodecane (0.5% Paranox 100)	dye did not disperse in the cake
Nylaflo	13 and 26	50:50 water-in-dodecane (1% Paranox 100)	dye dispersed throughout the cake
HTTuffryn (0.2)	13 and 26	50:50 water-in-dodecane (1% Paranox 100)	dye dispersed throughout the cake
Versapor (0.2)	13 and 26	50:50 water-in-dodecane (1% Paranox 100)	dye dispersed throughout the cake
Supor (0.1)	13	50:50 water-in-dodecane (1% Paranox 100)	dye dispersed throughout the cake
Supor (0.45)	13 and 26	50:50 water-in-dodecane (1% Paranox 100)	dye dispersed throughout the cake

3.4.4.1 Droplet size distribution

Figures 3.15-3.19 show the droplet size distributions for emulsions in Table 3.1 the distributions show the appearance of a normal curve (symmetrical and bell-shaped). The sample size measured was 300 droplets. The emulsions have a fairly uniform size distribution.

Table 3.3 shows the mean diameters of the emulsions in Table 3.1. The results show that as the water content increases from 20 vol % to 50 vol % the mean droplet size more than doubles (increases by 10.9 μm). Also when the water volume is 50 vol % and the surfactant concentration is increased from 0.5 w/w % to 2 w/w % the mean droplet size decreases. The difference in the mean droplet size (2.8 μm) for surfactant concentrations 1 w/w % and 2 w/w % is much smaller than the difference in the mean droplet size (11.4 μm) for surfactant concentrations 0.5 w/w % and 1 w/w %.

Figure 3.20 shows a sample of the droplets obtained in a 50:50 water-in-dodecane (1 % Paranox 100) emulsion. It is clear from the picture that the emulsion is monodispersed.

3.4.4.2 Emulsion viscosity

Figures 3.21 and 3.22 show the relationship between viscosity and shear rate. The viscosity was measured at 23^0C for all emulsions. The emulsions in Figure 3.21 resulted in the viscosity increasing with increase in shear rate. The measured viscosity was the apparent viscosity and is only accurate when the experimental parameters are kept the same. The increase in viscosity with an increase in shear rate characterises the dilatant fluid (shear thickening fluid). This type of non-Newtonian fluid is frequently

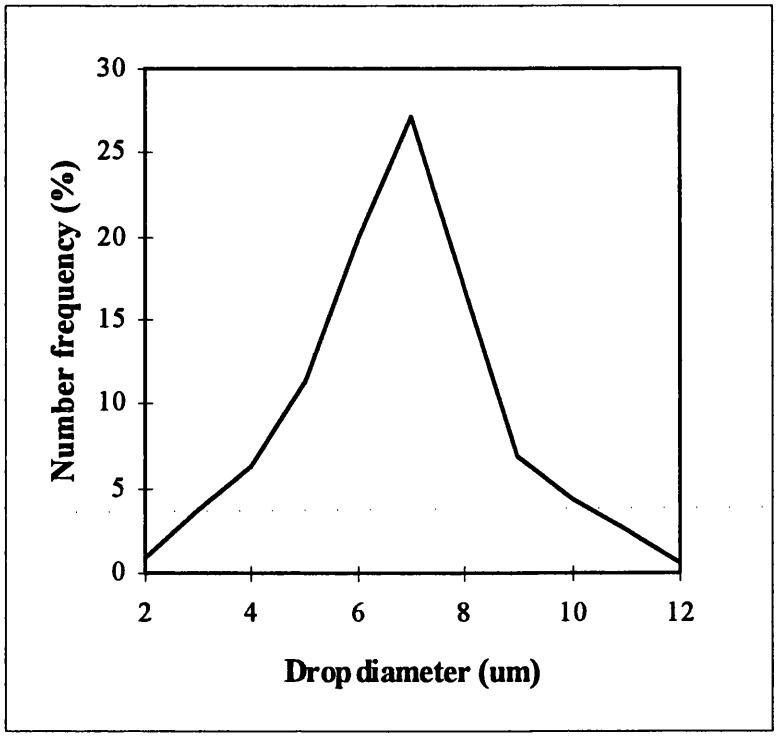

Fig 3.15 Drop size distribution for emulsion 50:50 water-in-dodecane (1 % Paranox 100). Homogenised at 8000 rpm for 3 minutes followed at 9500 rpm for 10 minutes

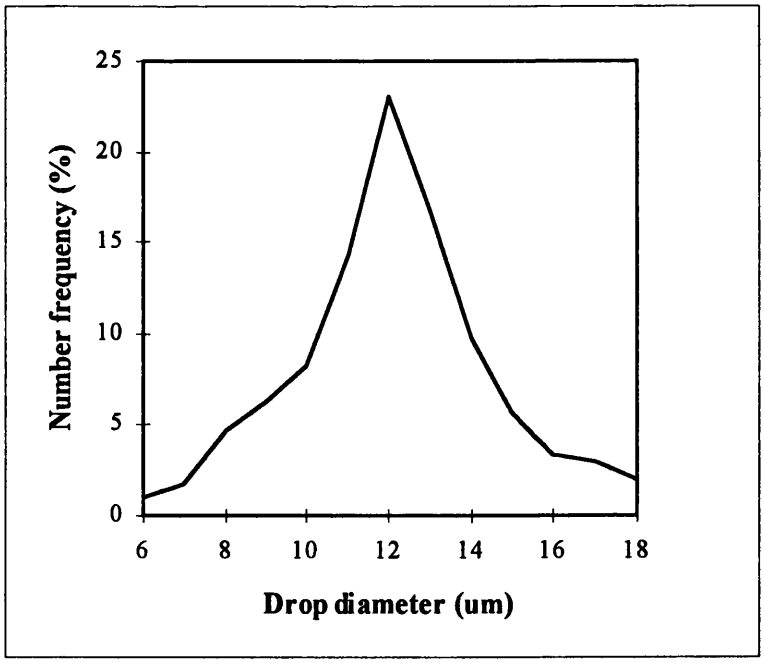

Fig 3.16 Drop size distribution for emulsion 50:50 water-in-dodecane (1 % Paranox 100). Homogenised at 8000 rpm for 13 minutes.

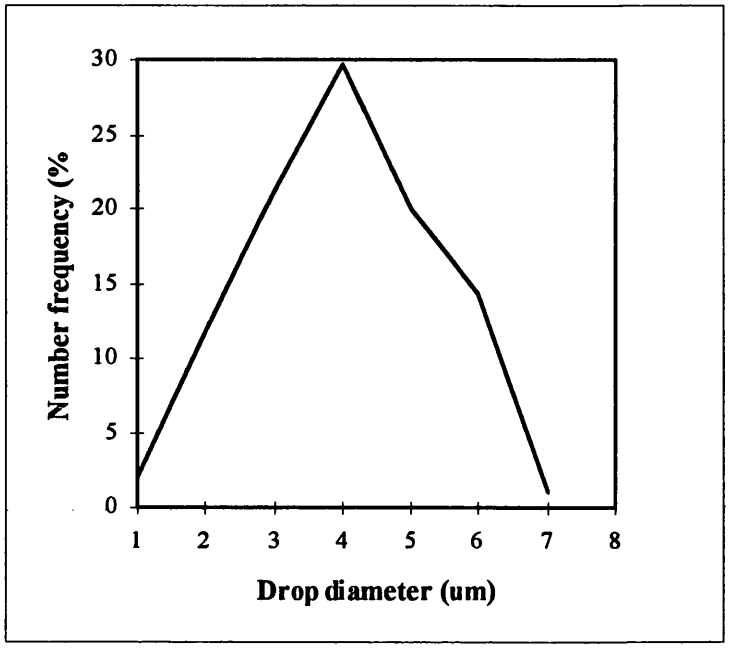

Fig 3.17 Drop size distribution for emulsion 50:50 water-in-dodecane (2 % Paranox 100). Homogenised at 8000 rpm for 3 minutes followed at 9500 rpm for 10 minutes

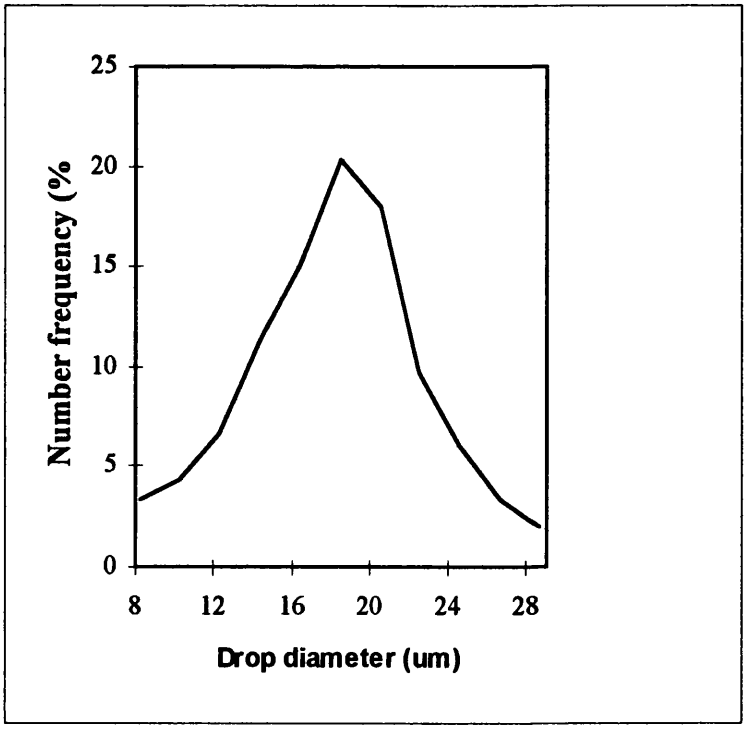

Fig 3.18 Drop size distribution for emulsion 50:50 water-in-dodecane (0.5 % Paranox 100). Homogenised at 8000 rpm for 3 minutes followed at 9500 rpm for 10 minutes.

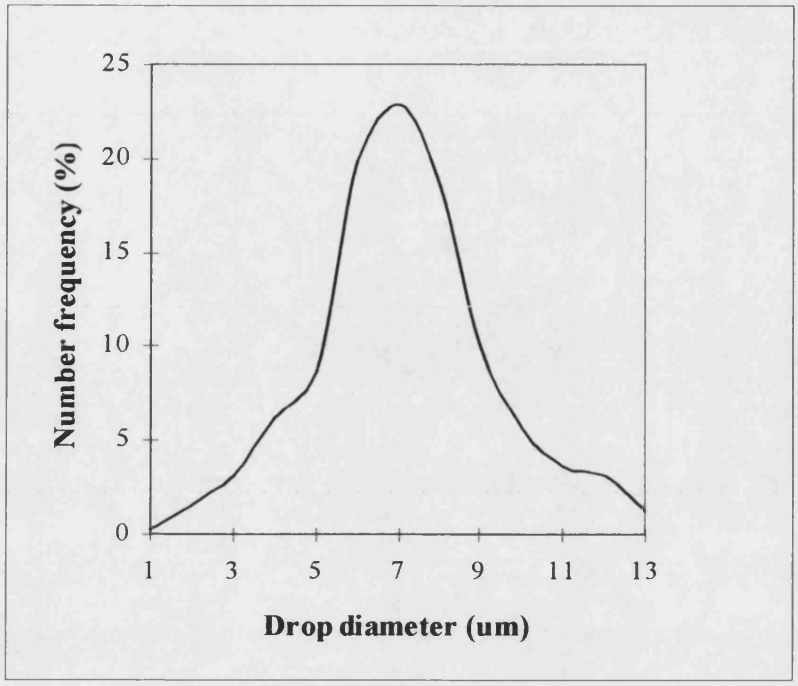

Fig 3.19 Drop size distribution for emulsion 20:80 water-in-dodecane (0.5 % Paranox 100). Homogenised at 8000 rpm for 3 minutes followed at 9500 rpm for 10 minutes.

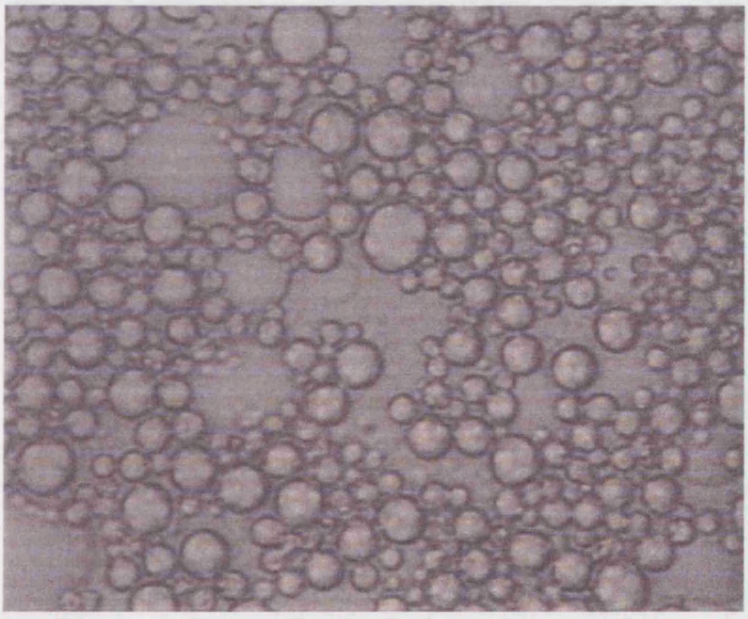

Figure 3.20 droplet size distribution for 50:50 water-in-dodecane (1 w/w % Paranox 100) emulsion.

observed in fluids containing high levels of deflocculated particles and is not observed for emulsions.

The emulsions in Figure 3.22 resulted in the viscosity remaining essentially constant as the shear rate was varied. This is typical of Newtonian fluids which means that the viscosity's quoted in Table 3.4 will remain constant regardless of the shear rate as long as the temperature is kept constant.

3.4.4.3 Surface tension, interfacial tension, density and water in the dodecane of the permeate for the emulsions and permeate components

Table 3.5 lists the results of the physical properties of the emulsion components before emulsification. The surface tension of water was close to the reported value of 72.4 $\times 10^{-3}$ N/m (Dean, 1992). The surface tension of dodecane was higher than the literature value of 25.1 $\times 10^{-3}$ N/m (Dean, 1992). The surfactant (Paranox 100) in the dodecane even at a concentration of 0.5 w/w % resulted in the surface tension being the same as that at a higher concentration (1 w/w % and 2 w/w %). The interfacial tension between the two phases (dodecane and water) decreases with increasing surfactant concentration. The interfacial tension reduced considerably when 0.5 w/w % of surfactant was added to the dodecane. On further addition of surfactant (1 w/w % and 2 w/w %) the interfacial tension was only reduced slightly.

The density of water was at the expected value of 1009 kg/m^3 but dodecane was at a slightly higher (761 kg/m^3) value than quoted in the literature (749 kg/m^3). It is believed that this was due to impurities in the dodecane and not due to the accuracy of the equipment (accuracy 1 kg/m^3). There could have been an error in the measurement but repeat measurements would have shown this (Standard deviation=0). Also the addition of surfactant to the dodecane phase did not affect the density.

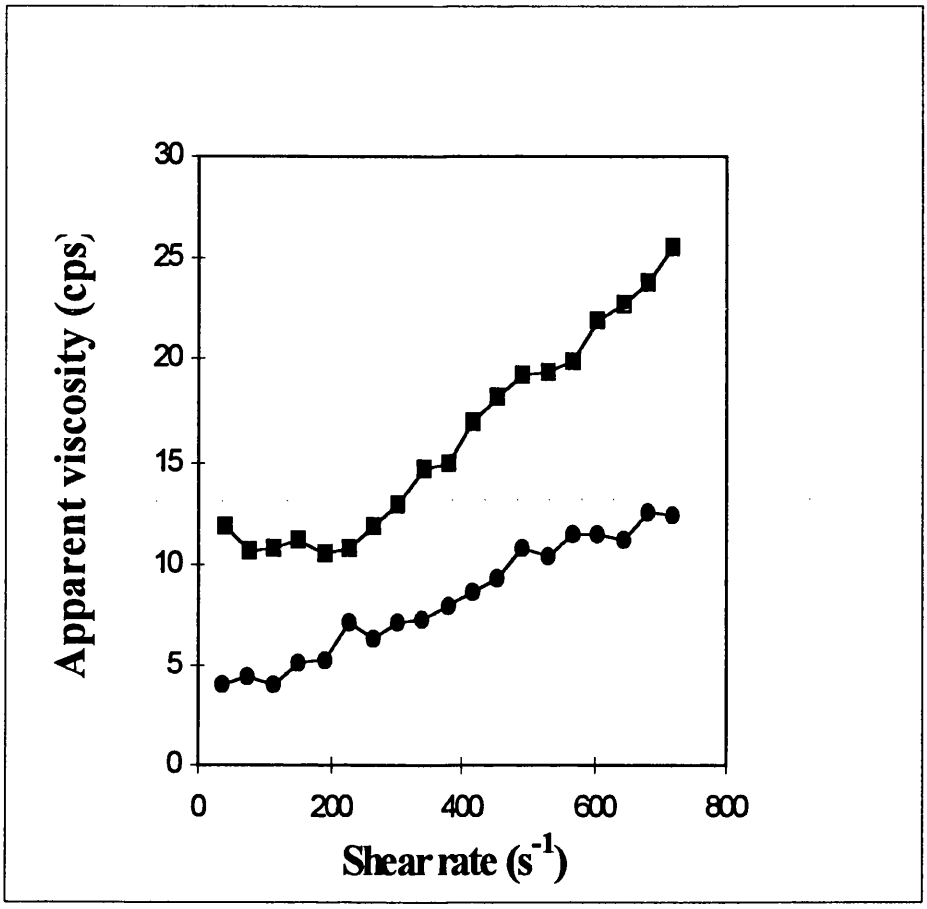

Figure 3.21 Apparent viscosity Vs shear rate for -■-50:50 water-in-dodecane (1% Paranox 100) where the homogeniser mixing speed was 8000 rpm. -●- 20:80 water-in-dodecane (0.5 % Paranox 100) emulsion where the homogeniser mixing speed was 9500 rpm.

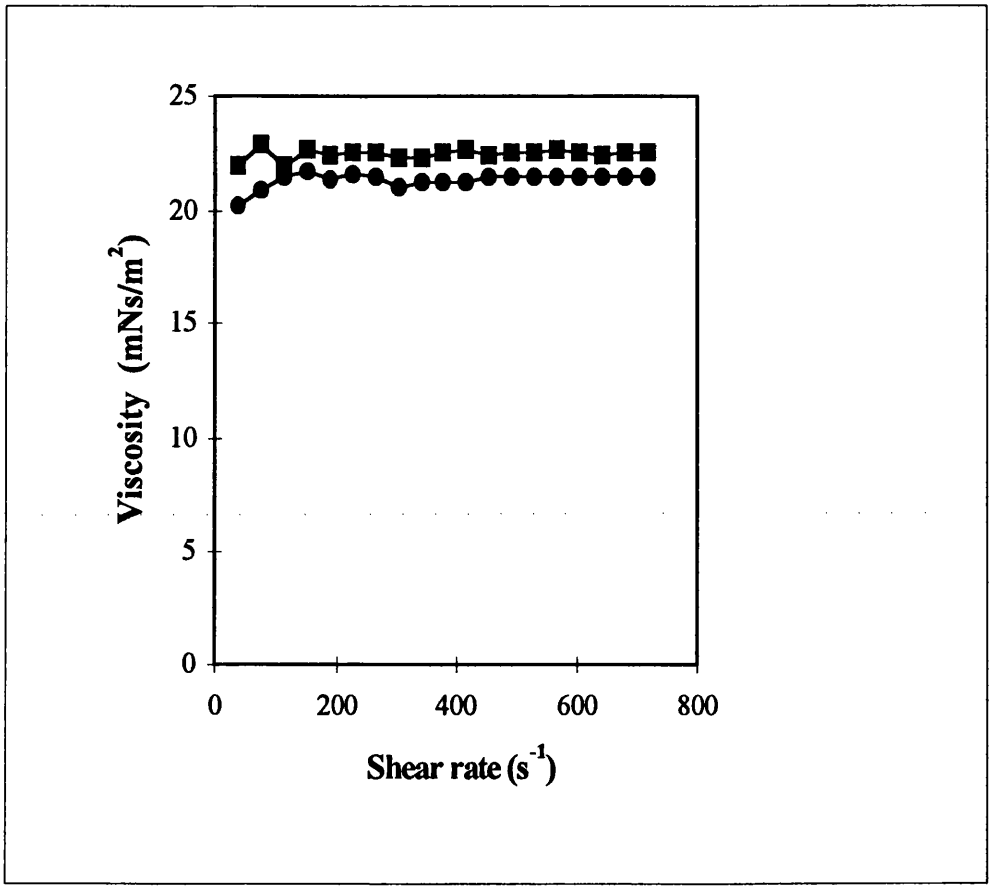

Figure 3.22 Viscosity Vs shear rate for -■-50:50 water-in-dodecane (2% Paranox 100) where the homogeniser mixing speed was 9500 rpm. -●- 50:50 water-in-dodecane (1% Paranox 100) emulsion where the homogeniser mixing speed was 9500 rpm.

Table 3.3 Mean droplet diameters for droplet size distributions in Figures 3.15-3.19

Phase ratio water:dodecane	homogeniser mixing speed (rpm)	surfactant concentration (w/w %)	Mean droplet size (μm)
50:50	9500	1	6.8
50:50	9500	2	4
50:50	8000	1	12.1
20:80	9500	0.5	7.3

Table 3.4 Viscosity of Newtonian emulsions

Phase ratio water:dodecane	homogeniser mixing speed (rpm)	surfactant concentration (w/w %)	Viscosity (mNs/m^2)
50:50	9500	1	21.5
50:50	9500	2	22.5

Table 3.6 summarises the results of the physical properties of the emulsions used. The surface tension of the emulsions were similar in all cases and were similar to the surface tension of the dodecane containing surfactant phases (Table 3.6). The density of the emulsions were between the density of water (1009 kg/m^3) and the density of dodecane 761 kg/m^3). Where the phase ratio was 50:50 and other parameters were changed (e.g. surfactant concentration, homogeniser speed) the densities were very similar. However, for the emulsion where the phase ratio was 20:80 (water/dodecane) the density was much lower (826 kg/m^3) than when the water phase was 50 % of the total emulsion volume. The presence of more dodecane resulted in the density of the emulsion becoming closer to the density of dodecane (762 kg/m^3).

Table 3.7 summarises the results of dodecane in the permeate. The dodecane had a very high purity in all cases (below 300 ppm of residual water, Table 3.7). The surface tension of the dodecane was similar to the surface tension of the dodecane in the original emulsion (Table 3.5). The accuracy of the equipment was -0.4 mN/m and the standard deviations are listed in table 3.7. It is clear that the precision is greater than the accuracy and therefore the uncertainty in the results can only be quoted to the first decimal place.

3.4.5 Emulsion Stability

Leakage of the internal phase products into the external phase was determined using the internal tracer technique. The emulsion conditions are given in Table 3.1. During emulsification four conditions were varied, phase ratio, surfactant concentration, homogeniser residence speed and temperature, to produce emulsions of varying stability. The initial temperatures of emulsification and final temperatures are presented in Table 3.8.

The effect of phase ratio on stability is shown in Fig 3.23. The emulsion with phase ratio 20:80 after 60 minutes of mechanical mixing showed little instability. The emulsion with phase ratio 50:50 exhibited considerable emulsion instability after just

15

Table 3.5 Physical properties of the emulsion components before emulsification. Temperature was kept at 23 °C and the accuracy of density meter and surface tension equipment was 1 kg/m^3 and -0.0004 N/m respectively.

Liquid	Density (kg/m^3)	Standard deviation (kg/m^3)	surface tension N/m 10^{-3}	Standard deviation N/m 10^{-3}	Interfacial tension N/m 10^{-3}	Standard deviation N/m 10^{-3}
Water	1009	1.6	72.0	0.2	-	-
Dodecane	761	0	27.3	0.2	44.9	0.3
Dodecane + 0.5 w/w % Paranox 100	762	0	26.3	0.1	7.28	0.27
Dodecane + 1w/w % Paranox 100	762	0.6	26.3	0.1	5.93	0.10
Dodecane + 2 w/w % Paranox 100	763	1.2	26.3	0.1	5.92	0.10

Table 3.6 Physical properties of the emulsions. Temperature was kept at 23 °C and the accuracy of density meter and surface tension equipment was 1 kg/m^3 and -0.0004 N/m respectively.

Emulsion	Density (kg/m^3)	Standard deviation (kg/m^3)	surface tension 10^{-3} (N/m)	Standard deviation 10^{-3} N/m
20:80 water-in-dodecane (0.5 w/w % Paranox 100)	826	0.6	26.4	0.2
50:50 water-in-dodecane (1 w/w % Paranox 100) *Homogeniser 8000 rpm throughout*	886	0.7	26.5	0.6
50:50 water-in-dodecane (1 w/w % Paranox 100)	880	0.8	26.3	0.5
50:50 water-in-dodecane (2 w/w % Paranox 100)	887	0.8	26.7	0.2

Table 3.7 Physical properties of the dodecane in the permeate. Temperature was kept at 23 °C and the accuracy of density meter and surface tension equipment was 1 kg/m^3 and -0.0004 N/m respectively.

Emulsion used		Membrane	Flux	surface	Standard	Interfacial	Standard	Water
phase ratio water/dodecane	Paranox 100 (w/w %)	and pore size	(l/h/m^2)	tension 10^{-3} (Nm^{-1})	deviation 10^{-3} (Nm^{-1})	tension 10^{-3} (Nm^{-1})	deviation 10^{-3} (Nm^{-1})	in the dodecane (ppm)
50:50	1	Supor (0.2 μm)	13	26.5	0.3	5.93	0.2	49.39
			26	26.5	0.3	5.92	0.2	71.13
			43.3	26.5	0.2	5.93	0.2	116.9
		HTTuffryn	13	26.4	0.4	5.93	0.1	228.4
			26	26.4	0	5.93	0.3	228.4
		Nylaflo	13	26.3	0.2	5.92	0.2	77.14
			26	26.3	0.1	5.92	0.3	-
50:50 *(8000 rpm)*	1	Supor (0.2 μm)	13	26.5	0.2	5.92	0.2	49.38
50:50	2		13	26.7	0.3	5.92	0.2	47.5
			26	26.5	0.3	5.92	0.1	95.32
20:80	0.5		13	26.7	0.3	7.21	0.1	42.36

minutes. After 60 minutes there was leakage of 16.1 (vol) % of the internal phase. The emulsification was carried out at room temperature or in an ice bath at temperatures below 5 °C (Table 3.8). There was a temperature rise during emulsification which resulted in the temperature of the final emulsion being considerably high for the emulsions that were not emulsified in an ice bath (Table 3.8). However, the temperature did not affect the stability of the emulsion.

The effect of surfactant concentration on stability is shown in Fig 3.24. At surfactant concentrations of 1 w/w % and 2 w/w % there was little leakage of the internal water phase. Breakage was high for the emulsion with 0.5 w/w % surfactant concentration, 16.1 (vol) % after 60 minutes of agitation. The temperature of the feed components before emulsification had little or no affect on the emulsion stability.

In Fig 3.25 the effect of homogeniser speed during emulsification on stability is shown. A lower emulsification speed produced an emulsion of greater stability but in both cases the emulsions were very stable. After 60 minutes the leakage of the internal phase to the external phase was less than 5 (vol) % for the emulsion at the higher emulsification speed (9500 rpm) and less than 3 % for the emulsion at the lower emulsification speed (8000 rpm).

At the start of stability tests the osmotic pressure in the internal phase was 35.3 atm and in the external phase it was zero. The osmotic pressure difference across the membrane was 35.3 atm in the direction of the internal phase. With such a large osmotic pressure difference emulsion swelling was expected. However, after 60 minutes the ratio of water in the external phase was approximately the same as the initial external water volume. There was a slight increase in volume in the external phase which was due to water leakage from the internal phase. Since the external volume remained the same there was no emulsion swelling by entrainment of the external phase.

Table 3.8 .Initial and final temperatures of emulsification ± 0.5 °C.

Phase (vol) ratio water:dodecane	Paranox 100 (w/w %)	homogeniser mixing speed (rpm)	Temperature before emulsification (°C)		Temperature after emulsification (°C)	
50:50	1	9500	2.8	23	13.2	29
50:50	1	8000	4.5	21	5.7	25
50:50	0.5	9500	4.5	22	16.7	36
50:50	2	9500	4.0	20	13.5	31.6
20:80	0.5	9500	4.0	21	20.0	34

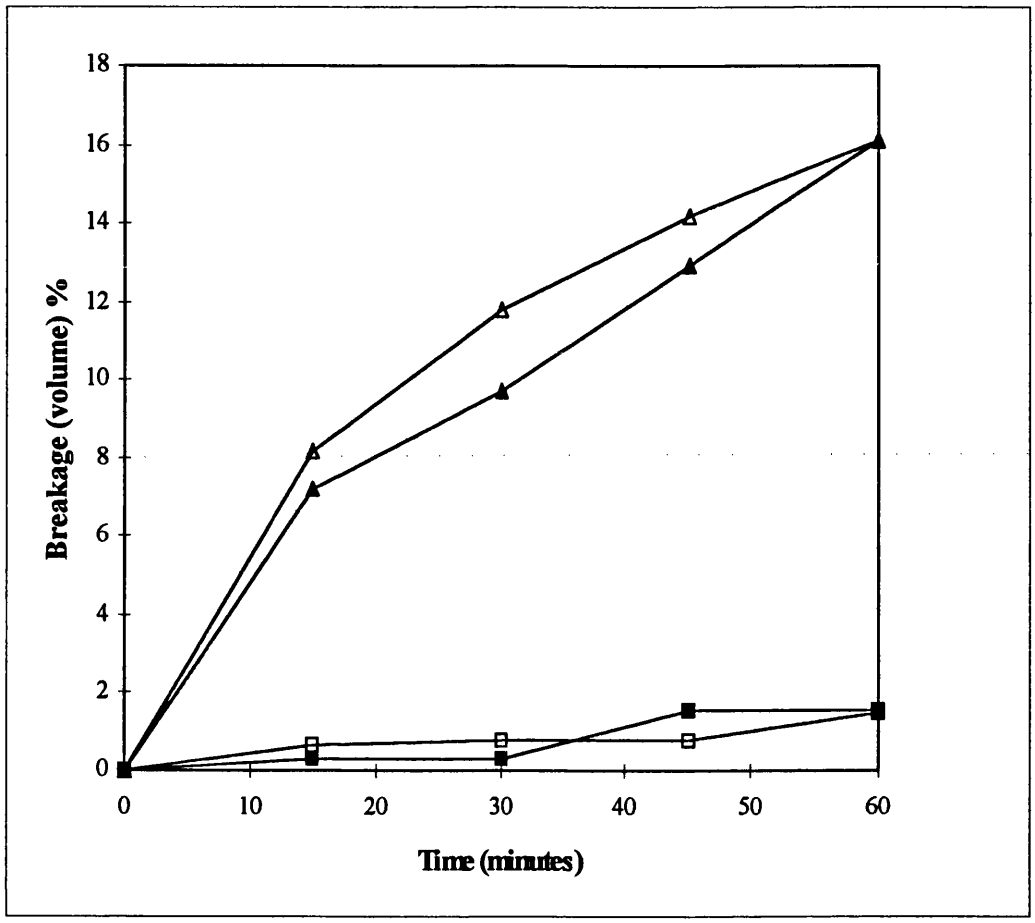

Figure 3.23 Effect of phase ratio on stability for a water-in-dodecane (0.5 w/w % Paranox 100). Homogenisation carried out in an ice bath: -Δ-50:50 phase ratio and -□- 20:80 phase ratio. Homogenisation carried out at room temperature: -▲- 50:50 phase ratio and -■- 20:80

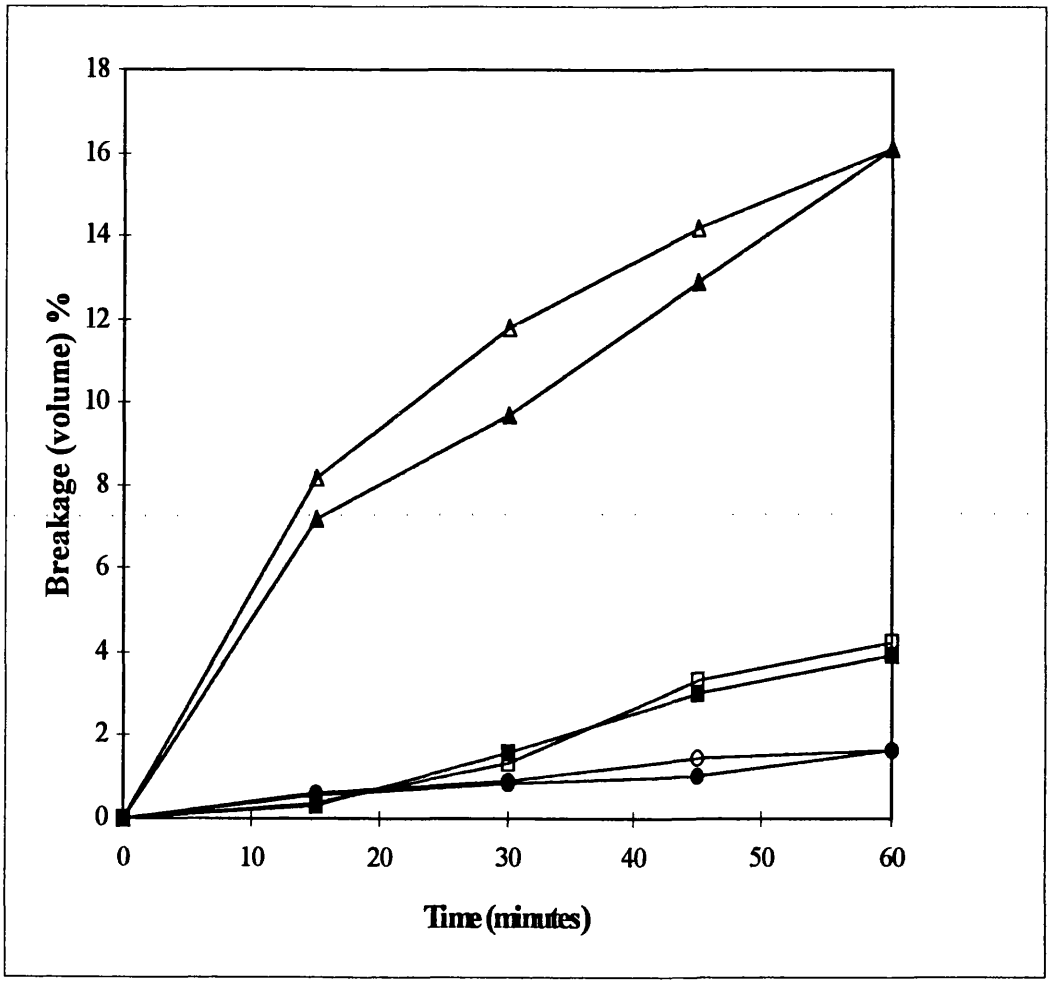

Figure 3.24 Effect of surfactant concentration on stability for a 50:50 water-in-dodecane emulsion. Homogenisation carried out in an ice bath: -Δ- 0.5 w/w % Paranox 100, -□- 1 w/w % Paranox 100 and -O- 2 w/w % Paranox 100. Homogenisation carried out at room temperature: -▲- 0.5 w/w % Paranox 100, 1 w/w %, -■- 1 w/w % Paranox 100 and -●- 2 w/w % Paranox 100.

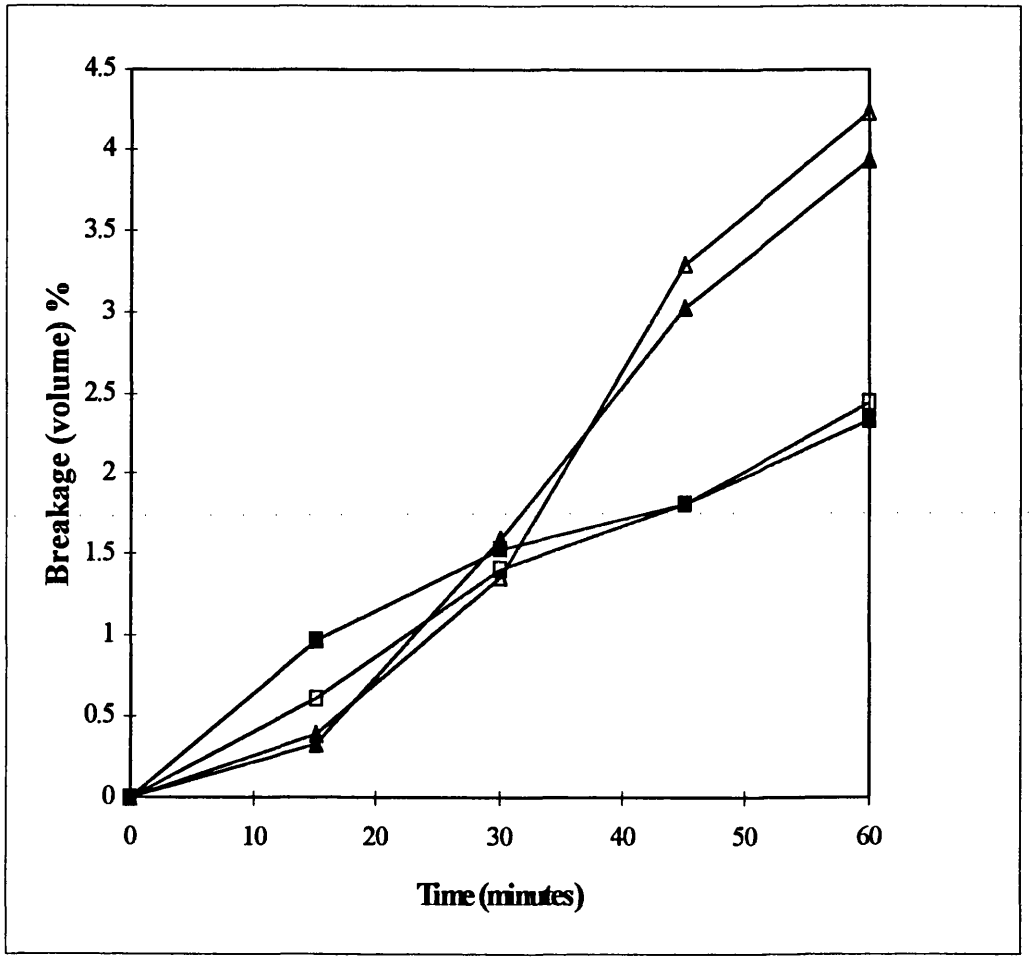

Figure 3.25 Effect of homogeniser speed on stability. Homogenisation carried out in an ice bath: -Δ- homogenisation speed 9500 rpm and -□- homogenisation speed 8000 rpm. Homogenisation carried out at room temperature: -▲- homogenisation speed 9500 rpm and -■-homogenisation speed 8000 rpm.

3.5 Discussion

The experimental results reported in Section 3.4 were for breakage of water-in-dodecane (stabilised by Paranox 100) emulsions using dead end microfiltration. The parameters which were varied were (1) size of the internal phase droplets (by changing the homogeniser speed, surfactant concentration and phase ratio of the internal to external phase), (2) flux, (3) membrane type and (4) membrane pore size. The physical properties (viscosity, surface/interfacial tension and density) of the emulsion and its constituents were measured to determine the breakage quality. Also the stability of emulsions of varying composition were measured using tracer techniques and only the emulsions where the stability was similar to liquid membrane emulsions were used in the breakage experiments. A detailed analysis of the filtration graphs is given in Chapter 4. In this section a general analysis is carried out.

3.5.1 Preliminary breakage

This method of emulsion breakage was fast and was used to give an indication of the feed flux needed to break the emulsion into dodecane and water. In all cases the emulsion separated into water and dodecane. However, at fluxes 57.1 $l/h/m^2$ and 142.8 $l/h/m^2$ (Fig 3.6 b and c) not all of the emulsion was demulsified. At these higher fluxes the emulsion passed through the membrane without the water droplets coalescing or the emulsion by-passed the membrane due to the 'o'- ring. At a flux of 28.6 $l/h/m^2$ the emulsion separated into water and dodecane. The hazy water phase was due to surfactant entrainment. The surfactant was not soluble in the water phase and the hazy appearance was an indication of this. Separation into two phases was possible at a flux of 28.6 $l/h/m^2$ and it was considered that at this flux and lower the emulsion breakage in the membrane rig would be possible (section 3.5.2).

3.5.2 Membrane filtration

Parameters such as flux, membrane material, membrane pore size and emulsion composition were varied. In some cases water and dodecane permeated through the membrane and in other cases only dodecane permeated through. At the end of each filtration experiment the content of the membrane module was analysed. A water soluble dye was added to the emulsion directly above the membrane (filtration cake) and if the dye dispersed this indicated that the water droplets had coalesced. The dye tests showed that in all cases (except for 20:80 water-in-dodecane stabilised with 0.5 w/w % Paranox 100) the emulsion was partially demulsified in the module.

3.5.2.1 Different hydrophilic membranes

In the case of membranes Supor 200, Httufryn, at all fluxes and Nylaflo at a flux of 13 l/h/m^2 (Figures 3.7-3.8) water was collected in the permeate and the demulsified emulsion filled half the module (concentrated emulsion). However, in the case of the Versapor membrane (Figure 3.9) water was not collected in the permeate and the demulsified emulsion filled half the module. The Nylaflo membrane at a flux of 26 l/h/m^2 was reported (Figure 3.7) to have no water collected in the permeate. However, water was collected in the permeate line but because there was a hold-up volume of 3.3 $\times 10^{-6}$ m^3 and the maximum pressure (6 bar) of the system was reached at 7.2 $\times 10^{-6}$ m^3 of the filtrate collected, only dodecane reached the permeate collection vessels at the end of the experiment.

For membranes where no water was collected in the permeate (Figure 3.9) it was considered that the pressure increased due to an increase in the concentrated emulsion until the maximum pressure of the system was reached 6 bar (3.3 $\times 10^{-6}$ to 4.2 $\times 10^{-6}$ m^3 of filtrate collected). The emulsion in the module depleted of dodecane by permeation through the membrane and this resulted in the emulsion gradually becoming concentrated until half the contents of the module was mainly partially broken droplets.

In the case of the membranes (Figures 3.7-3.8) where water was collected in the permeate, the pressure increased as described above until water permeated through the membrane. At this point there was an abrupt change in the slope (decrease). At the end of the filtration there was a similar amount of concentrated emulsion in the module as there was when no water permeated through the membrane (see above). The change in slope occurred at approximately the same volume (3.3×10^{-6} to 4.2×10^{-6} m^3 of filtrate collected). of filtrate collected in the permeate as for the experiments (Versapor, Figure 3.9) where no water was detected in the permeate. It was considered that the concentrated emulsion in the module did not increase very much after this change in slope which resulted in the final volume of concentrated emulsion in the module at the end of the experiment being similar to that found at the end of experiments where water did not permeate through the membrane. At the end of the filtration the percentage water in the permeate at a flux of 26 $l/h/m^2$ was greatest for the Supor 200 membrane (51 %) than the Httuffryn membrane (36 %). However, at the lower flux, 13 $l/h/m^2$ the water in the permeate was 44 % for all membranes (Figure 3.8).

Work by Tirmizi_et_al, 1996 showed that for water-in-tetradecane emulsions at surfactant concentrations 10, 20 kg/m^3 phase inversion was not observed. They also showed that the emulsions (water-in-tetradecane stabilised by ECA 5025) appeared thickened on the surface as the tetradecane content decreased due to permeation (concentrated emulsion layer). At lower concentration of surfactant 0.5 kg/m3, the phase inversion was complete and at constant flowrate a drop in pressure was recorded as the viscosity was reduced. For emulsions with surfactant concentration 2 kg/m^3 and higher there was partial phase inversion where the mixture on the membrane consisted of partly phase inverted emulsion and partly thickened emulsion.

3.5.2.2 Membrane pore size

The results in Figure 3.10 show that for a Supor membrane of various pore size 0.1-0.45 μm water only permeated through the membrane with the 0.2 μm pore size. At

the pore sizes either side there was no permeation. At 0.1 μm pore size the droplets were approx 60 times bigger than the pore and therefore this could have resulted in the water not permeating through. At 0.2 μm pore size the droplets were 30 times bigger and permeation was achieved but at 0.45 μm pore size where the droplets were only 15 times bigger there was no water permeation. At this higher pore size of the same material membrane it would have been expected that the water would have permeated through as dye tests showed that the emulsion was demulsified on the membrane surface.

All of the membranes in Figures 3.7 -3.10 were hydrophilic but made of different materials and initially it was considered that this could have prevented the permeation of the water phase for some of the membranes. However, the fact that no water permeated through a Supor membrane at 0.45 μm but water permeated through a Supor membrane of pore size 0.2 μm (emulsion demulsified on the surface of the membrane for both membranes) it was considered that the membrane structure could have prevented the water from permeating through. This is discussed in detail in Chapter 4.

3.5.2.3 Emulsion composition

The composition of the emulsion (Figure 3.12) was varied and it was determined that the higher the surfactant concentration (0.5-1 w/w %) the lower the phase separation. Water permeated through the membrane (Supor 200) but the water content at the end of filtration was much lower (20-22 %) for an emulsion with 2 w/w % Paranox 100 than for a similar emulsion with 1% Paranox 100 (44-51 %). The surfactant concentration was not the only difference between these two emulsions. The mean droplet size (Table 3.3) of the emulsions were 6.8 μm and 4 μm for surfactant concentrations 1 w/w % Paranox 100 and 2 w/w % Paranox 100 respectively. The viscosity (Newtonian) was similar for both emulsions (Table 3.4). It was considered that the droplet size and not the surfactant concentration was the result of the change

in the graphs in Figure 3.12. The proposed mechanism for this is explained in detail in Chapter 4.

When the homogeniser speed for emulsification (Figure 3.13) was kept at 8000 rpm for 13 minutes the resulting mean droplet size (12.1 μm) was much larger than for an emulsion emulsified at 8000 rpm for 3 minutes followed by 9500 rpm for 10 minutes (mean droplet size, 6.8 μm). It was considered that the larger droplet size aided phase separation (Chapter 4).

The pressure results for a 20:80 water-in-dodecane (0.5 w/w % Paranox 100) emulsion (Figure 3.14) were very different to all of the other experiments. The pressure initially increased in a similar manner to the emulsions of other compositions but at pressure 1bar there was a dramatic drop in pressure. No water permeated through the membrane during operation and when dye was added to the concentrated emulsion above the membrane the dye did not disperse (Table 3.3). It was considered that the dramatic drop in pressure was due to the cake forming rearranging itself into another packing structure, resulting in a decrease in the cakes specific resistance.

3.5.3 Emulsion breakage quality and physical properties of the emulsions.

Surface, interfacial tension and water content of the dodecane phase in the permeate were measured to determine if there was any change from the dodecane phase before emulsification. Also the water content of the dodecane phase was measured to determine the quality of phase separation. It was clear from the results in Table 3.7 that the amount of water in the permeate dodecane phase was below 300 ppm and this was considered low. The water content appeared to increase with flowrate, indicating that the higher fluxes (26 $l/h/m^2$ and 43.3 $l/h/m^2$) did not result in such a clear breakage separation.

3.5.3.1 Density

The density was measured to use in the surface and interfacial tension calculations. The measured density of dodecane, 0.761 g/cm^3 was slightly higher than values quoted in the literature, 0.749 g/cm^3. This was due to contamination of the dodecane. The measured density for 20:80 phase ratio emulsion, 0.826 g/cm^3 was considerably lower than the emulsions with 50:50 phase ratio, 0.886 g/cm^3. The reason for this was the presence of more dodecane in the 20:80 phase ratio emulsion that shifted the density of the emulsion closer to the density of dodecane. There were slight differences in the densities of the 50:50 phase ratio emulsions but these values were considered to be due to experimental error and not down to surfactant concentration.

3.5.3.2 Surface and interfacial tension

The surface tension (emulsion/air) of the emulsions of varying surfactant concentrations (0.5-2 w/w %) were found to be similar (26.5 $\times 10^{-3} \pm 0.2$ Nm^{-1}). These values were also similar to the value (26.3 $\times 10^{-3}$ Nm^{-1}) of the organic (dodecane + Paranox 100) phase and slightly less than the value (27.3 $\times 10^{-3}$ Nm^{-1}) of the surface tension of the pure dodecane phase (Tables 3.5-3.6). These values of surface tension indicated that the emulsion formed was water-in-dodecane. However, they did not show that the surfactant concentration was above the critical micelle concentration (cmc). Usually the surface tension of a solution of surfactant decreases steadily as the bulk concentration of surfactant is increased until the concentration reaches a value known as the cmc, above which the tension remains constant [Rosen, 1989]. The emulsions and the oil (dodecane + Paranox 100) phases all had the same surface tension but the reduction from the pure dodecane phase was only 1 $\times 10^{-3}$ Nm^{-1}. Where a reduction of about 20×10^{-3} Nm^{-1} [Rosen, 1989] was expected before the cmc was reached. Usually surface tension is measured between a solution of surfactant and air where the solution contains mainly polar molecules (aqueous phase) and the air consists of mainly nonpolar molecules. The surfactant migrates to the interface where the hydrophilic part remains in the polar phase and the hydrophobic

part of the surfactant sticks up into the air (nonpolar phase). Therefore, in an oil/surfactant solution the surface tension (oil/air) will not be reduced in the same manner. The oil phase and air are both nonpolar and therefore the surfactant will not be drawn to the interface (oil/air) since the surfactant has a greater affinity for the oil phase.

The interfacial tension measurements of the dodecane/water phase showed that the value reduced from 44.9 $\times 10^{-3}$ Nm^{-1} where there was no surfactant in the dodecane phase to 7.28 $\times 10^{-3}$ Nm^{-1} where the surfactant concentration was 0.5 w/w % Paranox 100. On further addition of surfactant (1-2 w/w %) the interfacial tension reduced to a constant value of 5.92 $\times 10^{-3} \pm 0.01$ Nm^{-1}. These results showed that on replacing the air surface with a water phase the surfactant was attracted to the interface (water/dodecane) where the hydrophilic part of the surfactant molecule stuck up out of the dodecane into the water phase (polar phase). At surfactant concentrations 1-2 w/w % the surfactant was considered to be above the cmc, indicated by the constant value with increase in surfactant concentration.

The surface tension results for reasons described above gave no indication of the surfactant concentration in the permeate (dodecane phase). However, the interfacial tension between water and dodecane was the same in the permeate as it was before emulsification. This did not indicate that no surfactant was absorbed on the membrane surface or lost to the water phase. What it did show was sufficient surfactant was not lost from the dodecane phase to bring the concentration below the cmc.

3.5.3.3 Droplet size distribution

In the treatment of water-in-dodecane emulsions the internal phase was increased from 20 vol % to 50 vol % and the surfactant concentration was increased from 0.5 w/w % to 2 w/w %. The results in Table 3.3 showed that the water/Paranox 100 ratio was important in determing the droplet size characteristics. At surfactant concentration of 0.5 w/w % and water volume 20 % the mean droplet size was 7.3

μm. However, when the water concentration was increased to 50 % the droplet size increased to 18.2 μm. At the higher water phase concentration the ratio of water to surfactant was in sufficient to completely surround the water droplets created by the homogeniser and therefore they coalesced producing an emulsion with a larger mean droplet size (larger droplets produce a smaller surface area and therefore less surfactant is required to stabilise the droplets). The 50 vol % emulsion showed evidence of instability and coalescence and stability tests (section 3.5.4) showed that the stability of this emulsion was unacceptable.

When an emulsion of 50 vol % water and Paranox 100 concentration of 1 w/w % was emulsified the mean droplet size was 6.8 μm which was approximately the mean droplet size of the emulsion with 20 vol % water and 0.5 w/w % Paranox 100.

The droplet size decreased with increasing Paranox 100 concentration. At concentration 2 w/w % Paranox 100 the mean droplet size was 4 μm, at concentration 1 w/w % Paranox 100 the mean droplet size was 6.8 μm and at concentration 0.5 w/w % Paranox 100 the mean droplet size was 18.2 μm. Again the affects of water/Paranox 100 ratio were apparent but these affects were not so great between 1 w/w % and 2 w/w %. The difference was greatest between 0.5 w/w % and 1 w/w %. This resulted from there being insufficient surfactant to stabilise the droplets produced by the homogeniser.

All the emulsions were prepared by adding the internal phase at 8000 rpm for 3 minutes followed by mixing for 10 minutes. The speed of the homogeniser during mixing was at 9500 rpm for four of the emulsions (Table 3.1). However one of the emulsions was homogenised during the mixing period at 8000 rpm and 9500 rpm. The higher stirring speed resulted in the droplets produced being of a smaller droplet size distribution where the mean droplet size was 6.8 μm. At the lower speed the mean droplet size was 12.1 μm which was approximately double the mean droplet size at the higher speed.

Published work by Lipp et al (1987) reported that the oil/surfactant ratio was important in determining the droplet size. They showed that the drop size distribution depended more on the ratio of oil to surfactant than on oil content.

3.5.3.4 Viscosity

For the two emulsions 50:50 water-in-dodecane at surfactant concentrations 1 w/w % and 2 w/w % the viscosity was the same at increasing shear rate (Figure 3.22) and therefore the emulsions were Newtonian fluids. The volume of the internal phase was not greater than 50 vol % so the droplets were not crowded and droplet size changes did not take affect (the viscosity would have resulted in non Newtonian behaviour). The reason the viscosity was much greater than the viscosity of the continuous phase was due to the high internal phase volume.

For low internal phase volumes the viscosity usually depends upon the viscosity of the continuous phase and at high internal phase volume the viscosity is influenced by (1) the volume ratio of the two phases, (2) particle size. The type of emulsion is not regarded as a major influence on viscosity despite the belief that o/w emulsions are thinner than w/o. This is only true as far as oils used are often more viscous than water. The viscosity of an emulsion is essentially the viscosity of the external phase as long as it represents more than half of the total volume [McKetta, 1983].

The viscosity of dodecane at 23°C is 1.42 mNs/m^2. The emulsion 20:80 water-in-dodecane contained more dodecane than water but the results in Figure 3.21 show that the emulsion viscosity was not the viscosity of the external phase. In fact the viscosity was much greater and increased with shear rate (non Newtonian). The results exhibited dilatancy which is frequently observed in fluids containing high levels of deflocculated solids but is not usually observed for emulsions (particles were treated as soft spheres since they are deformable)

Published work by Pal (1993) Investigated the rheological behaviour of water-in-oil emulsions where the water content varied from 0-75 vol % and the surfactant

concentration was varied between 1-50 wt %. He reported that for concentrated dispersions of soft spheres the viscosity increased with decrease in particle size. It was considered that this was due to several reasons (1) with decrease in droplet size the mean distance of separation between the droplets decreased leading to an increase in viscosity, (2) the thickness of the absorbed layer with respects to the droplet radius becomes important as the droplet size was decreased. He showed that for emulsions with phase ratio of >55 % the emulsions had a higher viscosity the smaller the droplet size. However, in all cases the non Newtonian behaviour was shear thinning. Work by Yan and Masliyah (1993) showed shear thickening in the emulsions they used but in their experiments solids were added to the emulsions and there was a transition from shear thinning to shear thickening. They showed that the higher the oil viscosity (dispersed phase) the more the oil droplets behaved like solid particles.

The two emulsions that showed shear thickening behaviour was the 20:80 water-in-dodecane emulsion (0.5 % Paranox 100) and the 50:50 water-in-dodecane (1 % Paranox 100) emulsion. In both cases the mean droplet size was greater than for the Newtonian emulsions. Therefore the droplets were not small enough to have behaved like solids. In light of this it was considered that the increase in viscosity with shear rate was due to the dispersed phase settling. However in most cases this would cause the viscosity to decrease. The mean droplet size for the emulsion described above was 7.3 μm (Table 3.3) which was not much greater than the mean droplet size (6.8 μm, Table 3.3) of the 50:50 water-in-dodecane emulsion which was Newtonian and showed no signs of the dispersed phase settling. If the dispersed phase was settling then the viscosity at low shear would be lower than the expected viscosity which was the case (Figure 3.21) as the shear rate increased the emulsion dispersed and therefore the viscosity increased. We see from Figure 3.21 that at shear rate 568 s^{-1} the viscosity becomes constant 11.5 mNs/m^2 and therefore the emulsion was fully dispersed.

The two emulsions that showed the viscosity increasing with shear rate (Figure 3.21) were not considered to be non Newtonian fluids. After emulsification it was observed that in the case of these two emulsions (Figure 3.21) sedimentation of the droplets

had occurred. This was not the case for the other two emulsions (Figure 3.22). All emulsions were fully dispersed before transfer to the viscometer. However, Setting up the viscometer and stabilising the temperature resulted in the emulsions in Figure 3.21 to sediment again before the viscometer was put into operation. Considering the filtration pressure results for these emulsions showed a similar trend to the filtration pressure results for the Newtonian emulsions it was concluded that the non-Newtonian behaviour was due to sedimentation.

3.5.4 Stability

Emulsions containing 0.5 w/w % Paranox 100 were more stable at a phase ratio of 20:80 than at 50:50 (Figure 3.23) this is because the lower water volume results in less surfactant being needed to stabilise each droplet. For the 50:50 emulsion there was not sufficient surfactant to stabilise all the droplets and therefore under shear the emulsion broke down. Both emulsions were homogenised at the same speed but resulted in different size distribution of droplets. The average droplet size in the 50:50 emulsion (18.2 μm) was much larger than in the 20:80 emulsion (7.3 μm). The larger droplets had a much smaller surface area for the surfactant to cover but due to the phase ratio being high there was not sufficient surfactant to keep the droplets stable and during agitation the droplets broke down

Emulsion stability improved with surfactant concentration (Figure 3.24). The mechanical strength of the surfactant increased with the amount present. In water-in-oil emulsions there is little or no charge and therefore no electrical barrier to prevent coalescence. It is mainly the mechanical strength of the interfacial film that prevents coalescence of the droplets. Therefore to survive under constant collision of other droplets the film must have great strength. When the system was subjected to shear these collisions were more frequent and to a greater intensity and therefore the strength of this interfacial film was of great importance. The more surfactant present the thicker this interface was [Rosen, 1989].

The effect of reducing the homogeniser speed (Figure 3.25) from 9500 rpm (mean droplet size 6.8 μm, Table 3.3) to 8000 rpm (mean droplet size 12.1μm, Table 3.3) was a much larger droplet size being formed. The larger droplet size emulsion under shear remained more stable. Again the larger droplet size emulsion had a smaller surface area to cover and therefore at surfactant concentration 1w/w % formed an interfacial film of greater mechanical strength.

Swelling of emulsions (increase of the internal phase volume) is caused by osmotic pressure differences or swelling attributed to the entrainment of the external water phase. Osmotic swelling occurs when there is a difference in osmotic pressures in the external and internal water phases and the surfactant acts as a water carrier. Since no swelling occurred Paranox 100 can be considered to not be a water carrier. Entrainment of the external phase into the emulsion accounts for swelling due to repeated coalescence and redispersion of the emulsion droplets during the dispersion operation. This usually occurs at high stirring speeds and can increase the internal phase up to 500 % [Ding and Xie, 1991]. A moderate stirring speed (170 rpm) was used and therefore prevented this happening.

The main mechanism of leakage was due to mechanical rupture of the microdroplets occurring when the emulsion droplets broke to form smaller emulsion droplets. The mechanical rupture of the micro and emulsion droplets were not two separate events. Leakage of the internal phase to the external phase can occur if the osmotic pressure difference across the two water phases is in the direction of the external phase. In all emulsion experiments the osmotic pressure difference was in the direction of the internal phase and therefore water leakage into the external phase by osmotic pressure was eliminated.

Shere and Cheng (1988) and Abou-Nemeh and Peterghem (1992) investigated the stability of liquid membrane emulsions using tracer techniques. They reported that the main mechanism of leakage was due to mechanical rupture of the internal phase droplets when the emulsion droplets were broken to form smaller emulsion droplets. Shere and Cheng (1988) used water-in-oil (stabilised with 1-4 w/w % span 80). The

oil phase (volume fraction 0.05-0.5) was Soltrol 220 (isoparaffinic solvent) and solvent extracted neutral oils S100N and S500N and the tracer used was 0.2 N sodium hydroxide. Abou-Nemeh and Peteghem (1992) used water-in-kerosene (stabilised with 3 vol % span 80) emulsions where the tracer metal was lithium (2000 ppm). They reported that ether-based and nitrogen containing surfactants should be used because of their better chemical stability and lower swelling properties.

Thien et al (1988) and Colinart et al (1984) reported that the stabilising ability of the surfactant varied greatly with the structure and amount of surfactant. They also reported that the hydration characteristics of the surfactant should be considered before being used in emulsion liquid membranes. Colinart et al (1984) showed that surfactants with certain chemical structures of HLB (hydrophilic - lipophilic balance) number swelled much more than others (HLB numbers between 2.5 -4.5 resulted in high swelling).

Paranox 100 is a nitrogen containing surfactant (Chapter 2) and this was considered the reason why the surfactant was not a water carrier. All of the emulsions tested except the 50:50 water-in-dodecane (0.5 % Paranox 100) emulsion were stable. The instability of the above emulsion was considered to be to high for the emulsion to be used in any of the filtration experiments. It is used later in the electrostatic coalescence experiments (Chapter 5).

Conclusions

* Hydrophilic membranes allow the permeation of both phases of an emulsion, provided phase inversion occurs and the membrane structure is fairly symmetrical. Phase inversion readily occurs in systems containing 1-2 w/w % Paranox 100, where the initial phase ratio is 50:50 (water/dodecane). Membranes such as HTTuffryn and Supor 200 are of the structure that result in permeation of both phases. With a Versapor membrane permeation of both phases was not possible.

* At the end of filtration the emulsion was demulsified in the module. Even in the cases where only dodecane permeated through the membrane the emulsion was demulsified in the module.

* The permeate dodecane phase contained as little as 49 ppm of water. Also the interfacial tension (oil/water) after one passage through the membrane was the same as the interfacial tension before emulsification.

CHAPTER 4

Comparison of Experimental Results and Constant Flux Equations to Predict the Mechanism of Breakage.

4.1 Introduction

Ideally a filter medium allows unrestricted passage of fluid through its pore structure while retaining the suspended particles. The particles may be retained entirely at the surface of the medium if all particles are larger than the pores and the pore structure of the medium consists of straight-through pores of equal size. However, the usual filtration system is much more complex. The filtration suspension may be well dispersed or partially or highly flocculated depending on the particle concentration and the chemical nature of the suspension particles. In most cases a wide range of effective particle size exists in the feed, either as a result of a wide particle size distribution or a condition of partial flocculation [Grace, 1954].

Blocking filtration mechanisms were first investigated by Hermans and Bredee (1935). Grace (1954) looked at the blocking mechanisms in relation to the performance of the filter media. He paid special attention to the standard blocking mechanism. Hermia (1982) looked at all four mechanisms: complete blocking, standard blocking, intermediate blocking and cake filtration, and formulated the mechanisms in the form of power law equations for Newtonian and non-Newtonian fluids.

All of the above authors investigated blocking laws for constant pressure. Grace (1954) was the only one who paid attention to constant flowrate blocking laws. However, important information was lost in lumping the parameters under one constant. Hlavacek and Bouchet (1993) developed constant flowrate blocking laws where the parameters were not combined.

Hermia (1982) suggested that the type of blocking depends on the operating conditions. The equation applicable to a given set of data depends on the size and concentration of the particles in the suspension to be filtered and the pore size of the membrane used.

Depending on the molecule to be deposited, blocking would start with standard blocking followed by complete blocking, intermediate blocking and the cake. If the molecule was greater than the pore the process would start with complete blocking followed by intermediate and finally cake filtration [Bowen et al, 1995]. If the particle is much greater than the pore size and the concentration is high>0.1% the process would start with standard followed by cake. It is fair to say that the higher the feed concentration the sooner the cake filtration mechanism will start. There would probably be some blocking even at high concentrations but it would only occur for the first few seconds.

The aim of this chapter is to describe the mechanism of emulsion breakage during dead-end microfiltration of concentrated water-in-dodecane emulsions through hydrophilic membranes in terms of the filtration laws and breakthrough pressures. The solutions are concentrated but Newtonian behaviour of the fluids was observed (Chapter 3).

4.2 Materials and Methods

4.2.1 Materials

All membranes used and other materials were outlined in Chapter 2. The method of emulsification has been described in Chapter 2. The emulsion composition and experimental conditions used are summarised in Table 4.1

4.2.2 Methods

4.2.2.1 Emulsification

4.2.2.2 Membrane module operation

The membrane module operation is outlined in Chapter 2

4.2.3 Analytical methods.

4.2.3.1 Dye tests

Methanol blue is a water soluble dye. It does not disperse in non polar solvents, it remains as black particles. In a polar solvent it disperses to give a bright blue colour. In an emulsion where water droplets, are surrounded by surfactant the addition of this dye will show no dispersion. In order to determine if the cake contains coalesced droplets and therefore emulsion breakage has occurred, the dye was introduced into the emulsion directly above the membrane.

4.3 Theory

In this section a description of each mechanism is given and all assumptions made are discussed.

4.3.1 Constant blocking laws.

There are assumptions that are specific to each of the blocking laws and they will be discussed in the individual sections.

The theory is based on the following assumptions. The membrane is considered to be a bundle of parallel straight pores with an initial radius r_0 and length L. The flow regime is assumed to be laminar and the flowrate Q is a constant equal to V/t (V is the

volumetric flowrate and t is the time). Each particle entering the membrane is captured.

Complete blocking and intermediate blocking mechanisms are based on pore plugging and therefore the relevant area used in the models is not the membrane area, A, but is the free pore area S_o. S_o can be related to the membrane area by porosity ε ($S_o = \varepsilon A$).

4.3.1.1 Complete blocking

Each particle coming into contact with the membrane plugs perfectly one pore. There is no superposition of particles. This is the complete blocking mechanism and Fig 4.1a is a schematic drawing of this mechanism. The reduction of the active surface due to blocking is proportional to the volume of the filtrate [Hlavacek and Bouchet, 1993].

$$S = eA - \sigma V \qquad \text{.....4.1}$$

Where e is the voidage, V is the filtrate volume and σ is the clogging coefficient and is a characteristic of the suspension.

The pressure drop is given by Darcy's Law [Hlavacek and Bouchet, 1993].

$$\Delta P = \frac{R_m \mu Q}{S} \qquad \text{....(4.2)}$$

Where R_m is the membrane resistance, μ is the viscosity of the filtrate, Q is the flowrate and S is the free pore surface.

By combining equation 4.1 and 4.2 , we find:

$$\frac{1}{\Delta P} = \frac{1}{\Delta P_0} - \frac{\sigma V}{R_m \mu Q} \qquad ...(4.3)$$

$$\Delta P_0 = \frac{R_m \mu Q}{eA}. \qquad ...(4.4)$$

There is an assumption implicit in Equation 4.1. The volume of particles projected on the filter membrane is σV^* and in equation 4.1

$$\left(\frac{V^* \gamma_S s}{\gamma_0}\right)\left(\frac{6}{\pi d^3}\right)\left(\frac{\pi d^2}{4\Psi}\right) = \sigma V^* = \sigma V \qquad ....(4.5)$$

Where V^* is the slurry volume

Equation 4.5 is only true for dilute solutions where $s < 0.1$ %, ie the filtrate and slurry volume are almost the same. For a concentrated system the filtrate volume at time t will fall short of the slurry volume by the percentage volume of solids in the slurry.

volume of slurry - volume of particles in slurry = volume of filtrate

$$V^* - V^* s_v = V \qquad ...(4.6)$$

$$V^*(1-s_v) = V \qquad ...(4.7)$$

$$V^* = V/(1-s_v) \qquad ...(4.8)$$

Thus a combination of equations 4.3-4.5 and 4.8 yields:

$$\frac{1}{\Delta P} = \frac{1}{\Delta P_0} - \frac{\sigma V}{R_m \mu Q(1-s_v)} \qquad ...(4.9)$$

4.3.1.2 Intermediate blocking

Each particle has the ability to deposit on any part of the membrane surface or any other particle. It means that superimposition is possible in this case. It is assumed that any particle depositing on a pore plugs it completely. The decrease in free surface dS is proportional to the free surface S. This reduction of free surface of pores is identical to the probability for a pore to get blocked (Figure 4.1b).

Combining Hermia's equation with the correction factor (Equation 4.8) for concentrated solutions developed here for Equation 4.3 yields:

$$\frac{dS}{dV} = -\sigma \frac{S}{eA(1-s_v)} \qquad .....(4.10)$$

By integrating Equation 4.10 we obtain:

$$S = eA \exp \frac{-\sigma V}{eA(1-s_v)} \qquad ...(4.11)$$

Combining Equations 4.2, 4.4 and 4.11 yields:

$$\Delta P = \Delta P_0 \exp \frac{\sigma V}{eA(1-s_v)} \qquad ....(4.12)$$

4.3.1.3 Standard blocking

Here the increase of the hydraulic resistance is the result of constant deposition of particles inside the pores along their complete length. For standard blocking to occur the particles need to be much smaller than the pores [Bowen et al, 1995]. During the time interval dt, the volume of filtered suspension is dV=Qdt (Figure 4.1c).

The free volume of N pores (the initial pore volume less the volume of deposited particles) is expressed by [Hlavacek and Bouchet, 1993]:

$$-N(2\pi r\, dr)L = CdV \qquad ...(4.13)$$

Where C is the volume of deposit per unit volume of filtered suspension. By integrating equation 4.13 we get:

$$r^2 = r_0^2 - \frac{CV}{\pi NL} \qquad ....(4.14)$$

The Hagen-Poiseuille law relates Q to the free pore radius by [Hlavacek and Bouchet, 1993:

$$Q = N\frac{\pi r^4 \Delta P}{8\mu L} \qquad ....(4.15)$$

Substituting equation 4.14 into equation 4.15 gives:

$$\frac{1}{\sqrt{\Delta P}} = \frac{1}{\sqrt{\Delta P_0}} - \frac{CV}{\sqrt{8\pi N\mu L^3 Q}} \qquad ....(4.16)$$

The porosity ε_0 is related to the radii R_0 by the following equation[Foley et al, 1995].

$$\varepsilon_0 = \frac{N\pi r_0^2}{A} \qquad ...(4.17)$$

Assuming that the flow in the pores is laminar, then

$$\frac{Q}{A} = \frac{\varepsilon_0 r_0^2 \Delta P}{8\mu L} \qquad ...(4.18)$$

Combining Equations 4.17 and 4.18 yields:

$$\frac{Q}{A} = \frac{\varepsilon_0^2 A \Delta P_0}{8\mu L N \pi} \qquad ...(4.19)$$

Rearranging Equation 4.19.

$$Q 8\mu L N \pi = \varepsilon_0^2 A^2 \Delta P_0 \qquad ...(4.20)$$

Combining Equation 4.16 and 4.20 yields:

$$\frac{1}{\sqrt{\Delta P}} = \frac{1}{\sqrt{\Delta P_0}} - \frac{CV}{\varepsilon_0 A L \sqrt{\Delta P_0}} \qquad ...(4.21)$$

4.3.2 Cake filtration law

Particles locate on other particles that have already arrived and blocked some of the pores. There is no room for these new particles to be in direct contact with the membrane so further obstruction of the membrane area is not possible. This is called cake filtration [Bowen et al, 1995].

The batch filtration starts with a clean membrane on which a cake layer of rejected particles accumulates with time as the filtration proceeds. When a suspension contains particles too large to enter the membrane pores then the surface filtration mechanism of sieving occurs. The retained particles accumulate on the membrane surface in a growing cake layer. The growing cake layer provides an additional increasing resistance to filtration so that in the case of constant pressure the permeate flux declines with time and for constant flux the pressure increases with time. For unstirred dead-end filtration, in which the fluid motion is normal to the membrane surface, the cake continues to grow until the process is stopped. When the sieving mechanism is dominant, a cake layer of rejected particles usually forms on the membrane surface as shown in Figure 4.1d.

The cake layer and membrane may be considered as two resistances in series and the pressure driven permeate flux is then described by Darcy's Law [Belfort,et al, 1994].

$$Q = \frac{A\Delta P}{\mu(R_m + \alpha M)} \qquad \text{.....(4.22)}$$

Where Q is the filtrate flow rate, μ is the filtrate viscosity, R_m is the membrane resistance, α is the specific cake resistance, ΔP is the pressure difference, A is the active membrane area and M is the cake mass per unit membrane area (M=W/A where W is the mass of cake).

Mass balance on the cake :

The mass of cake is equal to the mass of wet cake. since the cake is the slurry minus the mass of filtrate. Therefore the particles plus the remaining liquid is the cake:

Total mass of cake = mass of wet cake = W ..(4.23)

$$\frac{W}{W_D} = m \qquad \text{..(4.24)}$$

Where: W_D is the mass of dry cake, W is the mass of cake or wet cake and m is the mass ratio of wet to dry cake.

Rearranging Equation 4.24 gives [Hermia, 1982]:

mass of wet cake = $W = m \times W_D$ ..(4.25)

Also:

W_D = mass of solids in the slurry = (mass of slurry)s ..(4.26)

Where: s is the mass fraction of solids in the slurry.

W_D =(W + mass of filtrate)s = $(W + V\rho_f) \times s$ ..(4.27)

Where: V is the filtrate volume and ρ_f is the filtrate density.

Substituting Equation 4.27 into Equation 4.25 gives:

$W = ms(W + V\rho_f) = msW + msV\rho_f$ ..(4.28)

Rearranging Equation 4.28 yields [Hermia, 1982]:

$$W = \frac{ms\rho_f}{(1-ms)}V \quad ..(4.29)$$

It is clear from Equation 4.22 that at constant flux the increase in pressure is due to a combination of cake formation (increasing M) and membrane fouling (increasing R_m mostly before cake forms). Increasing R_m would be the result of blocking of the membrane pores by deposition or adsorption of the suspension components on to the membrane surface or the walls of the membrane pores (Foley et al, 1995).

From equation 4.22 M=W/A and by substituting for W with Equation 4.29 yields:

$$M = \frac{ms\rho_f}{(1-ms)A}V \quad ....(4.30)$$

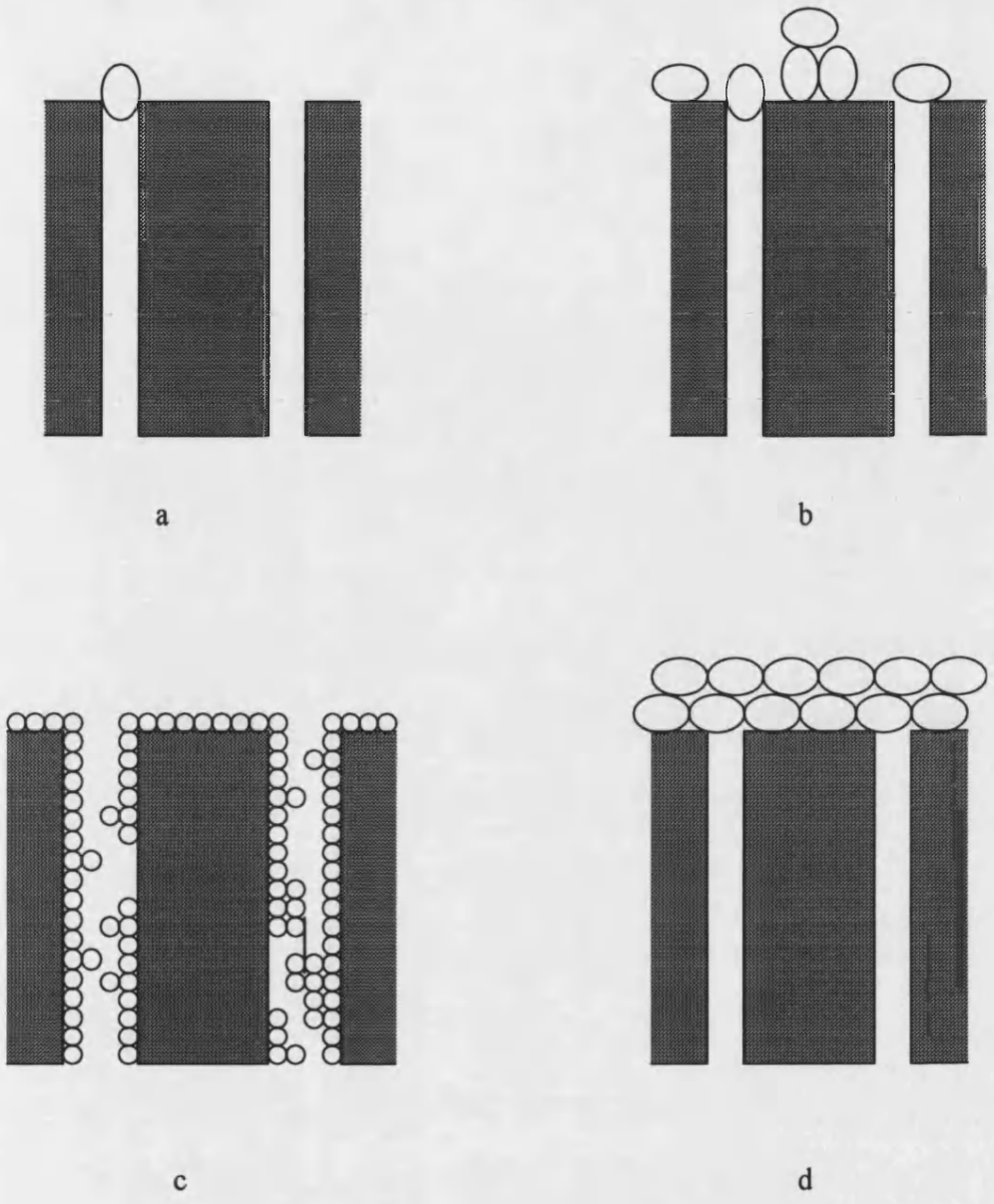

Fig 4.1 Schematic drawing of the fouling mechanisms. (a) Complete blocking, (b) Intermediate blocking, (c) Standard blocking and (d) Cake filtration.

Substituting Equation 4.30 into Equation 4.22 gives:

$$\Delta P = \frac{Q_0 \mu}{A}\left(R_m + \frac{\alpha \rho_f ms}{(1-ms)A}V\right) \qquad ..(4.31)$$

For constant flowrate $Q=Q_0$

$$\Delta P = \frac{Q_0 \mu R_m}{A}\left(1 + \frac{\alpha \rho_f ms}{(1-ms)R_m A}V\right) \qquad ...(4.32)$$

Substituting $\Delta P_0 = Q_0 \mu R_m / A$ into Equation 4.32 gives:

$$\Delta P = \Delta P_0\left(1 + \frac{\alpha \rho_f ms}{(1-ms)R_m A}V\right) \qquad ...(4.33)$$

Substitute for R_m in Equation 4.33

$$\Delta P = \Delta P_0 + K_C Q_0 V \qquad ...(4.34)$$

$$\text{Where } K_c = \frac{\mu \alpha}{A^2}\frac{\rho_f ms}{(1-ms)} \qquad ...(4.35)$$

Cake specific resistance (α):

Filter cakes are divided into two classes, incompressible cakes and compressible cakes. In the case of incompressible cake, the resistance to flow of a given volume of cake is not affected by either the pressure difference across the cake or by the rate of deposition of the material. In the case of a compressible cake increase of the pressure difference or the rate of flow causes the formation of a denser cake with a higher resistance. For incompressible cakes e in Equation 4.36 can be taken as constant.

Flow through packed beds under laminar conditions can be described by the "Carmen-Kozeny Equation" [Kirk-Othmer, 1994] as follows:

$$\frac{Q}{A} = \frac{\Delta P}{\mu L} \frac{e^3}{5(1-e)^2 S_A^2} \qquad ...(4.36)$$

Where Q is the flowrate, A is the active membrane area, L is the depth of the membrane, ΔP is the pressure difference, e is the voidage of the bed (porosity) and S_A is the volume specific surface of the bed and μ is the liquid viscosity.

The numerical constant in equation 4.36 is dependent upon the particle shape and voidage; it can be assumed to be 5 for low voidage. Equation 4.36 works reasonably well for incompressible cakes over a narrow voidage range. However, its use for compressible cakes is limited.

Darcy's law combines the constants in the last term of Equation 4.36 into one factor K, known as the permeability of the bed ie,

$$K = \frac{e^3}{5(1-e)^2 S_A^2} \qquad ...(4.37)$$

Where K is constant for compressible cakes (property of the particles forming the cake and is constant for a given material).

$$\alpha = \frac{5(1-e)^2 S_A^2}{e^3} \qquad ..(4.38)$$

Where: α is the specific cake resistance.

It is often convenient to define

$$\alpha = \frac{5(1-e)^2 S_A^2}{e^3 \gamma_s (1-e)} = \frac{5(1-e) S_A^2}{e^3 \gamma_s} \qquad ..(4.39)$$

Where γ_s is the density of the dispersed phase and 1-e is the solids volume fraction of the cake [Belfort et al, 1994].

Volume specific surface (S_A):

S_A is the specific surface area of the particles and is the surface area of a particle divided by its volume. For a sphere

$$S_A = \frac{\pi d^2}{\pi (d^3/6)} = \frac{6}{d} \qquad ...(4.40)$$

For non-spherical particles the equation can be written as

$$S_A = \frac{6}{d_p \Psi} \qquad ...(4.41)$$

Where d_p is the equivalent diameter of the particles and ψ is the shape factor (sphericity factor) [Howell et al, 1993]. ψ = surface area of a sphere of same volume of the particle/ surface area of the particle

Shape change from spherical to polyhedral

If the droplets are not spherical then the ψ value in Equation 4.41 will not be 1. When the droplets in an emulsion are squeesed together they change shape with a corresponding increase in surface area from a sphere to a polyhedral. For simplicity it is assumed that the droplets form polyhedrals of the form dodecahedrron. There are 12 faces and the profile is a pentagon.

Total area of the dodecahedron=20.65 a^2 ...(4.42)

Total volume of the dodecahedron=2.18 a^3 ...(4.43)

The volume of droplets in the cake is increased by squeezing out some of the dodecane phase. This is the same as saying that the percentage increase in the total volume of the spheres occupied is achieved without changing the total volume of the spheres or each sphere [Lissant, 1966].

Volume of a sphere = 4/3 π $(d/2)^3$ ...(4.44)

Combining Equations 4.43 and 4.44 yields:

Total volume of the dodecahedron=2.18 a^3=4/3 π $(d/2)^3$ ...(4.45)

Equation 4.45 allows for side a of the dodecahedron to be calculated and hence the surface area can be calculated from Equation 4.42. Also ψ in Equation 4.41 can be calculated ($\Psi = \frac{4\pi d^2}{20.65a^2}$).

Assumptions:

- All the solids in the slurry are retained by the membrane, no penetration of solids into the filtration medium (see Equations 4.23- 4.29) [Foley et al, 1995].

- The concept of the specific resistance used in Equation 4.22 is based on the following assumptions:

    - Flow is one dimensional
    - Growth of cake is unrestricted

- Only solid and liquid phases are present
- The feed is sufficiently dilute such that the solids are freely suspended
- The filtrate is free of solids
- Pressure losses in the feed and filtrate piping are negligible
- Flow is laminar (Laminar flow is a valid assumption in most cake formation operations of practical interest [McKetta, 1983].

A summary of constant flowrate filtration laws with their linearised form is given in Table 4.1.

4.3.3 Coefficient of linear regression

Experimental curves can be tested with the linearised equations described above. The coefficient of linear regression R^2 is calculated for each Law to find which is the most applicable and gives the best fit [Hlavacek and Bouchetl, 1993].

$$R^2 = 1 - \frac{\sum_{i=1}^{k}(y_i - y_i^*)}{\sum_{i=1}^{k}(y_i - y_i^m)} \qquad \text{....4.46}$$

Where k is the number of experimental points, yi is the ith experimental point, y_i*is the theoretical value and y_i^m is the mean value.

Table 4.1 Summary of constant flowrate filtration laws with their linearised form

Law	Equation	Linearised form
Cake	$\Delta P = \Delta P_0\left(1+\frac{\alpha\rho_f ms}{(1-ms)R_m A}V\right)$	$\Delta P = \Delta P_0 + K_C Q_0 V$
Standard blocking	$\frac{1}{\sqrt{\Delta P}} = \frac{1}{\sqrt{\Delta P_0}} - \frac{CV}{\varepsilon_0 AL\sqrt{\Delta P_0}}$	$\frac{1}{\sqrt{\Delta P}} = \frac{1}{\sqrt{\Delta P_0}} - K_s V$
Complete blocking	$\frac{1}{\Delta P} = \frac{1}{\Delta P_0} - \frac{\sigma V}{R_m \mu Q(1-s_v)}$	$\frac{1}{\Delta P} = \frac{1}{\Delta P_0} - K_b V$
Intermediate blocking	$Ln\Delta P = Ln\Delta P_0 + \frac{\sigma V}{eA(1-s_v)}$	$Ln\Delta P = Ln\Delta P_0 + K_i V$

4.3.4 Internal Pressure

The droplet internal pressure is defined by the following equation:

$\pi_i = 4\Upsilon/d$ ....(4.47)

Where π_I is the internal pressure of the droplet, Υ is the interfacial tension between water and dodecane and d is the diameter of the water droplet.

4.4 Results

4.4.1 Data Reduction

The blocking filtration and cake filtration equations given in Table 4.1 are all linearised equations. To determine the appropriate equation or equations to fit a given set of experimental data three steps were carried out. Figures 4.2 and 4.3 show a flowsheet of the steps for a 50:50 water-in-dodecane (1 w/w % Paranox 100) emulsion homogenised at 8000 rpm. All graphs, equations and Tables of the data used are indicated on the flowsheet. All other experimental data was analysed in a similar way to that reported in Figures 4.2 and 4.3.

Step 1 Filtration laws applied to entire data

The filtration laws were applied to the entire data to determine if one law would fit.

Step 2 Filtration laws applied to regions of the data

If one law did not fit all the data (step 1) the filtration laws were applied to regions of the experimental data where a linearised section for the law existed. As all the laws were linearised equations, calculation of the coefficient of linear regression was considered the best method of deciding if a law was to be rejected. By applying the law to different regions the number of data points and where the data points were taken partly predetermined the coefficient of linear regression and therefore there was a real chance of misrepresentation. As there was no abrupt change from one mechanism to another (more of a gradual shift) [Wei-Ming et al, 1997] it was uncertain where the mechanisms changed from one filtration law to another. To limit the error extra data was taken either side of the linear section where the law was applied. Next the coefficient of linear regression was calculated. The extra data was gradually reduced until the coefficient of linear regression was as close to, $R^2=1$ as possible. At the end of the analysis if the coefficient of linear regression, for any of

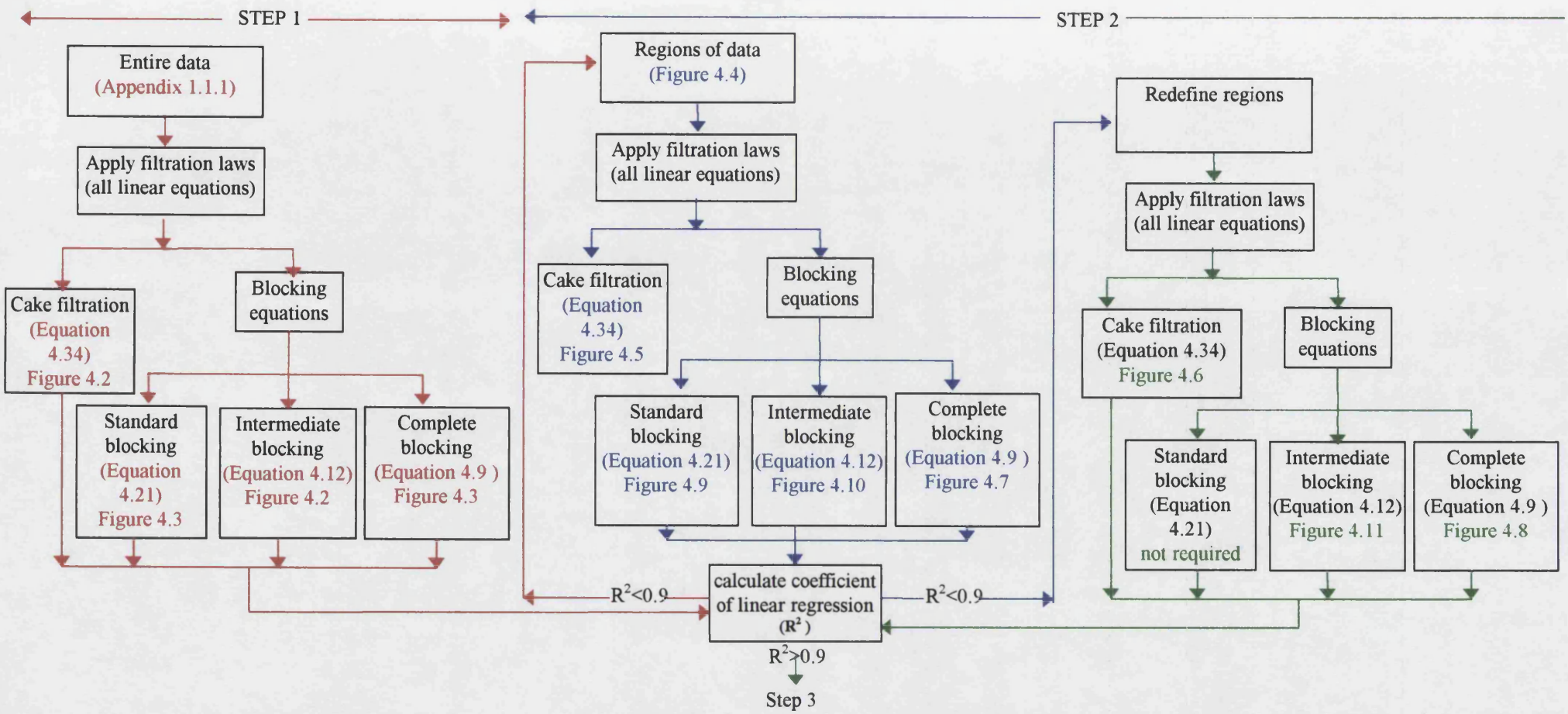

Figure 4.2 flowchart of steps 1-2 for a 50:50 water-in-dodecane (stabilised with 1 w/w % Paranox 100) emulsion homogenised at 8000 rpm for 13 minutes and a Supor 200 membrane at a flux of 13 l/h/m^2.

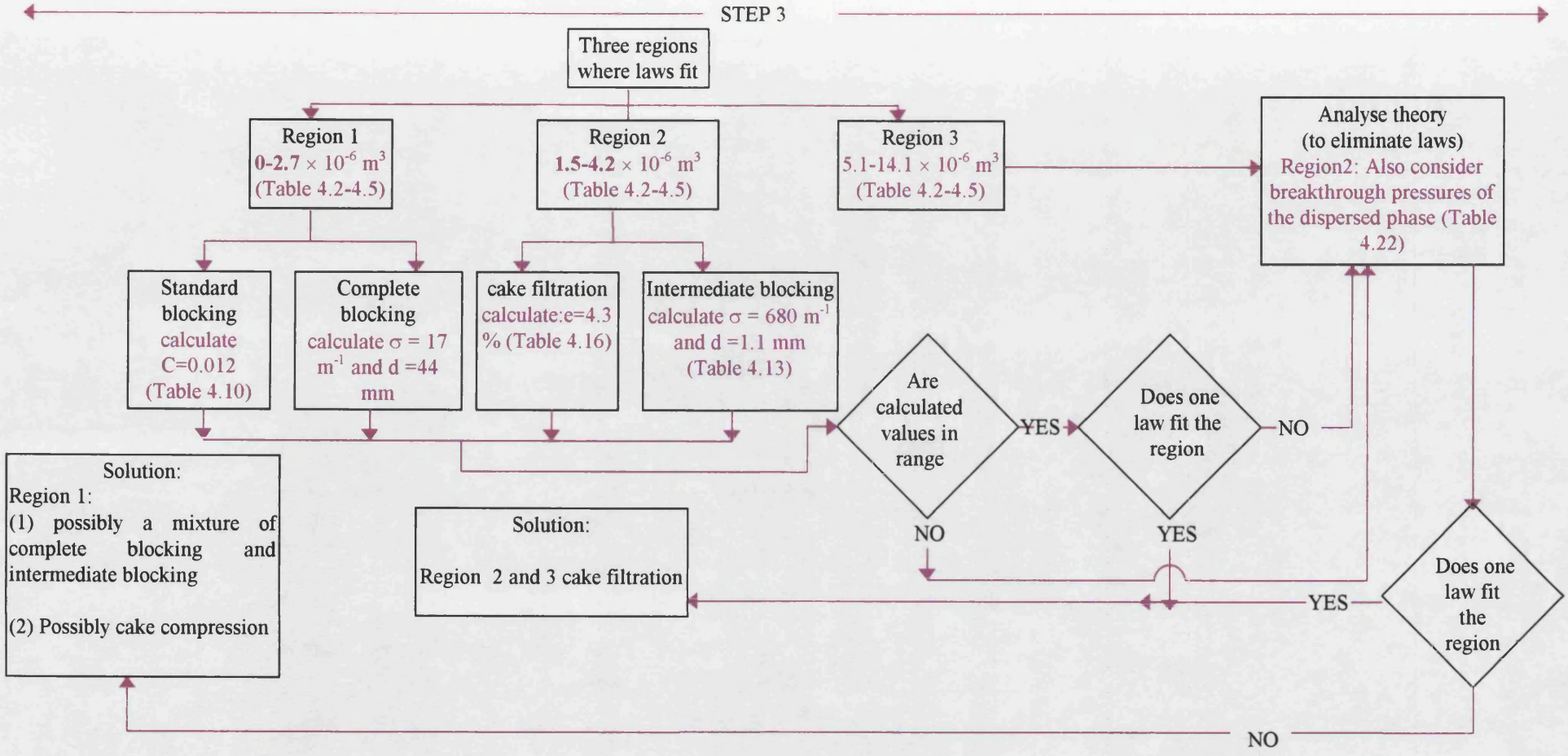

Figure 4.3 flowchart of step 3 for a 50:50 water-in-dodecane (stabilised with 1 w/w % Paranox 100) emulsion homogenised at 8000 rpm for 13 minutes and a Supor 200 membrane at a flux of 13 l/h/m^2.

the filtration laws applied, was R^2 >0.9 then the corresponding law or laws were considered to be the possible mechanism that applied to the region investigated.

Step 3 Analysis of the constants

If more than one model fits a set of data (R^2>0.9) or there was an overlap of data for more than one law (step 2) then analysis of the gradient of the linear section for each law was calculated. Also Hermia (1982) indicated that the type of equation applicable to a given system depends on the operating conditions and therefore, taking the theory into account and calculating the constants was necessary in order to determine which law applied to a given set of data.

4.4.2 Data Analysis

This section shows an example of the step by step analysis of the data (following the procedure outlined in section 4.4.1) for a 50:50 water-in-dodecane (1 w/w % Paranox 100) emulsion homogenised at 8000 rpm. Also a summary of a similar analysis carried out on the remaining experimental runs is reported.

4.4.2.1 Step 1: filtration laws applied to the entire data

Figures 4.4 and 4.5 show the graphs where the filtration laws were applied to the entire data, from the mean of three experiments, for an emulsion 50:50 water-in-dodecane (1 w/w % Paranox 100) homogenised at 8000 rpm . Figure 4.4 is for the cake filtration law and intermediate blocking law and Figure 4.5 for complete blocking law and standard blocking law. All of the filtration laws defined in the theory section were for straight lines and therefore it is clear that one law did not fit all the data.

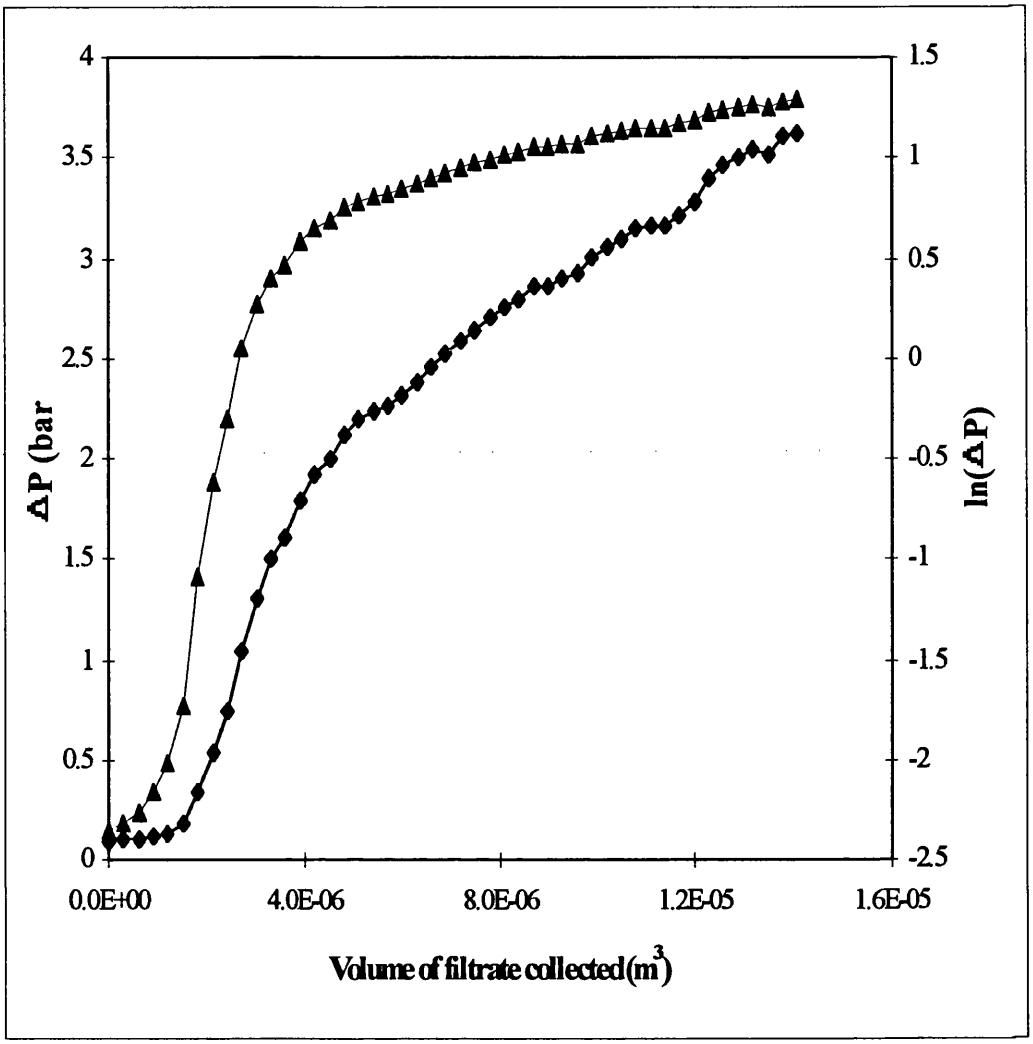

Figure 4.4 Cake filtration and intermediate blocking analysis for 50:50 water-in-dodecane (1 w/w % Paranox 100) homogenised at 8000 rpm for 13 minutes using a Supor 200 membrane at a flux of 13 l/h/m^2. -■- cake filtration law. -▲- intermediate blocking law.

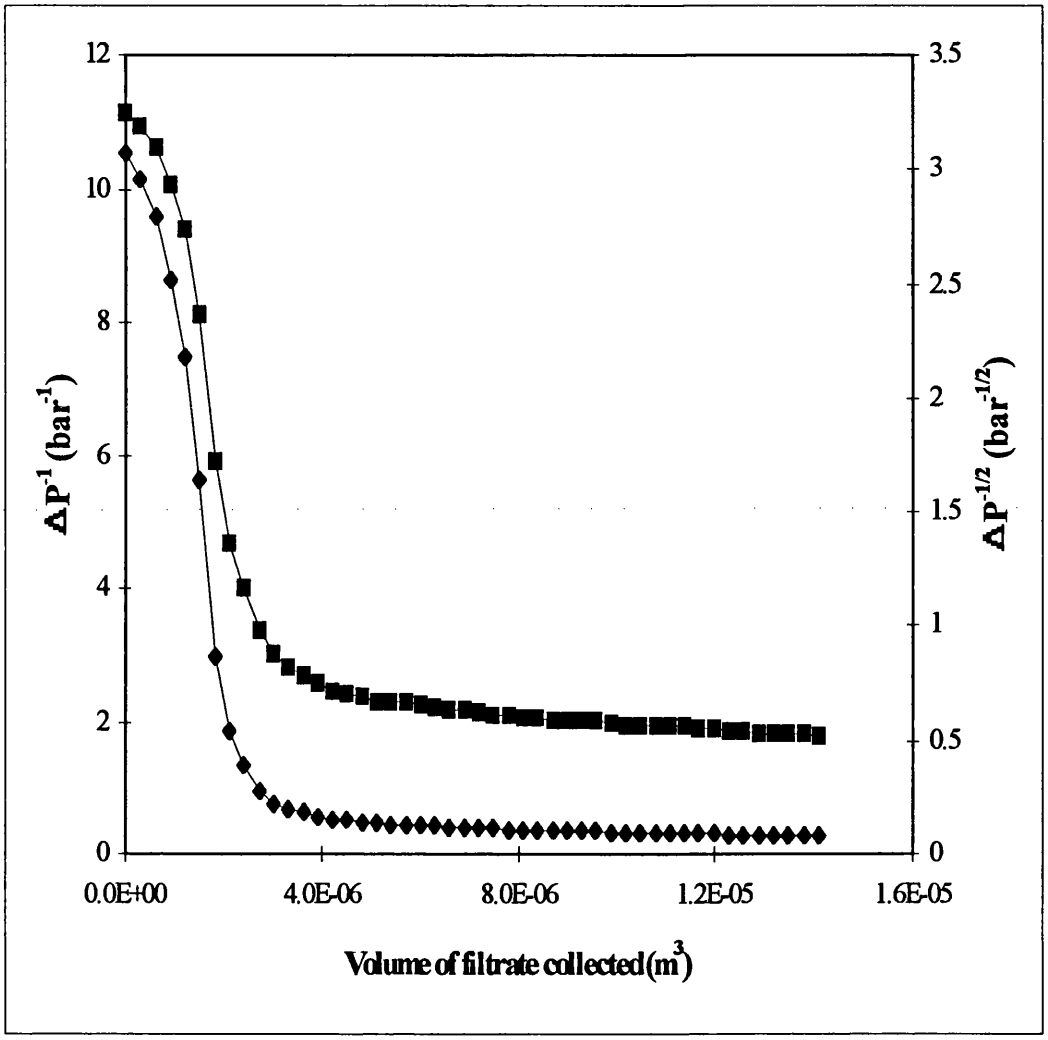

Figure 4.5 complete blocking and standard blocking analysis for 50:50 water-in-dodecane (1 w/w % Paranox 100) homogenised at 8000 rpm for 13 minutes using a Supor 200 membrane at a flux of 13 l/h/m^2. -■- standard blocking law and -◆- Complete blocking law.

4.4.2.2 Step 2: filtration laws applied to regions of the data

The regions referred to in this section were based on the change of shape of the graph when the individual laws were applied to the entire data (Figures 4.4 and 4.5). These regions are illustrated in Figure 4.6 for each law. For cake filtration and intermediate blocking there were three regions where a linearised section existed. For standard blocking and complete blocking there were two regions where a linearised section existed.

Cake filtration

Figures 4.7 and 4.8 show the cake filtration law applied to regions of the experimental data shown in Figure 4.4. The graph changed shape in three regions (Figure 4.6a). However, it was not clear where these regions started and finished and therefore in Figure 4.7 the regions were overlapped to avoid misrepresentation. Region 1: 0-1.5× 10^{-6} m^3, region 2: 1.5 × 10^{-6} - 5.1 × 10^{-6} m^3 and region 3: 3-14.1 × 10^{-6} m^3 of filtrate collected. The cake filtration law gave a reasonable fit in two of the regions and a poor fit in region 1 (indicated by coefficients of linear regression on the graph). In Figure 4.8 the regions where the filtration laws were applied were redefined and the cake filtration law gave an excellent fit (R^2 = 0.99) in regions 2 and 3 (1.5 ×10^{-6} -4.2 × 10^{-6} m^3 of filtrate collected and 3: 4.5-14.1 10^{-6} m^3 of filtrate collected respectively). However, region 1 still gave a poor fit (R^2=0.90).

Complete blocking

Figures 4.9 and 4.10 show the complete blocking law applied to regions of the experimental data shown in Figure 4.5. The graph changed shape in two regions (Figure 4.6b). However, it was not clear where these regions started and finished and therefore in Figure 4.9 the regions were overlapped to avoid misrepresentation. Region 1: 0-2.4× 10^{-6} m^3 of filtrate collected and region 2: 3 × 10^{-6} -14.1 × 10^{-6} m^3 of filtrate collected. The complete blocking law gave a poor fit in region 2 and a

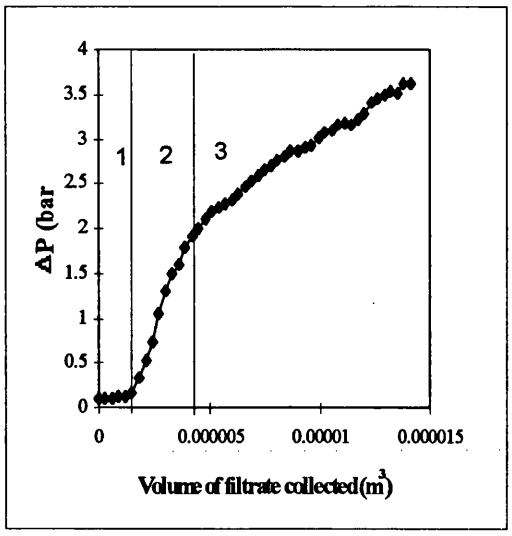

(a)

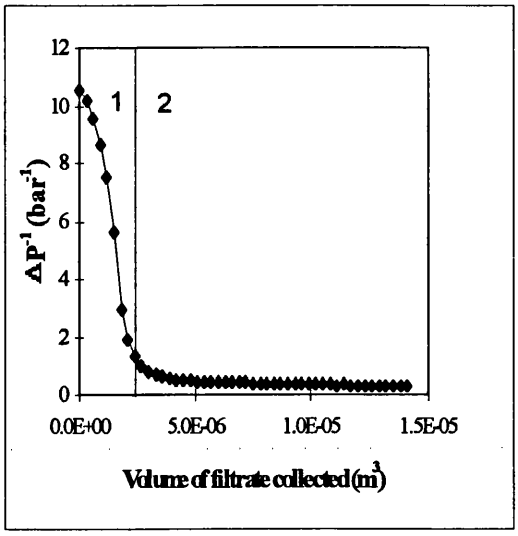

(b)

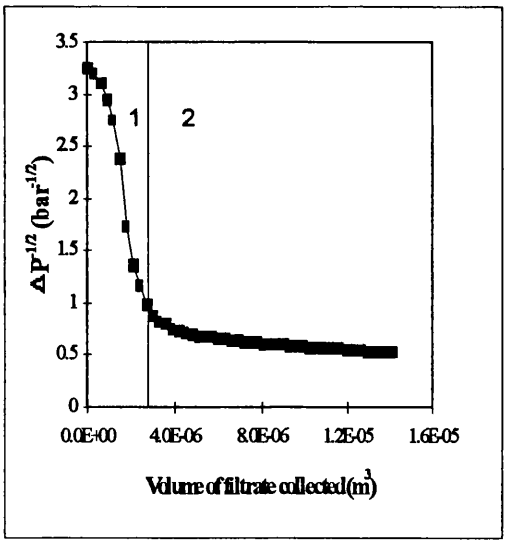

(c)

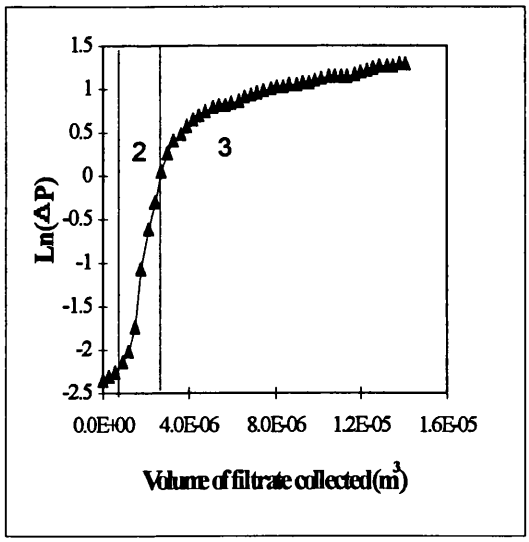

(d)

Fig 4.6 Linear regions (1, 2 and 3) for (a) Cake filtration law, (b) Complete blocking law, (c) Standard blocking law and (d) Intermediate blocking law.

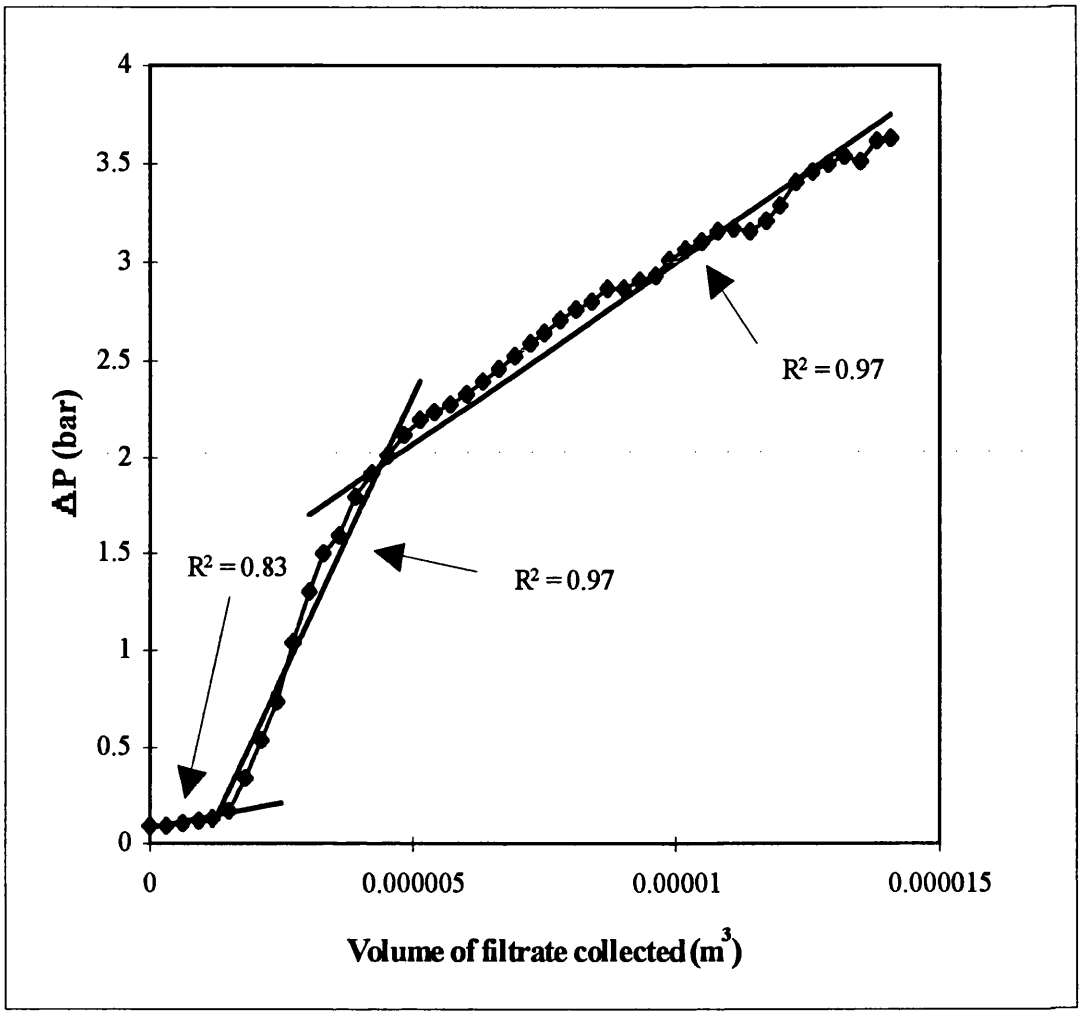

Fig 4.7 Cake filtration analysis for 50:50 water-in-dodecane (1 w/w % Paranox 100) homogenised at 8000 rpm for 13 minutes using a Supor 200 membrane at a flux of 13 l/h/m^2 applied to various sections of the data.

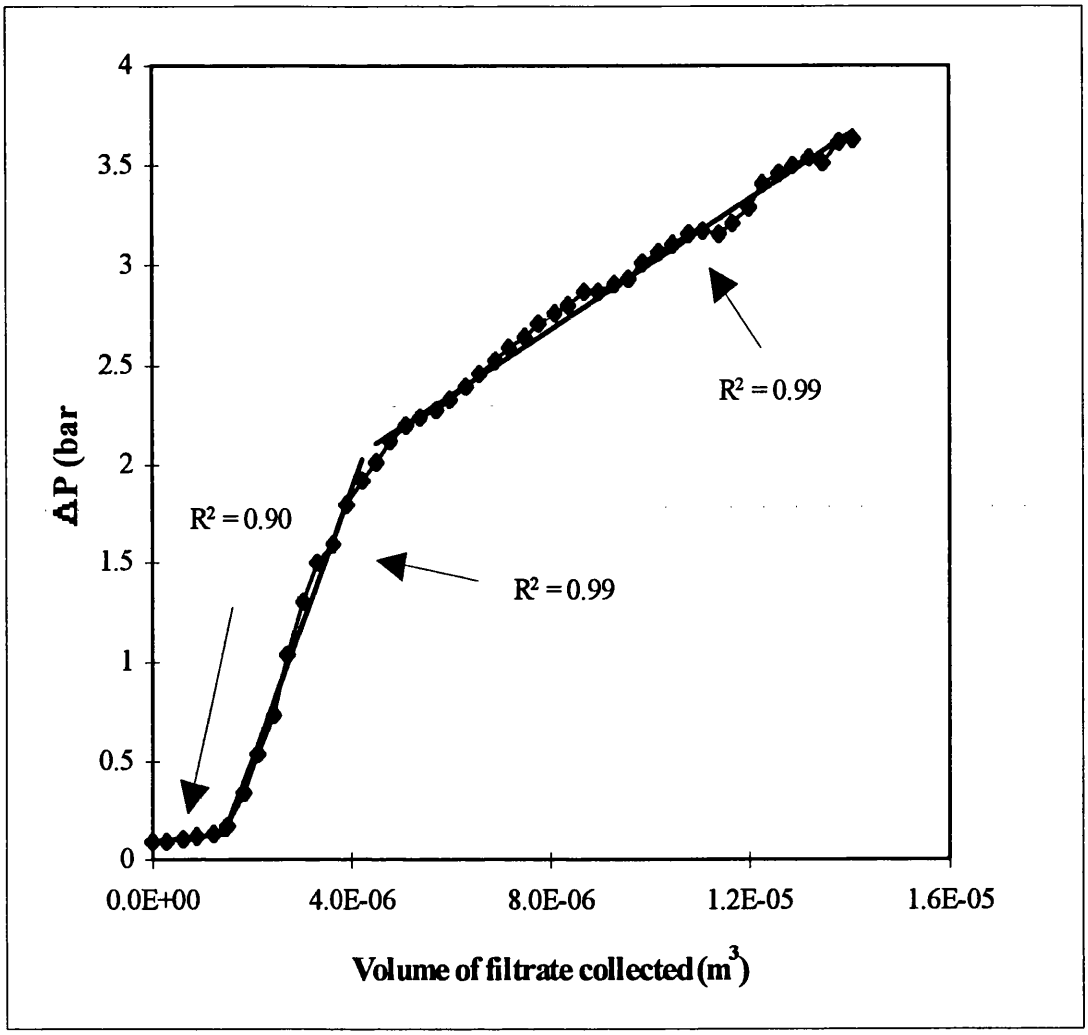

Fig 4.8 Cake filtration analysis for 50:50 water-in-dodecane (1 w/w % Paranox 100) homogenised at 8000 rpm for 13 minutes using a Supor 200 membrane at a flux of 13 l/h/m^2 applied to various sections of the data.

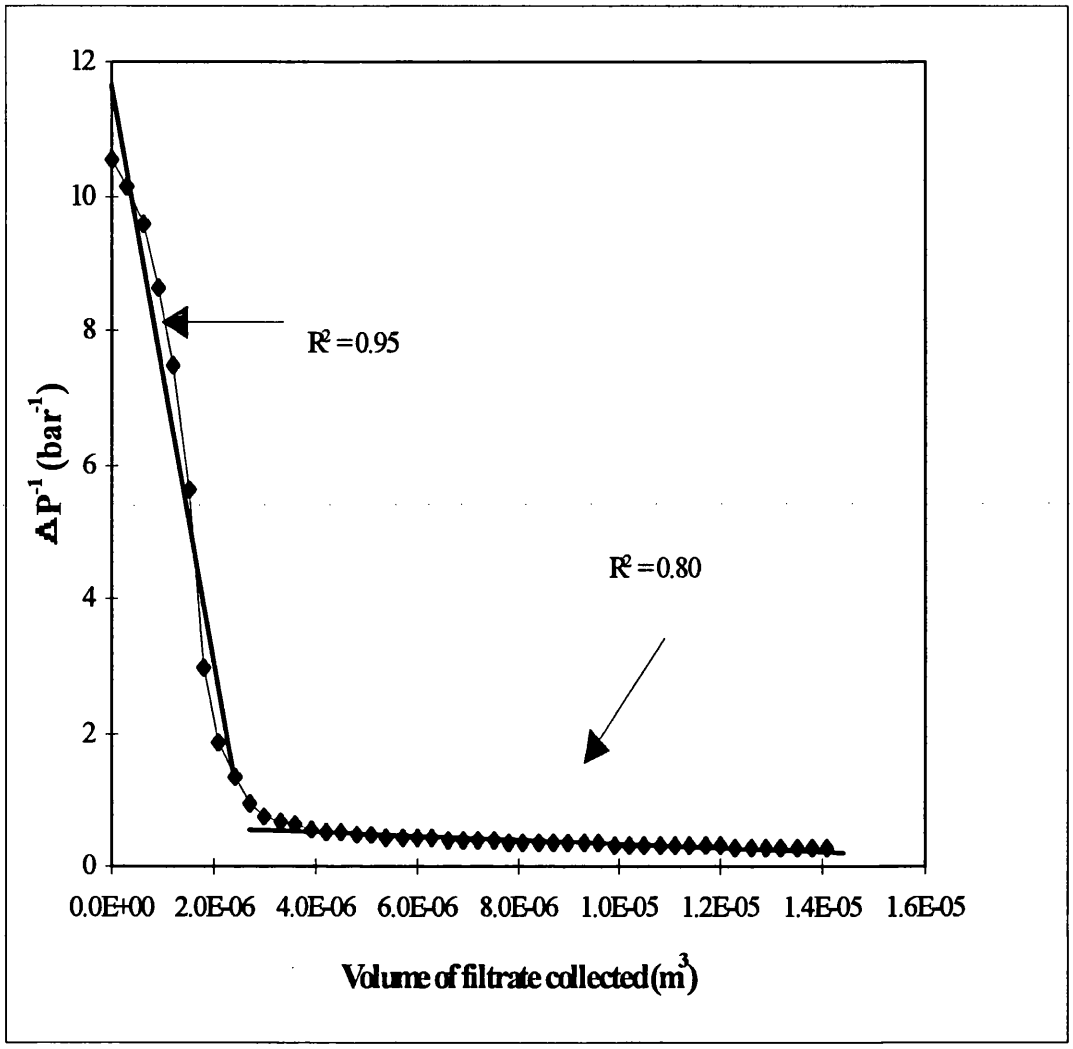

Fig 4.9 Complete blocking analysis for 50:50 water-in-dodecane (1 w/w % Paranox 100) homogenised at 8000 rpm for 13 minutes using a Supor 200 membrane at a flux of 13 l/h/m^2 applied to various sections of the data.

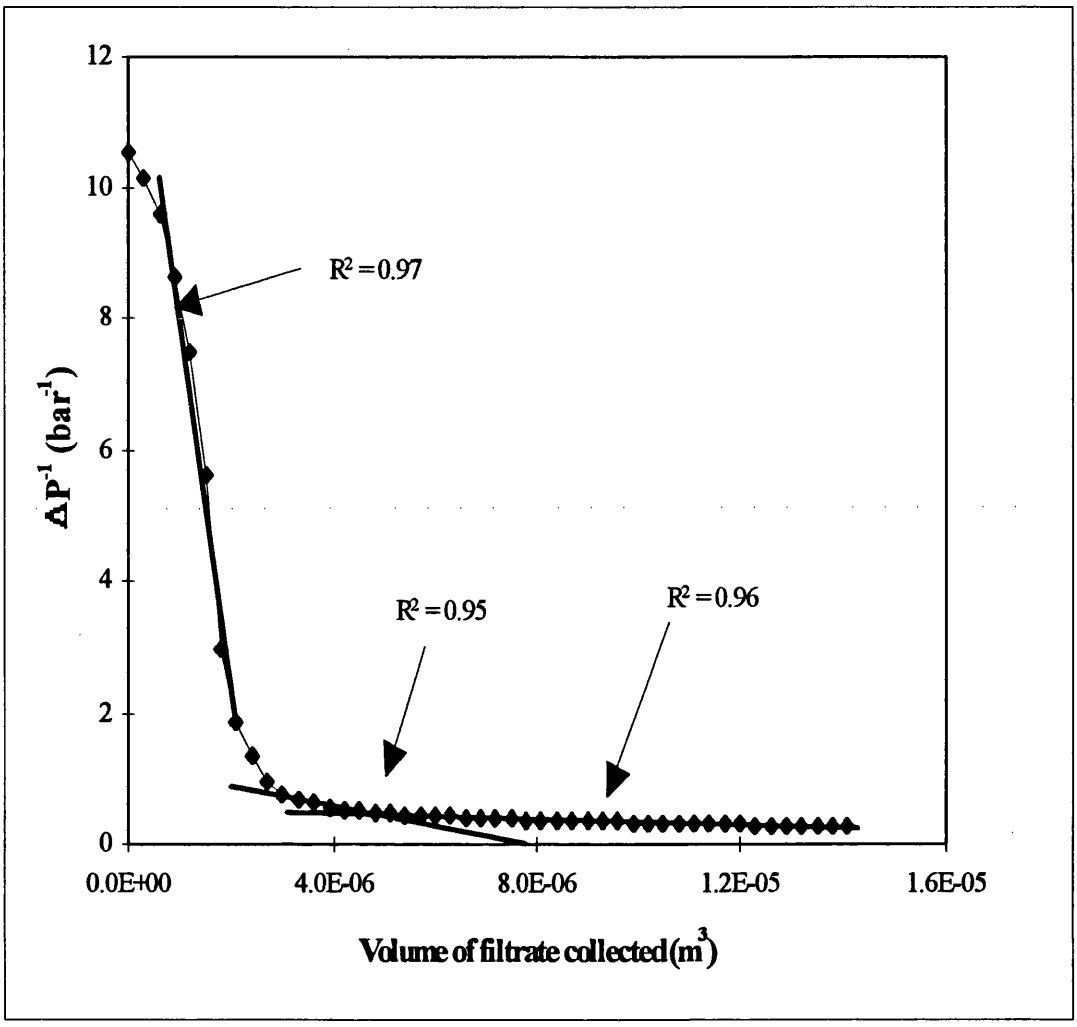

Fig 4.10 Complete blocking analysis for 50:50 water-in-dodecane (1 w/w % Paranox 100) homogenised at 8000 rpm for 13 minutes using a Supor 200 membrane at a flux of 13 l/h/m^2 applied to various sections of the data.

Reasonable fit in region 1 (indicated by coefficients of linear regression on the graph). In Figure 4.10 the regions were redefined and the complete blocking law gave a reasonable fit in three regions (R^2 >0.95). Region 2 was split into two regions (regions 2 and 3).

Standard blocking

The standard blocking graph (Figure 4.5) changed shape in two regions (Figure 4.6c) but the second region was further divided in to two regions. The law gave an excellent fit in regions 1 and 3 (Figure 4.11) and a moderate fit in region 2 (indicated by coefficients of linear regression on the graph). A better fit could not be obtained and this was considered the best fit by the standard blocking law for the data used.

Intermediate blocking

The intermediate blocking law (Figures 4.12-4.13) was applied to regions of the experimental data shown in Figure 4.4. The shape of the graph changed shape in three regions (Figure 4.6d). However, it was not clear where these regions started and finished and therefore in Figure 4.12 the regions were overlapped to avoid misrepresentation. Region 1: 0-2.4× 10^{-6} m^3 of filtrate collected and region 2: 3 × 10^{-6} -14.1 × 10^{-6} m^3 of filtrate collected. The intermediate blocking law gave an average fit in regions 1and 2 and a poor fit in region 3 (indicated by coefficients of linear regression on the graph). In Figure 4.13 the regions were redefined and the complete blocking law gave an average fit in region 1 (R^2=0.94) and a good fit in regions 2 and 3 (R^2>0.97).

Tables 4.2-4.5 show the summary of the filtration analysis (cake filtration, complete blocking, intermediate blocking and standard blocking) carried out on other experimental data. Where R^2 < 0.90 the analyse was rejected. There was no individual law for which a fit of all the data (mean of three experiments) resulted. It was found that the different filtration laws applied to three different regions. For each experiment regions 1, 2 and 3 for the standard law, complete blocking law and cake

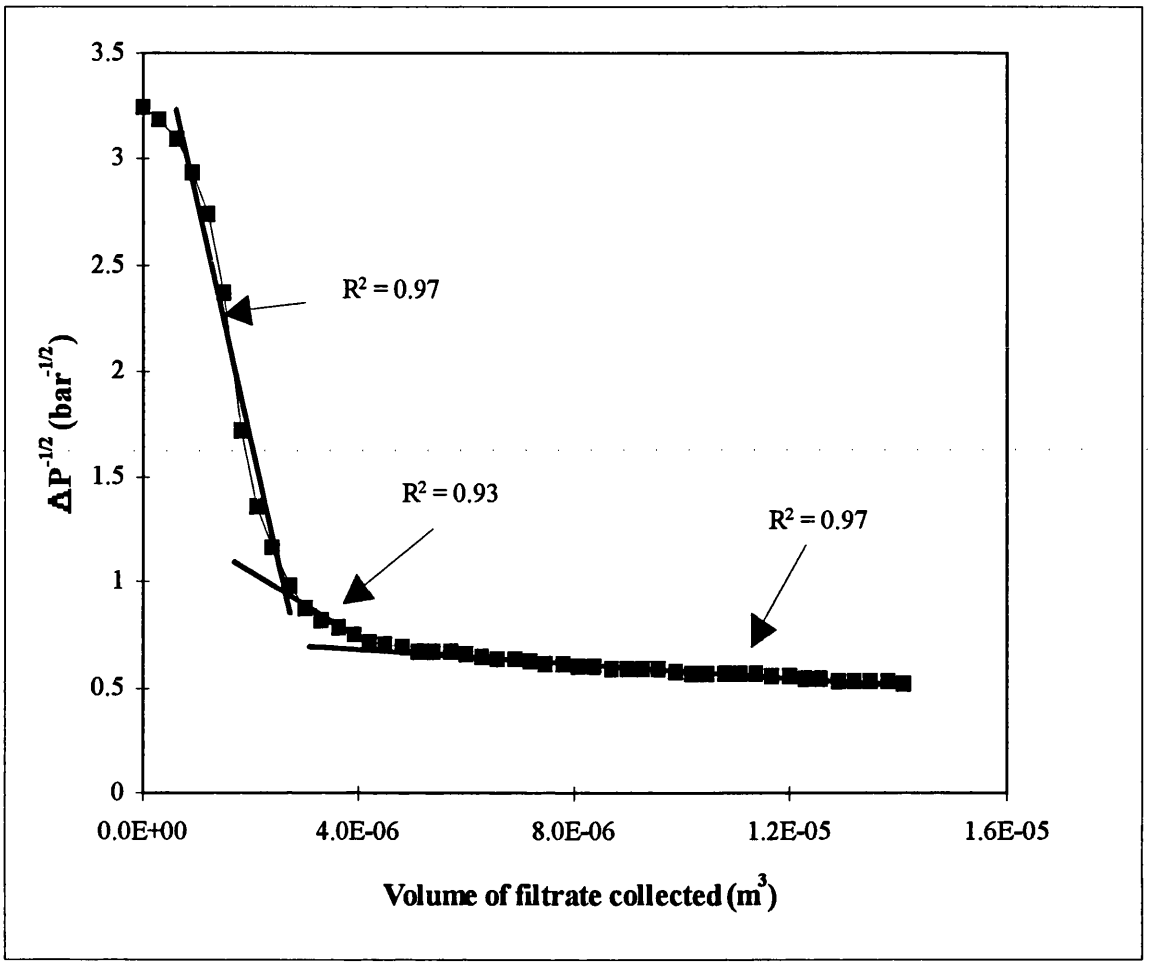

Fig 4.11 Standard blocking analysis for 50:50 water-in-dodecane (1 w/w % Paranox 100) homogenised at 8000 rpm for 13 minutes using a Supor 200 membrane at a flux of 13 l/h/m^2 applied to various sections of the data.

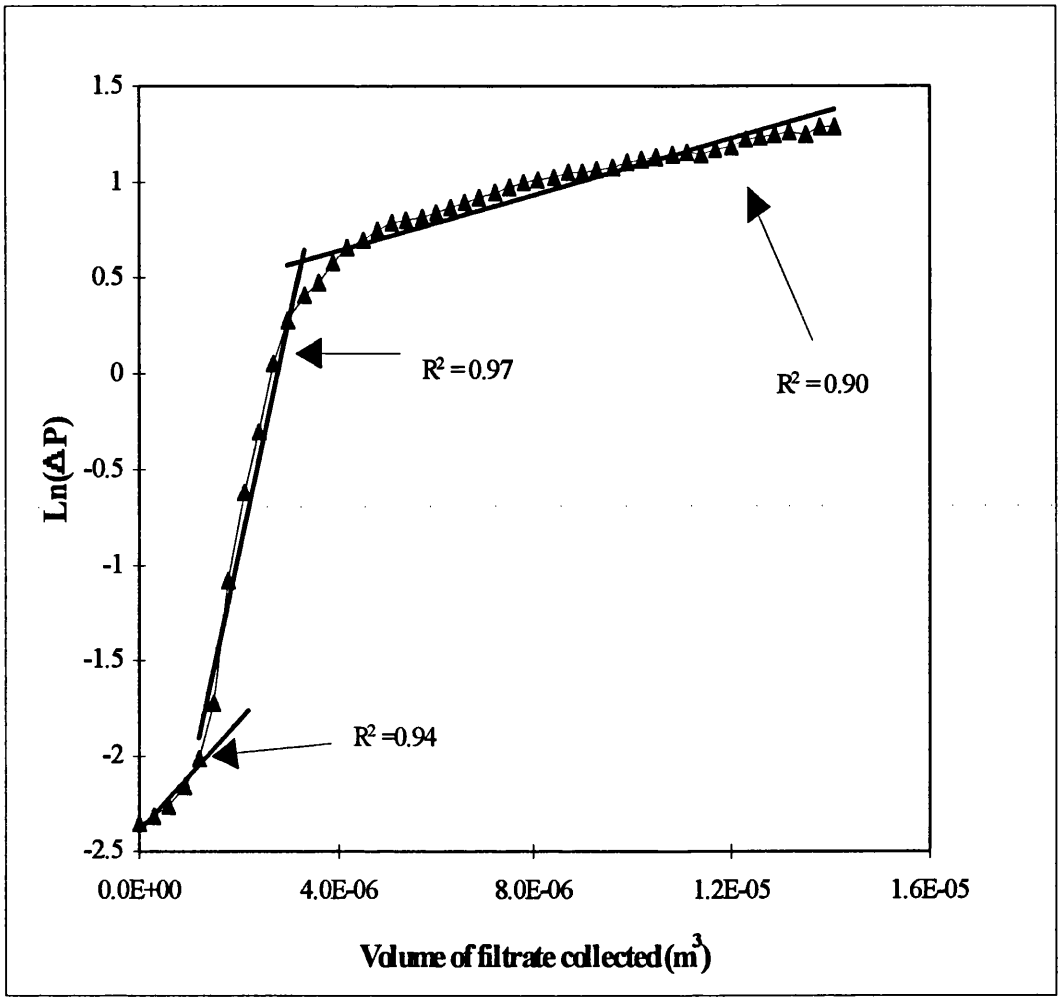

Fig 4.12 Intermediate blocking analysis for 50:50 water-in-dodecane (1 w/w % Paranox 100) homogenised at 8000 rpm for 13 minutes using a Supor 200 membrane at a flux of 13 l/h/m^2 applied to various sections of the data.

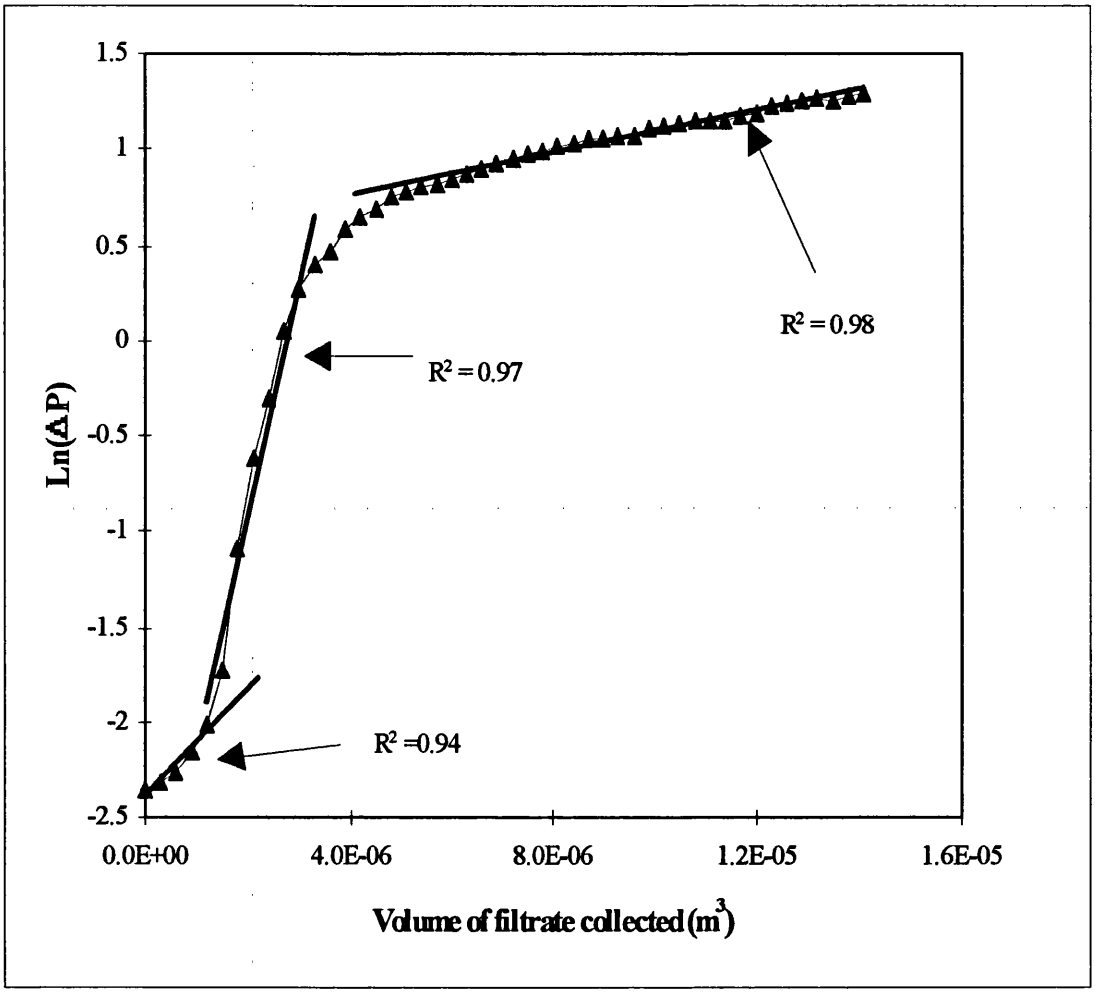

Fig 4.13 Intermediate blocking analysis for 50:50 water-in-dodecane (1 w/w % Paranox 100) homogenised at 8000 rpm for 13 minutes using a Supor 200 membrane at a flux of 13 l/h/m^2 applied to various sections of the data.

Table 4.2 Calculated coefficient of linear regression for sections of data for cake filtration law.

Emulsion composition	Membrane type	Flux ($l/h/m^2$)	volume of filtrate ($\times 10^{-6}$) collected (m^3)	R^2	if $R^2<0.9$ reject
50:50 water-in- dodecane (1 w/w % Paranox 100)	Supor 200	13	0-1.8	0.77	reject
			1.8-4.2	0.97	
			4.7-19.2	0.97	
		26	0-1.8	0.77	reject
			1.2-4.2	0.97	
			4.8-15	0.97	
		43.3	1-4	0.98	
			5-11	0.99	
50:50 water-in- dodecane (1 w/w % Paranox 100)		13	0-1.2	0.90	reject
			1.5-4.2	0.99	
			4.5-14.1	0.99	
50:50 water-in- dodecane (1 w/w % Paranox 100)	Httuffryn	13	0-1.2	0.89	reject
			1.2-3.3	0.99	
			3.6-9.9	0.99	
		26	0.6-6	0.99	
			6.6-13.8	0.99	
50:50 water-in- dodecane (1 w/w % Paranox 100)	Nylaflo	13	0-1.8	0.81	reject
			1.5-4.2	0.99	
			5.4-9.9	0.76	reject
		26	0-1.8	0.81	reject
			1.2-4.2	0.99	
			5.4-7.2	0.98	
	Versapor	13	0-1.8	0.76	reject
			1.8-3.6	0.99	
		26	0-1.8	0.72	reject
			1.8-3.3	0.99	
	Supor 100	13	0-1.8	0.71	reject
			1.8-4.2	0.99	
	Supor 450	26	0-1.8	0.78	reject
			1.8-4.2	0.99	
		13	0-1.8	0.74	reject
			1.8-3.9	0.99	
50:50 water-in- dodecane (2 w/w % Paranox 100)	Supor 200	26	0-1.5	0.77	reject
			1.5-4.2	0.98	
			4.5-8.7	0.97	
		13	0-1.8	0.68	reject
			1.8-4.2	0.99	
			4.2-7.2	0.95	

Table 4.3 Calculated coefficient of linear regression for sections of data for complete blocking law.

Emulsion composition	Membrane type	Flux ($l/h/m^2$)	volume of filtrate ($\times 10^{-6}$) collected (m^3)	R^2	if $R^2<0.90$ reject
50:50 water-in-dodecane (1 w/w % Paranox 100)	Supor 200	13	0.3-1.8	0.98	
			1.8-4.2	0.79	reject
			5.7-19.2	0.95	
		26	0-1.8	0.93	
			1.2-4.2	0.71	reject
			4.8-15	0.94	
		43.3	0-2	0.99	
			2-4	0.84	reject
			5-11	0.94	
50:50 water-in-dodecane (1 w/w % Paranox 100)		13	0.6-2.1	0.97	
			3-4.8	0.95	
			5.1-14.1	0.96	
50:50 water-in-dodecane (1 w/w % Paranox 100)	Httuffryn	13	0-1.8	0.88	reject
			2.1-3.3	0.97	
			3.6-9.9	0.99	
		26	0-1.8	0.92	
			1.8-6.6	0.80	reject
			6.6-13.8	0.98	
50:50 water-in-dodecane (1 w/w % Paranox 100)	Nylaflo	13	0.3-1.5	0.99	
			1.8-4.2	0.72	reject
			6.3-11.7	0.82	reject
		26	0-1.8	0.98	
			2.4-4.8	0.86	reject
			4.8-7.2	0.95	
	Versapor	13	0-1.8	0.98	
			1.8-3.9	0.87	reject
		26	0-1.8	0.98	
			1.8-3.3	0.66	reject
	Supor 100	13	0.6-2.1	0.99	
			2.1-4.2	0.60	reject
	Supor 450	13	0.3-1.8	0.99	
			1.8-4.2	0.71	reject
		26	0-1.8	0.99	
			1.8-4.2	0.79	reject
50:50 water-in-dodecane (2 w/w % Paranox 100)	Supor 200	13	0.3-1.5	0.96	
			1.8-4.2	0.70	reject
			4.2-8.1	0.91	
		26	0.6-1.8	0.98	
			1.8-4.2	0.66	reject
			4.2-8.4	0.87	reject

Table 4.4 Calculated coefficient of linear regression for sections of data for standard blocking law.

Emulsion composition	Membrane type	Flux ($l/h/m^2$)	volume of filtrate ($\times 10^{-6}$) collected(m^3)	R^2	if $R^2<0.90$ reject
50:50 water-in-dodecane (1 w/w % Paranox 100)	Supor 200	13	0.6-1.8	0.99	
			1.8-4.2	0.87	reject
			5.4-15	0.98	
		26	0.6-1.8	0.99	
			1.8-4.2	0.77	reject
			6-19.2	0.95	
		43.3	0-2	0.97	reject
			2-4	0.87	
			6-11	0.97	reject
50:50 water-in-dodecane (1 w/w % Paranox 100)		13	0.6-2.7	0.97	
			2.7-4.2	0.93	
			5.1-14.1	0.97	
50:50 water-in-dodecane (1 w/w % Paranox 100)	Httuffryn	13	0-1.8	0.91	
			1.8-4.2	0.90	reject
			4.8-9.9	0.99	
		26	0-1.8	0.97	
			1.8-6.6	0.87	reject
			6.6-13.8	0.98	
50:50 water-in-dodecane (1 w/w % Paranox 100)	Nylaflo	13	0.3-1.8	0.99	
			1.8-4.2	0.81	reject
			5.7-11.7	0.81	reject
		26	0-1.8	0.99	
			1.8-4.2	0.99	
			4.8-7.2	0.95	
	Versapor	13	0.3-1.8	0.99	
			1.8-3.9	0.82	reject
		26	0-1.8	0.98	
			1.8-3.3	0.91	
	Supor 100	13	0.9-2.4	0.99	
			2.4-4.2	0.63	reject
	Supor 450	13	0.3-1.8	0.99	
			1.8-4.2	0.81	reject
		26	0-1.8	0.99	
			1.8-4.2	0.86	reject
50:50 water-in-dodecane (2 w/w % Paranox 100)	Supor 200	13	0.3-1.8	0.98	
			1.8-4.2	0.78	reject
			4.2-8.1	0.92	
		26	0.6-1.8	0.97	
			1.8-4.2	0.96	
			4.2-8.4	0.88	reject

Table 4.5 Calculated coefficient of linear regression for sections of data for intermediate blocking law.

Emulsion composition	Membrane type	Flux ($l/h/m^2$)	volume of filtrate ($\times 10^{-6}$) collected (m^3)	R^2	if $R^2<0.90$ reject
50:50 water-in-dodecane (1 w/w % Paranox 100)	Supor 200	13	0.6-3.3	0.99	
			6-19.2	0.97	
		26	0.6-2.4	0.99	
			4.8-15	0.95	
		43.3	0-3	0.96	
			5-11	0.93	
50:50 water-in-dodecane (1 w/w % Paranox 100)		13	0-1.2	0.94	
			1.2-3.3	0.97	
			5.1-14.1	0.98	
50:50 water-in-dodecane (1 w/w % Paranox 100)	Httuffryn	13	1.2-3	0.99	
			3.6-9.9	0.99	
		26	0-3.0	0.99	
			6.6-13.8	0.98	
50:50 water-in-dodecane (1 w/w % Paranox 100)	Nylaflo	13	0.3-3	0.97	
			4.5-11.7	0.75	reject
		26	0-3.0	0.99	
			3.6-7.2	0.93	
	Versapor	13	0.3-3	0.99	
		26	0.6-3	0.97	
	Supor 100	13	1.2-2.7	0.98	
	Supor 450	13	0.3-3	0.99	
		26	0.6-3	0.99	
50:50 water-in-dodecane	Supor 200	13	0.3-3	0.99	
			4.5-8.1	0.94	
		26	0.6-3	0.96	
			4.2-8.4	0.89	reject

filtration law was for approximately the same range of data. However, region 1 for the intermediate law (Table 4.5) gave a fit in most cases for the data between regions 1 and 2 of the other laws. Region 3 for the intermediate law was for approximately the same range of data as for the other filtration laws.

4.4.2.3 Step 3 analysis of constants and theory

Complete blocking (Region 1)

The results in Tables 4.6-4.8 give the values of σ, σ/R_m and d derived from the linearised curves in Chapter 3. The σ/R_m values were in the same range for all membranes even where the resistance of the membrane was high (Supor 100 membrane). The clogging coefficient (σ) is an intrinsic property of the emulsion and should be the same for all experiments where the same emulsion was used (Tables 4.6 and 4.8).

Standard blocking (region 2)

Tables 4.9-4.11 show the $C/P^{1/2}\varepsilon$ and C values derived from the linearised curves in Chapter 3. The C values were in the same range for each emulsion and membrane used. The C value was not a measure of the concentration of droplets deposited on the pore walls as the droplets were too large for standard blocking. However, the surfactant molecules were small enough to enter the pores and if conditions were favourable adsorb on the pore walls this would have resulted in pore narrowing. The Surfactant concentration in the feed was 1 w/w % and 2 w/w % depending on the emulsion. However, The interfacial tension measurements (Table 3.7 Page 74) show the interfacial tension did not change. Taking into consideration that the surfactant concentration was above the cmc some surfactant could have adsorbed to the pores without causing any change to the interfacial tension values. However, as calculated concentrations (Tables 4.9-4.11) are higher than the surfactant concentrations used (1 w/w % and 2 w/w %) it is clear these values are not reasonable.

Table 4.6 Complete blocking analysis of the curves of pressure drop versus volume (Chapter 3). Determination of clogging coefficient (σ) and droplet diameter (d) for different membranes using emulsion 50:50 water-in-dodecane emulsion (1 % Paranox 100). Water was not collected in the permeate.

Filter media	region	Flux ($l/h/m^2$)	straight line slope $\times 10^6$	intercept	σ/R^m $\times 10^{-10}$	σ (m^{-1})	d (m)
Supor 100	1	13	-5.8	13.8	2.1	60	0.013
Supor 450	1	13	-6.4	12.3	2.2	11	0.068
	1	26	-6.1	11.6	4.3	21	0.035
Versapor	1	13	-5.6	11.1	2.0	21	0.035
	1	26	-5.9	10.9	4.3	45	0.017

Table 4. 7 Complete blocking analysis of the curves of pressure drop versus volume (Chapter 3). Determination of the clogging coefficient (σ) and droplet diameter (d) for Supor 200 membrane where the emulsions varied in composition. Water was collected in the permeate.

Filter media	region	Flux ($l/h/m^2$)	straight line slope $\times 10^6$	intercept	σ/R^m $\times 10^{-10}$	σ (m^{-1})	d (m)
50:50 water-in-dodecane (1 % Paranox 100)							
Homogenizer 8000 rpm	1	13	-5.63	12.5	2.0	18	0.042
for 3min and 9500 rpm	1	26	-6.13	12.0	5.4	48	0.016
for 10 min	1	43.3	-4.58	10.4	5.5	48	0.016
50:50 water-in-dodecane (1 % Paranox 100)							
Homogenizer 8000 rpm	1	13	-5.5	13.4	2.0	17	0.044
for 13 min							
50:50 water-in-dodecane (2 % Paranox 100)	1	13	-8.4	14.7	3.0	24	0.031
Homogenizer 8000 rpm	1	26	-7.3	15.6	5.2	42	0.017
for 3min and 9500 rpm							
for 10 min							

Table 4.8 Complete blocking analysis of the curves of pressure drop versus volume (Chapter 3). Determination of the clogging coefficient (σ) and droplet diameter (d) for different membranes using emulsion 50:50 water-in-dodecane emulsion (1 % Paranox 100). Water was collected in the permeate.

Filter media	region	Flux ($l/h/m^2$)	straight line slope $\times 10^6$	intercept	σ/R^m $\times 10^{-10}$	σ (m^{-1})	d (m)
Supor 200	1	26	-5.63	12.5	2.0	18	0.042
	1	13	-6.13	12.0	5.4	48	0.016
	1	43.3	-4.58	10.4	5.5	48	0.016
Nylaflo	1	13	-7.01	12.2	2.5	35	0.021
	1	26	-5.78	10.8	4.1	59	0.013
HTTuffryn	1	26	-5.89	10.2	4.2	53	0.014

Table 4.9 Standard blocking analysis of the curves of pressure drop versus volume (Chapter 3). Determination of C and $C/p^{1/2}\varepsilon$ for different membranes (of various pore size) using emulsion 50:50 water-in-dodecane emulsion (1 % Paranox 100). No water was collected in the permeate.

Filter media	region	Flux ($l/h/m^2$)	straight line slope $\times 10^6$	intercept	$C/p^{1/2}\varepsilon$ bar^{-1}	C
Versapor	1	13	-1.42	3.7	0.25	0.017
	1	26	-1.4 1	3.5	0.24	0.023
Supor 100	1	13	-1.5 0	4.4	0.31	0.034
Supor 450	1	13	-1.4 4	3.8	0.30	0.014
	1	26	-1.35	3.5	0.28	0.018

Table 4.10 Standard blocking analysis of the curves of pressure drop versus volume (Chapter 3). Determination of C and $C/p^{1/2}\varepsilon$ for Supor 200 membrane where the emulsions varied in composition. Water was collected in the permeate. permeate.

Filter media	region	Flux ($l/h/m^2$)	straight slope $\times 10^6$	line intercept	$C/p^{1/2}\varepsilon$ bar^{-1}	C
50:50 water-in-dodecane (1 % Paranox 100)						
Homogenizer 8000 rpm	1	13	-1.35	4.0	0.28	0.017
for 3min and 9500 rpm	1	26	-1.78	4.2	0.37	0.032
for 10 min	1	43.3	-1.08	3.3	0.22	0.025
50:50 water-in-dodecane (1 % Paranox 100) Homogenizer 8000 rpm for 13 min	1	13	-1.13	3.9	0.20	0.012
50:50 water-in-dodecane (2 % Paranox 100) Homogenizer 8000 rpm for3 min	1	13	-1.61	4.0	0.33	0.020
Homogenizer 9500 rpm for 10 min	1	26	-1.53	4.4	0.32	0.027

Table 4.11 Standard blocking analysis of the curves of pressure drop versus volume (Chapter 3). Determination of C and $C/p^{1/2}\varepsilon$ for different membranes using emulsion 50:50 water-in-dodecane emulsion (1 % Paranox 100). Water was collected in the permeate.

Filter media	region	Flux ($l/h/m^2$)	straight line slope $\times 10^6$	intercept	$C/p^{1/2}\varepsilon$ bar^{-1}	C
Supor 200						
	1	13	-1.35	4.0	0.28	0.017
	1	26	-1.78	4.2	0.37	0.032
	1	43.3	-1.08	3.3	0.22	0.025
Nylaflo	1	13	-1.47	3.7	0.25	0.020
	1	26	-1.34	3.4	0.23	0.026
HTTuffryn						
	1	13	-1.42	3.3	0.32	0.024
	1	26	-1.40	3.3	0.32	0.033

Intermediate blocking (region 1-2)

The results in tables 4.12-4.14 give the values of σ and σ/ε and the drop diameter (d) derived from the linearised curves in Chapter 3. The intermediate law predicts that the increase in pressure drop is inversely proportional to the membrane porosity. The results are in reasonably good agreement with the theory as all the membranes had the same porosity (0.8) and therefore all the σ/ε values were in the same range. The σ values and drop diameters calculated where the same emulsion but different membranes were used (Tables 4.12 and 4.14) were in the same range. This was to be expected as the clogging coefficient is an intrinsic property of the emulsion and did not depend on the membrane properties.

Cake filtration (region2 and 3)

Tables 4.15-4.17 show the cake voidage values derived from the linearised curves in Chapter 3. In Tables 4.15 and 4.17 for a given flux the voidage was in the same range for each membrane used which was to be expected as the same well dispersed emulsion was used. The membrane properties do not affect the cake if the cake covers all of the membrane area. In Table 4.16 for a given flux the voidage was in the same range for region 3 irrespective of the emulsion used but in region 2 there was some differences in the values calculated.

4.4.3 Clean Membranes

The pure dodecane permeability was checked routinely for each membrane and the average values are presented in Table 4.18. A new membrane was used for each experiment. The dodecane permeability tests were carried out at various fluxes which enabled the average flow resistance to be determined.

Table 4.12 Intermediate blocking analysis of the curves of pressure drop versus volume (Chapter 3). Determination of σ and σ/ε for different membranes (of various pore size) using emulsion 50:50 water-in-dodecane emulsion (1 % Paranox 100). No water was collected in the permeate.

Filter media	region	Flux ($l/h/m^2$)	straight slope $\times 10^6$	line intercept	σ/ε (m^{-1}) $\times 10^3$	σ (m^{-1}) $\times 10^2$	d (m) $\times 10^{-4}$
Versapor	1-2	13	1.6	-3.0	1.1	8.6	8.7
	1-2	26	1.7	-3.0	1.2	9.3	8.1
Supor 100	1-2	13	2.1	-4.7	1.4	10	6.5
Supor 450	1-2	13	1.5	-3.0	1.0	8.3	9.1
	1-2	26	1.5	-3.0	1.0	8.2	9.2

Table 4.13 Intermediate blocking analysis of the curves of pressure drop versus volume (Chapter 3). Determination of σ and σ/ε for Supor 200 membrane where the emulsions varied in composition. Water was collected in the permeate.

Filter media	region	Flux ($l/h/m^2$)	straight slope $\times 10^6$	line intercept	σ/ε (m^{-1}) $\times 10^3$	σ (m^{-1}) $\times 10^2$	d (m) $\times 10^{-3}$
50:50 water-in-dodecane (1 % Paranox 100)							
Homogenizer 8000 rpm	1-2	13	1.2	-3.1	0.83	6.7	1.1
for 3min and 9500 rpm	1-2	26	1.7	-3.3	1.2	9.6	0.78
for 10 min	1-2	43.3	1.2	-2.6	0.80	6.4	1.2
50:50 water-in-dodecane (1 % Paranox 100) Homogenizer 8000 rpm for 13 min	1-2	13	1.2	-3.4	0.85	6.8	1.1
50:50 water-in-dodecane (2 % Paranox 100) Homogenizer 8000 rpm for3 min	1-2	13	1.5	-3.1	1.0	8.0	0.93
Homogenizer 9500 rpm for 10 min	1-2	26	1.6	-3.5	1.1	8.6	0.87

Table 4.14 Intermediate blocking analysis of the curves of pressure drop versus volume (Chapter 3). Determination of σ and σ/ε for different membranes using emulsion 50:50 water-in-dodecane emulsion (1 % Paranox 100). Water was collected in the permeate.

Filter media	region	Flux ($l/h/m^2$)	Straight line Slope $\times 10^6$	intercept	σ/ε (m^{-1}) $\times 10^2$	σ (m^{-1}) $\times 10^2$	d (m) $\times 10^{-3}$
Supor 200	1-2	13	1.2	-3.1	8.3	6.7	1.1
	1-2	26	1.7	-3.3	15	9.6	0.78
	1-2	43.3	1.2	-2.6	8.0	6.4	1.2
Nylaflo	1-2	13	1.4	-2.8	9.6	7.7	0.98
	1-2	26	1.3	-2.4	9.3	7.4	1.0
HTTuffryn	1-2	13	0.64	-1.3	4.4	3.5	2.1
	1-2	26	1.3	-2.4	9.3	7.4	1.0

Table 4.15 Cake filtration constants for a 50:50 water-in-dodecane emulsion (1 % Paranox 100). Different membranes were used where no water was collected in the filtrate.

Membrane / pore size (μm)	Graph / region	Flux ($l/h/m^2$)	gradient (bar/m^3) $\times 10^6$	intercept (bar)	$\frac{\alpha \rho_F ms}{A^2(1-ms)}$ (bar min/m^6) $\times 10^{12}$	Cake voidage (%)
versapor (0.2)	Fig 4.16, region 2	13	2.83	-4.29	9.43	4.0
versapor (0.2)	Fig 4.16, region 2	26	2.86	-3.31	4.77	5.0
Supor (0.1)	Fig 4.15, region 2	13	2.27	-3.76	7.57	4.3
Supor (0.45)	Fig 4.14, region 2	13	2.32	-3.46	7.73	4.3
Supor (0.45)	Fig 4.14, region 2	26	2.21	-3.06	3.68	5.4

Table 4.16 Cake filtration constants Same membrane (Supor 200) but different emulsion compostion were used where water was collected in the filtrate.

Emulsion composition	Region	Flux ($l/h/m^2$)	Graph	straight slope $\times 10^6$	line intercept	$Kc=\frac{\alpha \rho_F ms}{A^2(1-ms)}$ (bar min/m^6) $\times 10^{12}$	Cake voidage (%)
50:50 water-in-dodecane (1 % Paranox 100) *Homogenizer 8000 rpm for 3min and 9500 rpm for 10 min*	2	13	Fig 4.17	1.02	-1.5	3.43	5.6
	3	13	Fig 4.17	0.14	2.4	0.472	2.2
	2	26	Fig 4.17	1.14	-0.93	1.90	6.8
	3	26	Fig 4.17	0.11	3.4	0.190	3.0
	2	43.3	Fig 4.18	1.17	-1.1	1.17	8.0
	3	43.3	Fig 4.18	0.19	3.2	0.191	3.0
50:50 water-in-dodecane (1 % Paranox 100) *Homogenizer 8000 rpm for 13 min*	2	13	Fig 4.24	0.68	-0.84	2.27	4.3
	3	13	Fig 4.24	0.16	1.4	0.544	1.4
50:50 water-in-dodecane (2 % Paranox 100) *Homogenizer 8000 rpm for 3min and 9500 rpm for 10 min*	2	13	Fig 4.23	1.63	-2.33	4.66	7.1
	3	13	Fig 4.23	0.395	2.7	0.496	2.2
	2	26	Fig 4.22	1.63	-2.33	2.72	8.6
	3	26	Fig 4.22	0.297	4.2	1.30	3.0

Table 4.17 Cake filtration analysisof the curves of pressure drop versus volume (Chapter 3). Determination of K_C for different membranes where water was collected in the permeate and the emulsion used was 50:50 water-in-dodecane emulsion (1 % Paranox 100).

Filter media	Region	Flux ($l/h/m^2$)	Graph	straight line slope $\times 10^6$	intercept	$Kc=\frac{\alpha\rho_F ms}{A^2(1-ms)}$ (bar min/m^6) $\times 10^{12}$	Cake voidage (%)
Supor 200	2	13	Fig 4.17	1.02	-1.5	3.43	5.6
	3	13	Fig 4.17	0.14	2.4	0.472	2.2
	2	26	Fig 4.17	1.14	-0.93	1.90	6.8
	3	26	Fig 4.17	0.11	3.4	0.190	3.0
	2	43.3	Fig 4.18	1.17	-1.1	1.17	8.0
	3	43.3	Fig 4.18	0.19	3.2	0.191	3.0
Nylaflo	2	13	Fig 4.20	1.26	-1.2	4.67	5.0
	3	13	Fig 4.20	0.142	4.6	0.476	2.2
	2	26	Fig 4.21	1.51	-1.4	2.52	6.0
	3	26	Fig 4.21	0.37	3.4	0.619	2.0
						0.472	
HTTuffryn	2	13	Fig 4.19	0.723	-0.34	2.41	6.3
	3	13	Fig 4.19	0.141	1.7	0.472	2.2
	2	26	Fig 4.19	0.844	-0.28	1.41	7.5
	3	26	Fig 4.19	0.119	4.3	0.198	3.0

Table 4.18 Measured pure dodecane permeability for membranes at 23 °C

Membrane type	Average pore size (μm)	Membrane thickness (μm)	Membrane resistance (m^{-1}) $\times 10^{11}$
Supor (udel polysulfone)	0.1	150	3.59
	0.2	150	1.08
	0.45	150	0.605
Httuffryn poly(arylenesulfone ether)	0.2	165	1.57
Nylaflo (nylon 6-6)	0.2	125	1.77
Versapor (polyvinylchloride and polyacrylonitrile)	0.2	191	1.32

4.4.4 Cake filtration law

The cake filtration law analysis is shown in Figures 4.14-4.24. Figures 4.14-4.16 were for membranes Supor 100, Versapor 200 and Supor 450. The emulsion used was 50:50 water-in-dodecane (1 % Paranox 100) in all cases. The filtration runs were plotted in terms of pressure (ΔP) vs volume of filtrate collected (equation 4.34) and there was one region of cake filtration. The filtration was stopped at about 6 bar which was the maximum pressure of the filtration system. Two fluxes were examined 13 l/h/m^2 and 26 l/h/m^2. The slope of the linearised portion of the graphs Figure 4.14-4.16 were tabulated in Table 4.15. From the slope, the K_c values were determined, the values were similar for each membrane where the flux was the same.

The Figures 4.17-4.21 were for membranes Supor 200, HTTuffryn and Nylaflo (average pore size 0.2 μm). The emulsion used was 50:50 water-in-dodecane (1 % Paranox 100) in all cases. The filtration runs were plotted in terms of pressure (ΔP) vs volume of filtrate collected (equation 4.34) and there were two regions of cake filtration. The process was stopped before the maximum pressure of 6 bar was reached. . Two fluxes were examined 13 l/h/m^2 and 26 l/h/m^2. The slope of the linearised portion of the graphs Figure 4.17-4.21 were tabulated in Table 4.17. From the slope, the Kc and voidage values were determined, the values were similar for each membrane where the flux was the same.

The graphs figure 4.22-4.24 are for Supor membrane (average pore size 0.2 μm) where the emulsions were varied in composition. In Figures 4.22-4.23 the emulsion used was a 50:50 water-in-dodecane (2 % Paranox 100). The filtration runs were plotted in terms of pressure (ΔP) vs volume of filtrate collected and there were two regions of cake filtration. The process was stopped at about 6 bar (maximum pressure of system). Two fluxes were examined 13 l/h/m^2 and 26 l/h/m^2. The slope of the linearised portion of the graphs Figure 4.22-4.23 were tabulated in Table 4.16. From the slope, the K_c and voidage values were determined and found to be slightly different for each flux. Figure 4.24 is the results for an emulsion 50:50 water-in-

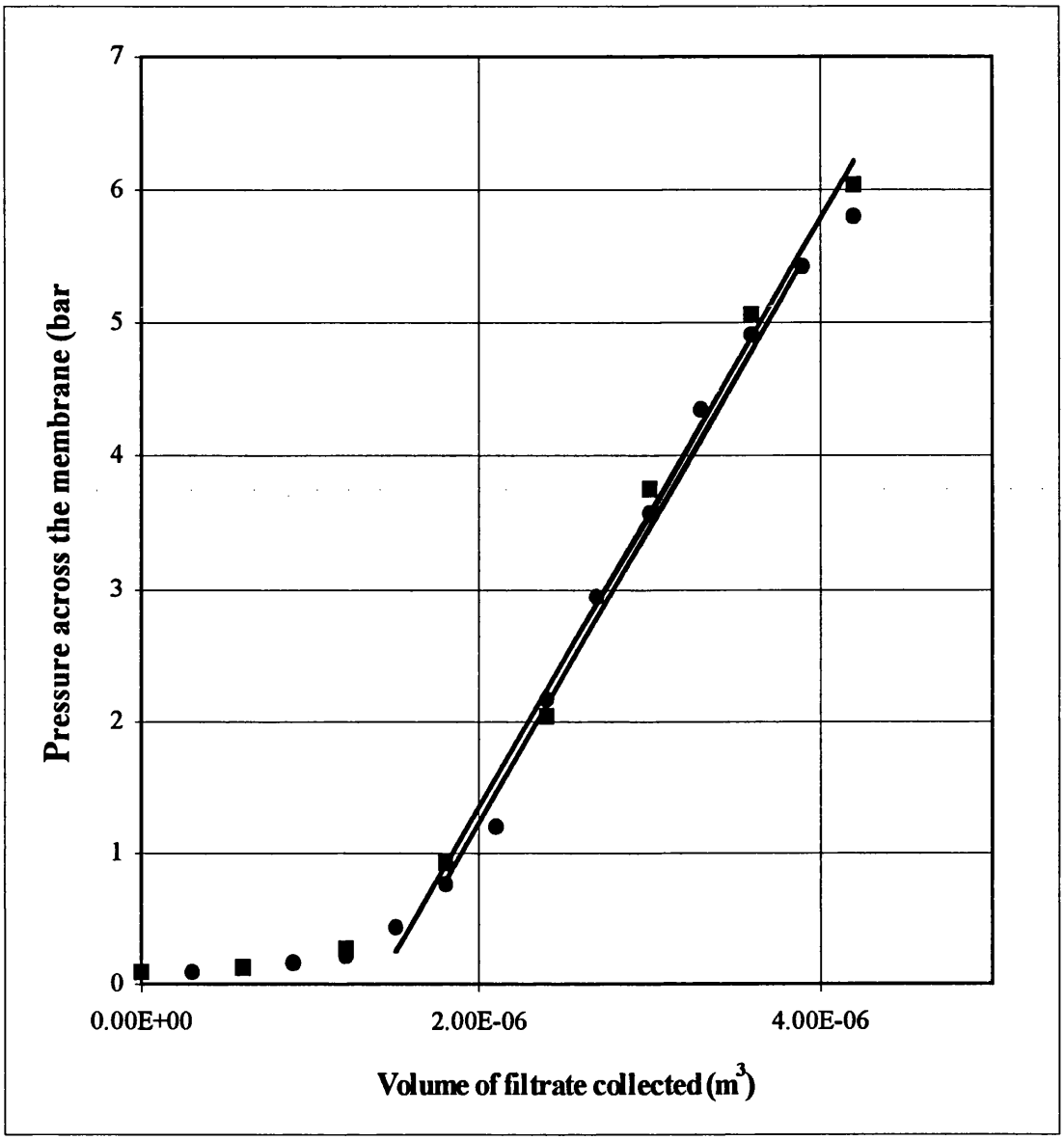

Figure 4.14 Cake filtration analysis for 50:50 water-in-dodecane emulsion at surfactant concentration 1 w/w % (Supor 450). -●- Flux 13 l/h/m^2 . -■- Flux 26 l/h/m^2.

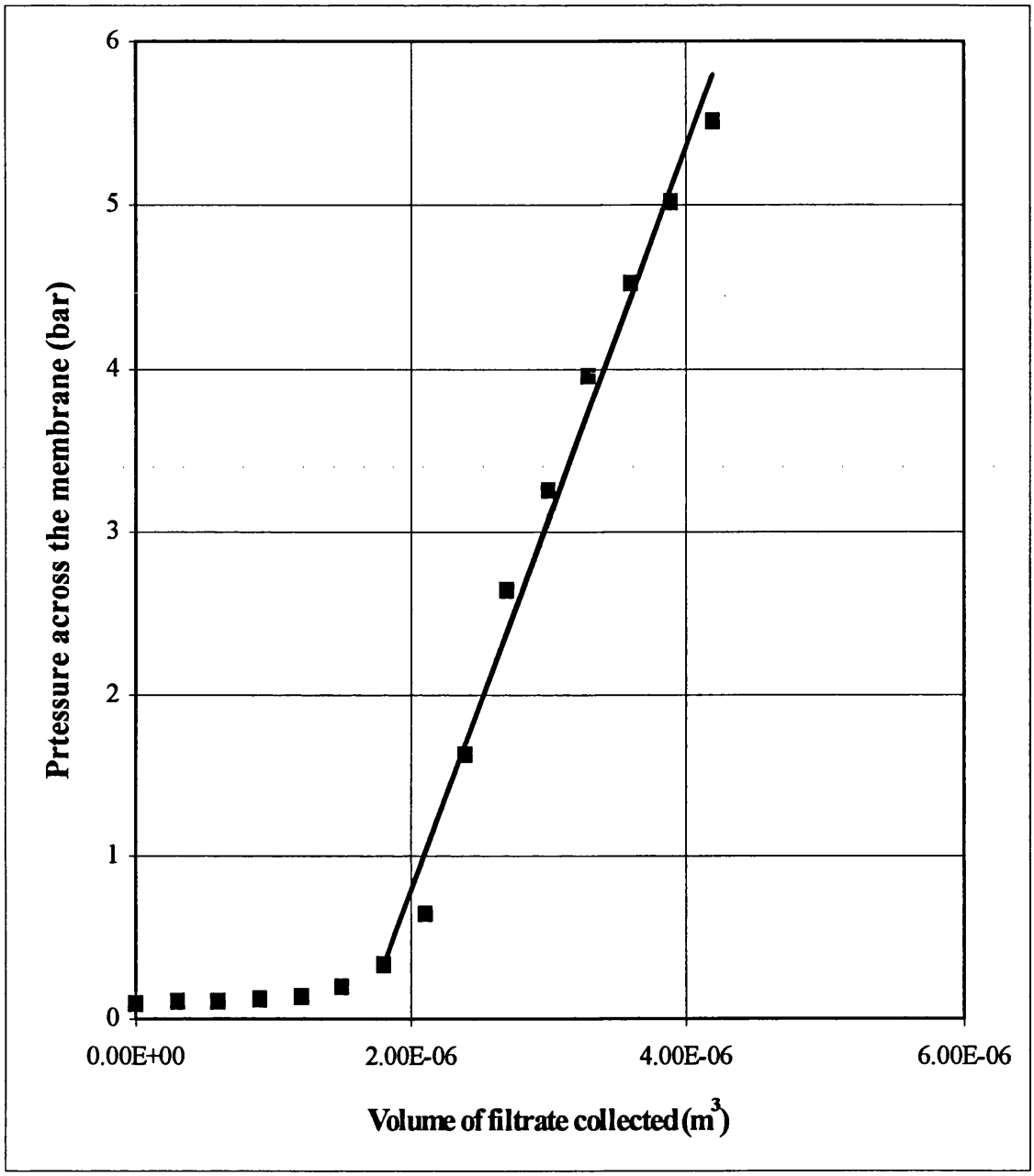

Fig 4.15 Cake filtration analysis for 50:50 water-in-dodecane emulsion at surfactant concentration 1 w/w % (Supor 100). -■- Flux 13 l/h/m^2.

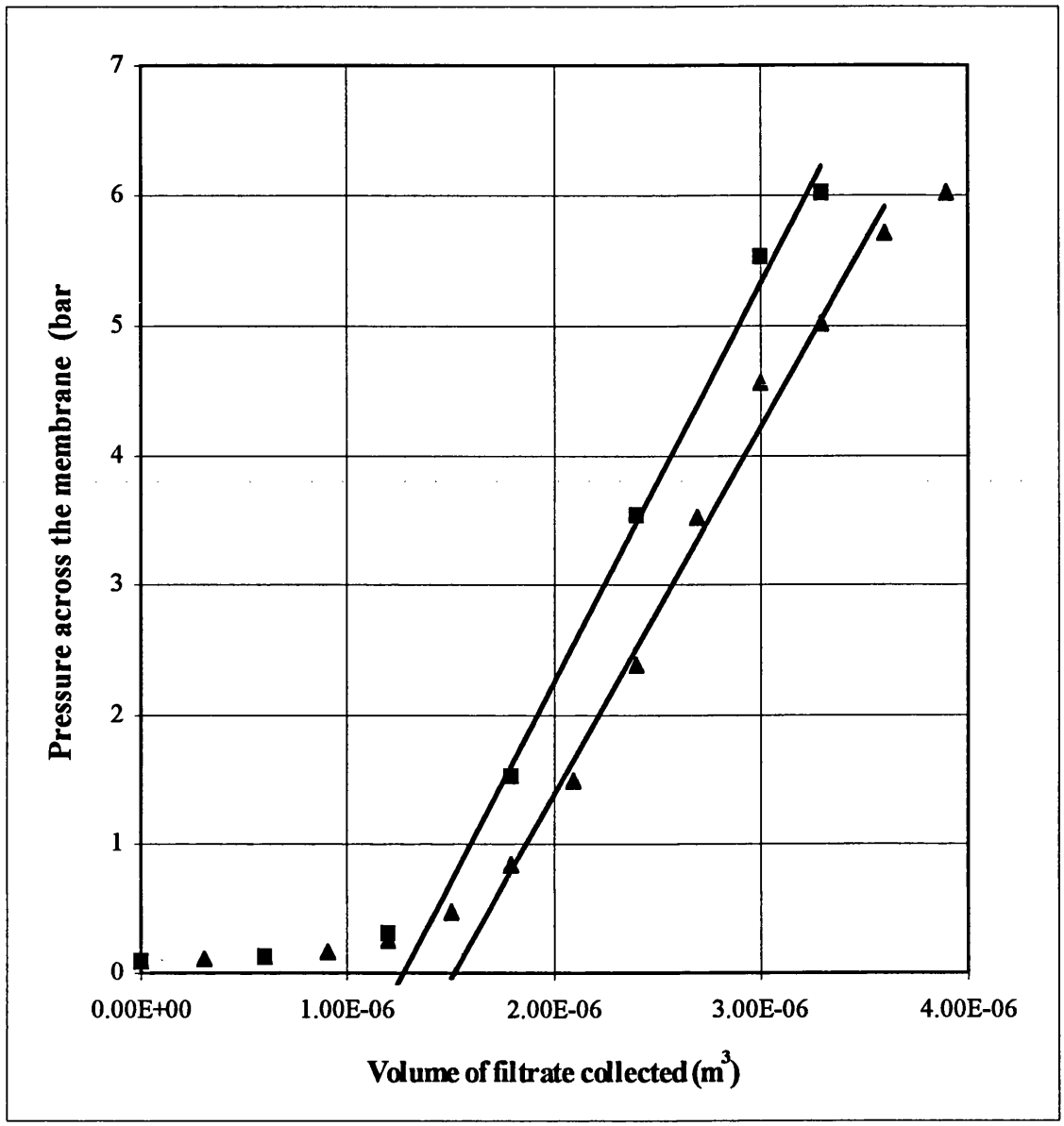

Fig 4.16 Cake filtration analysis for 50:50 water-in-dodecane emulsion at surfactant concentration 1 w/w % (Versapor). -▲- Flux 13 l/h/m^2. -■- Flux 26 l/h/m^2.

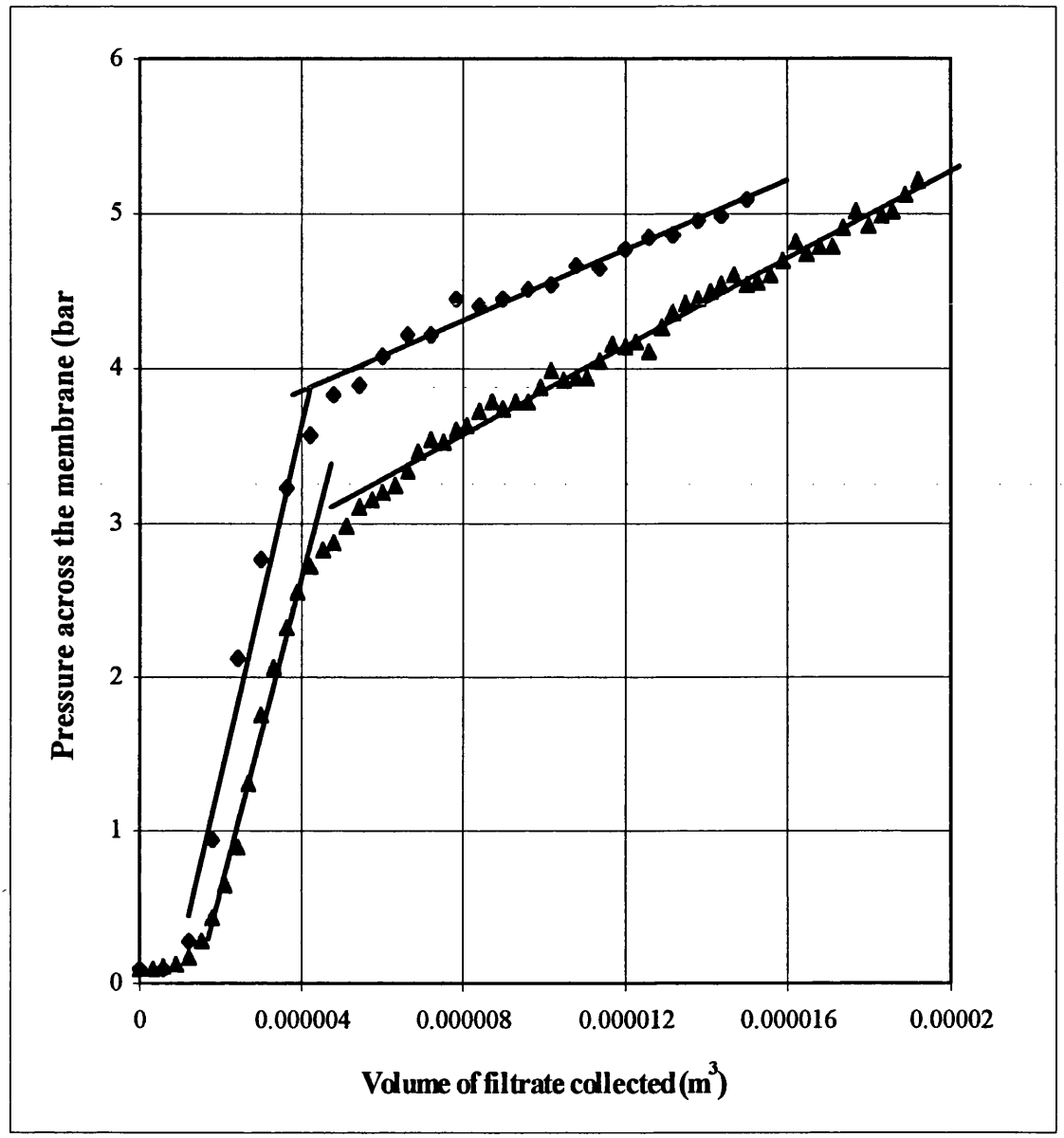

Fig 4.17 Cake filtration analysis for 50:50 water-in-dodecane emulsion at surfactant concentration 1 w/w %. -▲- Flux 13 l/h/m^2. -◆- Flux 26 l/h/m^2.

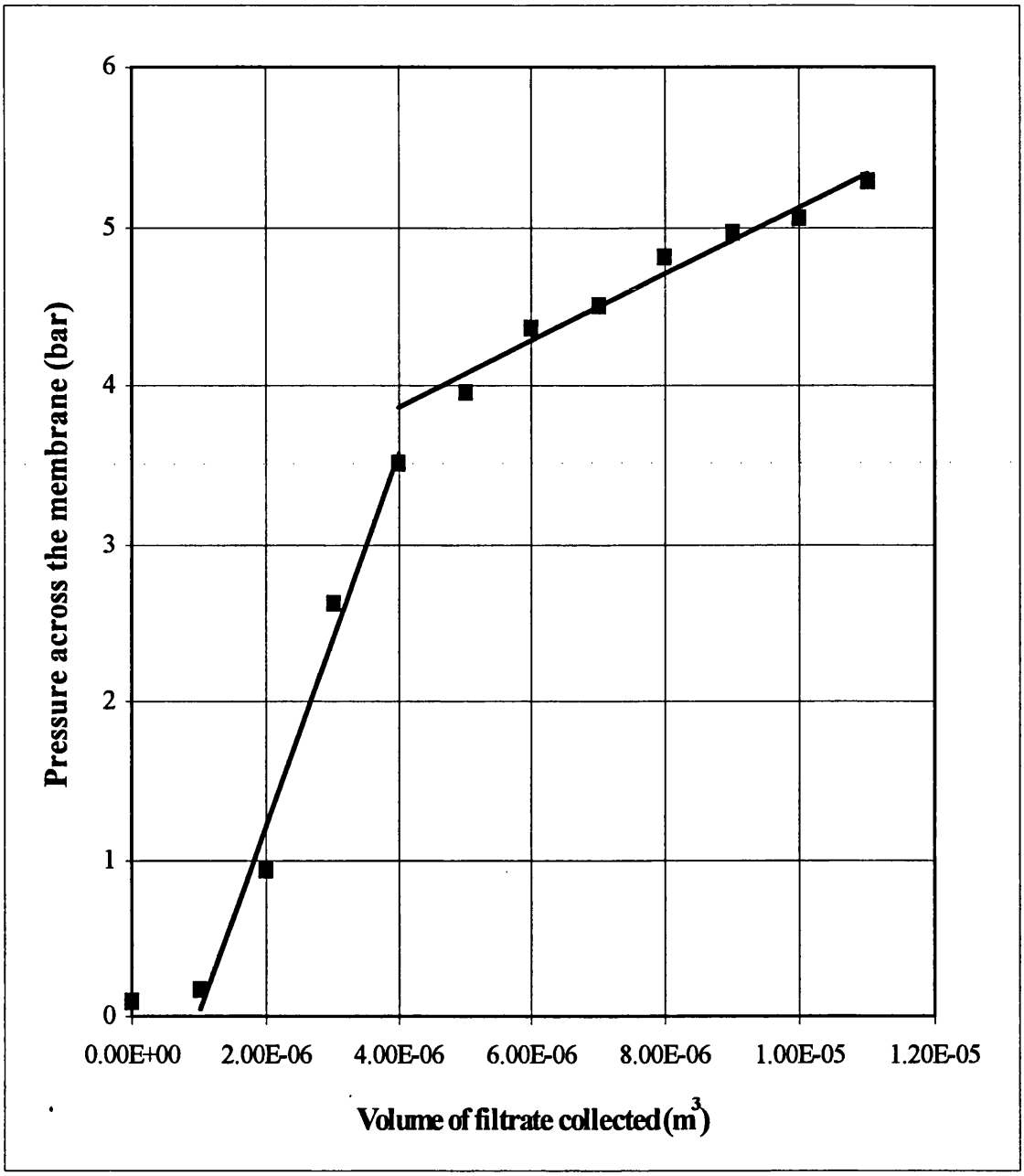

Fig 4.18 Cake filtration analysis for 50:50 water-in-dodecane emulsion at surfactant concentration 1 w/w % and flux 43.3 l/h/m^2.

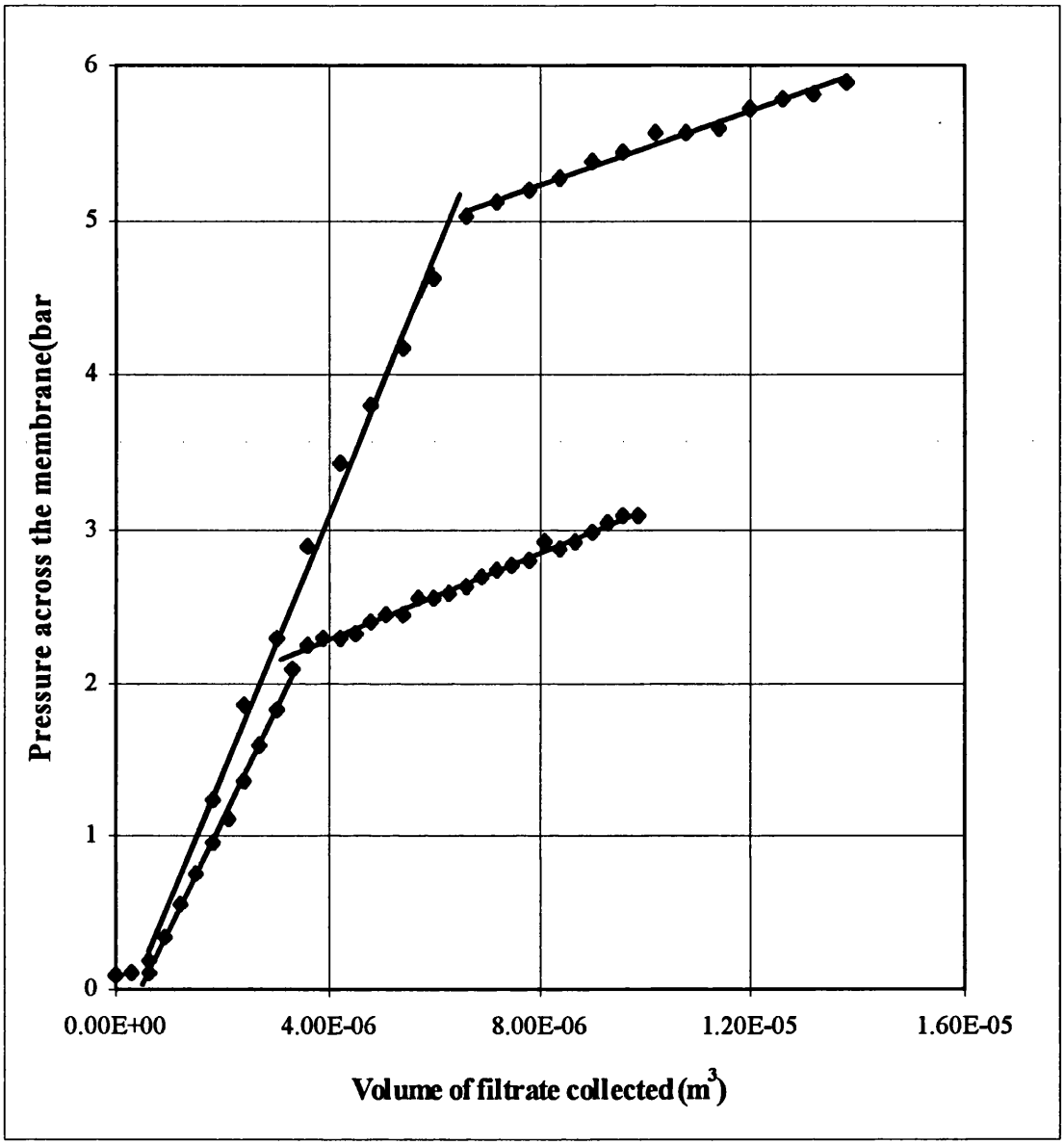

Fig 4.19 Cake filtration analysis for 50:50 water-in-dodecane emulsion at surfactant concentration 1 w/w % (membrane: HTTuffryn). -■-Flux 13 l/h/m^2. -◆- Flux 26 l/h/m^2.

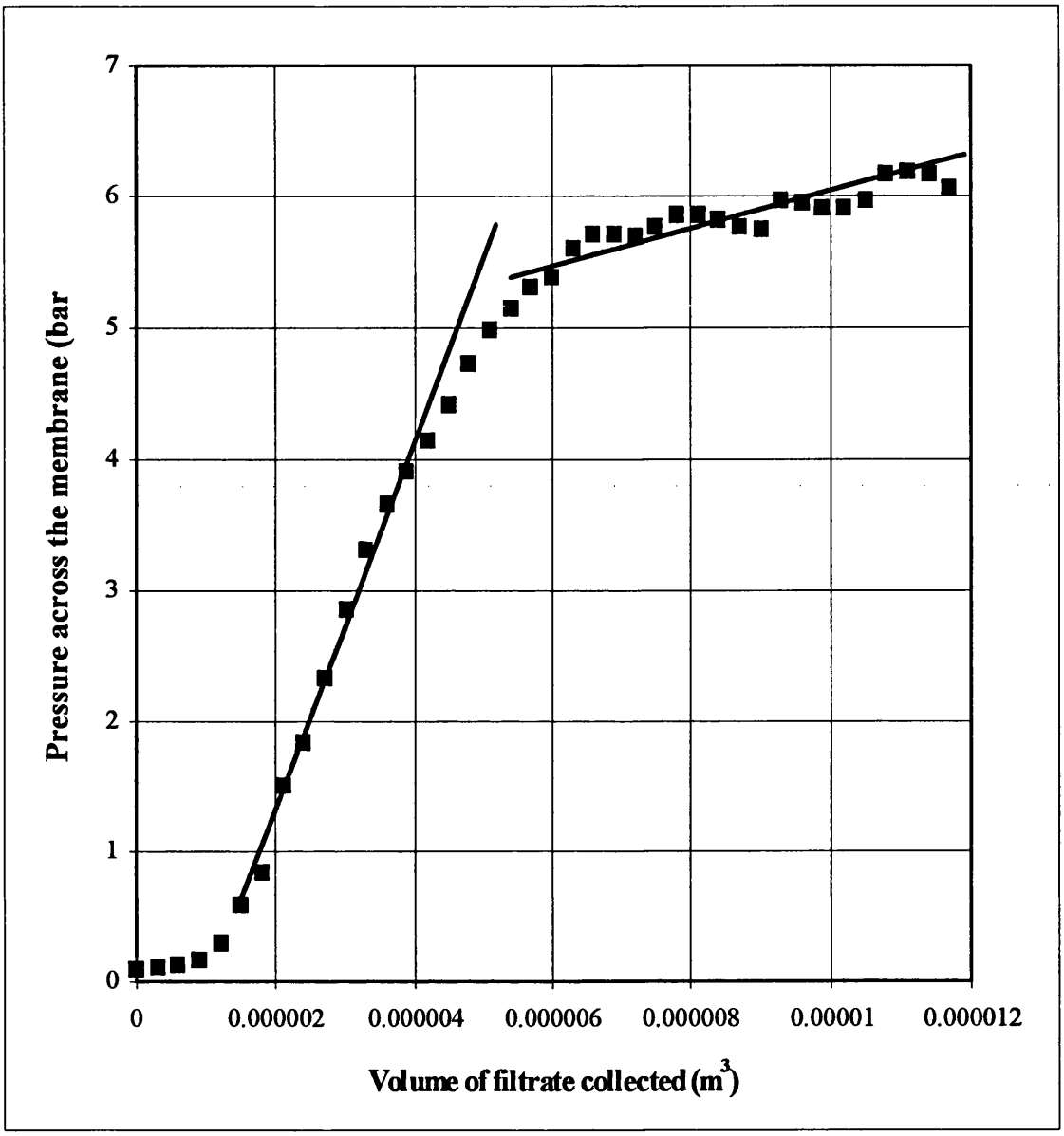

Fig 4.20 Cake filtration analysis for 50:50 water-in-dodecane emulsion at surfactant concentration 1 w/w % (membrane: Nylaflo) at a flux of 13 l/h/m^2.

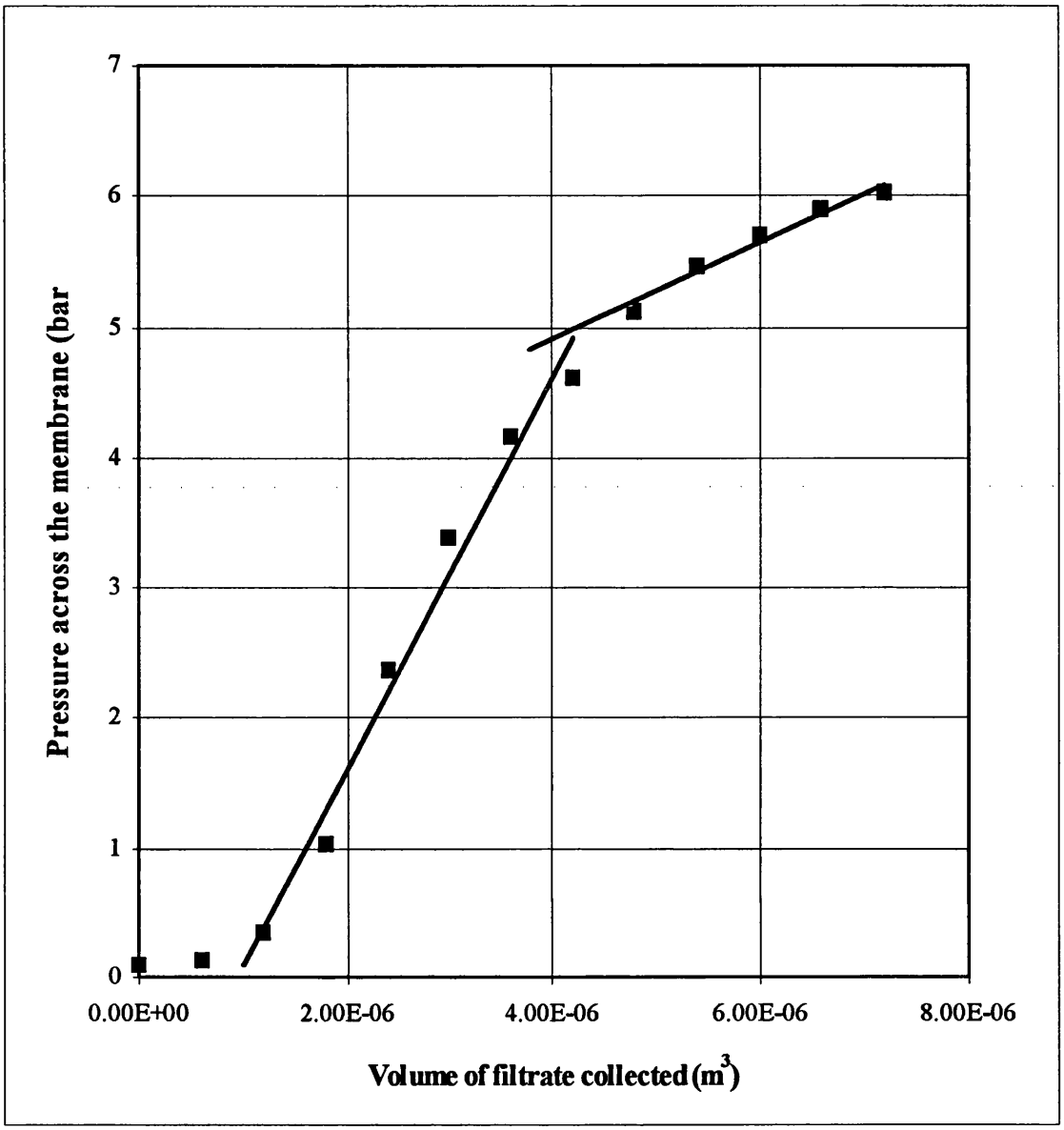

Fig 4.21 Cake filtration analysis for 50:50 water-in-dodecane emulsion at surfactant concentration 1 w/w % (membrane: Nylaflo) at a flux of 26 l/h/m^2.

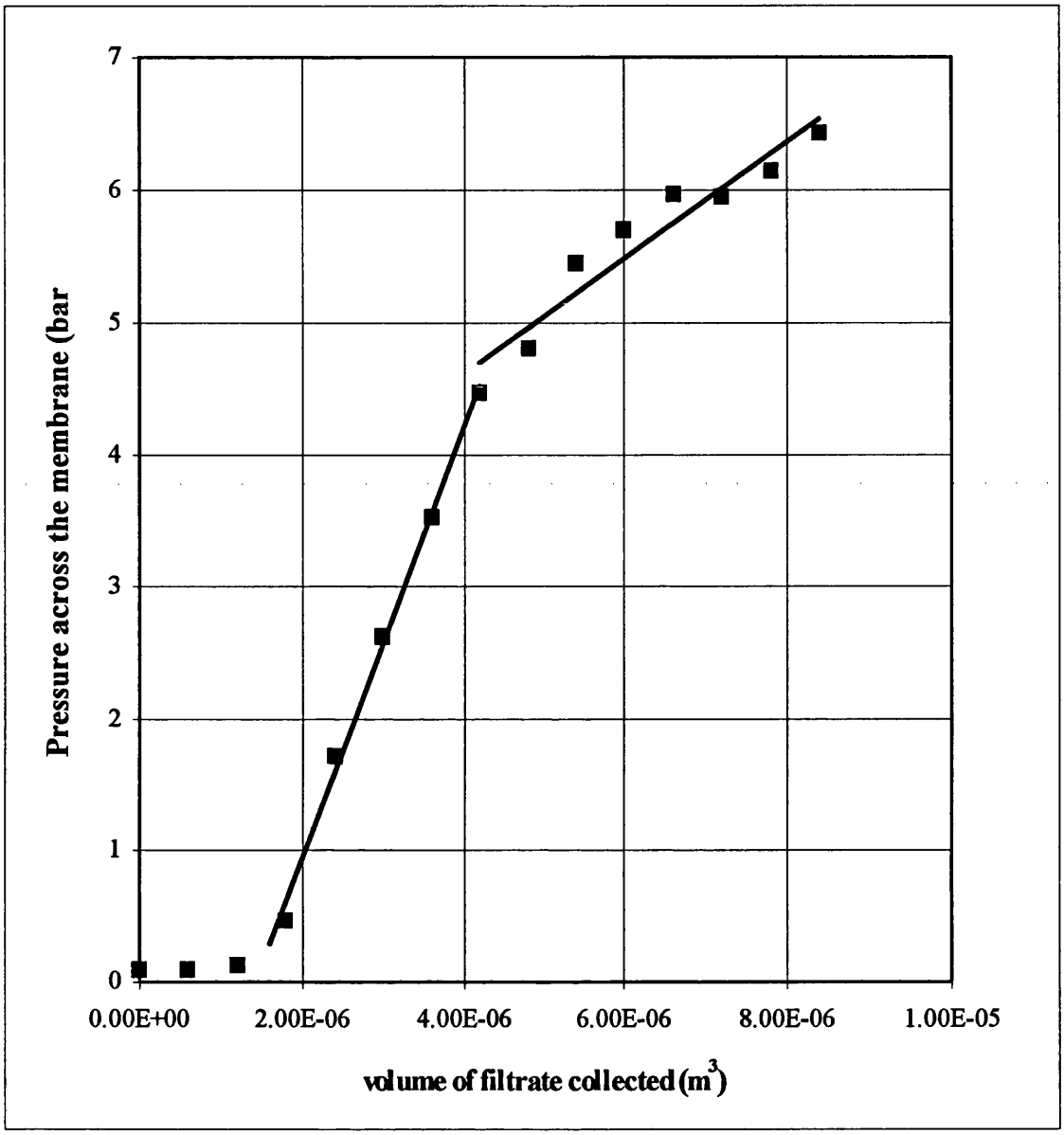

Fig 4.22 Cake filtration analysis for 50:50 water-in-dodecane emulsion at surfactant concentration 2 w/w % and flux 26 l/h/m^2.

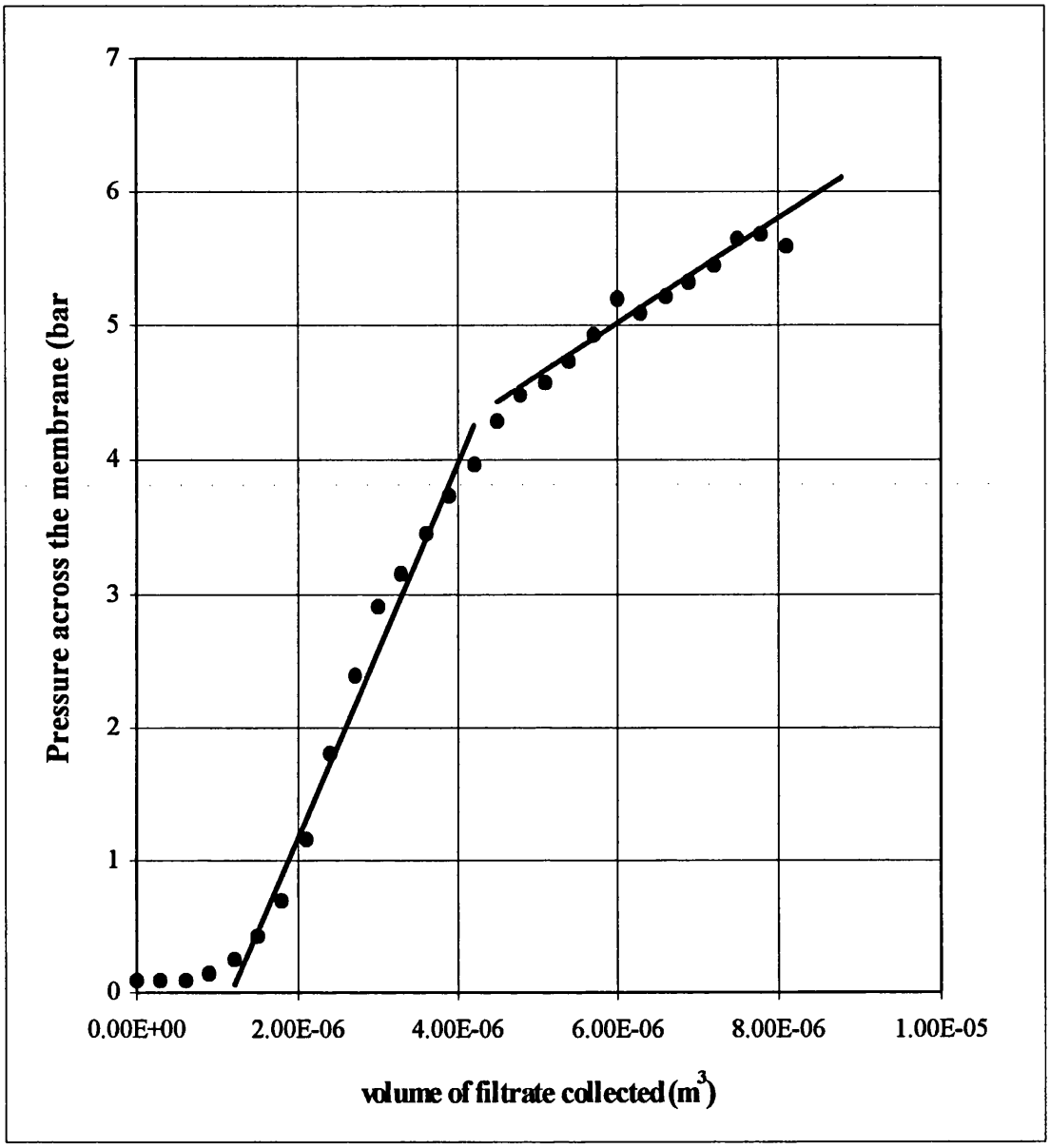

Figure 4.23 Cake filtration analysis for 50:50 water-in-dodecane emulsion at surfactant concentration 2 w/w % and flux 13 l/h/m^2.

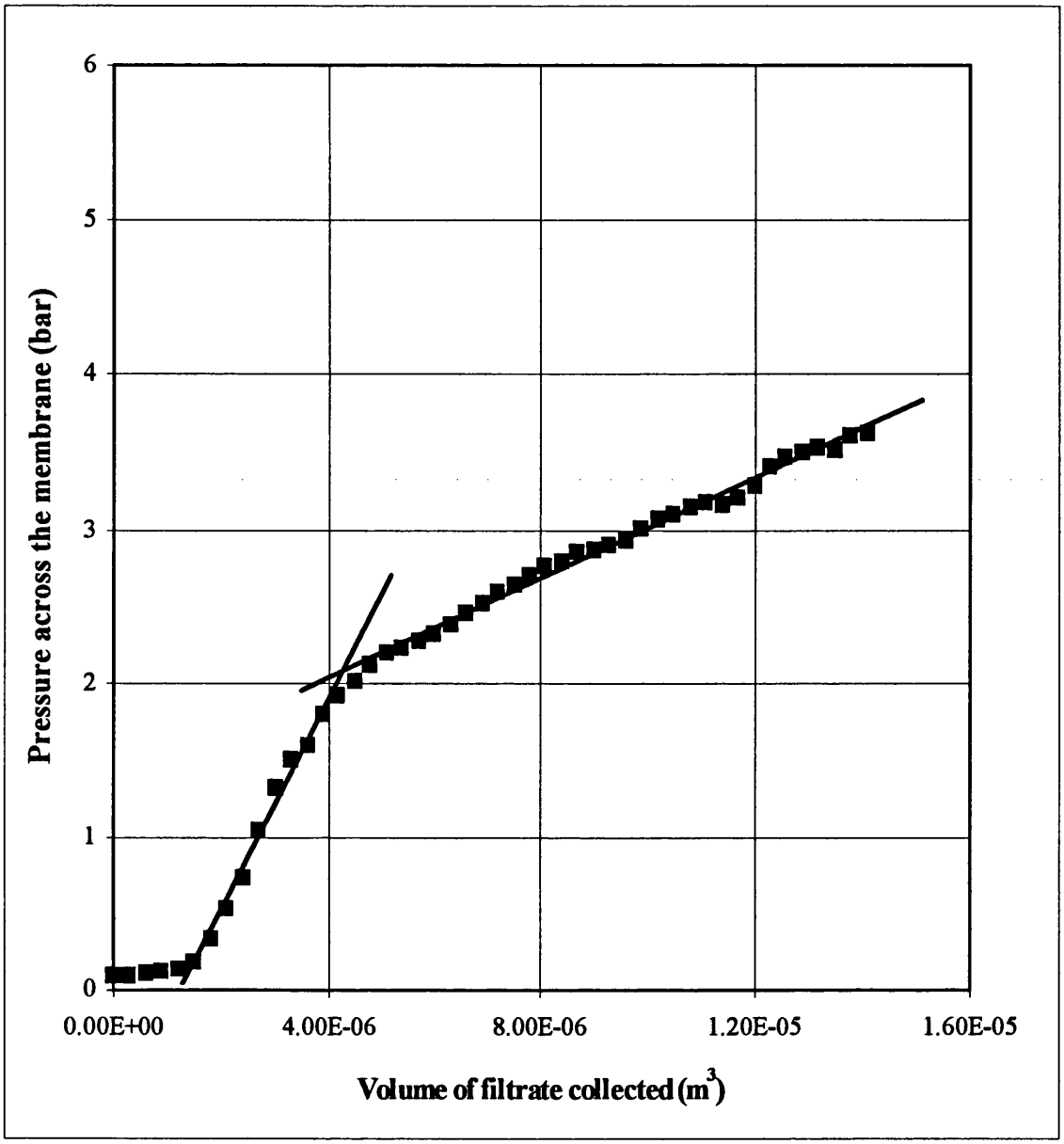

Figure 4.24. Cake filtration analysis for 50:50 water-in-dodecane emulsion at surfactant concentration 1 w/w % (Average droplet size 12 μm) and flux 13 l/h/m^2.

dodecane (1 % Paranox 100) where the droplet size was approx 12 μm. The filtration runs were plotted in terms of pressure (ΔP) vs volume of filtrate collected and there were two regions of cake filtration. The process was stopped at about 4 bar. One flux was examined 13 l/h/m^2. The slope of the linearised portion of the graph, Figure 4.24, was tabulated in Table 4.16. From the slope, the K_c and voidage values were determined.

Table 4.19 shows the dye test results. Dye was added to the cake formed on top of the membrane after the filtration process. The emulsion used in all experiments was water-in-dodecane. The dye methylene blue was only soluble in water and as the droplets were surrounded by surfactant the water was only detected if the droplets had broken. The dye dispersed throughout the emulsion for all of the emulsions except in the case of the 20:80 water-dodecane emulsion. The difference between the dye dispersed in the emulsion with no dispersion is shown in Figure 4.25.

The results in Table 4.20 were the pressures resulting at the end of region 2 in Figures 4.17-4.21. The results show that using the same membrane (Supor 200) and well dispersed emulsion but different fluxes the pressure where region 2 changed to region 3 was not the same. This was not the case for all membranes. Nylaflo membrane and the Supor membrane where the emulsion composition varied resulted in the pressure at the end of region 2 being similar for both fluxes tested.

Table 4.21 shows how the applied pressure compares to the internal pressure (Equation 4.47) of the undeformed droplet. In region 1 the droplets were touching each other and therefore any pressure increase caused distortion of the droplets. The applied pressure at the start of region 2 was greater than the internal pressure before the droplet was deformed and therefore the droplet was no longer spherical but polyhedral. Throughout region 2 the pressure increases. The pressure drop is greatest across the cake of droplets. Therefore, a pressure gradient exists at which the pressure on the droplets near the membrane surface is smallest. The pressure applied to the droplets increases through the cake towards the bulk solution.

Table 4.19 Summary of dye test results from Chapter 3

Membrane/pore size (μm)	Flux ($l/h/m^2$)	Emulsion (composition)	Results
Supor 0.2	13 and 26	50:50 water-in-dodecane (1% Paranox 100)	dye dispersed throughout the cake (Fig 4.25a)
	13	50:50 water-in-dodecane (1% Paranox 100) "homogenizer kept at 8000 rpm"	dye dispersed throughout the cake (Fig 4.25a)
	13 and 26	50:50 water-in-dodecane (2% Paranox 100)	dye dispersed throughout the cake (Fig 4.25a)
	13	20:80 water-in-dodecane (0.5% Paranox 100)	dye did not disperse in the cake (Fig 4.25b)
Nylaflo	13 and 26	50:50 water-in-dodecane (1% Paranox 100)	dye dispersed throughout the cake (Fig 4.25a)
HTTuffryn (0.2)	13 and 26	50:50 water-in-dodecane (1% Paranox 100)	dye dispersed throughout the cake (Fig 4.25a)
Versapor (0.2)	13 and 26	50:50 water-in-dodecane (1% Paranox 100)	dye dispersed throughout the cake (Fig 4.25a)
Supor (0.1)	13	50:50 water-in-dodecane (1% Paranox 100)	dye dispersed throughout the cake (Fig 4.25a)
Supor (0.45)	13 and 26	50:50 water-in-dodecane (1% Paranox 100)	dye dispersed throughout the cake (Fig 4.25a)

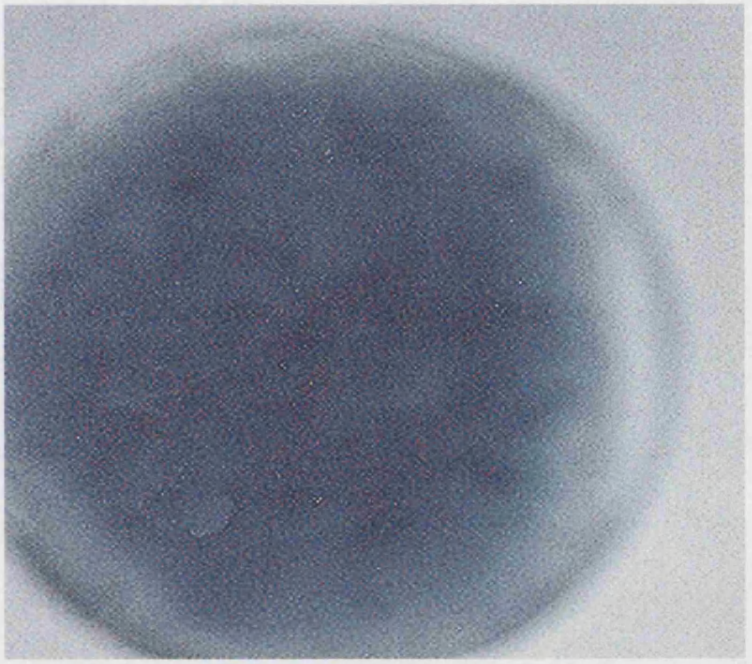

(a)

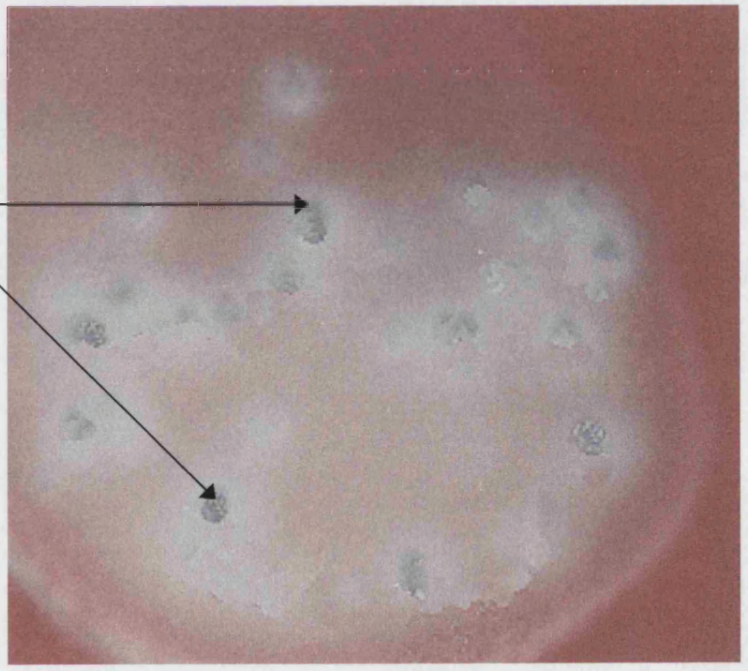

(b)

Figure 4.25 Dye tests on the cake after filtration (a) Dye disperses throughout cake and (b) No dispersion of dye in the cake.

Table 4.22 shows the breakthrough pressure for water when the pores contained dodecane, and dodecane and Paranox 100. The breakthrough pressure of water when the pore contained dodecane and Paranox 100 was very low (< 0.5 bar) for the Nylaflo, HTTuffryn and Supor 200 membranes. However, the breakthrough pressure of water was very high for the Supor 100, Supor 450 and Versapor membranes (> 0.94 bar). It was expected that for the larger pore size of the Supor membrane (0.45 μm) the breakthrough pressure would have been lower than for the Supor membrane with a smaller pore size (0.2 μm).

Figure 4.26 and 4.27 show the SEM of the membranes used. Figure 4.26 displays the membranes where there was no water permeation. The structures were very similar. The membranes appeared to be asymmetric in structure. That is visually it looked like the morphology of the membrane was not the same across the entire thickness of the membrane. The SEM's in Figure 4.26 were taken from the top of the membrane but it is clear that two layers existed. A thin top layer of material which had a tighter structure than the layer below (a porous support layer, with a very open structure). This could have resulted in the membrane resistance increasing.

Figure 4.27 is the SEM for the membranes where water permeation occurred. These membranes appeared some what more symmetrical. The pores were single channels and did not branch as much. This would have resulted in the resistance of the membranes being lower than for those of similar nominal pore size in Figure 4.26. For water to pass through the membranes the breakthrough pressure of water in the presence of dodecane had to be reached. If the membrane consisted of pores that branch and blind the breakthrough pressure would be higher.

Table 4.20 Pressure recorded at the end of region 2 of Figures 4.17- 4.24

Membrane/pore size (μm)	Emulsion (composition)	Pressure at end of region 2 at different fluxes (bar)		
		13	26	43.3
Supor 0.2	50:50 water-in-dodecane (1% Paranox 100)	2.7	3.6	3.5
	50:50 water-in-dodecane (2% Paranox 100)	4.0	4.5	-
	50:50 water-in-dodecane (1% Paranox 100) "homogenizer kept at 8000 rpm"	1.9	-	-
Nylaflo	50:50 water-in-dodecane (1% Paranox 100)	4.6	4.13	-
HTTuffryn (0.2)	50:50 water-in-dodecane (1% Paranox 100)	2.0	4.6	-

Table 4.21 Pressure in droplet compared to applied pressure to determine deformation of the droplet.

Membrane	Emulsion compostion	Flux ($l/h/m^2$)	Applied pressure P_A (bar)	Interfacial tension (Nm^{-1})	droplet size (m)	Internal pressure of the droplet P_I (bar)	$P_A < P_I$ or $P_A > P_I$	Comments
Supor 200	50:50 water-in-dodecane (1 % Paranox 100)	13	0.4.3	0.0062	6.8 E-6	0.036	$P_A > P_I$	polyhedral
		26	0.28	0.0062	6.8 E-6	0.036	$P_A > P_I$	polyhedral
		43.3	0.94	0.0062	6.8 E-6	0.036	$P_A > P_I$	polyhedral
Versapor		13	0.85	0.0062	6.8 E-6	0.036	$P_A > P_I$	polyhedral
		26	0.32	0.0062	6.8 E-6	0.036	$P_A > P_I$	polyhedral
Supor 450		13	0.75	0.0062	6.8 E-6	0.036	$P_A > P_I$	polyhedral
		26	0.93	0.0062	6.8 E-6	0.036	$P_A > P_I$	polyhedral
Supor 100		13	0.33	0.0062	6.8 E-6	0.036	$P_A > P_I$	polyhedral
HTTuffryn		13	0.53	0.0062	6.8 E-6	0.036	$P_A > P_I$	polyhedral
		26	0.18	0.0062	6.8 E-6	0.036	$P_A > P_I$	polyhedral
Nylaflo		13	0.28	0.0062	6.8 E-6	0.036	$P_A > P_I$	polyhedral
		26	0.35	0.0062	6.8 E-6	0.036	$P_A > P_I$	polyhedral
Supor 200	50:50 water-in-dodecane (1 % Paranox 100)	13	0.18	0.0062	12.1 E-6	0.021	$P_A > P_I$	polyhedral
	50:50 water-in-dodecane (2 % Paranox 100)	13	0.25	0.0062	4 E-6	0.062	$P_A > P_I$	polyhedral
		26	0.47	0.0062	4 E-6	0.062	$P_A > P_I$	polyhedral

Table 4.22 Breakthrough pressure of water where the pores are filled with dodecane, and dodecane and Paranox 100.

Membrane/pore size (μm)	Breakthrough pressure water/dodecane (bar)	Breakthrough pressure water/dodecane/Paranox 100 (bar)
Supor (0.45)	1.5	0.94
Supor (0.2)	1.0	0.4
Versapor (0.2)	2.0	1.6
Supor (0.1)	3.0	2.5
Nylaflo (0.2)	1.1	0.46
HTTuffryn (0.2)	0.51	0.28

Table 4.23 Pressure recorded at the end of the intermediate law

Membrane/pore size (μm)	Emulsion (composition)	Pressure at the end of intermediate law at various fluxes (bar)	
		13	26
Versapor (0.2)	50:50 water-in-dodecane (1% Paranox 100)	4.6	5.5
Supor (0.1)	50:50 water-in-dodecane (1% Paranox 100)	2.7	-
Supor (0.45)	50:50 water-in-dodecane (1% Paranox 100)	3.6	3.8

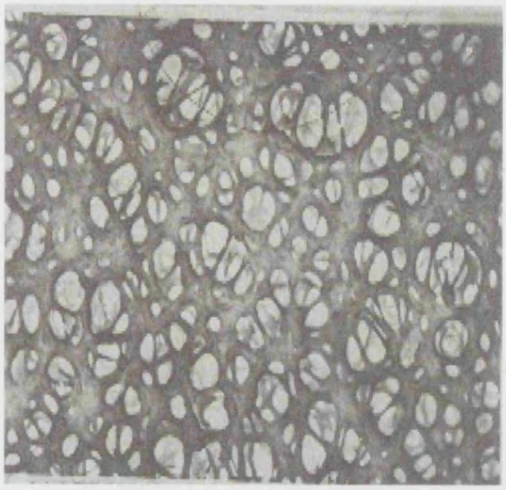

(a)

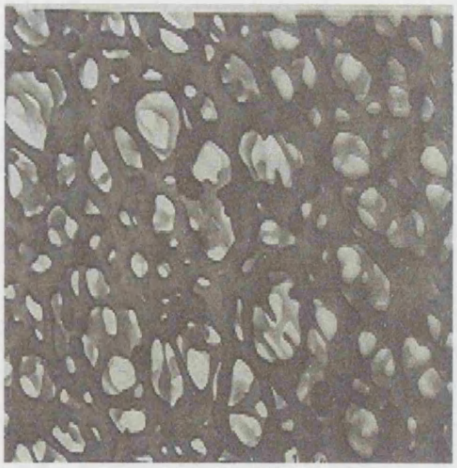

(b)

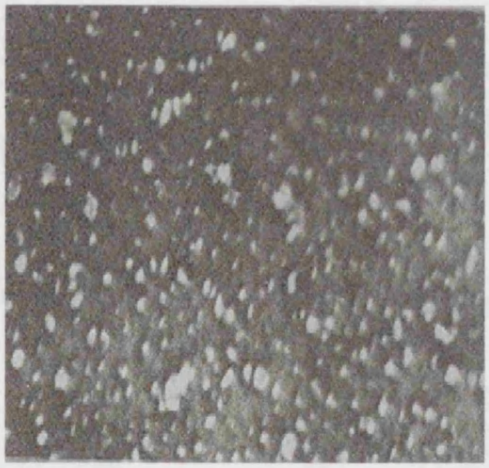

(c)

Fig 4.26 SEM of the top surface of three membranes (a) Versapor 200 hydrophilic membrane (magnification x 7500), (b) Supor 450 hydrophilic membrane (magnification x 7500) and (c) Supor 100 hydrophilic membrane (magnification x 7500).

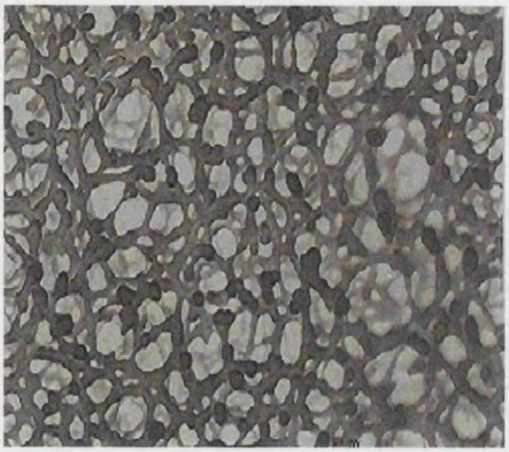

(a)

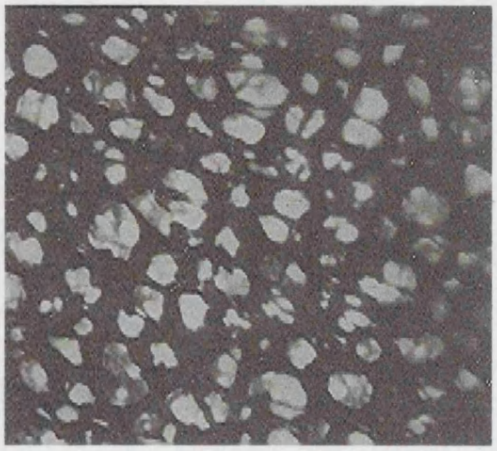

(b)

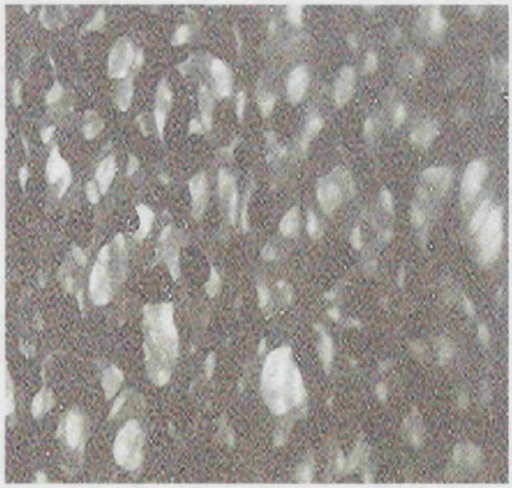

(c)

Fig 4.27 SEM of the top surface of three membranes (a) Supor 200 hydrophilic membrane (magnification x 7500), (b) Nylaflo 200 hydrophilic membrane (magnification x 7500) and (c) HTTuffryn 200 hydrophilic membrane (magnification x 7500).

4.5 Discussion

To make it easy to read through the discussion, Figures 4.28 and 4.29 show which sections are relevant to each step of determining the breakage mechanism. In the results section two similar flowsheets (Figures 4.2 and 4.3) were used to outline the steps involved in analysing the data. Graphs, equations and tables were indicated on the flowsheets. In Figures 4.28 and 4.29 the sections where the results are discussed are indicated on the flowsheets. It was outlined in the results, Section 4.4, that three steps were followed in order to determine which law gave the best fit for each set of data recorded. Steps 1 and 2 were where the filtration laws were applied to part or all of the recorded data. Step 3 was where physical restrictions were invoked when more than one law gave a good fit (Steps 1 and 2) to a set of data points. The aim of the three steps was for only one law to fit a section of each set of data points.

4.5.1 Step 1 and 2

The analysis of the filtration data for a 50:50 water-in-dodecane (1 w/w % Paranox 100) emulsion, homogenised at 8000 rpm was carried out and reported step by step in section 4.4.

All of the filtration laws defined in the theory section were for straight lines and therefore it was clear that one law did not fit all the data for a single experiment. However, it appeared that the models did fit sections of the curves. As we were considering straight lines the coefficient of linear regression was considered the first step in determining which law/laws gave the best fit. The coefficient of linear regression R^2 was calculated for each law and the one that gave the best fit was deemed the most applicable. Great care was taken in deciding where the laws should be applied (law should start and end) as the parameters calculated from the slopes of the graphs would be greatly affected by this. Initially the curves in Figures 4.4 and 4.5 were <u>not</u> split in to regions for fear of misrepresentation.

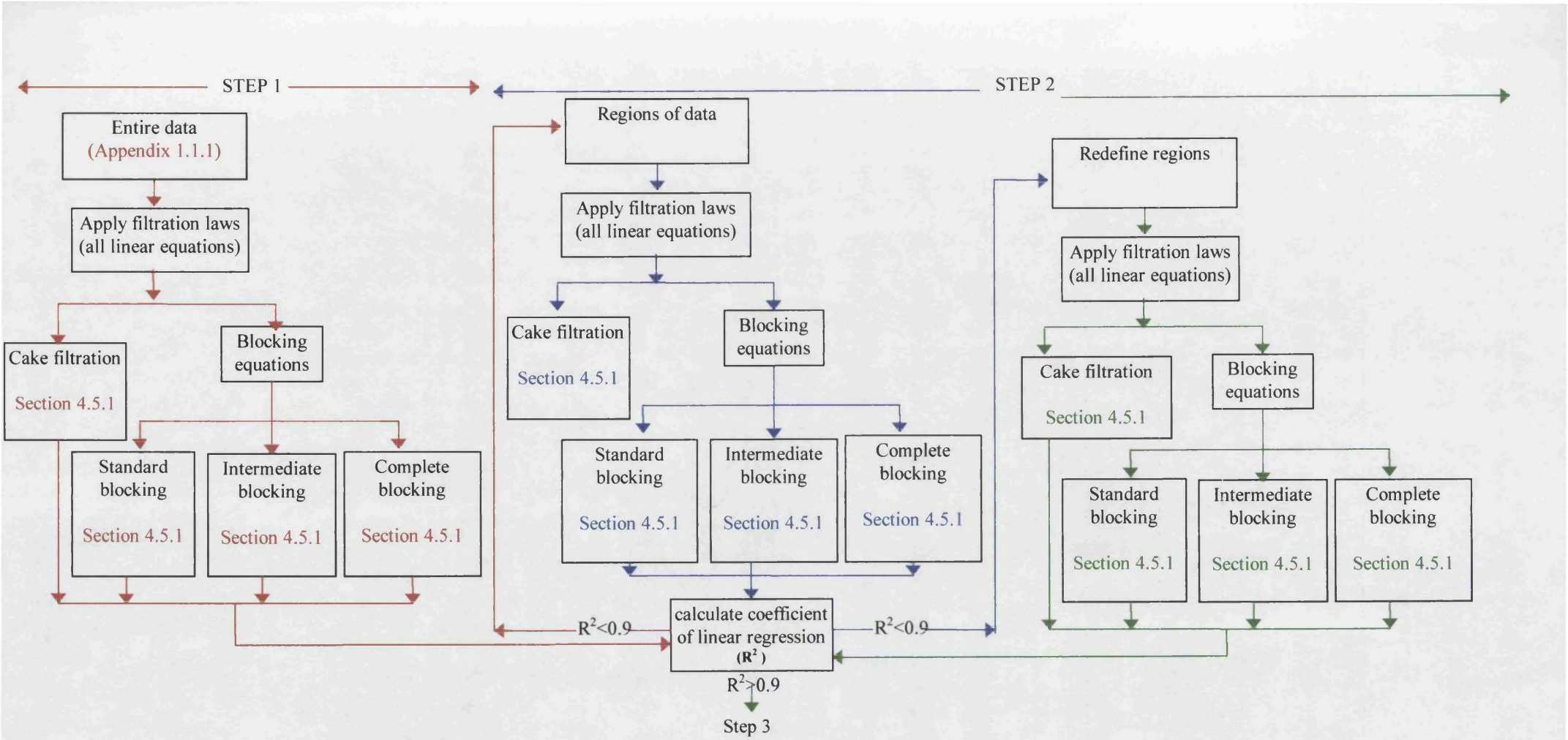

Figure 4.28 flowchart of steps 1-2 for water-in-dodecane (stabilised with Paranox 100) emulsions of various composition and using various membranes at fluxes 13 l/h/m^2 and 26 l/h/m^2.

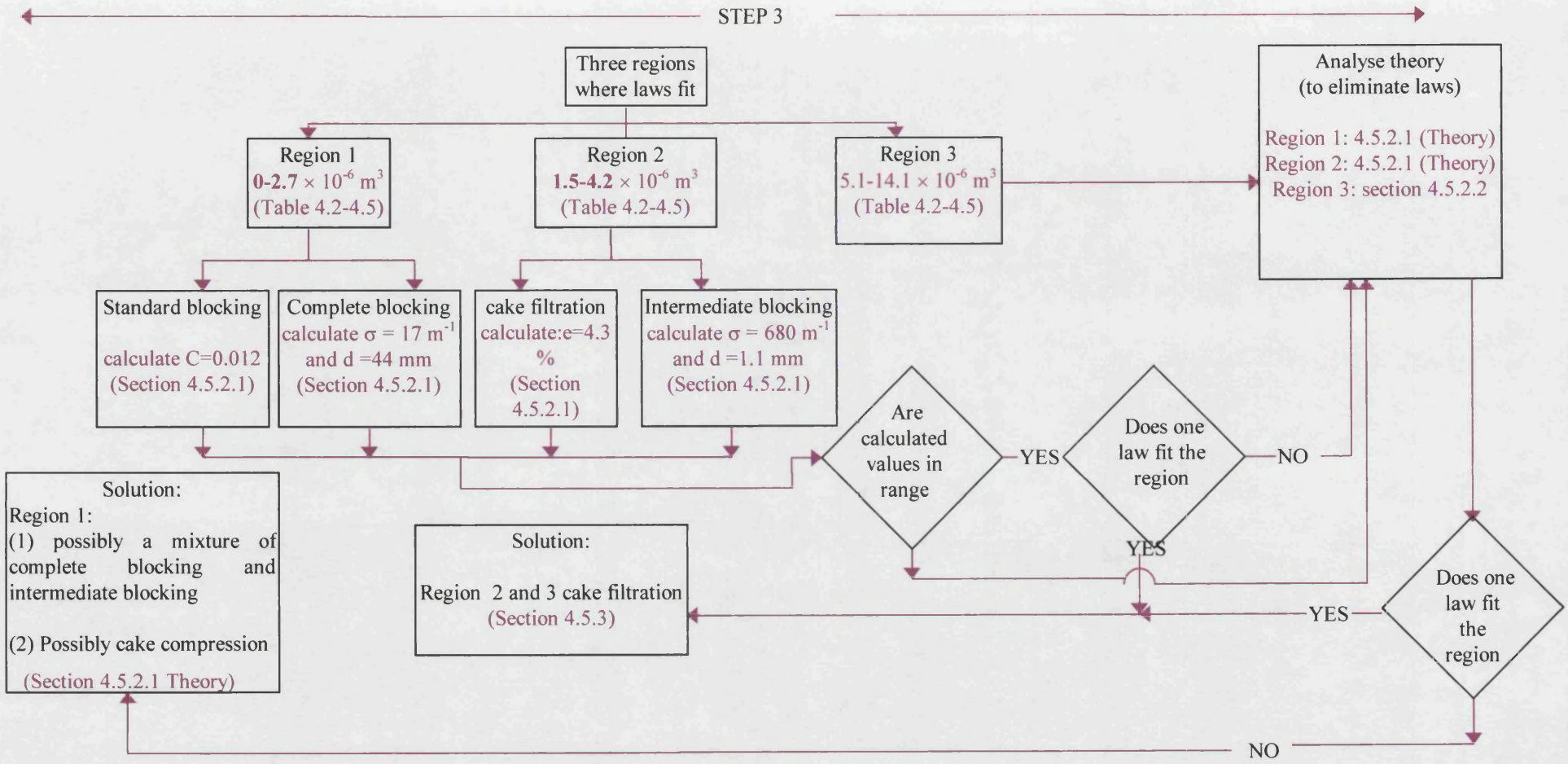

Figure 4.29 flowchart of step 3 for water-in-dodecane (stabilised with Paranox 100) emulsions of various composition and using various membranes at fluxes 13 l/h/m^2, 26 l/h/m^2 and 43.3 l/h/m^2.

The filtration laws were initially applied to sections of the curve (Figures 4.7, 4.9 and 4.10) based on the shape of the curve in Figures 4.6 (curves changed shape in three regions in Figure 4.6a and 4.6d and in two regions in Figure 4.6b and 4.6c). However, it was not clear where the regions started and finished and to avoid misrepresentation the regions were initially overlapped. The filtration laws gave a poor to average fit in all cases and the regions where the laws were applied had to be redefined. Figures 4.8, 4.10 -4.11 and 4.13 show the best fits for each law that were possible and the results were summarised in Tables 4.2-4.5. The cake filtration law gave an excellent fit (R^2 =0.99) between 1.5-14.1×10^{-6} m^3 of filtrate collected (90% of data). Complete blocking only gave a good fit (R^2<0.97) between 0.6-2.1×10^{-6} m^3 of filtrate collected. The intermediate blocking law gave a fit of R^2=0.97 and R^2=0.98 for two regions of the data 1.2-3.3 ×10^{-6} m^3 of filtrate collected and 5.1-14.1×10^{-6} m^3 of filtrate collected respectively. The standard law gave a good fit (R^2=0.97) for two regions of data 0.6-2.7 ×10^{-6} m^3 of filtrate collected and 5.1-14.1×10-6 m^3 of filtrate collected.

The analysis of the filtration data for all experiments was carried out similar to the 50:50 water-in-dodecane (1 w/w % Paranox 100) emulsion, homogenised at 8000 rpm and the results were summarised in Tables 4.2-4.5. Cake filtration, standard blocking law and complete blocking laws were tested across three regions. However, these regions (volume of filtrate collected) were different for each law and each experiment. Therefore no great importance was connected to the volume of filtrate collected when the change occurred. The region was allocated to the change in shape of the graph depending on the filtration law applied (for example in Figure 4.4 it was clear that the shape changed in three regions). Regions 1,2,and 3 for the standard law (Table 4.4), complete blocking law (Table 4.3) and cake filtration law (Table 4.2) were for approximately the same range of data. However, the intermediate law (Table 4.5) in region 1 was in most cases for a region between 1 and 2 for all the other laws. In order to discuss the results in Tables 4.2-4.5 the three regions are indicated on the plot of pressure across the membrane vs volume of filtrate collected (Figure 4.30). The results showed that complete blocking and standard blocking gave

a reasonable fit in region 1 (R^2>0.90) for all membranes and emulsions used except for the HTTuffryn membrane, where only standard blocking gave a R^2>0.90. In region 2 (Figure 4.30) cake filtration gave an excellent fit for the entire range and the intermediate law gave a good fit across region 1 and 2. However, it did not apply across the entire range. In the third region all of the filtration laws gave a good fit R^2>0.90. Since the cake filtration gave an excellent fit (R^2>0.99) across 99 % of the data in regions 2 and 3 it was initially considered that cake filtration was the controlling mechanism. However, there was a possibility that one of the other mechanisms could have accounted for the results in regions 2 and 3 therefore the coefficient of linear regression was considered not to be enough to determine the law which applied to each region.

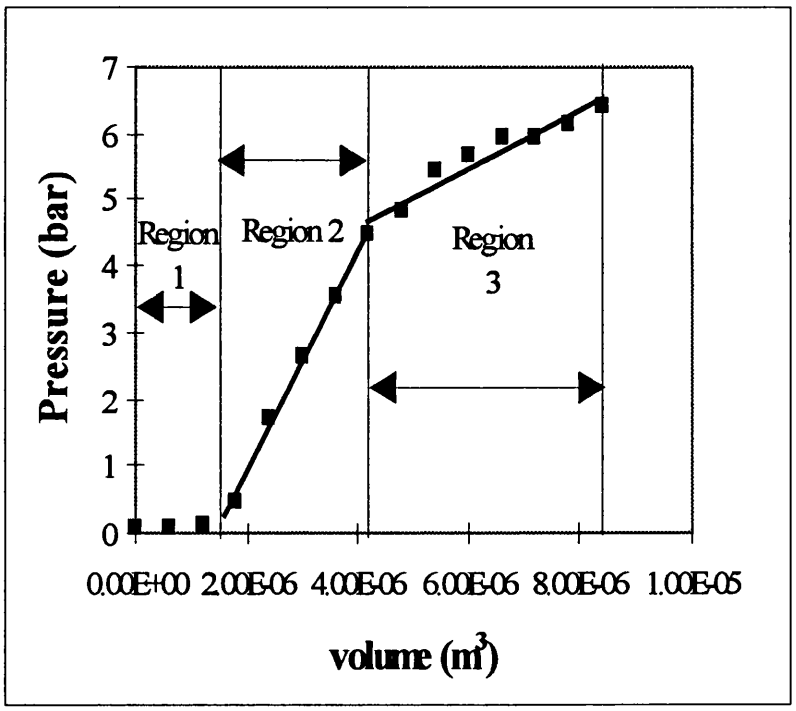

Fig 4.30 The regions in which the filtration is represented in the discussion.

4.5.2 Step 3: Analysis of constants and theory

4.5.2.1 region 1-2

Intermediate blocking (region 1-2)

The blocking law theory is based on the clogging coefficient σ value being an intrinsic property of the fouling ability of the emulsion and it does not depend on the membrane. Therefore, for different membranes where the emulsion used was the same, the clogging coefficient was expected to be the same. This assumption seems to be a good approximation as the values of the clogging coefficient were in the same range for the same well dispersed emulsion (Tables 4.12 and 4.14) and for all different membranes (different material, pore size and structure). When the emulsion properties were varied it was expected that the clogging coefficient would change. For the three emulsions in Table 4.13 the droplet size was 4μm, 6.8 μm and 12.1 μm but the clogging coefficients were in the same range for each emulsion. It was considered that the clogging coefficients were similar because the droplets form aggregates. These aggregates were very large such that they were not dependent on the individual droplet size. Even though the model gave a good fit in region 1-2 intermediate blocking was unlikely to have been the filtration mechanism. The emulsions used were 50 vol % internal phase and at these concentrations a cake would have formed in the first few seconds.

Complete blocking (region 1)

The pressure of the membrane depends on the global term $\frac{\sigma V}{R_m \mu Q(1-s_v)}$ at a given Flux, viscosity and particle concentration the fouling rate is proportional to σ/R_m.

The theory predicts that fouling would be worse for a membrane with a low membrane resistance, this is because at a lower resistance at given Flux the pressure required to block the pores will be lower The results in Tables 4.6-4.7 were for

membranes where the resistance changed. The values of σ/R_m were in the same range for all membranes. Even the Supor 100 membrane where the resistance was very high, (Table 4.4) compared to all the other membranes, resulted in a value similar to the other membranes. Also the calculated droplet diameter in all cases was $\times 10^{-3}$ m. At such a large droplet size compared to the pore diameter (0.1,0.2 and 0.45 μm). The fact that there was no relationship between the membrane resistance and σ/R_m, and the calculated droplet size was so large lead to the conclusion that complete blocking law was not the mechanism in region 1.

Standard blocking (region 1)

The standard law is such that each particle arriving to the membrane is deposited (adsorption) on to the pore walls leading to the decrease in the pore volume. For this to apply the droplets need to be smaller than the pores. The droplet size in the emulsions used was >1 μm (average droplet sizes for the three emulsions in Table 4.10 were 4 μm, 6.8 μm and 12.1 μm) and the average pore size of the membranes was 0.45 μm for the Supor 450 membrane (Table 4.9), 0.1 μm for the Supor 100 membrane (Table 4.9) and 0.2 μm for all other membranes (Tables 4.9-4.11). In all cases the emulsion droplets were greater than the membrane pore size. It was clear that the standard law could not be considered for the adsorption of water droplets on the pore walls. However, during this initial period dodecane and surfactant permeated the membrane and the surfactant could have adsorbed on the pore walls. The measured surfactant concentration in the emulsions was 0.02 (mass fraction) for one of the emulsions in Table 4.10. All other emulsions (Table 4.9 and 4.11) had a surfactant concentration of 0.01 (mass fraction). The calculated values of the concentration (Tables 4.9-4.11) were in the same range but were much higher than the measured values. The calculated values for the emulsion with 0.02 surfactant was close to the measured value but it was considered that standard blocking was not the mechanism in region 1 because the interfacial tension measurements of the permeate, which were recorded in Chapter 3, were the same value as that of the emulsion before

emulsification. In order for them to be the same the surfactant concentration could not have reduced very much in the permeate (only a small amount of adsorption on the pore walls would have occurred).

Cake filtration (region 2)

The cake filtration gave a good fit in regions 2 where R^2>0.97 (90% of R^2>0.99) and region 3 R^2>0.97. This section discusses the analysis the constants (K_c and cake voidage) from the calculated gradient to determine if they were values to be expected. Kc was calculated directly from the gradient. Equation shows that K_c is a function of the cake specific resistance and mass of cake per unit area. All of the constants except the voidage were measured and the results were reported in Chapter 3. The voidage was calculated from the gradient of the ΔP vs Volume of filtrate collected (Figures 4.14-4.23).

The calculated values for the slope of the graphs were tabulated in Tables 4.15-4.17. From this data, values of K_c and voidage of the cake were calculated. Usually the specific cake resistance is calculated directly from the slope. In this case it was not possible because of the following:

The last term in Equation 4.35 is the concentration of the cake, where m is a function of the voidage of the cake. In order to determine the specific cake resistance directly from the slope of the line a value for the voidage would have had to be substituted because specific cake resistance and m were both a function of voidage.

Published work by Lipp et al (1988) showed that calculated values for α were taken from the slopes without having to put a value in for the voidage. The system was constant pressure and the filtration equation was as follows.

$$\frac{t}{V} = \frac{R_m \mu}{\Delta P A} + \frac{K_c}{2\Delta P} V \qquad \text{...(4.48)}$$

$$\text{slope} = K_C = \frac{\alpha\mu C}{A^2} \qquad ..(4.49)$$

Where t is the filtration time, V is the volume of the filtrate, R_m is the membrane resistance, μ is the filtrate viscosity, ΔP is the pressure difference, A is the membrane area, α is the cake specific resistance and C is the solids concentration in the slurry.

Equation 4.48 and 4.49 only consider the concentration of the solids in the feed (slurry) and as such the volume of solids and liquid retained in the cake is considered to be negligible. At low concentrations this assumption is considered to be reasonable. The emulsions used by Lipp et al (1988) were oil-in-water where the concentration of the oil phase ranged from 0.5-10 vol %, which were low dispersed phase concentrations.

The emulsions used in this study were of high concentration 50 vol % and therefore only considering the feed concentration of dispersed phase would have lead to high errors. Correcting this meant that the specific cake resistance could not be calculated directly from the slope.

The results in Tables 4.15-4.17 showed that the voidage of the cake was in the same range for all membranes and emulsions used. The value of approx 5% was to be expected as the droplets were packed close together and deformed due to depletion of the dodecane (continuous) phase. This is explained in detail later (section 4.5.6)

Theory

Analysis of the constants in regions 1 and 2 was not enough to determine which of the filtration laws applied and therefore the definition of the theory needed to be considered.

Region 1

The lack of knowledge concerning the mechanism occurring during the initial period of filtration results largely from the short duration of its existence. As the initial period was so short it was not surprising that a fit of the blocking laws was not conclusive. The short duration meant that only a few data points were available and therefore applying any of the laws would have resulted in possible misrepresentation. However, the initial period can be considered to be due to one or more of the following:

* Pore blocking (complete, standard or intermediate) [Grace, 1954]

* This initial lag period can be attributed to imperfect retention of fine particles [Hlavacek and Bouchet, 1993 and Wei-Ming et al, 1997]. However, during the initial period no water was detected in the permeate.

* compressible cake filtration. Negative intercepts on P vs V plots and thus negative filter medium resistances is a well known phenomenon in compressible cake filtration [Kamst et al, 1997]. Tiller et al (1995) reported that the specific cake resistance may change many fold for highly compactible material. If the slurry is dilute and cake build-up is slow and there will be a long period before there is any effects due to variable specific cake resistance. For concentrated slurries the initial period with variable specific cake resistance may last no more than a few seconds. The emulsions used in this study were highly concentrated (50 vol %) and deformable also the initial period lasted a few minutes. Therefore the initial period could be explained by compressible filtration..

Granger et al (1985) studied the initial filtration for periods of the order of a few minutes. They found at concentrations as low as 20μl/l a cake formed in the first few minutes even when the particle size was smaller than the pore size. In this study the concentrations were as high as 50 vol % (internal phase) and the pressure drop during

this period could have been cake filtration. The fact that the pressure did not increase linearly with volume of filtrate collected could have been due to the deformable nature of the droplets.

As the particle concentration in the feed is decreased below 0.01 % by volume the duration of the initial period of filtration before formation of a cake is extended to such an extent that study of the mechanism involved becomes practical [Grace, 1954 and Wei-Ming et al, 1997]. Granger (1985) showed that for concentrations as low as 20 ul/l a cake formed in the first few minutes. Which brings us to region 2 of the experiments in this Chapter. In this region water was not permeating the membrane until the end and therefore at concentrations of 50 % by volume of droplets the filtration law could not according to the theory have been one of blocking laws.

Region 2

Analysis of the constants showed that both cake filtration and intermediate blocking gave a good fit to the data in region 2 and 1and 2 respectively. However, intermediate blocking according to the theory results in the reduction of the free surface of the pores and therefore an increase in the membrane resistance. If this was the case the breakthrough pressure of water for the Supor 450 (0.94 bar, Table 4.22), Supor 100 membrane (2.5 bar, Table 4.22) and Versapor (1.6 bar, Table 4.22) would have been reached (Table 4.23) and therefore water would have permeated through the membrane. As this was not the case it was concluded that intermediate blocking was not the filtration law that applied across regions 1 and 2. Also at the end of the filtration runs the module consisted of a concentrated emulsion (Chapter 3) directly above the membrane. This concentrated emulsion was a fully formed cake.

The membranes where water permeated through, were Supor 200, Nylaflo and HTTuffryn and it was considered that region 2 for these membranes was also cake filtration and not intermediate blocking. The type of blocking equation applicable to a given system depends on the operating conditions. In particular the equation

applicable to a given set of data depends on the size and concentration of the particles in the suspension to be filtered and on the pore size of the membrane used [Granger et al, 1985 and Hermia, 1982]. The constants calculated from the gradient of both laws (cake filtration and intermediate blocking) did not depend on the properties of the membrane used and as the emulsion used in the experiments for the Supor 100, Supor 450 and Versapor membranes was the same as the emulsion used in the Supor 200, Nylaflo and HTTuffryn membrane experiments. It would be expected that the same filtration law would apply to region 2. It as already been mentioned that for the Supor 200, Nylaflo and HTTuffryn membranes water permeated through the membrane at the end of region 2. This was due to the breakthrough pressure of water (when the pores contain dodecane and Paranox 100) being reached for these membranes (Section 4.5.5 discusses this in detail).

Grace (1954) reported that when filtering suspensions containing more than 1 vol % of solids the pore blocked with cake in the first few seconds or fraction of a second and a continuous cake covered the surface of the membrane. This cake immediately become the active filter surface and the particle passage through or penetration of the filter medium (which causes plugging) occurred for only a very short period at the start of the filtration cycle . Although a short duration, this plugging period eventually resulted in blinding of the filter medium.

It is clear that cake filtration occurred in regions 1 and 2. In region 1 the increase in cake resistance was due to the deformable nature of the droplets (the specific cake resistance changed many fold until at the end of region 1). In region 2 the straight line indicated that the specific resistance of the cake remained constant and any further compression of the cake was only small. Therefore the pressure increase was due to an increase in the cake thickness.

4.5.2.2 Region 3

In region 3 water and dodecane permeated through the membrane at a ratio of approximately 50:50. It was unclear exactly how much water was in the permeate but it was clear that the amount retained by the membrane was small and therefore region 3 was considered to be a region of dilute filtration. In step 2 it was determined that all the laws gave an acceptable fit $R^2>0.9$ in region 3. However, unlike region 1 and 2 calculation of the constants was not straight forward, due to the fact that the amount of water retained (s) by the membrane was not measurable. In order to eliminate the laws that applied to region 3 the theory of each law was taken into consideration. Hermia (1982) indicated the type of equation applicable to a given system depends on the operating conditions . In particular the equation applicable to a given set of data depends on the size and concentration of the particles in the suspension to be filtered and pore size of the membrane used.

Standard law

The standard law assumes that the number of pores remains constant but the pore volume decreases proportionally to the filtrate volume by particle deposition on the pore walls [Mueller et al, 1997]. Therefore the droplets in the emulsion must be smaller than the pores but in all cases the droplets were much larger than the pores. There was a possibility that the surfactant (Paranox 100) could have absorbed to the pore walls which would have resulted in pore narrowing. However, interfacial tension experiments (Chapter 3) showed that the concentration of the surfactant in the permeate was the same as the surfactant concentration in the feed therefore the surfactant (Paranox 100) did not absorb on the pore walls of the membrane.

Complete blocking law

The complete blocking law assumes that the membrane consists of parallel pores that each particle reaching the membrane participates in blocking by sealing off pores. The

droplets in the emulsion in the cake had partially coalesced which was shown by dye tests (Table 4.19) and the two phases in the permeate were two distinct phases where the surfactant concentration was unchanged in the dodecane phase (Chapter 3). It was therefore considered that the droplets would not have plugged the pores as this would have required the surfactant to have remained around the droplets before entering the pores. Experiments (Table 4..19) have shown that the emulsion was broken before entering the membrane pores.

Intermediate blocking

The intermediate law is derived assuming that in addition to particles blocking and sealing off pores the particles reaching the membrane can also dispose on other particles [Granger et al, 1985]. In region 2 a cake formed and therefore the cake was between the membrane and new particles reaching the membrane in region 3. It was considered that the intermediate law did not apply.

Cake filtration

Increase in resistance according to the definition is due to an accumulation of particles as a filter cake. It was clear that cake filtration occurred in region 3. In region 2 a cake formed and if water did not permeate through the membrane (Supor 450, Supor 100 and Versapor) the pressure increased until the maximum pressure of the system was reached (6 bar). When water permeated through the membrane, (Supor 200, HTTuffryn and Nylaflo) at the end of region 2, the gradient of the slope decreased due to the fact most of the dispersed phase passed through the membrane. The exact amount of water retained by the membrane was unknown but a value of 1vol % (0.01mol %) was considered a reasonable value. Tables 4.16-4.17 show the K_c and cake voidage values calculated for this region where the mass fraction of solids (s) was 0.011. Tables 4.15 and 4.17 show that for each flux the K_c and voidage values were in the same range whatever membrane was used. This was to be expected as the voidage was a property of the cake and did not depend on the properties of the

membrane. The voidage of the cake was at the expected value of < 5 vol % (droplets will not rupture in the cake at a higher value) [Bibette, 1992] for all emulsions and membranes used (See Section 4.5.6).

4.5.3 Cake filtration (Regions 2 and 3)

It was determined in Section 4.5.1-4.5.2 that cake filtration was the filtration law that fit the data best. However the calculated value of the voidage of the cake was not explained and the relationship between different operating conditions, membrane type (Pore size, material and structure) was not compared. In this section it was assumed that a cake was being formed during filtration. Also the mechanism that resulted in the breakage of the water droplets is investigated and a relationship is explained between the different experiments.

Figures 4.14-4.24 were the filtration runs plotted in terms of pressure (ΔP) vs volume of filtrate collected. The data was shown for the entire run and there were two regions of cake filtration for each graph. In order to discuss the graphs they have been sectioned into three regions (Fig 4.30). In region 1, the pressure increased only slightly or not at all (Section 4.5.2.1). In region 2 (Section 4.5.2.1), the first cake model was tested and in region 3 the cake changed and the second cake model was shown to fit (Section 4.5.2.2).

4.5.3.1 Cake filtration in region 2

When a cake under constant flux starts to be created pressure should increase slowly and should be independent of the membrane pore size, given that the cake covers most of the porous area. It would therefore be expected for the same well dispersed emulsion (membranes were of different pore size but all hydrophilic) the value of K_c would be almost constant for all membranes if, as assumed the cake has a unique compaction and thickness. The results in Table 4.15 (region 2) show that for each flux K_c and the voidage were in the same range but at the different fluxes the K_c and

voidage values were different. At half the flux the K_c value should have been equal to the value at the higher flux (26 l/h/m^2) since the cake produced had a unique compaction and thickness. However, this was not the case. It was observed that by increasing the flux the gradient of the data was observed to not increase in the expected manner (at double the flux, 26 l/h/m^2, it was expected that the gradient would double) but it was found that the gradient was approximately the same at both fluxes. It was considered that the cake that formed at the lower flux (13 l/h/m^2) was different to that produced at the higher flux (0.6 x 10^{-6} m^3min^{-1}). It was also considered that region 1 was due to compression of the cake. This being the case helps to explain why the cake formed at the two fluxes were different. No water permeated through these membranes in region 2 and therefore all of the water (dispersed) phase was retained by the membrane. The voidage was in the same range at a given flux 4.0-4.3 % (Table 4.15) at a flux of 13 l/h/m^2 and 5-5.4 % (Table 4.15) at flux of 26 l/h/m^2. At the lower flux the voidage of the cake was lower. The emulsion used had a mean droplet size of 6.8 μm but the distribution was such that smaller droplets could have packed between the larger droplets so that a tighter structure was produced that compressed to a smaller voidage at the lower flux.

Results in Table 4.16-4.17 showed that for each flux K_c and the voidage were different. At half the flux the K_c values should have been equal to the value at the higher flux (26 l/h/m^2) since the cake produced had a unique compaction and thickness. However, this was not the case and it was observed that by increasing the flux the gradient of the data was observed to not increase in the expected manner (at double the flux, 26 l/h/m^2, it was expected that the gradient would double). Also in Table 4.17 the same well dispersed emulsion was used and therefore for different membranes (Supor 200, Nylaflo and HTTuffryn) it was expected that the voidage would have been similar as was observed for the versapor, Supor 100 and Supor 450 membranes. It was clear that there were other factors that caused the results in region 2. The results in Tables 4.16-4.17 were where water permeated through the membrane at the end of region 2. It was considered due to this leakage the value of the mass fraction of dispersed phase (s) in equation 4.35 was no longer 50 %. A

small decrease in s would have resulted in an error in the calculation of the voidage. However, the emulsion where the homogeniser speed was lower (8000 rpm for the entire emulsification process) and the mean droplet size was 12.1 μm the voidage was similar to the voidage in Table 4.15. This was because water did not permeate through the membrane until region 3 and therefore the mass fraction of dispersed phase (s) substituted in equation 4.33 was the correct value (s = 50 vol %).

Bowen (1995) reported that cake was independent of the pore size of the membrane and that the slope of the graph should be constant for all membranes. Also Published work by Grace (1954) showed that the pore size could effect the calculated values for the constants if the cake formed was not macroscopic (not all of the membrane area is covered by cake). He reported that the specific cake resistance could vary due to not all the area of the membrane being covered. He showed that the values of α, for the regions of cake filtration of various membranes varied over a tenfold range (same well dispersed emulsion used). He also showed that with tight media two successive regions of cake filtration resulted. The values of α, were much higher than expected if they represented a true cake over the entire surface of the membrane. It was determined that no macroscopic cake was formed on the membrane even at the end of the cycle and that a changing cake surface area during the period of cake filtration probably accounted for the successive regions of cake filtration for tight media. No cake could be seen on the surface.

The presence of water in the permeate led to the conclusion that the cake filtration mechanism was not the only cause of pressure increase in region 2 (Table 4.16-4.17). If the pressure increase in region 2 was solely due to the cake that formed then according to Equation 4.22 the cake resistance and membrane resistance acted in series. The pressure required for a certain volume of dodecane to pass through the membrane depended on the membrane resistance (which is usually considered to be constant) and the resistance due to the cake would continuously change with time due to the thickness of the cake increasing. The pressure increase would be only due to the cake and not blocking of the membrane. With this being the case water could not

have entered the pores as the pressure difference across the membrane was too small and independent of the total system pressure. The increase in the system pressure would be entirely due to the increased pressure drop required to maintain constant flow across the cake of ever increasing thickness. In order for the water to have entered the pores the pressure across the membrane must have increased and therefore the membrane resistance was changing not just at the start of filtration but all the way through

4.5.3 Break through pressures

Since water was present in the permeate the break through pressure of water needed to be reached before it could pass through the membrane. The break through pressure of the membranes, (Supor 200, Nylaflo and HTTuffryn) for water when the pores contained dodecane + Paranox 100, was due to the resistance of the membrane increasing during filtration. This would have been the result of blocking of the membrane pores by deposition or adsorption of the emulsion droplets onto the membrane surface or the walls of the membrane pores [Foley et al, 1995]. The increase in membrane resistance would have occurred in the following manner:

* In region 1 the pressure increased slightly for all membranes used and at the start of region 2 the pressure (Table 4.22) was greater than the breakthrough pressure of the water phase (Table 4.25). However, no water permeated through the membranes until the end of region 2. If the breakthrough pressure of water (when the pores contain dodecane and Paranox 100) was reached in region 1 (by membrane fouling) then water would have permeated through the membrane all the way through region 2. It was therefore considered that region 1 was due to a compressible cake forming.

* The membrane resistance increased in region 2 but because the pressure increase due to membrane resistance was small compared to the pressure increase due to the cake a linear relationship was still maintained. The membranes where water

permeated through (Supor 200, Nylaflo, Httuffryn) the breakthrough pressure of water was only small 0.28-0.46 bar (Table 4.22) and it was considered that when the droplets coalesced on the membrane surface (Section 4.5.6) the membrane fouled slightly.

considering that a cake started to form (region 1 of Figures 4.14 to 4.24) the water droplets in the cake were squeezed closer together due to depletion of dodecane. The voidage in the cake was decreased, and at the point where the volume fraction of water droplets was greater than 74 % [Princen, 1986 and Lissant and Mayhan, 1973] in the cake the droplets distorted. It was discussed above how the droplets distorted to form polyhedrals and at 95 % volume of water the emulsion demulsified. The voidage in region 2 remained relatively constant but the partially demulsified emulsion was considered to have fouled the membrane and this resulted in the breakthrough pressure for water being reached (different for each membrane) so that water permeated through the pores. Water did not enter the pores until the critical pressure was exceeded (Table 4.22). The critical pressure (ΔP_{Ca}) depended on the interfacial tension (γ), contact angle (θ) and the size (r) and shape of the openings in the membrane (Equation 4.50). Membranes consisted of a wide distribution of pore size and flow into the larger pores occurred at a lower pressure. However, pressure continued to increase until flow was continuous.

$$\Delta P_{Ca} = \frac{2\gamma \cos\theta}{r} \qquad ..(4.50)$$

Flow of water into the pores for membranes in Table 4.16 and Table 4.17 occurred before and at the point of breakthrough. If the breakthrough pressure was considered to be reached at the point where region 2 ended (Fig 4.17 to 4.24) the results can then be explained in the following manner. Table 4.20 shows the pressures at the end of region 2. For a 50:50 water-in-dodecane (1 % Paranox 100) emulsion using a Supor 200 membrane the break through pressures at fluxes 26 l/h/m^2 and 43.3 l/h/m^2 were almost the same which was to be expected for the same well dispersed emulsion being

used for the same membrane. At the lower flux of 13 l/h/m^2 the breakthrough of water was about 1 bar less. If at the lower flux the membrane fouled at a faster rate then the breakthrough pressure would have been different. This explains why at the two higher fluxes the cake filtration (in region 3) gave similar K_c constants for the slope. As the cakes formed were similar the breakthrough pressures were similar. There was no time for coalescence to occur before the water entered the pores once the water was flowing the proportion of water to dodecane was the same at both fluxes and therefore there was no reason to think that the cake in region 3 would have formed differently at either Flux (26 l/h/m^2 and 43.3 l/h/m^2). However at the lower flux the break through pressure was lower due to a different cake structure being formed and therefore the cake continued to be different in region 3.

The rate of filtration depends upon the pressure drop viscosity, and the resistances of both cake and the membrane. Conventional theory has assumed that the medium resistance Rm is constant. Leu and Tiller (1983) reported for constant pressure cake filtration that membrane resistance changed not only in the first few seconds of a filtration operation but throughout the entire process. Tarleton and Willmer (1997) reported for a dead-end pressure filter cell using aqueous calcite and zinc sulphide suspensions that the filter medium was generally seen to increase with applied pressure. It was observed that by increasing the pressure the gradient of the data (cake filtration) decreased in the expected manner at low pressures (1-3 bar). However, at pressures between 4-6 bar the decrease in gradient became progressively smaller as the pressure was raised. The system became more extreme when very incompressible (zinc sulphide suspension at pH =10.5) systems were used. There was an overlay of t/V vs V data in the range 4-6 bar.

4.5.4 Membrane compressibility

The increase in resistance in region 2 could not have resulted from membrane compressibility. In region 2 the pressure increased to a value greater than 2 bar. The breakthrough pressure of water for almost all the membranes was lower than this

value. Therefore, if the increase in resistance was due to membrane compressibility then the pressure drop across the membrane would have been big enough for the breakthrough of water and water would have been detected in the permeate. However, water was not detected in the permeate until the end of region 2.

Bowen et al (1993) reported that using polysulfone films compression was observed by the loss of permeation rate at high applied pressures. In their system constant pressure was applied where the pressure in some cases was high enough to compress the membrane.

In the work presented here a constant flux system was used where the resulting pressure for the applied flux was small. Total pressure increase in the system was due to a cake that formed on the membrane.

4.5.5 Membrane swelling

Dodecane could have caused swelling of the membrane that could have resulted in the pressure increasing in region 2. If the pore structure of the membranes used were homogeneous then swelling of the membranes would have led to a dilation of the pore structure. Which would have led to the pore size increasing and the resistance to flow decreasing. This would have resulted in the structure being more open so the pressure would have not increased so that the flux remained constant. However, if the membrane structure is such that the membrane surface layer is different to the rest of the membrane. The surface layer could swell differently to the rest of the membrane. This could lead to pore constriction and an increase in membrane resistance.

Lencki et al (1994) looked at the effects of solvents on membranes. They reported that if the membrane layer was denser and/or of different chemical properties to the support, the membrane layer could swell more relative to the porous support, leading to an increase in the membrane resistance.

Membranes Supor 450, Supor 100, Supor 200, Nylaflo and HTTuffryn were not supported membranes. The surface layer and the rest of the membrane were of the same material (membranes were essentially homogeneous). Versapor was a supported membrane (non-woven nylon support). It was possible for the top layer of the versapor membrane to swell differently to the support and therefore cause the membrane resistance to increase. However, as the experimental data in region 2 for versapor, Supor 100 and Supor 450 was similar membrane swelling was not the cause of pressure increase in region 2.

4.5.6 Droplet breakdown

4.5.6.1 Droplet breakdown

It has been established that cake filtration was occurring throughout all of the runs. In region 1, the emulsion depleted of dodecane which forced the droplets to come closer together forming a cake where the droplets deformed. In region 2 the cake formed in region 1 increased in thickness which was the main cause of pressure increase. During this period the destorted droplets coalesced as the voidage between the droplets was < 5 vol % (Tables 4.15-4.17).

The original emulsion consisted of 50:50 water -in-dodecane. Very little dodecane was needed to be removed for the volume fraction of the droplets in the cake to be greater than 74 %. The results in Table 4.21 showed that the relationship between applied pressure and internal droplet pressure at the start of region 2 was at the limit of $P_A >> P_I$. Therefore, the droplets were polyhedral in shape. The increase in surface area from a sphere to a polyhedral caused the voidage in the cake to decrease. When the volume fraction of the water in the cake was near 95 % (e = 5 %) [Bibette et al, 1992] the surfactant layer was destroyed and the droplets were able to coalesce with other droplets. The presence of water in the permeate was an indication that the voidage was about 95 %.

Work by Bibette (1992) and Bibette et al (1992) demonstrated by using an osmotic stress technique that the surfactant film was ruptured. An emulsion (silicone oil-in-water stabilised by sodium dodecyl sulfate) was enclosed in a dialysis bag and immersed in a larger reservoir of a ternary mixture of water, surfactant and hydrophilic polymer. The bags were made of a cellulosic membrane with a MW cut-off of 50,000, which was permeable to water and surfactant but impermeable to the oil droplets and polymer molecules. The effect of the applied osmotic pressure was to squeeze the water out from the emulsion. This resulted in deforming the droplets like a mechanical piston would do on the droplets alone. Since the droplets could no longer remain spherical they pressed against each other and formed facets at each contact. The surface area of the droplets increased from a spherical shape to a polyhedral shape at constant volume. They also reported that emulsions stabilised by surfactant below the cmc were always unstable and above the cmc the emulsion became unstable when most of the water was squeezed out (oil volume of 95 %). They caused the rupture of thin films by gradually increasing the osmotic pressure applied on the emulsion until the pressure reached the critical disjoining pressure. They found that the osmotic pressure required for droplets to reach the critical pressure depended upon the diameter of the undeformed droplet. For very small droplets where the radius d/2 was less than the critical radius of curvature R* the Laplace pressure,$\pi_o=4\gamma/d$ was above the critical value π_i, before the droplets were deformed (droplets already unstable). Where $d>>2R^*$ the droplets were compressed until they were polyhedral before reaching the critical value in this limit $\pi_I=\pi$.. They also showed that the degree of deformation of the droplets was determined by the ratio $\pi d/\Upsilon \propto \pi/\pi_o$. In the limit $\pi << \pi_o$, the droplets were weakly deformed spheres and pressed against each other across small nearly circular facets. Here $\pi_I=\pi_o$ and the osmotic pressure required to cause rupture vanished. In the limit $\pi >> \pi_o$, the droplets become nearly polyhedral and $\pi_I=\pi$ where the critical osmotic pressure π^* equals the critical pressure of the droplet π_I^* (critical disjoining pressure).

Work by Lissant (1966) showed that the spheres were undistorted until the volume fraction of the internal phase reached the critical volume fraction where spheres first

touched their neighbours. The critical volume fraction for spheres arranged on a simple cubic lattice was 52 %, on a tetrakaidecahedral lattice 68 %, and on a rhomboidal dodecahedral lattice was 74 %. Above this volume fraction the spheres distorted. He showed that between internal phase volumes 68-74 % that the tetrakaidecahedral packing occurred but the system was unstable and could rearrange to a system of undistorted spheres. In the region between 74-94 vol % rhomboidal dodecahedral packing was preferable and above 94 vol % tetrakaidecahedral packing was again preferred. These packings were also reported to occur at the same phase ratios by Bohlen et al (1992). Distortion of the droplet was investigated by several authors. Sherwood (1992) investigated the filtration behaviour of emulsions. He assumed that the droplets distorted from a sphere to a cube so that the cake formed a cubic array. In his experiments the water droplets came together to form a filter cake without coalescence and therefore unlike Bibette (1992) he was not looking at the maximum stress that could be supported by an emulsion before it demulsified. He was looking at a filtration system where the droplets were retained by the membrane and the applied pressure was sufficient to drive fluid through the medium on which a filter cake of particles built up. The water droplets did not breakdown and wet the filter medium.

Region 3

The water retained by the membrane was estimated to be 1.1 (mass) % and the voidage calculated was 3% at a flux of 26 l/h/m^2 and 2.2 % at 13 l/h/m^2 for all membranes and emulsions used. The voidage calculated in this region was different to the voidage calculated in region 2 but we have to consider that the exact voidage was in error due to the membrane resistance changing throughout the filtration and not just at the start. However, if we consider that the change in the membrane resistance was similar for the same emulsion then we can determine that the since the voidages were the same for a given flux then the amount of water retained by the membrane was the same (but not necessarily 1.1 %). We know that for all experiments that water and dodecane in region 3 permeated through the membrane at the same ratio

(Chapters 3 and 5) and therefore it was expected that the same amount of water was retained by the membrane. Also in order for the droplets to have broken the voidage in the cake had to be at < 5% and as the calculated values (Tables 4.16-4.17) were around this value, the estimated value of the retained phase was a good approximation.

4.5.7 Breakage Mechanism

There are two possible mechanisms to explain the breakage phenomenon described above.

4.5.7.1 Mechanism 1

The results suggest that the breakage mechanism (Figure 4.31) was one where the droplets were broken by squeezing them (by depletion of dodecane) so that the surface area was increased from a sphere to a polyhedral. The surfactant could no longer stabilise the droplet and the emulsion then broke down on the surface of the membrane (Figure 4.31 b). Once the breakthrough pressure was reached for the permeation of water/surfactant through the membrane, water from the collapsed droplets in the cake and dodecane from fresh emulsion directly above the cake permeated through the membrane (Figure 4.31c). The new cake formed from the depletion of dodecane replaced the cake permeating through the membrane (cascade affect). However, the ratio of cake removal to cake replacement was not equal. A small amount of cake was still being formed (cake thickness was still increasing). The breakage of the droplets occurred at about 1-1.2 bar but the water did not enter the pores until the breakthrough pressure for water, where dodecane was in the membrane pores, was reached. The various membranes had different breakthrough pressures (Table 4.22) and therefore the lower the pressure was the sooner water passed through the membrane. The Httuffryn membrane (flux 13 l/h/m^2) had the lowest breakthrough pressure. After breakthrough of water occurred water and dodecane permeated through the membrane at approx the same ratio as that entering

the system. Some membranes (Versapor, Supor 450 and Supor 100) did not allow the permeation of water through the membrane but the droplet breakage (Figure 4.31a-b) still occurred on the membrane surface. The pressure in the system just continued to increase until the maximum pressure was reached (6 bar). This resulted from the breakthrough pressure for water through a Supor 100, Supor 450 and Versapor being so high that the demulsified emulsion on the membrane was prevented from entering the pores. This mechanism was very successful where the membrane had a low breakthrough pressure (for the permeation of water). The mechanism indicates that the membrane surface acts as a wetting and a coalescing medium and the concentrated emulsion formed on the surface acts as a barrier to prevent flow which leads to a pressure increase that deforms the droplets within the concentrated emulsion and eventually leads to their rupture. The permeation of both phases through the membrane that follows, allows for complete separation of the two phases.

4.5.7.2 Mechanism 2

Another possible mechanism that explains the results is shown in Figure 4.32. The schematic diagram of demulsification of water-in-oil emulsions by using hydrophilic membranes shows that the droplets gather on the membrane surface, but do not coalesce with each other due to the presence of the surfactant film. The droplets gathered on the membrane surface can enter the pore if the operating pressure exceeds the capillary pressure (Figure 4.32a). If the pore diameter on the membrane is so large that the droplets can easily pass through, the emulsion will not be demulsified. If the pore diameter of the membrane is smaller than the size of droplets, the droplets must deform to enter the pore (Figure 4.32b). The deformation of the droplets entering the pore causes a change in the distribution of the surfactant around

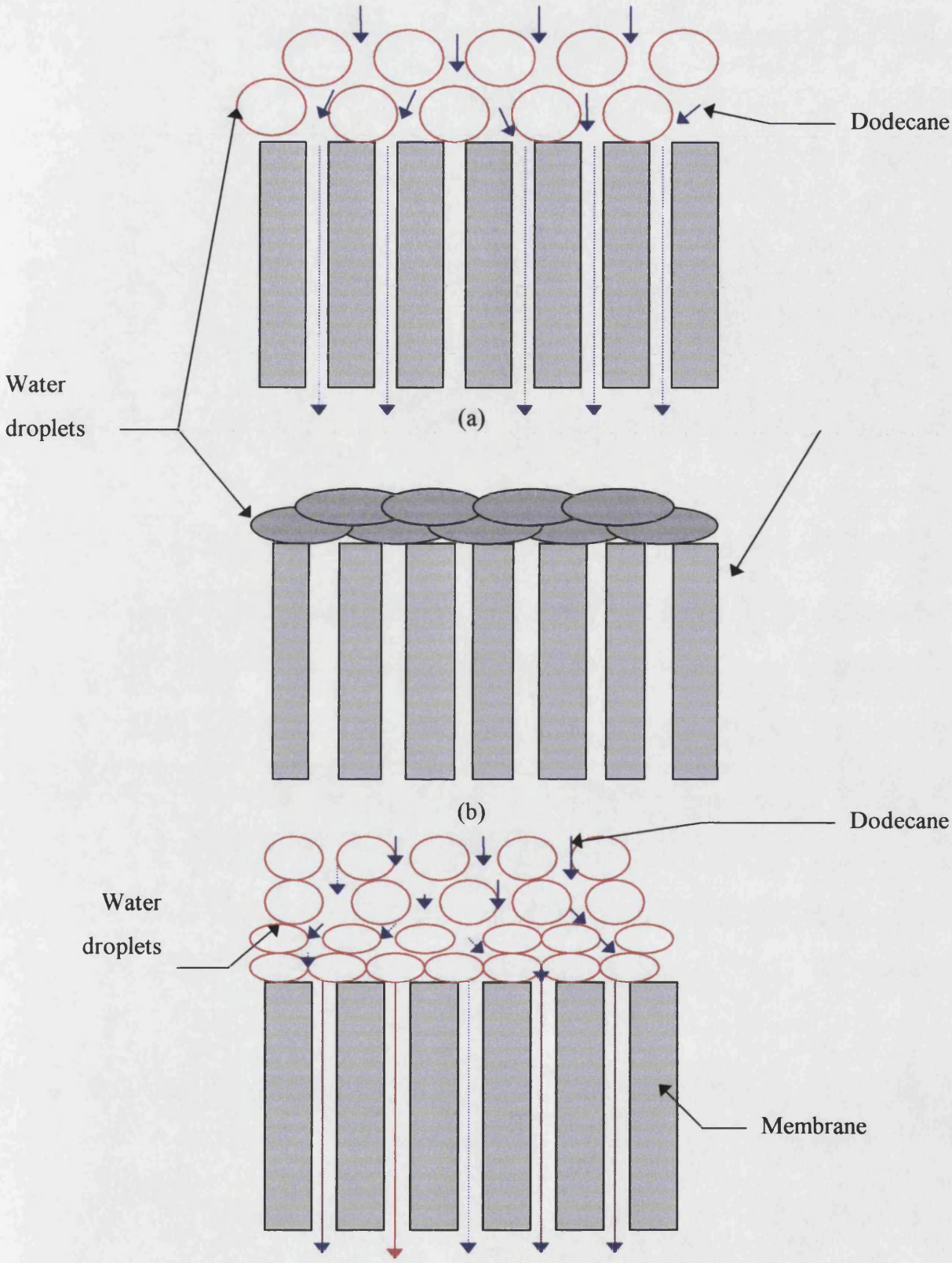

Fig 4.31 Breakage mechanism 1 on surface of the membrane (a) Depletion of dodecane from the emulsion, (b) Droplets distort and the passage of dodecane is restricted and (c) Cake is destroyed and formed simultaneously.

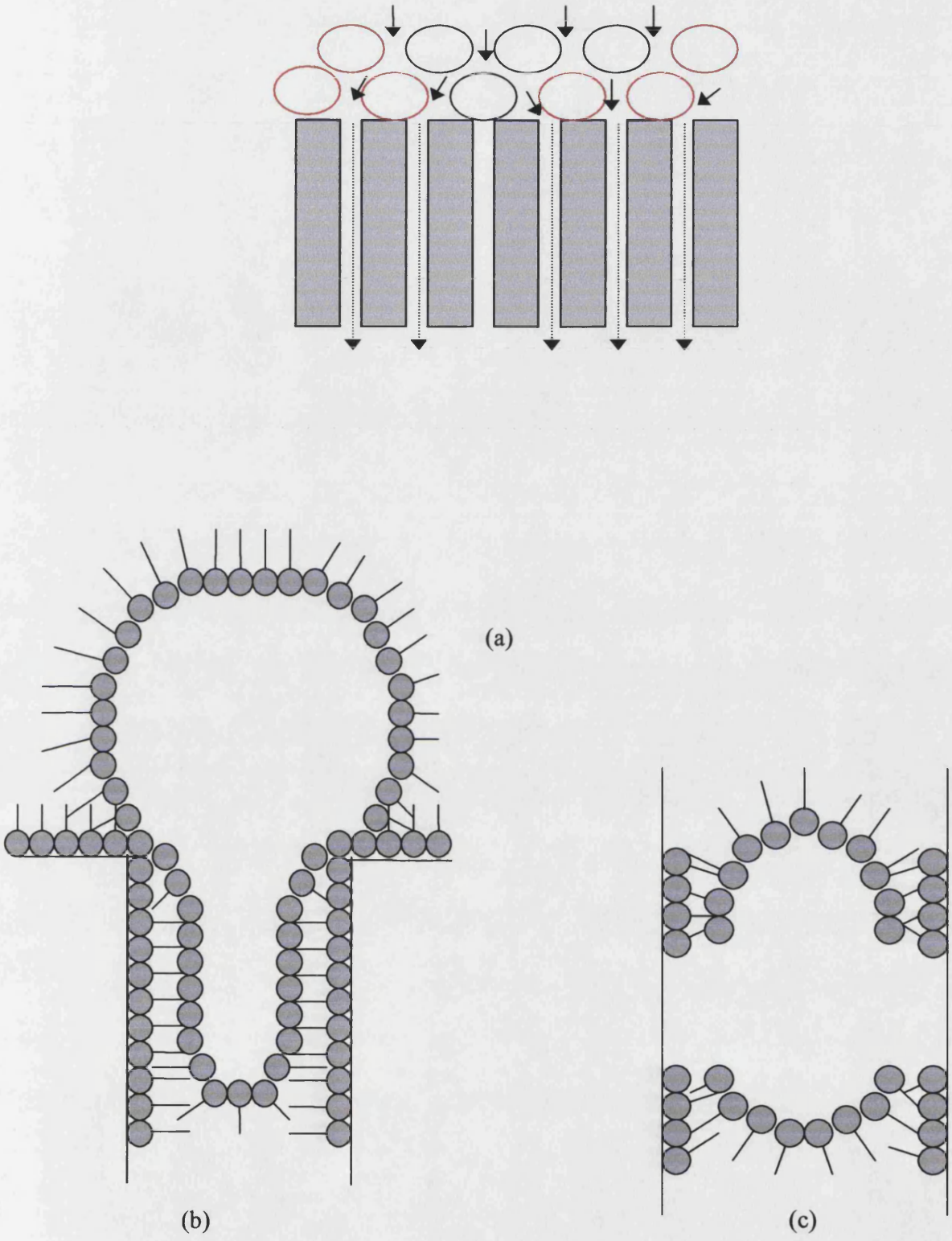

Fig 4.32 Breakage mechanism 2 in the membrane pores (a) Depletion of dodecane from the emulsion (b) Droplets entering into smaller pores must deform and (c) droplets in the pore are broken and adsorbed on the pore wall.

Fig 4.32 Breakage mechanism 2 in the membrane pores (a) Depletion of dodecane from the emulsion (b) Droplets entering into smaller pores must deform and (c) droplets in the pore are broken and adsorbed on the pore wall.

the droplet and makes it easy for the film to rupture in the membrane pore. The deformed droplets are squeezed and broken in the pores (Figure 4.32 c) so that the water phase is released and makes contact with the pore walls. The water phase that is adsorbed on the pore walls will coalesce with water from other broken droplets and therefore increase in size. Finally, under the action of pressure the water phase will flow out of the pore. This mechanism indicates that the membrane material acts as a wetting and a coalescing medium and the pore size and pressure exerted cause the droplets to deform and enter the membrane pore and eventually rupture. This mechanism may have played a small role in the demulsification experiments but not the leading role. The fluxes at which the filtration was run were very low (and the resistance of the membrane also being low resulted in a low pressure. The droplets in the emulsion were nearly thirty times greater in size than the pores and therefore the droplets would have needed to be distorted to enter the pores. The pressure that resulted from the membrane resistance to flow of dodecane was not sufficient. The increase in pressure in the system to an adequate value so that the droplets were distorted was the result of the following:

* In the first few minutes there was just permeation of dodecane and surfactant. This depletion of dodecane from the emulsion resulted in the droplets being squeezed closer together so that they deformed in to polyhedrals

* The increase in the concentrated emulsion on the membrane surface resulted in the pressure increasing so that the flux remained constant. During cake formation the membrane became fouled which resulted in an increase in the membrane resistance so that the breakthrough of water occurred.

* The increase in the concentrated emulsion on the membrane surface resulted in the pressure increasing so that the flux remained constant. During cake formation the membrane became fouled which resulted in an increase in the membrane resistance so that the breakthrough of water occurred.

The results in Figure 4.33 showed that when the filtration was halted after 4.5 minutes there was no permeation of water through the pores. Therefore, the pressure across the membrane was not sufficient to overcome the capillary pressure. Also the cake on the membrane did not consist of emulsified droplets. In fact the emulsion had demulsified and the water droplets were no longer surrounded by surfactant. The dye tests showed that the dye was dispersed throughout the cake after 4.5 minutes to the same extent as when the experiment was allowed to continue for 20 minutes. If the

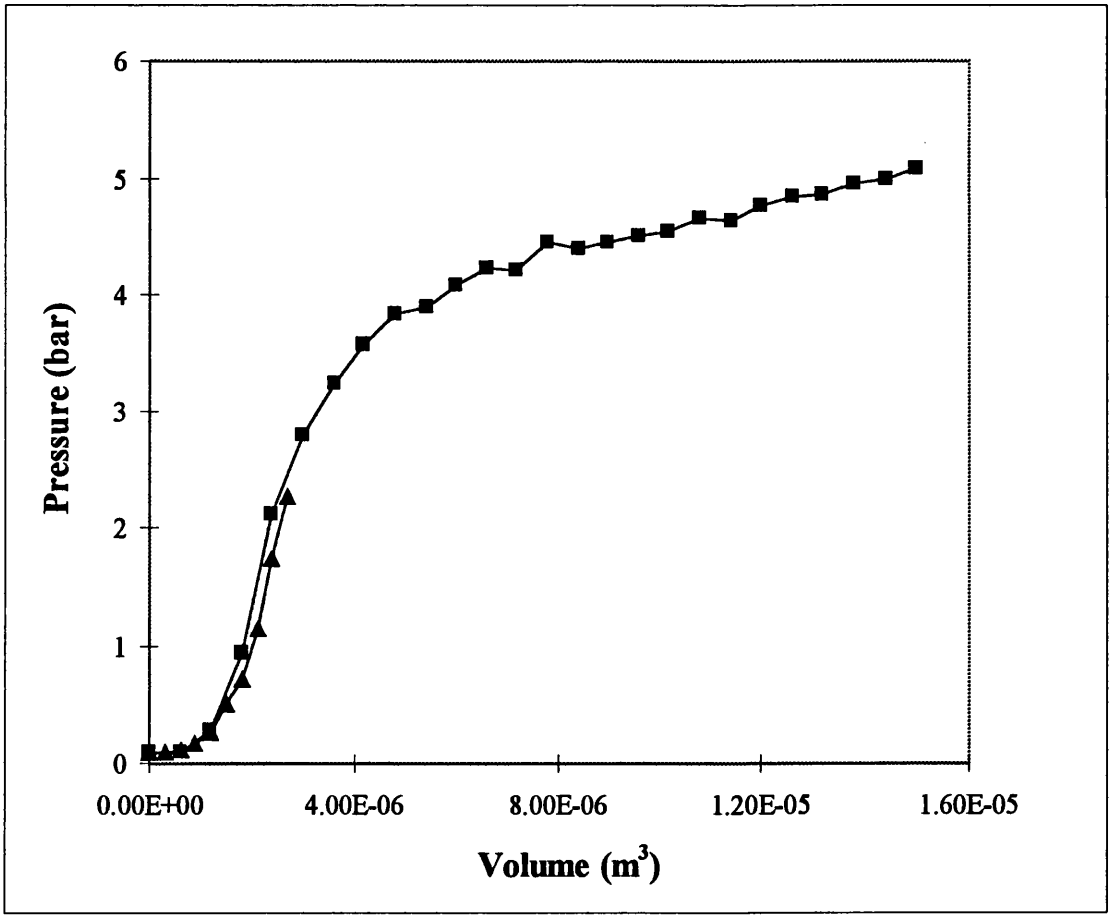

droplets had not broken until they entered the pores the dye would not have dispersed in the cake at 4.5 minutes as no water at this time interval had passed through the membrane pores. There was however, demulsified water droplets on the surface of the membranes which indicated that emulsion breakage had occurred and was probably due to the droplets being squeezed within the cake so that they became unstable.

Lee et al (1984|) showed that for the ultrafiltration of water-in-oil (stabilised with 0.2-1 vol % of surfactant) there was permeation of the dispersed phase when the operating pressure exceeded the capillary pressure. They reported that as the operating pressure increased, the number of pores where the operating pressure exceeded the capillary pressure increased , and thus pore plugging and membrane fouling became more important. The capillary pressure was estimated to be about -4 bar and membrane fouling was more important when the pressure was operated at above 3 bar

Published work by Hlavacek (1995) showed that for an oil-in-water emulsion (composition of emulsion was not disclosed) of internal oil phase between 2.8-3.2 vol % the mechanism of breakage was in the pore (Figure 4.32). A constant pressure (20-50 kPa), crossflow system with a hydrophobic membrane (pore size of 0.2 μm) was used. The emulsion droplets were of a narrow distribution 1.7 ± 0.5 μm. The droplets were approx 10 times bigger than the pores. In order for the droplets to enter the pore they had to be deformed. If the operating pressure was greater than the capillary pressure of the oil drops in the membrane pores then the emulsified drops deformed and entered the pores. Hlavacek also reported that for a cross flow velocity range of 0.5-3 m/s there was no change to the permeation rate. There was also no oil retention as the retentate concentration remained constant and the same as in the feed. As this was the case the system could have been run in dead end mode.

Daiminger et al (1995) looked at the demulsification of isododecane-in-water emulsions, containing 0.1 $kmolm^{-3}$ of surfactant bis(2-ethylhexyl)-phosphate (DEPA),

using hydrophobic membranes as a coalescer. The average pore size of the membranes ranged between 0.22-5 μm. The droplet size was approx 5 μm and therefore the droplets were 30 times bigger for the smaller pore and same size at the largest pore size. Their work showed that separation did not occur where membranes of small pore diameters (0.22 and 1 μm) were used. A high degree of separation was achieved 80-90 % when membranes with a pore size equal to the droplet size were used. The work also showed that the degree of coalescence was independent of the oil concentration (5g/l to 25g/l).

Published work by Sun et al (1998) showed that the mechanism for breakage of a water -in-kerosene emulsion using a porous glass membrane (hydrophilic) was due to breakage in the pores mechanism Figure 4.32. Their results showed that the demulsification efficiency increased with pore diameter. The droplets of the emulsion were between 2-10 μm and the membranes used had an average pore size between 0.5-80 μm. For the membranes with an average pore size bigger than the droplets the demulsification was poor (approx 41% for 80 μm pore) because the emulsion could easily enter and pass through the membrane pore. When a membrane with an average pore size smaller than the droplets diameter was used demulsification efficiency increased (approx 97.2 % for 0.5 μm pore) because the droplets had to be deformed to enter the pores. They also investigated the effect of phase ratio on the demulsification efficiency. They reported that the ratio of oil phase to water phase had no effect on the demulsification. The oil phase was increased up to 50 vol % and they claimed that the mechanism was in the pores.

All of the above literature involved constant pressure crossflow microfiltration where the applied pressure was greater than the capillary pressure of the emulsified drop in the pore structure. This resulted in both phases passing through the membrane. However, the surfactant concentrations were either low or not given. It is considered that at high surfactant concentrations or where the mechanical properties of a surfactant are strong, confined flow through a pore will not be sufficient to destabilise the surfactant layer and the droplets will remain emulsified drops.

Work by Tirmizi et al (1996) showed for a constant pressure (34.5 kpa) system where the pressure was kept below the breakthrough pressure of the nonwetting fluid and the surfactant concentrations were between 10-20 kg/m^3 phase inversion was not observed. They also showed that the emulsions (water-in-tetradecane stabilised by ECA 5025) appeared thickened on the surface as the tetradecane content decreased due to permeation. At lower concentration of surfactant 0.5 kg/m^3, the phase inversion was complete. For emulsions with surfactant concentration 2 kg/m^3 and higher there was partial phase inversion where the mixture on the membrane consisted of partly phase inverted emulsion and partly thickened emulsion. It should be noted that the operating pressure was kept below the breakthrough pressure of water.

The literature and findings reported here indicate that Mechanism 1 (Figure 4.31) explains the experimental data best.

Chapter 5

A Comparison Between Dead-End Filtration and Pulsed D.C. Electrostatic Coalescence

5.1 Introduction

The time it takes for an emulsion droplet to coalesce inhibits the use of emulsion liquid membranes. The process of coalescence is divided into three distinct stages (1) the collision of the droplets, (2) the thinning of the film between the droplets; and (3) the final breaking of the film to achieve a single droplet. In order for this to occur it is necessary to weaken or remove the interfacial film, the successful weakening and ultimate removal of this film will be accomplished by understanding the factors that influence the stability. Some of these include viscosity of the oil; density difference; interfacial viscosity; droplet size; surfactant concentration; interfacial tension; film compressibility; and operating conditions. The ultimate goal is to weaken or remove the surfactant layer as fast as possible so this too will limit the method used [Grace., 1992]. This phenomenon applies to breakage by both electrostatic coalescence and filtration using membranes. For each method the factors that influence the coalescence of the water droplets will be discussed later.

There are also other factors that influence demulsification, which are specific to the individual breakage method:

Electrostatic coalescence: Applied voltage, frequency, wave form, stirring of the emulsion, temperature and insulation material.

Membrane filtration: Applied pressure, temperature, pore size of the membrane, membrane material.

Some of these factors will be discussed later. Coalescence is brought about by collision of the droplets. How this occurs in each method (electrostatic coalescence and membrane filtration) is discussed below.

5.1.1 Electrostatic Coalescence

This form of demulsification is a physical process which makes recycle of the oil phase possible. A high electric field can be established across an emulsion because the oil phase is non-conducting [Larson et al, 1994]. The three main field types are AC, DC and pulsed DC. DC is the oldest of the three and is used in the breakage of crude oil emulsions in production and refining. DC, is used for resolving emulsions with low water content (at high water content short circuiting can occur by the droplets forming chains between the electrodes) and pulsed DC with insulated electrodes, is used for the breakage of emulsions with high water content (very useful for the breakage of emulsion liquid membranes) [Taylor, 1996].

When a DC field is applied the water droplets orient and move rapidly in the direction of the applied field (electrophoresis). When an AC field is applied droplets move in the direction of maximum field strength [Larson et al, 1994]. The ever-changing nature of the electric field (usually sinusoidal, operating at a frequency of 50-60 Hz) ensures the dipoles are maintained [Taylor, 1996]. The electrostatic forces causing coalescence are, (1) Dipole interaction (Fig 5.1), A water droplet in an electric field polarises, this means that an induced charge is created on the surface of the droplet and two polarised droplets will attract each other [Urdahl, 1996], (2) Electrophoresis (Fig 5.2), droplets that come into contact with the electrode they are attracted to, will recharge and change polarity. Following this the droplets will move rapidly to the other electrode. The charged droplets can also transport charge to other droplets. Electrophoresis and contact charging causes random motion of the droplets which results in random collision and this can lead to coalescence [Grace, 1992]. Electrophoresis requires the droplets to be in direct contact with the electrodes and therefore will only apply to DC and (3) Dielectrophoresis (Fig 5.3), unlike

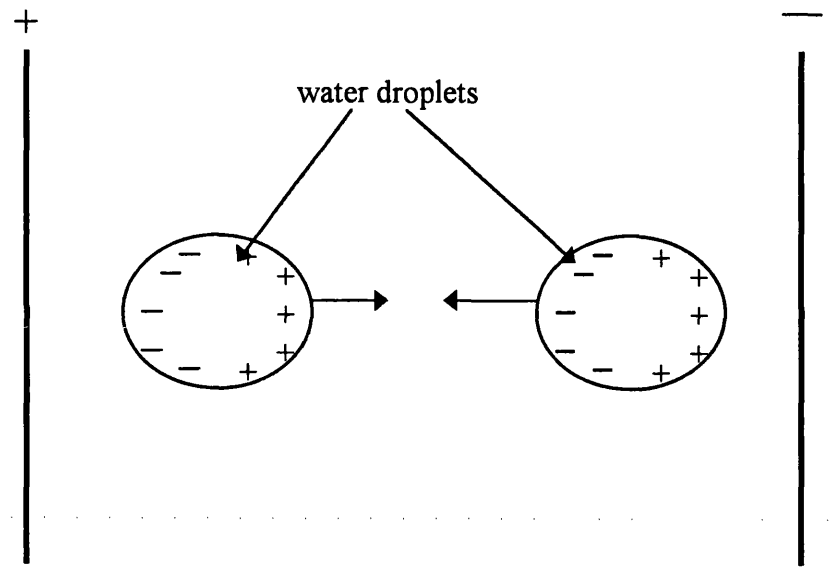

Figure 5.1 Dipole dipole interaction

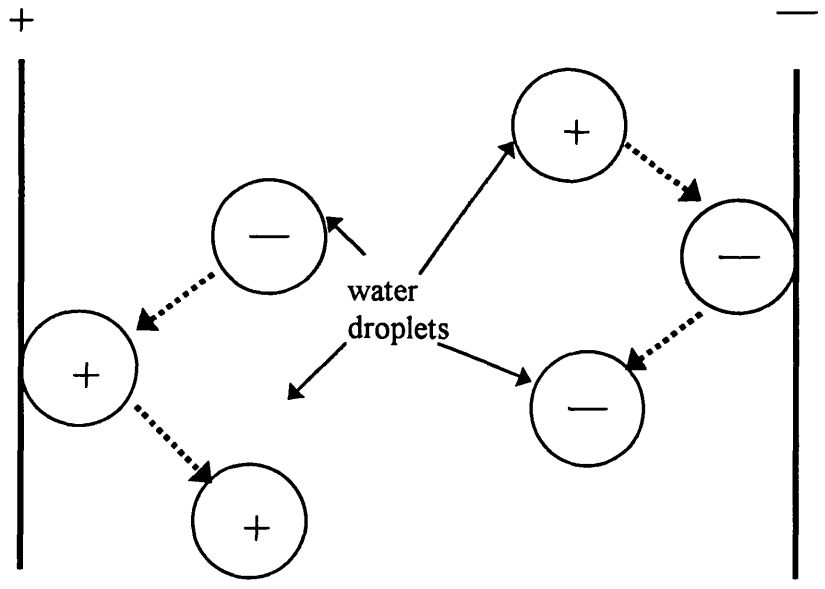

Figure 5.2 Electrophoresis.

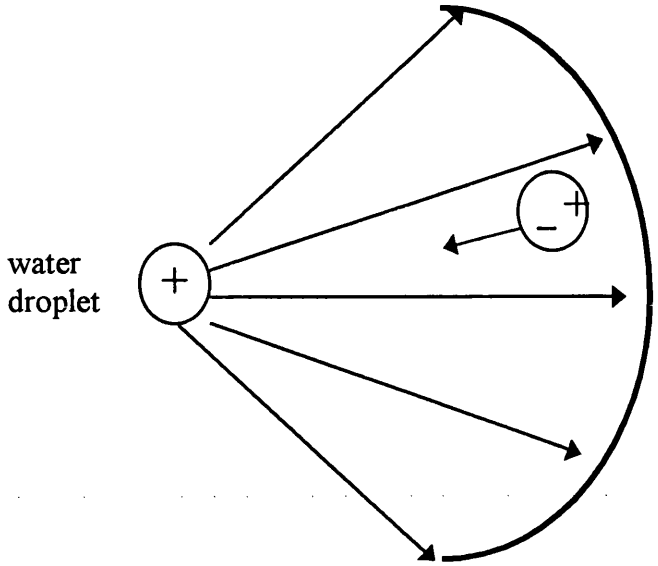

Figure 5.3 Dielectrophoresis.

electrophoresis, movement of the droplets is to both electrodes, the direction of movement of the droplets is always towards the higher electric field strength. It is independent of polarity [Yamaguchi et al, 1987]. The forces acting on the emulsion are proportional to the square of the electric field and are independent of the shape and kind (AC or DC) of voltage. Published work implies that DC is inferior to pulsed DC. Draxler et al. (1986) regards pulsed DC fields of the square shape to be superior to all other DC. Most authors prefer high voltage pulsed DC or AC [Taylor, 1996 and Hano et al, 1990].

5.1.2 Membrane filtration

The coalescence of the water droplets as been discussed in Chapters 3 and 4 and will be discussed in further detail later in this chapter.

The rest of this chapter is divided into two sections. The first examines emulsion breakage using electrostatic coalescence. By investigating the factors which affect the coalescence, such as phase ratio, surfactant concentration and frequency, the capabilities of this method of emulsion breakage (for a stable emulsion of water-in-dodecane emulsion stabilised by Paranox 100) can be determined. The second section looks at emulsion breakage using hydrophilic membranes. The mechanism of this form of emulsion breakage has been described in Chapters 3 and 4.

The aim of this chapter is to investigate whether breakage of stable emulsions using membranes is superior to emulsion breakage using pulsed DC electrostatic coalescence. Emulsion breakage using pulsed DC is a well established process. However, there are limitations on how effective this process is in breaking stable high water content emulsions. The ultimate objective of this work is to show that where electrostatic coalescence fails to break emulsions that have a high water content and are stabilised by a surfactant of high mechanical ability, membranes are not only successful but there is high water phase recovery.

5.2 Theoretical considerations of the mechanism of emulsion breakage.

5.2.1 DC electric fields.

The emulsion breakage process consists of three major steps: (1) movement of droplets due to gravity; (2) drainage of the film between the droplets; and (3) rupture of the film between the droplets and coalescence [Kriechbaumer et al, 1985 and Taylor, 1996].

The electric field promotes the movement of droplets which leads to coalescence, and finally to oil and water separation. The electrical field does not influence film drainage, but there is an influence on film rupture. The coalescence rate is increased by electrically induced movement of the droplet. Induced movement in pulsed DC is caused by dipole interaction. Dipole attraction (Fig 5.1) arises from the polarisation of the water droplets in the applied electric field and does not depend on them possessing a net charge. The electric field polarity has no affect on the force of attraction between droplets, and the dielectric constant of the droplet phase must be much larger than the dielectric constant of the oil phase. The dipole attraction between droplets is usually small but as the droplets come closer the force increases and becomes dominant.

The force acting on the droplets can be described by the following equation [Taylor, 1996]:

$$F = K\frac{E^2 r^6}{d^4} \qquad \text{.....(5.1)}$$

Where F is the attractive force between the droplets, E is the electric field strength, r_d is the droplet radius, d is the droplet separation and K is a constant.

From Equation 5.1 it is clear that a pair of droplets must first be brought into close proximity with one another (in a stationary system this is brought about by Brownian

motion, sedimentation and flocculation). In a flowing system liquid shear aids in bringing droplets into close contact. Therefore collisions in a flowing system are more frequent than in a stationary system [Urdahl et al, 1996]. Also force between the water droplets is proportional to the square of the applied field strength and therefore high voltages are commonly used in electrostatic coalescers. As the droplets coalesce and grow they settle rapidly due to gravitational forces [Larson et al, 1994]. The droplet diameter will also affect the force of attraction. Very small droplets will reduce the force by a factor of r_d^6 and will not coalesce. In the case of very small droplets DC fields are applied [Taylor, 1996].

5.2.2 Membrane Filtration

The mechanism for emulsion breakage has been described in Chapter 4

5.3 Materials and Methods

5.3.1 Materials

Dodecane (99 %) was obtained from BDH Laboratory Supplies (Poole, England). Paranox 100 was obtained from Exxon Chemicals (Southampton, England). Nickel II nitrate was purchased from Fluka (Gillingham, Dorset, England).

5.3.2 Experimental

5.3.2.1 Emulsification

The method of emulsification has been described in Chapter 2. The emulsion composition and experimental conditions used are summarised in Table 5.1.

5.3.2.2 Electrostatic coalescence unit and operation

The equipment used was a parallel plate type coalescer (Fig 5.5a). The cell configuration and operating details are given in Table 5.2. The inside dimensions of the cell were, length 10 cm , width 10 cm and height 10 cm. Prior to start-up the cell contained two phases (equal amounts of dodecane and aqueous phase) which lay at the interface to the emulsion feed inlet. An insulated glass spiral tube containing salt solution and a metal electrode were placed in the dodecane phase as shown in Fig 5.5a. At the bottom of the aqueous phase was a metal electrode. The distance between the electrodes was 8.0 cm. However, the aqueous phase plays the role of an electrode and therefore the distance between upper electrode and the water phase is 1.5 cm. The top electrode (positive) was connected to a high voltage DC generator and the lower electrode grounded.

Operation

The emulsion was fed through the emulsion inlet, as shown in Fig 5.5a, into the apparatus from the feed tank until the thickness of the emulsion layer was 5 mm. Demulsification experiments were performed by applying low frequency pulsed DC (10 kV and 10 Hz) as developed by Bailes. The frequency was kept constant for the first set of breakage experiments. Experiments were repeated for the most unstable emulsions in Table 5.1, and this time frequency was varied between 0-200 Hz. The experiments were carried out batchwise.

The operation conditions for breakage using the electrostatic coalescer in batch mode were varied to investigate the best way to break the emulsions. The parameters studied were: frequency and electrode position. Also emulsion composition was varied to determine how emulsion stability effects breakage.

Table. 5.1: The emulsion composition and conditions for homogenisation.

Emulsion phase volume ratio aqueous: organic	Surfactant concentration (w/w %)	Homogeniser		Breakage method
		speed (rpm)	residence time (min)	coalescer or filtration
50:50	1	9500	10	F,C
50:50	1	8000	10	F,C
50:50	2	9500	10	F
20:80	0.5	9500	10	F
50:50	0.5	9500	10	C

Where F= filtration and C= electrostatic coalescence.

Table. 5.2 : Specifications for electrostatic coalescence.

Power	Pulsed d.c
Residence time for breaking the emulsion	10 min
Electric field	Parallel
Shape of electrostatic coalescer	Parallel plate horizontal
Earthed electrode	Metal electrode
Insulated electrode	Spiral tube containing salt solution and a metal electrode

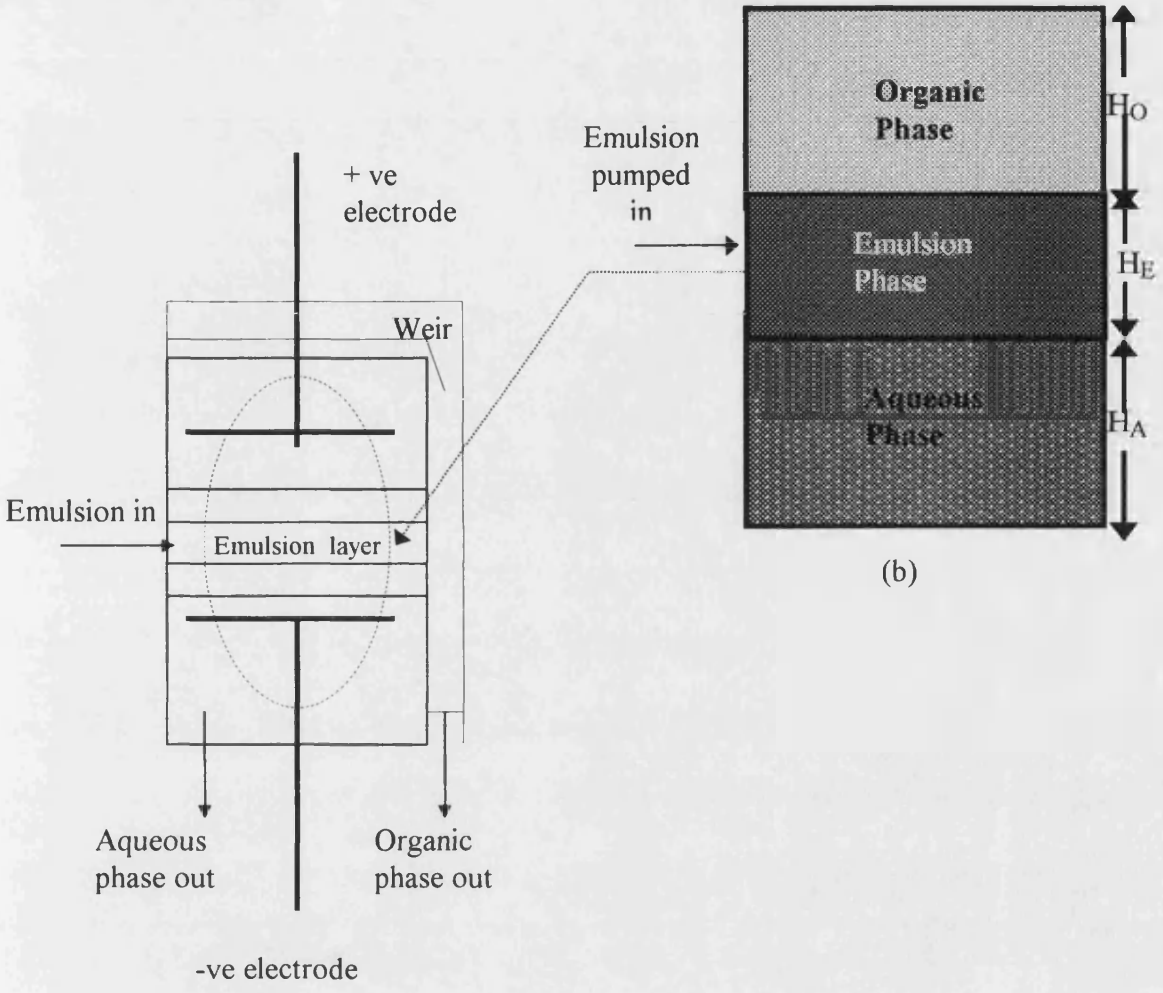

Figure. 5.5 (a) Schematic diagram of the electrostatic coalescer used for the breakage of emulsions and (b) Loading of the aqueous, oil and emulsion phases (H_O -height of the oil phase, H_E -height of the emulsion phase and H_A -height of the aqueous phase).

5.3.2.3 Membrane module operation

The membrane module operation is outlined in Chapter 2.2. The characteristics of the membranes used are given in Table 5.3.

5.3.3 Analytical Methods

Emulsion breakage using either an electrostatic coalescer or a membrane module was determined by the separation of water from dodecane. The details of how the water content is represented for each process is outlined below:

5.3.3.1 Electrostatic coalescer performance

The initial conditions of the electrostatic coalescer are shown in Fig. 5.5b. Once the electrostatic coalescer has operated, an additional layer, Δh_e (Fig. 5.7) formed between the emulsion and the water phase when first signs of demulsification occurred. This layer contained emulsion that is whiter than the emulsion above it.

If the water droplets coalesce and sediment there will be another layer found, Δh_w (Fig 5.8) which will lie between the water phase and Δh_e. By measuring the thickness (proportional to phase volume ratios) of Δh_e the separation of water from dodecane can be determined.

5.3.3.2 Membrane module

By measuring the water content in the permeate (collection in 1.5 ml vials) at 2 minute intervals for a flux of 13 l/h/m^2 and at 1 min intervals for a flux of 26 l/h/m^2 and representing it as a percentage of the total permeate at time t, the permeate water content can be compared with the original emulsion water content at any time.

Table. 5.3. Membrane characteristics, Gelman Science

Name	Membrane thickness (μm)	Membrane porosity %	Pore size range (μm)	Hydrophilic membrane material
Supor	150	70-80	0.2, 0.45 and 0.1	udel polysulfone
Nylaflo	125	70-80	0.2	nylon 6-6
HTtuffryn	165	70-80	0.2	poly(arylenesulfone ether)
Versapor	125	70-80	0.2	polyvinylchloride and polyacrylonitrile

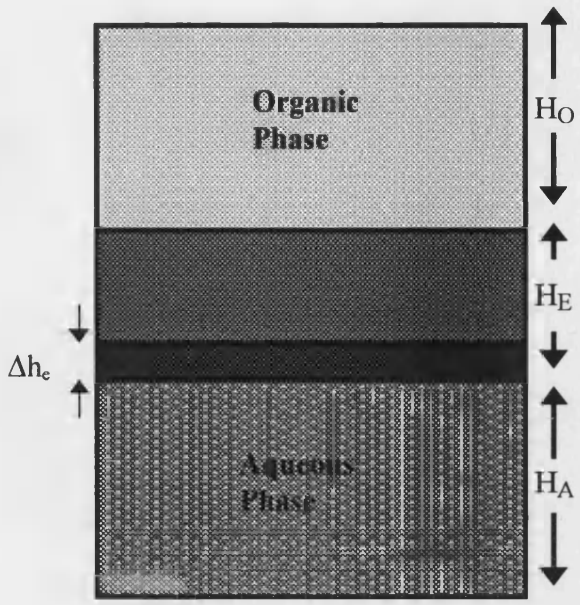

Fig. 5.7. Sedimentation of water droplets to form an additional layer. (H_O -height of the oil phase, H_E -height of the emulsion phase, H_A -height of the aqueous phase and Δh_e -height of the sedimentation).

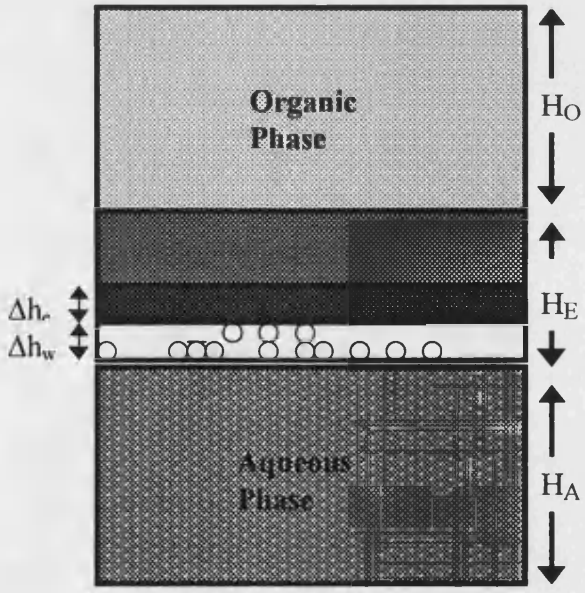

Fig. 5.8. Sedimentation of water droplets to form an additional layer. (H_O -height of the oil phase, H_E -height of the emulsion phase, H_A -height of the aqueous phase and Δh_e -height of the sedimentation).

5.4 Results

Coalescence of the water droplets of emulsions of varying composition were investigated using DC electrostaic coalescence and membrane filtration. The emulsions used in the experiments (Table. 5.1) had surfactant concentrations between 0.5-2 w/w % and phase ratios of 50:50 and 20:80. The emulsion which was only used in the electrostatic coalescer was considered to be very unstable and was used to help determine the demulsification rate. In the case of filtration an emulsion with 2 % Paranox 100 (surfactant) was used to show breakage of a very stable system. This emulsion was not used in the electrostatic coalescer for reasons described below.

5.4.1 Electrostatic coalescence

All operation conditions for breakage using the electrostatic coalescer in batch mode were kept constant except for frequency which was varied to investigate its effect on the emulsions breakage. Also emulsion composition (Table. 5.1) was varied to determine how emulsion stability affects breakage.

5.4.1.1 Visual results

The initial conditions of the electrostatic coalescer are shown in Fig 5.9. Once the coalescer had been operated the lower part of the organic phase became cloudy.

5.4.1.2 Effect of varying emulsion composition.

Tables 5.4, 5.5 and 5.6 show the breakage results for emulsions that vary in composition. In all cases Δh_e and Δh_w were zero and therefore the emulsions were not demulsified..

5.4.1.3 Effect of varying the frequency of the DC .

Table 5.7 shows the breakage results where the frequency was varied between 10 and 200 Hz. Only the most unstable emulsions in Table 5.1 were used and there was no water separation (Δh_e and Δh_w were zero).

5.4.2 Droplet coalescence in the membrane module

Experiments were performed on four membrane types in the same manner. A fresh membrane was used for each run and the pore size for membranes: (Table. 5.3) versapor (polyvinylchloride and polyacrylonitrile), Nylaflo (nylon 6-6) and HTTuffryn (poly(arylenesulfone)ether) was 0.2 μm. The pore sizes used for Supor (udel polysulphone) were 0.1 μm, 0.2 μm and 0.45 μm. The permeability of each membrane for fresh dodecane was checked before each run (see Chapter 2, for materials and methods and Chapter 3 for the results).

5.4.2.1 Effect of surfactant concentration

Figure 5.10 shows a time course for emulsion breakage. The percentage water content (vol %) of the permeate is plotted against time as a function of flux and surfactant concentration. The water initially appeared in the permeate at the same time (10.5 minutes for a flux of 26 l/h/m^2 and 21 minutes for a flux of 13 l/h/m^2) irrespective of surfactant concentration. Prior to this only dodecane was collected, 3 x 10^{-6} m^3 for both fluxes and surfactant concentrations. The water in the permeate increased after its initial appearance in the same manner (for both 1 w/w % and 2 w/w % Paranox 100) up to 27 min at flux 13 l/h/m^2 and 13.5 min at a flux of 26 l/h/m^2 and after this period the 2 w/w % Paranox 100 emulsion was at the maximum pressure of the system but the 1 w/w % Paranox 100 emulsion continued to increase steadily to a water content in the permeate of 44 % and 51 % for fluxes 13 l/h/m^2 and 26 l/h/m^2 respectively. This was approximately the percentage water in the original emulsion (50 v/v %).

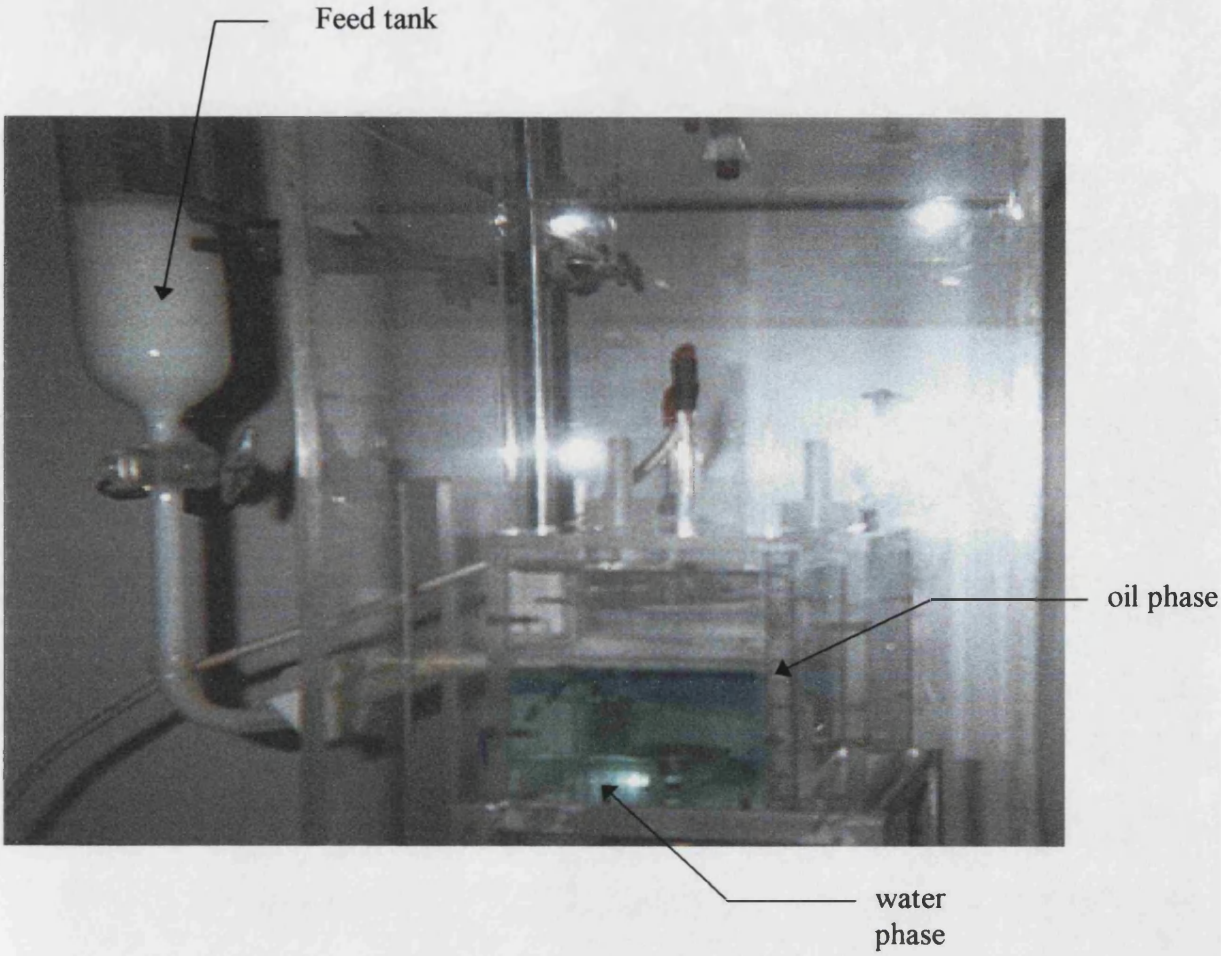

Fig 5.9 Electrostatic coalescer before operation.

Table.5.4. Emulsion Breakage in the electrostatic coalescer for varying surfactant concentration.

Surfactant concentration (w/w %)	Time (min)	Current (mA)	H_E (cm)	Δh_E (mm)	Δh_W (mm)
0.5	20	0.72	0.5	0	0
1	20	0.82	0.5	0	0

50:50 emulsion at surfactant concentrations 0.5 and 1 w/w %. The voltage of 10 kV and frequency of 10 Hz. were kept constant.

Table.5.5. Emulsion Breakage in the electrostatic coalescer for varying average droplet size.

Homogeniser mixing speed (rpm)	Time (min)	Current (mA)	H_E (cm)	Δh_E (mm)	Δh_W (mm)
8,000	20	0.78	2.3	0	0
9,500	20	0.82	0.5	0	0

50:50 emulsion (1 w/w % Paranox 100) at mixing speed 9500 and 8000 rpm (for 10 minutes). The voltage of 10 kV and frequency of 10 Hz were kept constant.

Table.5.6. Emulsion Breakage in the electrostatic coalescer for varying phase ratio

Phase ratio A:O	Time (min)	Current (mA)	H_E (cm)	Δh_E (mm)	Δh_W (mm)
50:50	20	0.72	0.5	0	0
20:80	20	0.66	0.5	0	0

50:50 and 20:80 emulsion with surfactant concentration 0.5 w/w %. The voltage of 10 kV and frequency of 10 Hz. were kept constant.

Table.5.7. Emulsion Breakage in the electrostatic coalescer at varying frequency.

Surfactant concentration w/w %	Time minutes	Homogeniser mixing speed rpm	Current mA	H_E CM	Δh_E (mm)	Δh_W (mm)
0.5	20	8,000	0.74	0.5	0	0
1	20	9,500	0.66	0.5	0	0

50:50 (0.5 % and 1% Paranox 100) emulsion. For the 1w/w % Paranox 100 emulsion the mixing speed was 8000 rpm. The voltage of 10 kV was kept constant and the frequency was varied between 10 -200 Hz.

5.4.2.2 Effect of droplet size.

Fig 5.11 shows the percentage water in the permeate as a function of time for a 50:50 water-in-dodecane (1 w/w % Paranox 100) emulsion with average droplet size 6.8 μm and 12.1 μm. The water initially appeared in the permeate at 21 minutes for the emulsion with average droplet size 6.8 μm but there was a longer delay (25 minutes) before water was detected in the permeate for the emulsion with average droplet size 12.1 μm. During the time interval 21 minutes and 25 minutes air bubbles were detected in the permeate line and flux was not constant. The water in the permeate increased rapidly to a final value of 51 % for the emulsion with an average droplet size of 12.1 μm and 44 % for the emulsion with an average droplet size of 6.8 μm. This was approximately the percentage water in the original emulsion (50 v/v %).

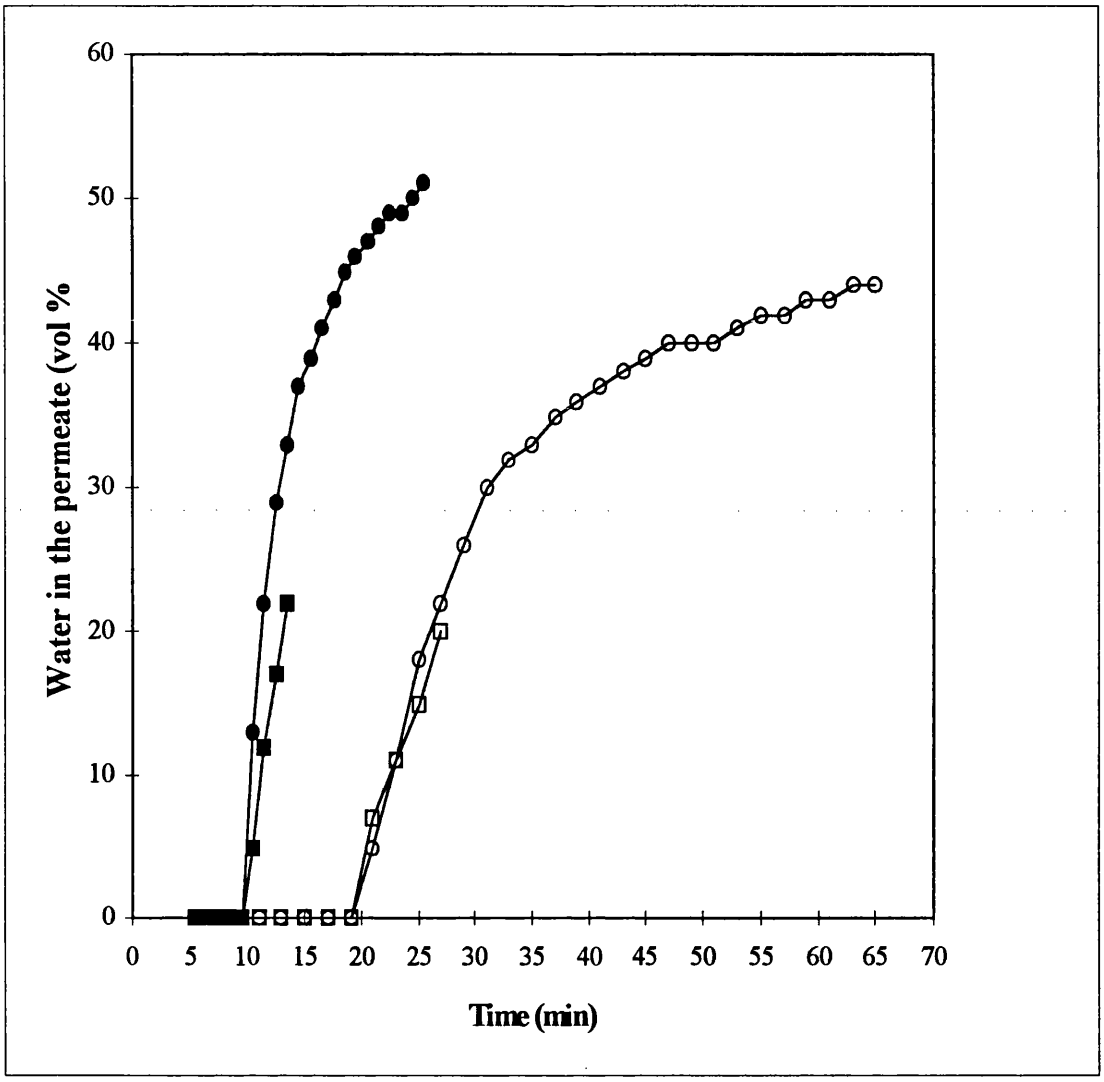

Fig 5.10. Water content in the permeate for 50:50 water-in-dodecane emulsion at surfactant concentration 1 w/w % and 2 w/w %. Flux 13 l/h/m^2 -□- 2 w/w % Paranox 100, -O- 1 w/w % Paranox 100. Flux 26 l/h/m^2 -■- 2 w/w % Paranox 100, - • - 1 w/w % Paranox 100.

5.4.2.3 Effect of type of membrane

Fig 5.12 shows the water in the permeate for a 50:50 water-in-dodecane (1 w/w % Paranox 100) emulsion. Three different membranes were used Nylaflo, HTTuffryn and Supor (pore size 0.2 μm). Water initially appeared in the permeate at the same time (10.5 minutes for a flux of 26 l/h/m^2) irrespective of the membrane type. After this initial period the water content in the permeate increased rapidly to a value of 51 % and 36 % for Supor and HTTuffryn respectively. At the lower flux 13 l/h/m^2 the water content in the permeate increased rapidly and in the same manner for membranes Nylaflo and HTTuffryn but at a more steady rate for Supor. At the end of the runs the percentage water in the permeate was 44 % for membranes Supor, Nylaflo and HTTuffryn. Table 6.8 shows that no water was collected in the permeate for membranes Nylaflo (at a flux of 26 l/h/m^2) and Versapor at a fluxes 13 l/h/m^2 and 26 l/h/m^2.

5.4.2.4 Effect of pore size.

Table 5.9 shows that there is no water detected in the permeate at pore sizes 0.1μm and 0.45 μm (for fluxes 26 l/h/m^2 and 13 l/h/m^2).

5.4.2.5 Effect of flux

Fig 5.13 shows the water in the permeate for a 50:50 water-in-dodecane (1 w/w % Paranox 100) emulsion at three different fluxes (13 l/h/m^2, 26 l/h/m^2 and 43.3 l/h/m^2). The water initially appeared in the permeate at 10.5 minutes for the 26 l/h/m^2 flux, 21 minutes for the 13 l/h/m^2 flux and 7.3 minutes for the 43.3 l/h/m^2 flux. These values corresponded to 3 x 10^{-6} m^3 of dodecane being collected before any water was detected in the permeate for the two lower fluxes and 4 x 10^{-6} m^3 of dodecane for the 43.3 l/h/m^2 flux. For a short period before water was collected in the permeate, at a flux of 43.3 l/h/m^2, air bubbles were detected in the permeate line at this point the flux was not constant. At the end of operation the percentage water in the permeate was 51 %, 44 % and 35 % for fluxes 13 l/h/m^2, 26 l/h/m^2 and 43.3 l/h/m^2 respectively.

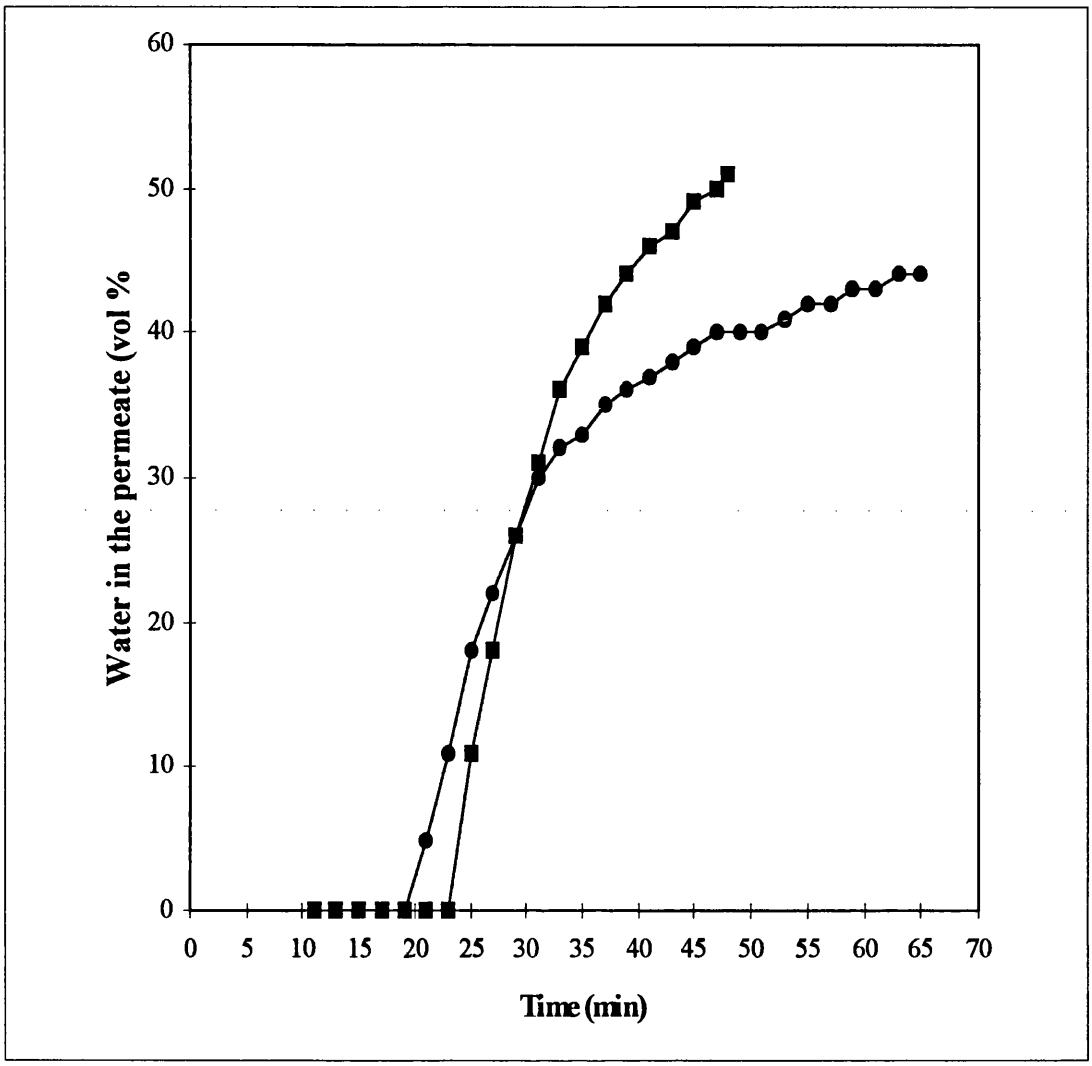

Fig 5.11. Water content in the permeate for 50:50 water-in-dodecane (1 w/w % Paranox 100) emulsion. Flux 13 l/h/m^2: -■- average droplet size 12.1 μm, -•- average droplet size 6.8 μm.

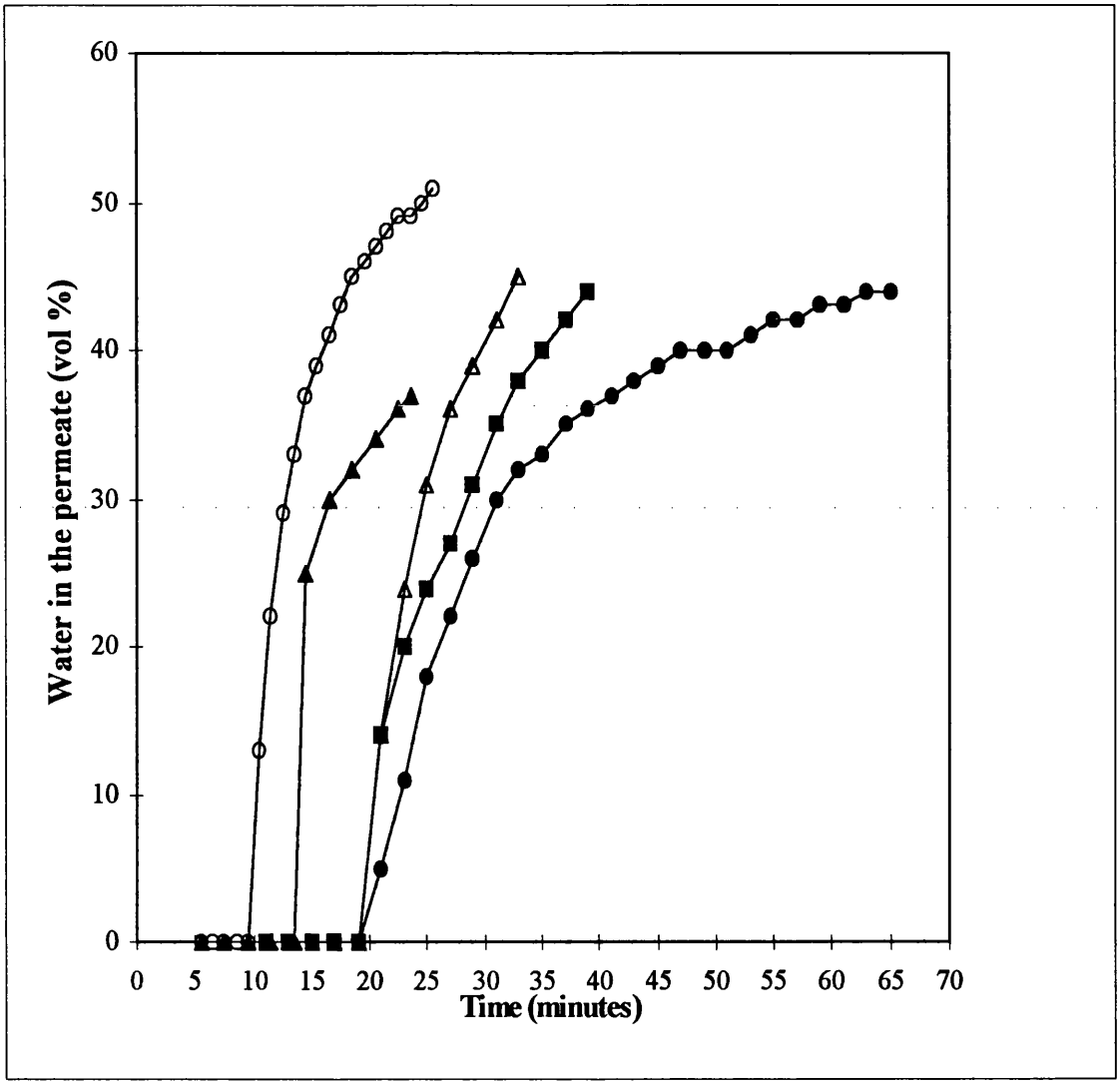

Fig 5.12. Water content in the permeate for 50:50 water-in-dodecane emulsion at surfactant concentration 1 w/w % using membranes HTTuffryn, Nylaflo and Supor 200. Flux 13 l/h/m^2 -Δ- HTTuffryn, -■- Nylaflo and -●- Supor 200. Flux 26 l/h/m^2 -▲- HTTuffryn and -○- Supor 200.

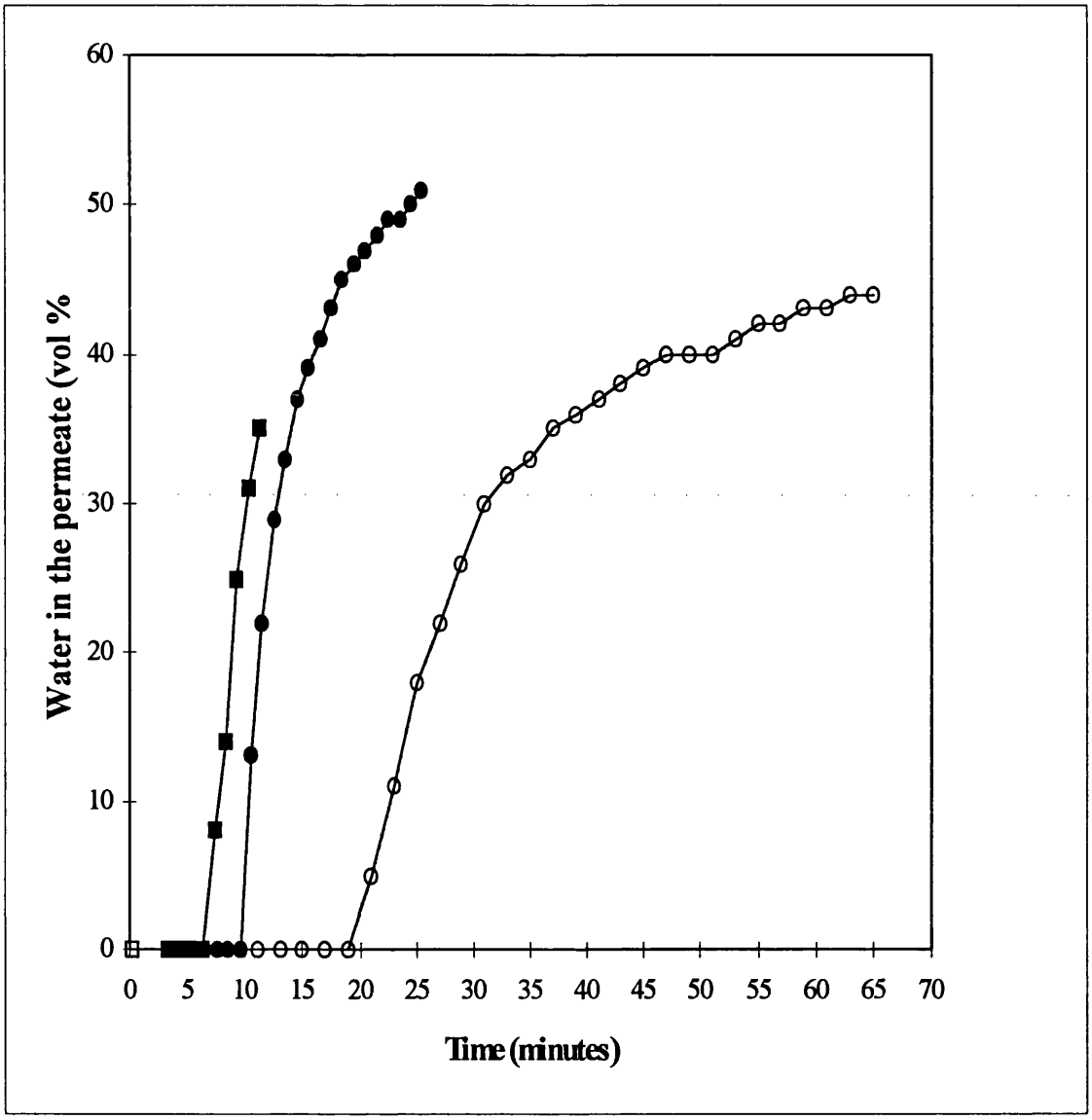

Fig 5.13. Water content in the permeate for 50:50 water-in-dodecane emulsion at surfactant concentration 1 w/w % . Fluxes -O- 13 l/h/m^2, - • - 26 l/h/m^2 and -■- 43.3 l/h/m^2.

Table 5.8. Water content in the permeate at fluxes 0.3 x 10^{-6} m^3 min^{-1} and 0.3 x 10^{-6} m^3 min^{-1} for membranes Nylaflo and Versapor.

Membrane	pore (μm)	Flux ($l/h/m^2$)	water content in permeate (%)
Versapor	0.2	0.3	0
		0.6	0
Nylaflo	0.2		0

Table 5.9 Water content in the permeate at a flux of 13 $l/h/m^2$ for a 20:80 water-in-oil (0.5 w/w %) emulsion.

Membrane	pore (μm)	Flux ($l/h/m^2$)	water content in permeate (%)
Supor	0.2	13	0

Table 5.10 Water content in the permeate at fluxes 13 $l/h/m^2$ and 26 $l/h/m^2$ the for a 50:50 water-in-oil (1 w/w %) emulsion. Supor membrane used with pore sizes 0.1, 0.2 and 0.45 μm.

Membrane	pore (μm)	Flux ($l/h/m^2$)	water content in permeate (%)
Supor	0.1	0.3	0
	0.2	0.3	44 %
	0.45	0.3	0
	0.1	0.6	0
	0.2	0.6	51 %
	0.45	0.6	0

5.5 Discussion

5.5.1 Electrostatic Coalescer

During emulsion breakage experiments the organic phase became cloudy in almost all cases. However, this was not due to demulsification but to dispersion of the emulsion in the organic phase, caused by the electric field. The droplets move due to Brownian motion and sedimentation. When an electric field is applied this movement is magnified and eddies are formed. The cloudy phase was simply entrained aqueous phase, there was no evidence of emulsion breakage.

Tables 5.4, 5.5 and 5.6 show that there was no breakage of the emulsions at a frequency of 10 Hz and applied voltage 10 kV even though this has been stated to be the optimum frequency of the system (Bailes and Larkai, 1981). The coalescer was then run over a range of frequencies 10-200 Hz to investigate if coalescence would occur at higher frequencies. The results in Table 5.7 show that emulsion breakage did not even occur at 10 kV and 200 Hz. It may be considered that the surfactant (Paranox 100) used and the way in which it interacted with the emulsion components, and the high water content of the emulsions was what prevented the water droplets coalescing. The high water content emulsions lowered the electric field strength so that the droplets received little force (equation 5.1). Equation 5.1 suggests that the forces acting on the dipoles are proportional to the square of the electric field and to the sixth power of the droplet diameter. It also shows that the electric field strength, not the conduction current is the main cause of droplet coalescence and therefore with the high water content emulsions used here, the electric field strength was low. The surfactant mechanical properties for Paranox 100 were high and therefore helped to prevent droplet coalescence. The emulsions in Table 5.4 were stabilised with Paranox 100 at concentrations 0.5 and 1 w/w %. However the emulsion in both cases was above the cmc and therefore the droplet size distribution was the same for both. This showed that the surfactant concentration was not one of the controlling steps that prevented droplet coalescence. In order for surfactant concentration to have affected the coalescence rate it would have needed to be below the cmc resulting in a wider

droplet size distribution. A larger droplet size would have improved the possibility of coalescence according to equation 5.1. In view of this, breakage of emulsions at surfactant concentration 2 w/w % were not deemed necessary. The applied voltage could not be increased above 10 kV due to the properties of the electrode insulation. However, increasing voltage above 10 kV was unlikely to promote coalescence as the high water content of the emulsions would have reduced the electric field strength. Breakage of emulsions, stabilised by Paranox 100 and of high water content, using DC electrostaic coalescence was not possible given the results reported here. It may have been possible to break these emulsions using AC electrostatic coalescence.

Bailes and Larkai (1982), reported that the optimum frequency is determined by the relaxation time of the insulation and the continuous phase only. When the insulation is absent the optimum frequency is determined by the relaxation time of the continuous phase. For the emulsion they used (dilute sulphuric acid-20 % LIX 64N in kerosene and surfactant Escaid 100) the optimum frequency was:

τ =0.00291 s

$$f_m = \frac{1}{2\pi\tau} \qquad \text{.....(5.2)}$$

f_m = 54.7 Hz

Where f_m is the optimum frequency and τ is the relaxation time of the continuous phase. The calculated frequency is consistent with that used in the oil industry. The relaxation time used in Equation 5.2 is only for the continuous phase and the dispersed phase is not taken into consideration. This is not a true prediction of the optimum frequency since a small amount of water will produce a conduction current. Which means that k will be much larger than that of the continuous phase only. if k is large τ will decrease and the frequency will increase.

$$\tau = \frac{\varepsilon_b \ \varepsilon}{k_e} \qquad \text{.....(5.3)}$$

Where k_e is the conductivity of the external phase, ε_b is the permittivity of the continuous phase and ε is the permittivity of free space.

For an insulated electrode Bailes and Larkai (1982) calculated the relaxation time at the interface and the optimum frequency using:

$$\tau = \frac{d_a\varepsilon_b + d_b\varepsilon_a}{d_a k_b + d_b k_a} = 0.0158 \text{ s} \qquad \text{.....(5.4)}$$

$f_m = 10$ Hz

Where d_a, k_a and ε_a are the thickness, conductivity and permittivity of the insulation and d_b, k_b and ε_b are the thickness, conductivity and permittivity of the continuous phase. Their calculated value is consistent with their results. The reason for this is they used unstable emulsions in which the dispersed phase settled out leaving the oil phase. The oil phase then prevented the dispersed phase from affecting the frequency. This can be seen clearly by a later paper by Bailes and Larkai (1984) where they reported that phase ratio did not effect the frequency. They accepted the concept that before coalescence the droplets formed chains which were responsible for the conduction of current. If the phase ratio was increasing then so would the conduction current and therefore k_b in equation 5.4 would be large and f_m would increase. If their emulsions had been stable increasing the water content would have increased the frequency. The reason the emulsions did not break was a result of surfactant mechanical properties and high water content. Bailes and Larkai (1984), also reported that the electric field strength decreased with increase in phase ratio and therefore coalescence performance depended on factors other than just field strength. A decrease in electric field strength was to be expected when the water content in the emulsion was increased. The higher the water content the higher the conductivity of

the emulsion. A large number of chains of drops form a conducting path making it difficult to maintain a high electric field strength. The emulsions they used were unstable which is what led them to believe that as phase ratio increased so did the coalescence.

Joos and Snaddon (1985) remodelled Bailes and Larkai equipment as a resistor - capacitor network and found a maximum field strength at 22 Hz acting on the emulsion at a constant source voltage V_0. They did not find a maximum coalescence efficiency at low frequencies neither did they find a maximum at high frequency. However, they found that the coalescence efficiency increased steadily with frequency and they attributed the results to field strength effect.

Kataoka and Nishiki (1995) reported that emulsions stabilised by ECA 4360J of polyamine were more difficult to demulsify than emulsions stabilised by Span 80. Emulsions stabilised with ECA 4360J of polyamine could only be demulsified at voltages above 2.5 kV. However in their experiments the water phase was only 0.5 wt %. It is clear that surfactant mechanical properties were not the only factor preventing emulsion breakage in the results presented in table 5.7. Kizling and Stenus (1983) reported for micro emulsions above the cmc a decrease in the surfactant concentration resulted in a decrease in the number of micelles. The micelle structure and droplet size were unaffected.

Taking into consideration the above, the controlling steps in droplet coalescence for DC electrostatic coalescence were, (1) the type of surfactant and not surfactant concentration (if the surfactant concentration is above the cmc) and (2) the water content.

When the voltage applied is AC the distribution of voltage across the emulsion and insulation changes as frequency changes. At low frequency the voltage across the emulsion is low but at higher frequencies (optimum frequency) the voltage distribution is greatest across the emulsion. Also for a DC system (with insulated electrodes) the voltage across the emulsion is very low because the resistance of the

emulsion compared to the resistance of the insulation is very low and therefore almost all of the voltage is dissipated by the insulating material [Biggan, 1993]. This explains why demulsification using AC voltage is superior to demulsification using DC voltage.

5.5.2 Membrane module

Chapters 3 and 4 have shown that the breakage mechanism occurs on the surface of the membrane. It was concluded that the breakage on the surface was the result of the droplets being pressed together by squeezing dodecane out of the emulsion. Depletion of the dodecane caused the pressure applied on the emulsion to increase to a critical pressure where rupture of the surfactant film took place. This mechanism was first introduced by Bibette (1982) where he used an emulsion enclosed in a dialysis bag. The effect of the applied osmotic pressure is to squeeze the water out of the emulsion. This results in compressing the droplets (like a mechanical piston would do on the droplets alone). Since the droplets can no longer stay spherical, they press against each other and form facets at each contact. He also reported that there was a critical pressure (disjoining pressure) and a critical mean radius of curvature at which rupture of the surfactant film is likely to happen. This implies that the larger and smaller droplets can reach the same internal pressure for different osmotic pressures. Small droplets have an initial internal pressure close to the critical value and need only a small osmotic pressure to become unstable. Each surfactant as a single critical pressure. This theory is used to explain the results in Fig 5.10, 5.11, 5.12, 5.13. It is clear from Fig 5.10 since at any time in the individual runs the dodecane /water ratio in the permeate is the same. It maybe considered that surfactant concentration did not hinder coalescence where the emulsions used were all above the cmc. The mean droplet size was different for each emulsion but the threshold pressure (Bibette et al, 1982) was at the critical pressure and therefore rupture of the film and coalescence of the droplets occurred at the same time. The surfactant concentration did not affect the coalescence of the droplets.

Fig 5.11 shows that there was a longer delay before water was detected in the permeate for the emulsion with an average droplet size of 12.1 μm. This delay was

believed to be the result of air trapped in the module and was not the result of the difference in droplet size. For average droplet sizes 6.8 μm and 12.1 μm the threshold pressure (Bibette et al, 1982) was at the critical pressure and therefore rupture of the film and coalescence of the droplets occurred at the same time.

Fig 5.12 shows that the ratio of water to dodecane in the permeate was in the same proportions. So in the case of these membranes membrane structure was similar (chapter 4). Tables 5.9 and 5.10 show that no water was detected in the permeate. However, dye tests (Chapter 3) carried out on the contents of the module showed that coalescence had occurred but the water had not entered the pores. It was considered that the breakthrough pressure of water in the presence of dodecane for certain types of pore structure was extremely high and resulted in the pressure across the membrane never being reached (discussed in detail in Chapter 4).

The results in Fig, 5.10, 5.12 and 5.13 showed that what ever the flux a certain amount of dodecane needed to be removed before the droplets coalesced and as already mentioned surfactant concentration did not affect coalescence as, the droplet size was > 6.8 μm in all cases, the pressure was at the critical value and surfactant rupture occurred. Therefore, once the appropriate amount of dodecane was removed the droplets coalesced. The amount removed was the same for almost all the emulsions and fluxes. For emulsions where there was a longer delay in the water being collected in the permeate or where no water was detected in the permeate the reason was attributed to one of the following (1) Air was trapped in the module, where it was compressed and caused a drop in the flux. (2) If the breakthrough pressure of the membrane is very high, water will have coalesced on the surface of the membrane but will not enter the pores until the breakthrough pressure is reached. This was discussed in detail in chapter 4.

Published work by Bibette (1982) and Bibette et al (1982) showed, using an osmotic stress technique, that the applied osmotic pressure presses the oil droplets together by squeezing water out of the system. By varying the surfactant concentration and osmotic pressure and keeping the droplet size at 1.6 μm they produced a set of

stability criteria for an emulsion. The stability diagram shows that below the cmc (critical micelle concentration) the emulsions are always unstable but above the cmc their stability is controlled by osmotic pressure and is insensitive to surfactant concentration. They also reported that by keeping the surfactant concentration above the cmc and varying the osmotic pressure and droplet size a stability diagram could be developed that represents the threshold osmotic pressure π^* (atm) as a function of droplet diameter, σ (μm), on a semilog scale (Fig 5.14). The osmotic pressure, π^*, dropped to almost zero for very small droplets (about 0.3 μm) and monotonically increased for larger droplets. With increasing droplet diameter π^* reached asymptotically a constant value of about 1 atm. However these values were for an emulsion consisting of silicone oil, sodium dodecyl sulfate (SDS) and water. In order to know the threshold values for an emulsion of water-in-dodecane stabilised by Paranox 100, appropriate experiments would have to be carried out. The stability diagram would be similar to the one shown in Fig 5.14. It is clear from the stability diagram for droplet sizes 6.8 μm and 12.1 μm the threshold pressure was at the same value which resulted in the droplets for either emulsion coalescing at the same time. If droplets coalesce at the same time then the amount of water in the permeate was the same at any time t.

5.5.3 Membrane filtration verses electrostatic coalescence

The results for membrane filtration and electrostatic coalescence showed demulsification was only achieved by membrane filtration. However, in general the demulsification process is influenced by similar factors. The influencing parameters are outlined below:

Surfactant: The mechanism of coalescence is not a function of surfactant concentration for electrostatic coalescence or membrane filtration. However, if the surfactant concentration was below the cmc then one of the controlling steps would be surfactant concentration.

Droplet size: Droplet size distribution greater than 4 μm will not effect the coalescence performance of the water droplets for the membrane filtration process. This is because above 4 μm the droplets will require the same amount of pressure to deform the droplet to a radius where the internal pressure of the droplet is equal to the critical pressure for surfactant rupture. However, for electrostatic coalescence the larger the droplet size the greater the force required (equation 5.1).

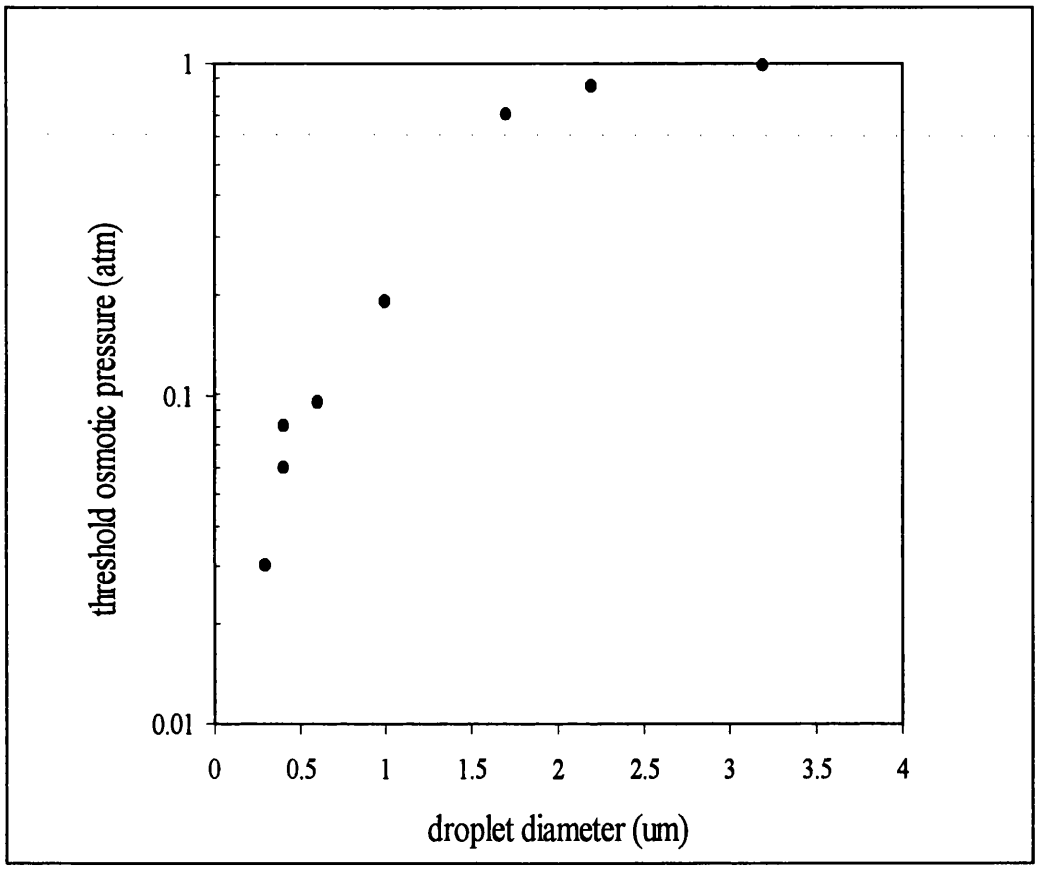

Fig 5.14. Stability diagram of an emulsion. The threshold osmotic pressure (atm) is plotted as a function of the droplet diameter μm (Bibette,1982)

Applied force: Both systems require a force for coalescence to occur. In the membrane system there is a critical pressure at which the droplets coalesce and any pressure increase above this value is wasted. However, as mentioned in Chapter 4 the break through pressure of water in the presence of dodecane was very high for certain types of membrane (e.g versapor, Supor 450 and Supor 100) and therefore extra pressure was needed in order for the coalesced droplets to enter the pores. In

electrostatic coalescence, the greater the force (equation 5.1) the greater the coalescence of water droplets. However, in this research no coalescence was observed this was due to the reduction of the force caused by the emulsion being a high current conductor (which is usually the case for high water content emulsions). The electric field strength was reduced and hence the force.

Chapter 6

Conclusions and Future Work

6.1 Conclusions

The aim of this research was to study the breakage of stable water-in-dodecane emulsions stabilised by Paranox 100 by membrane filtration. It was also decided to compare the breakage results from the filtration experiments with the best method of emulsion breakage available which was electrostatic coalescence. The main conclusions are summarised in this chapter.

6.1.1 Emulsion breakage using hydrophilic membranes as a coalescing aid

6.1.1.1 Preliminary breakage

A compression/tension device (Instron 112) was used as a syringe press to transport emulsion at a constant flowrate to the membrane module. This technique was used to determine if the emulsion could be separated into two phases and if so what sort of flux could be used. A flux of 26 l/h/m^2 was determined experimentally to give good phase separation. No attempt was made to optimise the experimental conditions as this was considered a cheap (only 20 ml of emulsion was required to load and run experiments) and a fast way of determining the initial feed conditions for breakage.

The flux (28.6 l/h/m^2) determined using the Instron could be used directly on the membrane rig. However, a lower value was used so that a clearer separation of water and dodecane in the permeate was obtained.

6.1.1.2 Membrane filtration

The ability of microfiltration hydrophilic membranes to demulsify water -in-dodecane emulsions has been demonstrated. Good separation can be achieved provided that the membranes are of a certain pore structure and pore size. The effect of operating parameters on emulsion breakage by membrane filtration have been studied.

* The performance of the Supor (udel polysulfone) and HTTuffryn (polyarylenesulfone ether) membrane at pore size 0.2 μm were superior to the other membranes (Nylaflo, nylon 6-6; Versapor, polyvinylchloride and polyacrylonitrile; Supor 100 and Supor 450, udel polysulfone) used for the demulsification of water-in-dodecane emulsions. This was attributed to the pore structure of the Supor and HTTuffryn membranes which reduces the breakthrough pressure of the membrane for the dispersed phase.

* The lower the flux the lower the breakthrough pressure required for permeation of the dispersed phase. This was due to the droplets having a longer time to coalesce after surfactant rupture before entering the pores. For the Supor 200 membrane water was detected in the permeate at 2.8 bar and 1.8 bar at fluxes of 26 l/h/m^2 and 13 l/h/m^2 respectively but the slope of the graph did not change until 3.6 bar and 2.7 bar at fluxes 26 l/h/m^2 and 13 l/h/m^2 respectively. This was attributed to water permeating through the larger pores at the lower pressure but pressure increased until the breakthrough pressure of the smaller pores was reached. At the higher flux of 43.3 l/h/m^2 the breakthrough pressure was 3.5 bar which is not very different to the pressure at the flux, 26 l/h/m^2. This was the result of the emulsion being demulsified on the membrane surface to a similar degree.

* Increasing the surfactant concentration in the emulsion decreased the amount of water collected in the permeate and the maximum pressure of the system was reached for a lower amount of filtrate collected. However, because the emulsions formed at surfactant concentrations 1 w/w % and 2 w/w % also had different average droplet size and size distribution it was difficult to tell if the changes were

due to surfactant concentration or droplet size. Other results showed that the smaller the droplet size in the original emulsion the higher the pressure required for the water phase to permeate through. In all cases prior to permeation of both phases the surfactant layer was ruptured and the droplets were partially broken (surfactant concentration did not affect this). After this the role of the surfactant would have been to reduce the interfacial tension and wetting angle. However, the results showed that an increase in pressure was required for both phases to pass through the membrane. This was attributed to droplet size, in the original emulsion. The smaller the droplet size, for the same volume of internal phase, the more coalescence that needs to take place after surfactant rupture for the emulsion to be completely demulsified. Hence larger droplets, after surfactant rupture, will be closer to complete phase separation than the smaller ones.

* Decreasing the homogeniser speed during emulsification resulted in a larger mean droplet size emulsion and this led to an increase in the percentage water in the permeate and a lower breakthrough pressure. The amount of filtrate collected was greater for a much lower pressure increase.

* The breakthrough pressure of water in the presence of dodecane was > 1 bar for the Supor 100, Versapor and Supor 450 membranes. However, the pressure across the membrane (before and after fouling) was not sufficient for the demulsified water phase to enter the membrane pores. In the case of the Nylaflo, HTTuffryn and Supor 200 membranes the breakthrough pressure of water was < 0.5 bar which resulted in the applied pressure being greater than the breakthrough pressure. The breakthrough pressure was dependent on :

Flux: The lower the flux the longer the droplets have to demulsify before entering the pores.

Initial droplet size: The larger the droplet size in the initial emulsion the lower the

breakthrough pressure. e.g emulsion breakage using a Supor membrane for emulsions with an average droplet size of 12.1 μm. and 6.8 μm showed that the breakthrough pressure was lower for the emulsion with the larger initial droplet size (12.1 μm).

In all cases the droplets were partially broken on the membrane surface before permeation of both phases occurred. There was no permeation of both phases until the surfactant layer had been ruptured.

6.1.1.3 Stability

The stability tests showed that the emulsions used in the filtration experiments were extremely stable. The five emulsions studied, for internal phase leakage using tracer experiments, showed that four of the emulsions had internal leakage of less than 5 vol % of which three of the emulsions was below 2 vol %. However, one of the emulsions had a leakage of 18 vol%. This emulsion was considered to be too unstable to be used in the filtration experiments. The same emulsions used in the filtration experiments were used in the D.C electrostatic coalescence experiments. Breakage was determined to be impossible and it was therefore considered necessary to use the most unstable emulsion of water leakage of 18 vol % to determine if this too would not break under DC electrostatic coalescence.

6.1.2 Comparison between experimental results and constant flux equations to predict the mechanism of breakage

Permeation of both phases was determined by the successful rupture of the surfactant layer and the breakthrough pressure of the membrane. Rupture of the surfactant layer was dependent on the close compaction of the droplets (which occurs on depletion of the dodecane phase) and the applied pressure being sufficient for surfactant rupture. If either of these two constraints were not present during filtration the droplets did not break. e.g In the case of the 20:80 water-in-dodecane emulsion the pressure rose to a value that was sufficient to rupture the surfactant layer but the amount of depleted dodecane was not enough and the droplets were not close enough to deform the dye

tests showed that the droplets were not broken. The breakthrough pressure was determined by the pore size of the membrane, the interfacial tension between the two liquids and the contact angle of the water phase with the membrane in the presence of the dodecane phase as described by the Laplace Law. A choice of large pore size and low interfacial tension of the water/dodecane/Paranox 100 system will result in a low breakthrough pressure. However, there are limits :

* If the pore size is too large (bigger than the droplet size) the droplets will pass through the membrane without demulsifying.

* The breakthrough pressure of the membrane needs to be higher than the pressure for surfactant rupture or the droplets could deform and enter the pores before they have broken on the membrane surface. If the droplets are not partly broken before entering the pores the surfactant will not be removed and the emulsion will not demulsify.

Once both phases permeated through the membrane at similar volumes to that in the original emulsion the cake filtration theory explained the membrane fouling.

6.1.3 A comparison between dead-end filtration and pulsed D.C. electrostatic coalescence

Demulsification by electrostatic coalescence was found to be unsuccessful for all emulsions considered and at all operating conditions. It was determined that this was due to the following:

* The water phase was so high that the electricfield strength was lowered so that the droplets received little force.

* The surfactant concentration and its mechanical properties formed a very stable emulsion which could not be ruptured (again not sufficient force).

* No optimum frequency was found and increasing the frequency did not result in the droplets breaking. Again this was attributed to the lowering of electricfield strength by internal phase concentration.

Both filtration and DC electrostatic use the same principles to promote emulsion breakage (both require a force to rupture the surfactant layer). In filtration the force is supplied by the applied pressure and in electrostatic coalescence it is supplied by the electricfield strength. In the filtration experiments the applied pressure will only not rupture the surfactant layer if the droplets are not closely packed (sufficient dodecane as not been removed). Therefore, the higher the initial internal phase the less the continuous phase that needs to be removed. In DC electrostatic coalescence the higher the internal phase the lower the electricfield strength and hence, the lower the force supplied.

I t was determined that DC electrostatic coalescence could not be used to demulsify emulsions with high water content unless the emulsions were initially unstable. However stable emulsions could be broken if the water content was low. Therefore, the use of DC electrostatic coalescence for the demulsification of liquid membrane emulsions was not successful.

6.2 Future work

A number of areas of this work are unresolved or require further study and include the following:

* During filtration the membranes creased. Attempts were made to stop this happening and the membrane creasing was reduced but not eliminated. However, Using a rigid membrane, e.g. ceramic [Marshal, et al, 1996], would eliminate this problem. The more flexible the membrane the greater the creasing problem.

* The emulsions, where the surfactant concentration was between 1-2 w/w % resulted in the emulsion droplet size and distribution being different for each emulsion. In order to determine the affect of surfactant concentration on filtration the water droplets need to be the same whatever the surfactant concentration. This can be achieved by making an emulsion with 1 w/w % surfactant and then after emulsification the extra surfactant can be added. The droplet size will not change on addition of more surfactant.

* It is possible to measure pressure using the compression/tension device (Instron 1122). But for the results to be used a plastic syringe is not suitable. The liquids loaded in the syringe caused a resistance on the syringe which was not constant. It was therefore difficult to know from the pressure recordings which were due to filtration and those due to resistance. A pneumatic piston would reduce this resistance to a negligible value and allow not only flux to be determined but also pressure conditions. This information could be obtained quickly and prevent the chances of bad membrane rig design for any filtration system.

* The breakthrough of the two phases was determined to be down to the droplet size after surfactant rupture. Therefore after surfactant rupture is reached the permeate line should be closed so that the pressure is maintained in the system. The droplets will be free to coalesce to a larger size. Once an adequate time interval is passed the filtration can be continued. This will allow for all of the water to permeate through the membrane and for the cycle to begin again. The result will be operation at lower pressures and longer use of the membranes before cleaning.

* The filtration technique should be applied to other emulsions and different membranes. A knowledge of the emulsion chemistry is needed to assist the choice of suitable membrane therefore, the task could be difficult with complex industrial emulsions where the composition in not available.

* Further experiments concerning the influence of droplet size and membrane structure are important for the evaluation of the operation of the dead-end filtration system as well as for the investigation of the mechanism of emulsion breakage.

* The emulsion breakage mechanism requires the droplets to be closely packed and therefore crossflow operation would not be feasible. From an industrial point of view it would be necessary to operate in dead-end mode by use of a pressure filter. The liquid is pumped up through the centre of the filter shell and into the element, where it is dispersed across the filter bed and paper on each plate. Any portion of the liquid only has a single pass through the filter media. This is similar to operation under dead-end reported in this thesis.

References

Armstrong, D. and Li, W. (1988). Highly selective protein separations with reversed micellar liquid membranes. Analytical Chemistry, **60**, 86-88.

Abou-Nemeh, I. and Peterghem, A.P. (1992). Kinetic study of the emulsion breakage during metals extraction by liquid surfactant membranes (LSM) from simulated and industrial effluents. Journal of Membrane Science, **70**, 65-73.

Bailes, P.J. and Larkai, S.K.L. (1981). An experimental investigation into the use of high voltage D.C. fields for liquid phase separation. Trans IChemE, **59**, 229-237.

Bailes, P.J. and Larkai, S.K.L. (1982). Liquid phase separation in pulsed D.C. fields. Trans IChemE, **60**, 115-121.

Bailes, P.J. and Larkai, S.K.L. (1984). Influence of phase ratio on electrostatic coalescence of water - in - oil dispersions. Chemical Engineering research and design, **63**, 305-311.

Bailes, P.J. and Larkai, S.K.L. (1987). Correspondence. Chemical Engineering Research and Design, **65**, September, 445-447.

Belfort, G., Davis, R.H. and Zydney, A.L. (1994). The behavior of suspensions and macromolecular solutions in cross flow microfiltration. Journal of Membrane Science, **96**, 1-58.

Bevis, A. and Cobham, A. (1992). The treatment of oily water by coalescing. Filtration and Separation, 295-303.

Bhattacharyya, D., Jumawan, A.B., Grieves, R.B. and Harris, L.R. (1979). Ultrafiltration characteristics of oil - detergent - water systems: membrane fouling mechanisms. Separation Science and Technology, **14**, (6), 529-549.

Bhave, R.R. and Fleming, H.L. (1988). Removal of oily contaminants in wastewater with microporous alumina membranes. AIChE Symposium Series, **84**, 19-27.

Bibette, J. (1992). Stability of thin films in concentrated emulsions. Langmuir, **8**, 12, 3178-3182.

Bibette, J., Morse, D.C., Witten, T.A. and Weitz, D.A. (1992). Stability criteria for emulsions. Physical Review Letters, **69**,(16), 2439-2442.

Boey, S.C., Garcia del Cerro, M.C. and Pyle, D.L. (1987). Extraction of citric acid by liquid membrane extraction. Chemical Engineering Research and Design, **65**, 218-223.

Bohlen, D.S., Davis, H.T. and Scriven, L.E. (1992). Surfaces of constant mean curvature with prescribed contact angle. Langmuir, **8**, 3, 982-988.

Bowen, W.R., Calvo, J.I. and Hernandez, A. (1995). Steps of membrane blocking in flux decline during protein microfiltration. Journal of Membrane Science, **101**, 153-165.

Coulson, J.M. and Richardson, J.F. Chemical Engineering volume 2. Pergman, 1978, Oxford.

Cussler, E.L. Diffusion, Mass Transfer in Fluid Systems. Cambridge University Press, (1986), New York.

Dahuron, L. and Cussler, E.L. (1988). Protein extractions with hollow fibres. American Institute of Chemical Engineers Journal, **34**, (1), 130-136.

Daiminger, U., Nitsch, W., Plucinski, P. and Hoffmann, S. (1995). Novel techniques for oil/water separation. Journal of Membrane Science, **99**, 197-203.

Davis, S.S. and Burbage, A.S. (1977). Electron micrography of water-in-oil-in-water emulsions. Journal of Colloid and Interface Science, **62**, (2), 361-363.

Dean, J.A. Langes Handbook of Chemistry. McGraw Hill, 1992, NewYork.

Delaine, J. (1985). Separating oil from water offshore. Chemical Engineer, November, 31-34

Ding, X.C. and Xie, F.Q. (1991). Study of the swelling phenomena of liquid surfactant membranes. Journal of Membrane Science, **59**, (2), 183-188.

Draxler, J., Furst, W. and Marr, R. (1988). Separation of metal species by emulsion liquid membranes. Journal of Membrane Science, **38**, 281-293.

Draxler, J. and Marr, R. (1986). Emulsion liquid membranes. Part 1: Phenonmenon and industrial application. Chemical Engineering Process, **20**, 319-329.

Farnand, B.A., Sawatzky, H. and Poirier, M.A. (1985). An evaluation of the use of porous membranes for the dewatering of wellhead bitumen / water / mineral emulsions. Separation Science and Technology, **20**, (2,3),193-303.

Florence, A.T. and Whitehill, D. (1981). Some features of breakdown in water-in-oil-in-water multiple emulsions. Journal of colloid and Interface Science, **79**, (1), 243-256.

Foley, G., MacLoughlin, P.F. and Malone, D.M. (1995). Membrane fouling during constant flux crossflow microfiltration of dilute suspensions of active dry yeast. Separation Science and Technology, **30**, (3), 383-398.

Fuller, E.J. and Li, N.N. (1984). Extraction of chromium and zinc from cooling tower blowdown by liquid membranes. Journal of Membrane Science, **18**, 251-271.

Grace, H.P. (1954). Structure and performance of filter media. Journal A.I.Ch.E, **2**, 3, 307-

Grace, R. (1992). Commercial emulsion breaking. American Chemical Society, 313-339.

Granger, J., Dodds, J. and Leclerc, D. (1985). Filtration of low concentrations of latex particles. Filtration and Separation.

Hano, T., Ohtake,T. and Hori, F. Kinetic study of electrostatic demulsification contributions of oil and water phases properties. Water Treatment, **5**, 202-213.

Hano, T., Matsumoto., M. and Ohtake, T. (1994). Continuous extraction of Penicillin G with liquid surfactant membrane using vibro mixer. Journal of Membrane Science, **93**, 61-68.

Hermans, P.H. and Bredee. (1935). Kenntnis der filtrationsgesetze. Rec. Trav Chim des Pays-Bas, **54**, 680.

Hermia, J. (1982). Constant pressure blocking filtration laws- application to power law non-newtonian fluids. Trans IchemE, **60**, 183-187.

Hlavacek, M. (1995). Break-up of oil-in-water emulsions induced by permeation through a microfiltration membrane. Journal of Membrane Science, **102**, 1-7.

Hlavacek, M. and Bouchet, F. (1993). Constant flowrate blocking laws and an example of their application to dead-end microfiltration of protein solutions. Journal of Membrane Science, **82**, 285-295.

Howell, J.A., Sanchez, V. and Field, R.W. Membranes in Bioprocessing, Theory and Applications. Blackie A and P, 1993, London.

Hsu, E.C. and Li, N.N. (1985). Membrane recovery in liquid membrane separation processes. Separation Science and Technology, **20**, (2,3), 115-130.

Izatt, R.M., Dearden, D.V., McBride, D.W., Oscarson, J.L., Lamb, J.D. and Christensen, J.J. (1983). Metal separations using emulsion liquid membranes. Separation Science and Technology, **18**, (12 & 13), 1113-1129.

Jeater, P., Rushton, E. and Davies, G.A. (1980). Coalescence in fibre beds. Filtration and Separation, 129-133.

Joos, F.M and Snaddon, R.W.L. (1985). On the frequency dependance of electrically enhanced emulsion separation. Chemical Engineering Research and Design, **62**, 305-311.

Joos, F.M and Snaddon, R.W.L. (1987). Correspondence. Chemical Engineering Research and Design, **65**, September, 448.

Juang, R. and Jiang, J. Application of batch ultrafiltration to the separation of w/o emulsions in liquid surfactant membrane processes. Journal of Membrane Science, **96**, 193-203.

Kamst, G.F., Bruinsma, O.S.L. and Graauw, J. (1997). Permeability of filtration cakes of palm oil in relation to mechanical expression. AIChE Journal, **43**, (3), 673-680.

Kataoka, T. and Nishiki, T. (1990). Development of a continuous electric coalescer of w / o emulsions in liquid surfactant membrane process. Separation Science and Technology, **25**, (1,2), 171-185.

Kato, S. and Kawasaki, J. (1987). A new technique for the mechanical demulsification of o / w emulsions. Journal of Chemical Engineering of Japan, **20**, (3), 232-237.

Kato, S. and Kawasaki, J. (1988). Continuous demulsification of o / w emulsions by a mechanical technique. Journal of Chemical Engineering of Japan, **21**, (3), 321-323.

Kirjassoff, D.E., Pinto, S.D. and Hoffman, C.R. (1980). Ultrafiltration of waste latex solutions. Chemical Engineering Progress, **76**, 58-61.

Kirk-Othmer. Encyclopedia of Chemical Technology. John Wiley, 1994, New York, Vol 9 and 10.

Kita, Y., Matsumoto, S. and Yonezawa, D. (1977). Viscometric method for estimating the stability of w/o/w type multiple phase emulsions. Journal of Colloid and Interface Science, **62**, (1), 87-94.

Kizling, J. and Stenius, P. (1987). Microemulsions formed by water, aliphatic - hydrocarbons and pentaethylene glycol dodecyl ether- the temperature- dependence of aggregate size. Journal of Colloid and Interface Science, **118**, (2), 482-492.

Koltuniewicz, A.B., Field, R.W. and Arnot, T.C. (1995). Cross-flow and dead-end microfiltration of oily-water emulsion. Part1: Experimental study and analysis of flux decline. Journal of Membrane Science, **102**, 193-207.

Kriechbaumer, A. and Marr, R. (1985). Emulsion breaking in electrical fields. American Chemical Society, 381-398.

Kutowy, O., Thayer, W.L., Tigner, J. and Sourirajan, S. Tubular cellulose acetate reverse osmosis membranes for treatment of oily wastewaters. Industrial Engineering Chemical Production research and development, **20**, 354.

Larson, K., Raghuraman, B. and Wiencek, J. (1994). Electrical and chemical demulsification techniques for microemulsion liquid membranes. Journal of Membrane Science, **91**, 231-248.

Lee, S., Aurelle, Y. and Roques, H. (1984). Concentration polarization, membrane fouling and cleaning in ultrafiltration of soluble oil. Journal of Membrane Science, **19**, 23-38.

Lencki, R.W. and Williams, S. (1994). Effect of nonaqueous solvents on the flux behavior of ultrafiltration membranes. Journal of Membrane Science, **101**, 43-51.

Leu, W. and Tiller, F.M. (1983). Experimental study of the mechanism of constant pressure cake filtration: Clogging of filter media. Separation Science and Technology, **18**, (12 and 13), 1351-1369.

Li, N (1968). Separating hydrocarbons with liquid membranes. U.S. Patent 3,410,794.

Li, N. (1978). Demulsification by centrifugation followed by strong shearing. U.S. Patent 4 125 461.

Li, N.N. and Shrier, A.L. (1972). Liquid membrane water treating. Recent Developments in Separation Science, **1**, 163-174.

Lipp, P., Lee, C.H., Fane, A.G. and Fell, C.J.D. (1988). A fundamental study of the ultrafiltration of oil-water emulsions. Journal of Membrane Science, **36**, 161-177.

Lissant, K.J. (1966). The geometry of high-internal- phase -ratio emulsions. Journal of Colloid and Interface Science, **22**, 462-468.

Lissant, K.J. and Mayhan, K.G. (1973). A study of medium and high internal phase ratio water/polymer emulsions. Journal of Colloid and Interface Science, **42**,1, 201-208.

Lu, W., Tung, K.L. and Hwang, K.J. (1997). Effect of woven structure on transient characteristics of cake filtration. Chemical Engineering Science, **52**, 1743-1756.

Marr, R. and Kopp, A. (1982). Liquid membrane technology - a survey of phenomena, mechanisms, and models. International Chemical Engineering, **22**, (1), 44-60.

Marshall, A.D., Munro, P.A. and Tragardh, G. (1996). Design and development of a cross-flow membrane rig to compare constant pressure and constant flux operation in ultrafiltration and microfiltration. Trans IChemE, **74**, Part C, 92-99.

Matsumoto, S. and Kohda, M. (1980). The viscosity of w/o/w emulsions: an attempt to estimate the water permeation coefficient of the oil layer from the viscosity changes in diluted systems on ageing under osmotic pressure gradients. Journal of Colloid and Interface Science, **73**, (1), 13-20.

May, S.W and Li, N.N. (1972). The immobilisation of urease using liquid surfactant membranes. Biochemical and Biophysical Research Communications, 68, (3), 786-792.

McKetta, J.J. Encyclopedia of Chemical Processing and Design. Marcel and Dekker, 1983, NewYork, Vol 18, 90-108.

Mohan, R. and Li, N.N. (1975). Nitrate and nitrate reduction by liquid membrane-encapsulated whole cells. Biotechnology and Bioengineering, **17**, 1137-1156.

Mueller, J., Cen Y. and Davis, R.H. (1997). Crossflow microfiltration of oily water. Journal of Membrane Science, **129**, 221-235.

Pal, R. (1993). Rheological behaviour of surfactant - flocculated water-in-oil emulsions. Colloids and Surfaces A: Physicochemical and Engineering Aspects, **71**, 173-185.

Parkinson, G., Short, H. and McQueen, S. (1983). Liquid membranes - are they ready? Chemical Engineering, August 22, 22-27.

Pickering, P.J. and Chaudhuri, J.B. (1997). Enantioselective extraction of (D)-phenylalanine from racemic (D/L) - phenylalanine using chiral emulsion liquid membranes. Journal of Membrane Science, **127**, 115-130.

Prasad, R. and Sirkar, K.K. (1987). Solvent extraction with microporous hydrophilic and composite membranes. AIChE Journal, **33**, (7), 1057-1066.

Princen, H.M. (1986). Osmotic pressure of foams and highly concentrated emulsions 1. theoretical considerations. Langmuir, **2**, 4, 519-524.

Rosen, M.J. (1989). Surfactants and interfacial phenomena. 2nd edition, John Wiley. New York, pp 308.

Scheper, T., Likidis, Z., Makryaleas, K., Nowottny, C.H. and Schugerl, K. (1987). Three different examples of enzymatic bioconversion in liquid membrane reactors. Enzyme and Microbial Technology, **9**, (10), 625-631.

Scott, K., McConvey, I.F. and Adhamy, A. (1992) Application of crossflow microfiltration to emulsion separation in extraction processes. Journal of Membrane Science, **72**, 245-257.

Scott, K., Adhamy, A., Atteck, W. and Davidson, C. (1994). Crossflow microfiltration of organic / water suspensions. Water research, **28**, (1), 137-145.

Shaw, D.J. Introduction to Colloid and Surface Chemistry. Butterworth, 1980, London.

Shere, A.J. and Cheung, M.H. (1988). Modeling of leakage in liquid surfactant membrane systems. Chemical Engineering Communications, **68**, 143-164.

Sherwood, J.D. (1993). A model for static filtration of emulsions and foams. Chemical Engineering Science, **48**, 19, 3355-3361.

Sun, D., Duan, X., Li, W. and Zhou, D. (1998). Demulsification of water-in-oil emulsion by using porous glass membrane. Journal of Membrane Science, **146**, 65-72.

Sutheim, G. (1947). Introduction to emulsions. Chemical Publishing. New York.

Tarleton, E.S. and Willmer, S.A. (1997). The effects of scale and process parameters in cake filtration. Institution of Chemical Engineers, **75**, Part A, 497-507.

Taylor, S.E. (1996). Theory and practice of electrically enhanced phase separation of water-in-oil emulsions. Trans IChemE, **74**, 526-540.

Terry, R.E., Li, N.N and Ho, W.S. (1982). Extraction of phenolic compounds and organic acids by liquid membranes. Journal of Membrane Science, **10**, 305-323.

Thien, M.P., Hatton, T.A. and Wang, D.I.C. (1986). Liquid emulsion membranes and their applications in biochemical separations. In separation Recovery, and Purification in Biotechnology, eds. Asenjo, J.A. and Hong, J., pp 67-77. American Chemical Society Symposium Series, 314

Thien, M.P., Hatton, T.A. and Wang, D.I.C. (1988). Separation and concentration of amino acids using liquid emulsion membranes. Biotechnology and Bioengineering, **32**, 604-615.

Tiller, F.M., Hsyung, N.B. and Cong, D.Z. (1995). Role of porosity in filtration: Xll. Filtration with sedimentation. AIChE Journal, **41**, (5), 1153-1164.

Tirmizi, N.P., Raghuraman, B. and Wiencek, J. (1996). Demulsification of water/oil/solid emulsions by Hollow-fiber membranes. Journal of AIChE, **42**, 1263-1276.

Toms, A.W. (1987). Design and performance of oleophilic porous media coalescing oil / water separators. Filtration and Separation, 188-190.

Urdahl, O., Williams, T.J., Bailey, A.G. and Thew, M.T. (1996). Electrostatic destabilization of water-in-oil emulsions under conditions of turbulent flow. Trans IChemE, **74**, 158-165.

Wei-Ming, L., Kuo-Lun., T. and Kuo-Jen, H. (1997). Effect of woven structure on transient characteristics of cake filtration. Chemical Engineering Science, **52**, 11, 1743-1756.

Xinsheng, M., Jin, W., Bangqing, N. and Yajun, S. (1995). Demulsification of w/o emulsion by sintered glass plate.

Yan, Y. and Masliyah, J.H. (1993). Effect of oil viscosity on the rheology of oil-in-water emulsions with added solids. The Canadian Journal of Chemical Engineering, **71**, 852-858.

Yamaguchi, M., Kobayashi, A. and Kataayama, T. (1987). International Chemical Engineer, **27**, 3, 506-513.

Zhong, Y. , Siya. L., Yaochuan. Y. and Xuelun. Z. (1987). An investigation into the breaking-down of water-in-oil type emulsions by means of pulsed voltage. Desalination, **62**, 323-328.

Zhong, Y. , Siya. L., Weiha, Z., Liancheng, W. and Peiyan, L. (1990). An investigation into the breakdown of w/o type emulsions by pulsed voltage, **5**, 127-135.

Appendix 1

Experimental data

A1.1 Emulsion breakage by filtration

The pressure across the membrane recorded in the tables below is the mean value of three experiments. Also the standard deviation (SD) for the three repeat experiments is recorded.

A1.1.1 Pressure across the membrane and filtrate collected

50:50 water-in-dodecane emulsion (1 % Paranox 100). Homogenised at 8000 rpm for 3 minutes followed at 9500 rpm for 10 minutes

Supor 200 membrane at flowrate 0.6×10^{-6} m^3/min

Time (min)	Volume of filtrate collected (m^3) 10^{-6}	Pressure across the membrane (bar)		Time (min)	Volume of filtrate collected (m^3) 10^{-6}	Pressure across the membrane (bar)	
		pressure	SD			pressure	SD
0	0	0.090	0.006	13	7.8	4.4	0.4
1	0.6	0.10	0.02	14	8.4	4.4	0.4
2	1.2	0.278	0.1	15	9.0	4.5	0.4
3	1.8	0.939	0.04	16	9.6	4.5	0.4
4	2.4	2.1	0.2	17	10.2	4.5	0.4
5	3.0	2.8	0.1	18	10.8	4.7	0.4
6	3.6	3.2	0.1	19	11.4	4.6	0.5
7	4.2	3.6	0.1	20	12.0	4.8	0.4
8	4.8	3.8	0.2	21	12.6	4.8	0.3
9	5.4	3.9	0.4	22	13.2	4.9	0.4
10	6.0	4.1	0.4	23	13.8	5.0	0.3
11	6.6	4.2	0.3	24	14.4	5.0	0.4
12	7.2	4.2	0.5	25	15.0	5.1	0.4

Supor 200 membrane at flowrate 0.3×10^{-6} m^3/min

Time (min)	Volume of filtrate collected (m^3) 10^{-6}	Pressure across the membrane (bar) pressure	SD	Time (min)	Volume of filtrate collected (m^3) 10^{-6}	Pressure across the membrane (bar) pressure	SD
0	0	0.096	0.0006	33	9.9	3.9	0.4
1	0.3	0.098	0.002	34	10.2	4.0	0.4
2	0.6	0.105	0.007	35	10.5	4.0	0.4
3	0.9	0.13	0.02	36	10.8	4.0	0.3
4	1.2	0.17	0.05	37	11.1	4.0	0.3
5	1.5	0.27	0.01	38	11.4	4.1	0.3
6	1.8	0.43	0.01	39	11.7	4.2	0.3
7	2.1	0.65	0.07	40	12.0	4.2	0.4
8	2.4	0.89	0.02	41	12.3	4.2	0.2
9	2.7	1.31	0.1	42	12.6	4.1	0.3
10	3.0	1.75	0.07	43	12.9	4.3	0.3
11	3.3	2.07	0.02	44	13.2	4.4	0.3
12	3.6	2.3	0.1	45	13.5	4.4	0.4
13	3.9	2.6	0.3	46	13.8	4.5	0.3
14	4.2	2.7	0.3	47	14.1	4.5	0.3
15	4.5	2.8	0.4	48	14.4	4.5	0.3
16	4.8	2.9	0.4	49	14.7	4.6	0.4
17	5.1	3.0	0.4	50	15.0	4.5	0.4
18	5.4	3.1	0.4	51	15.3	4.5	0.2
19	5.7	3.1	0.2	52	15.6	4.6	0.2
20	6.0	3.2	0.3	53	15.9	4.7	0.3
21	6.3	3.25	0.3	54	16.2	4.8	0.3
22	6.6	3.34	0.3	55	16.5	4.7	0.5
23	6.9	3.46	0.3	56	16.8	4.8	0.3
24	7.2	3.5	0.2	57	17.1	4.9	0.3
25	7.5	3.52	0.3	58	17.4	4.9	0.3
26	7.8	3.59	0.4	59	17.7	5.0	0.4
27	8.1	3.6	0.3	60	18.0	4.9	0.6
28	8.4	3.7	0.3	61	18.3	5.0	0.4
29	8.7	3.8	0.3	62	18.6	5.0	0.3
30	9.0	3.7	0.3	63	18.9	5.1	0.4
31	9.3	3.8	0.4	64	19.2	5.2	0.4
32	9.6	3.8	0.4				

Nylaflo membrane at flowrate 0.6×10^{-6} m^3/min

Time (min)	Volume of filtrate collected (m^3) 10^{-6}	Pressure across the membrane (bar) pressure	SD
0	0	0.091	0
1	0.6	0.135	0.0005
2	1.2	0.35	0.09
3	1.8	1.04	0.01
4	2.4	2.4	0.2
5	3.0	3.383	0
6	3.6	4.159	0
7	4.2	4.61	0.06
8	4.8	5.12	0.07
9	5.4	5.46	0.1
10	6.0	5.7	0.1
11	6.6	5.90	0.05
12	7.2	6.02	0.09

Nylaflo membrane at flowrate 0.3×10^{-6} m^3/min

Time (min)	Volume of filtrate collected (m^3) 10^{-6}	Pressure across the membrane (bar) pressure	SD
0	0	0.094	0
1	0.3	0.101	0.0005
2	0.6	0.124	0.005
3	0.9	0.17	0.01
4	1.2	0.283	0.007
5	1.5	0.583	0.009
6	1.8	0.832	0.0005
7	2.1	1.51	0.06
8	2.4	1.84	0.04
9	2.7	2.3	0.1
10	3.0	2.9	0.2
11	3.3	3.3	0.3
12	3.6	3.6	0.3
13	3.9	3.9	0.3
14	4.2	4.1	0.3
15	4.5	4.4	0.3
16	4.8	4.7	0.3
17	5.1	5.0	0.2
18	5.4	5.1	0.2
19	5.7	5.30	0.07
20	6.0	5.4	0.2
21	6.3	5.60	0.09
22	6.6	5.709	0
23	6.9	5.707	0
24	7.2	5.686	0
25	7.5	5.756	0
26	7.8	5.863	0
27	8.1	5.858	0
28	8.4	5.821	0.007
29	8.7	5.760	0
30	9.0	5.74	0.02
31	9.3	5.965	0
32	9.6	5.951	0
33	9.9	5.912	0
34	10.2	5.901	0
35	10.5	5.963	0
36	10.8	6.163	0
37	11.1	6.19	0.01
38	11.4	6.156	0
39	11.7	6.05	0.01

Supor 100 membrane at flowrate 0.3×10^{-6} m^3/min

Time (min)	Volume of filtrate collected (m^3) 10^{-6}	Pressure across the membrane (bar) pressure	SD	Time (min)	Volume of filtrate collected (m^3) 10^{-6}	Pressure across the membrane (bar) pressure	SD
0	0	0.097	0	8	2.4	1.63	0.03
1	0.3	0.098	0.002	9	2.7	2.6	0.2
2	0.6	0.101	0	10	3.0	3.26	0.04
3	0.9	0.114	0.009	11	3.3	3.95	0.2
4	1.2	0.138	0.007	12	3.6	4.5	0.1
5	1.5	0.198	0.005	13	3.9	5.0	0.1
6	1.8	0.33	0.02	14	4.2	5.51	0.08
7	2.1	0.65	0.05				

HTTuffryn membrane at flowrate 0.3×10^{-6} m^3/min

Time (min)	Volume of filtrate collected (m^3) 10^{-6}	Pressure across the membrane (bar) pressure	SD	Time (min)	Volume of filtrate collected (m^3) 10^{-6}	Pressure across the membrane (bar) pressure	SD
0	0	0.095	0.001	17	5.1	2.45	0.09
1	0.3	0.11	0.02	18	5.4	2.5	0.1
2	0.6	0.115	0.001	19	5.7	2.55	0.01
3	0.9	0.342	0.003	20	6.0	2.56	0.04
4	1.2	0.56	0.01	21	6.3	2.583	0.007
5	1.5	0.756	0.004	22	6.6	2.63	0.05
6	1.8	0.96	0.01	23	6.9	2.69	0.05
7	2.1	1.12	0.03	24	7.2	2.737	0.009
8	2.4	1.355	0.005	25	7.5	2.77	0.07
9	2.7	1.60	0.03	26	7.8	2.80	0.09
10	3.0	1.83	0.01	27	8.1	2.92	0.02
11	3.3	2.095	0.005	28	8.4	2.88	0.03
12	3.6	2.24	0.04	29	8.7	2.92	0.02
13	3.9	2.28	0.05	30	9.0	2.980	0.009
14	4.2	2.29	0.05	31	9.3	3.04	0.03
15	4.5	2.32	0.05	32	9.6	3.095	0.003
16	4.8	2.4	0.1	33	9.9	3.10	0.05

HTTuffryn membrane at flowrate 0.6×10^{-6} m^3/min

Time (min)	Volume of filtrate collected (m^3) 10^{-6}	Pressure across the membrane (bar) pressure	SD	Time (min)	Volume of filtrate collected (m^3) 10^{-6}	Pressure across the membrane (bar) pressure	SD
0	0	0.088	0.002	13	7.8	5.2	0.1
1	0.6	0.18	0.04	14	8.4	5.3	0.1
2	1.2	0.56	0.04	15	9.0	5.39	0.07
3	1.8	1.23	0.07	16	9.6	5.4	0.1
4	2.4	1.8	0.2	17	10.2	5.6	0.2
5	3.0	2.3	0.2	18	10.8	5.56	0.03
6	3.6	2.89	0.07	19	11.4	5.6	0.2
7	4.2	3.4	0.2	20	12.0	5.7	0.2
8	4.8	3.8	0.2	21	12.6	5.8	0.1
9	5.4	4.18	0.04	22	13.2	5.81	0.09
10	6.0	4.63	0.09	23	13.8	5.9	0.1
11	6.6	5.0	0.1				
12	7.2	5.1	0.1				

Supor 450 membrane at flowrate 0.6×10^{-6} m^3/min

Time (min)	Volume of filtrate collected (m^3) 10^{-6}	Pressure across the membrane (bar) pressure	SD	Time (min)	Volume of filtrate collected (m^3) 10^{-6}	Pressure across the membrane (bar) pressure	SD
0	0	0.087	0.0005	4	2.4	2.03	0.09
1	0.6	0.119	0.008	5	3.0	3.8	0.2
2	1.2	0.28	0.01	6	3.6	5.1	0.2
3	1.8	0.933	0.002	7	4.2	6.0	0.1

Supor 450 membrane at flowrate 0.3×10^{-6} m^3/min

Time (min)	Volume of filtrate collected (m^3) 10^{-6}	Pressure across the membrane (bar) pressure	SD	Time (min)	Volume of filtrate collected (m^3) 10^{-6}	Pressure across the membrane (bar) pressure	SD
0	0	0.092	0.005	8	2.4	2.2	0.2
1	0.3	0.092	0.004	9	2.7	2.9	0.1
2	0.6	0.122	0.002	10	3.0	3.6	0.3
3	0.9	0.160	0.008	11	3.3	4.4	0.3
4	1.2	0.220	0.009	12	3.6	4.9	0.3
5	1.5	0.43	0.03	13	3.9	5.4	0.3
6	1.8	0.753	0.001	14	4.2	5.8	0.2
7	2.1	1.203	0.005				

Versapor membrane at flowrate 0.6×10^{-6} m^3/min

Time (min)	Volume of filtrate collected (m^3) 10^{-6}	Pressure across the membrane (bar) pressure	SD	Time (min)	Volume of filtrate collected (m^3) 10^{-6}	Pressure across the membrane (bar) pressure	SD
0	0	0.093	0	4	2.4	3.53	0.03
1	0.6	0.125	0.005	5	3.0	5.5	0.3
2	1.2	0.32	0.03	6	3.3	6.0	0.2
3	1.8	1.53	0.04				

Versapor membrane at flowrate 0.3×10^{-6} m^3/min

Time (min)	Volume of filtrate collected (m^3) 10^{-6}	Pressure across the membrane (bar) pressure	SD	Time (min)	Volume of filtrate collected (m^3) 10^{-6}	Pressure across the membrane (bar) pressure	SD
0	0	0.096	0	8	2.4	2.387	0.002
1	0.3	0.102	0.0006	9	2.7	3.523	0.002
2	0.6	0.123	0.005	10	3.0	4.566	0.0006
3	0.9	0.159	0.002	11	3.3	5.009	0.004
4	1.2	0.256	0.001	12	3.6	5.712	0.003
5	1.5	0.473	0.004	13	3.9	6.023	0.004
6	1.8	0.847	0.002				
7	2.1	1.493	0.003				

50:50 water-in-dodecane emulsion (2 % Paranox 100). Homogenised at 8000 rpm for 3 minutes followed at 9500 rpm for 10 minutes using a Supor 200.

flowrate 0.6 × 10^{-6} m^3/min.

Time (min)	Volume of filtrate collected (m^3) 10^{-6}	Pressure across the membrane (bar) pressure	SD	Time (min)	Volume of filtrate collected (m^3) 10^{-6}	Pressure across the membrane (bar) pressure	SD
0	0	0.090	0	8	4.8	4.8	0.1
1	0.6	0.092	0	9	5.4	5.4	0.2
2	1.2	0.130	0.005	10	6.0	5.7	0.2
3	1.8	0.47	0.04	11	6.6	5.96	0.06
4	2.4	1.72	0.03	12	7.2	5.9	0.1
5	3.0	2.63	0.08	13	7.8	6.137	0.0005
6	3.6	3.52	0.06	14	8.4	6.42	0.03
7	4.2	4.5	0.3				

flowrate 0.3 × 10^{-6} m^3/min

Time (min)	Volume of filtrate collected (m^3) 10^{-6}	Pressure across the membrane (bar) pressure	SD	Time (min)	Volume of filtrate collected (m^3) 10^{-6}	Pressure across the membrane (bar) pressure	SD
0	0	0.087	0	15	4.5	4.29	0.07
1	0.3	0.087	0	16	4.8	4.49	0.07
2	0.6	0.092	0.003	17	5.1	4.58	0.03
3	0.9	0.149	0	18	5.4	4.7	0.2
4	1.2	0.25	0.02	19	5.7	4.9	0.2
5	1.5	0.44	0.01	20	6.0	5.195	0
6	1.8	0.70	0.05	21	6.3	5.10	0.09
7	2.1	1.15	0.05	22	6.6	5.23	0.04
8	2.4	1.8	0.1	23	6.9	5.32	0.07
9	2.7	2.4	0.1	24	7.2	5.5	0.2
10	3.0	2.90	0.09	25	7.5	5.648	0.003
11	3.3	3.15	0.03	26	7.8	5.68	0.03
12	3.6	3.460	0.0006	27	8.1	5.58	0.06
13	3.9	3.7	0.2				
14	4.2	4.0	0.2				

50:50 water-in-dodecane emulsion (1 % Paranox 100). Homogenised at 8000 rpm for 3 minutes followed at 8000 rpm for 10 minutes using a Supor 200.

Supor 200 membrane at flowrate 0.3 × 10^{-6} m^3/min

Time (min)	Volume of filtrate collected (m^3) 10^{-6}	Pressure across the membrane (bar) pressure	SD	Time (min)	Volume of filtrate collected (m^3) 10^{-6}	Pressure across the membrane (bar) pressure	SD
0	0	0.095	0	24	7.2	2.6	0.1
1	0.3	0.099	0	25	7.5	2.64	0.05
2	0.6	0.105	0.005	26	7.8	2.70	0.09
3	0.9	0.12	0.01	27	8.1	2.76	0.06
4	1.2	0.13	0.03	28	8.4	2.80	0.08
5	1.5	0.18	0.07	29	8.7	2.86	0.08
6	1.8	0.4	0.1	30	9.0	2.87	0.07
7	2.1	0.5	0.1	31	9.3	2.9	0.1
8	2.4	0.74	0.3	32	9.6	2.9	0.1
9	2.7	1.0	0.3	33	9.9	3.01	0.08
10	3.0	1.3	0.2	34	10.2	3.07	0.09
11	3.3	1.5	0.2	35	10.5	3.10	0.09
12	3.6	1.6	0.3	36	10.8	3.2	0.1
13	3.9	1.8	0.2	37	11.1	3.2	0.1
14	4.2	1.9	0.1	38	11.4	3.2	0.1
15	4.5	2.0	0.1	39	11.7	3.2	0.1
16	4.8	2.1	0.1	40	12	3.29	0.07
17	5.1	2.20	0.09	41	12.3	3.405	0.008
18	5.4	2.23	0.09	42	12.6	3.46	0.02
19	5.7	2.3	0.1	43	12.9	3.50	0.02
20	6.0	2.31	0.02	44	13.2	3.54	0.06
21	6.3	2.4	0.2	45	13.5	3.51	0.08
22	6.6	2.5	0.2	46	13.8	3.612	0.004
23	6.9	2.52	0.08	47	14.1	3.627	0.008

20:80 water-in-dodecane emulsion (0.5 % Paranox 100). Homogenised at 8000 rpm for 3 minutes followed at 8000 rpm for 10 minutes using a Supor 200.

Supor 200 membrane at flowrate 0.3×10^{-6} m^3/min

Time (min)	Volume of filtrate collected (m^3) 10^{-6}	Pressure across the membrane (bar) pressure	SD	Time (min)	Volume of filtrate collected (m^3) 10^{-6}	Pressure across the membrane (bar) pressure	SD
0	0	0.096	0.001	20	6.0	0.87	0.02
1	0.3	0.098	0.002	21	6.3	0.82	0.03
2	0.6	0.099	0.004	22	6.6	0.79	0.04
3	0.9	0.102	0	23	6.9	0.77	0.03
4	1.2	0.115	0.001	24	7.2	0.74	0.04
5	1.5	0.125	0.002	25	7.5	0.73	0.05
6	1.8	0.152	0.001	26	7.8	0.71	0.05
7	2.1	0.21	0.02	27	8.1	0.70	0.05
8	2.4	0.284	0.005	28	8.4	0.69	0.04
9	2.7	0.427	0.009	29	8.7	0.68	0.06
10	3.0	0.598	0.0006	30	9.0	0.68	0.07
11	3.3	0.70	0.01	31	9.3	0.65	0.07
12	3.6	0.91	0.05	32	9.6	0.65	0.06
13	3.9	1.05	0.02	33	9.9	0.65	0.05
14	4.2	1.12	0.05	34	10.2	0.64	0.05
15	4.5	1.11	0.04	35	10.5	0.63	0.06
16	4.8	1.058	0.008	36	10.8	0.62	0.07
17	5.1	1.006	0.003	37	11.1	0.62	0.06
18	5.4	0.970	0.009	38	11.4	0.62	0.06
19	5.7	0.908	0.006				

A1.1.2 Percentage water collected in the permeate

50:50 water-in-dodecane emulsion (1 % Paranox 100). Homogenised at 8000 rpm for 3 minutes followed at 9500 rpm for 10 minutes

Supor 200 membrane at flowrate 0.6×10^{-6} m^3/min

Time (min)	Volume of filtrate collected (m^3) 10^{-6}	Water collected in the permeate (vol %)	Time (min)	Volume of filtrate collected (m^3) 10^{-6}	Water collected in the permeate (vol %)
5.5	3.3	0	16.5	9.9	41
6.5	3.9	0	17.5	10.5	43
7.5	4.5	0	18.5	11.1	45
8.5	5.1	0	19.5	11.7	46
9.5	5.7	0	20.5	12.3	47
10.5	6.3	13	21.5	12.9	48
11.5	6.9	22	22.5	13.5	49
12.5	7.5	29	23.5	14.1	49
13.5	8.1	33	24.5	14.7	50
14.5	8.7	37	25.5	15.3	51
15.5	9.3	39			

Supor 200 membrane at flowrate 1×10^{-6} m^3/min

Time (min)	Volume of filtrate collected (m^3) 10^{-6}	Water collected in the permeate (vol %)	Time (min)	Volume of filtrate collected (m^3) 10^{-6}	Water collected in the permeate (vol %)
3.3	3.3	0	8.3	8.3	14
4.3	4.3	0	9.3	9.3	25
5.3	5.3	0	10.3	10	31
6.3	6.3	0	11.3	11	35
7.3	7.3	8			

Supor 200 membrane at flowrate 0.3×10^{-6} m^3/min

Time (min)	Volume of filtrate collected (m^3) 10^{-6}	Water collected in the permeate (vol %)	Time (min)	Volume of filtrate collected (m^3) 10^{-6}	Water collected in the permeate (vol %)
11	3.3	0	39	11.7	36
13	3.9	0	41	12.3	37
15	4.5	0	43	12.9	38
17	5.1	0	45	13.5	39
19	5.7	0	47	14.1	40
21	6.3	4.9	49	14.7	40
23	6.9	11	51	15.3	40
25	7.5	18	53	15.9	41
27	8.1	22	55	16.5	42
29	8.7	26	57	17.1	42
31	9.3	30	59	17.7	43
33	9.9	32	61	18.3	43
35	10.5	33	63	18.9	44
37	11.1	35	65	19.5	44

HTTuffryn membrane at flowrate 0.6×10^{-6} m^3/min

Time (min)	Volume of filtrate collected (m^3) 10^{-6}	Water collected in the permeate (vol %)	Time (min)	Volume of filtrate collected (m^3) 10^{-6}	Water collected in the permeate (vol %)
5.5	3.3	0	17.5	10.5	30
7.5	4.5	0	19.5	11.7	32
9.5	5.7	0	21.5	12.9	34
11.5	6.9	0	23.5	14.1	36
13.5	8.1	0			
15.5	9.3	25			

HTTuffryn membrane at flowrate 0.3×10^{-6} m^3/min

Time (min)	Volume of filtrate collected (m^3) 10^{-6}	Water collected in the permeate (vol %)	Time (min)	Volume of filtrate collected (m^3) 10^{-6}	Water collected in the permeate (vol %)
11	3.3	0	25	7.5	31
13	3.9	0	27	8.1	36
15	4.5	0	29	8.7	39
17	5.1	0	31	9.3	42
19	5.7	0	33	9.9	45
21	6.3	14			
23	6.9	24			

Nylaflo membrane at flowrate 0.3×10^{-6} m^3/min

Time (min)	Volume of filtrate collected (m^3) 10^{-6}	Water collected in the permeate (vol %)	Time (min)	Volume of filtrate collected (m^3) 10^{-6}	Water collected in the permeate (vol %)
11	3.3	0	27	8.1	27
13	3.9	0	29	8.7	31
15	4.5	0	31	9.3	35
17	5.1	0	33	9.9	38
19	5.7	0	35	10.5	40
21	6.3	14	37	11.1	42
23	6.9	20	39	11.7	44
25	7.5	24			

50:50 water-in-dodecane emulsion (2 % Paranox 100). Homogenised at 8000 rpm for 3 minutes followed at 9500 rpm for 10 minutes using a Supor 200.

Supor 200 membrane at flowrate 0.6×10^{-6} m^3/min

Time (min)	Volume of filtrate collected (m^3) 10^{-6}	Water collected in the permeate (vol %)	Time (min)	Volume of filtrate collected (m^3) 10^{-6}	Water collected in the permeate (vol %)
5.5	3.3	0	10.5	6.3	5
6.5	3.9	0	11.5	6.9	12
7.5	4.5	0	12.5	7.5	17
8.5	5.1	0	13.5	8.1	22
9.5	5.7	0			

Supor 200 membrane at flowrate 0.3×10^{-6} m^3/min

Time (min)	Volume of filtrate collected (m^3) 10^{-6}	Water collected in the permeate (vol %)	Time (min)	Volume of filtrate collected (m^3) 10^{-6}	Water collected in the permeate (vol %)
11	3.3	0	21	6.3	7
13	3.9	0	23	6.9	11
15	4.5	0	25	7.5	15
17	5.1	0	27	8.1	20
19	5.7	0			

50:50 water-in-dodecane emulsion (1 % Paranox 100). Homogenised at 8000 rpm for 3 minutes followed at 8000 rpm for 10 minutes using a Supor 200.

Supor 200 membrane at flowrate 0.3×10^{-6} m^3/min

Time (min)	Volume of filtrate collected (m^3) 10^{-6}	Water collected in the permeate (vol %)	Time (min)	Volume of filtrate collected (m^3) 10^{-6}	Water collected in the permeate (vol %)
11	3.3	0	31	9.3	31
13	3.9	0	33	9.9	36
15	4.5	0	35	10.5	39
17	5.1	0	37	11.1	42
19	5.7	0	39	11.7	44
21	6.3	0	41	12.3	46
23	6.9	0	43	12.9	47
25	7.5	11	45	13.5	49
27	8.1	18	47	14.1	50
29	8.7	26			

A1.2 Emulsion viscosity

50:50 water-in-dodecane emulsion (2 % Paranox 100). Homogenised at 8000 rpm for 3 minutes followed at 9500 rpm for 10 minutes

Shear rate (s^{-1})	Viscosity ($mNsm^{-2}$)	Temperature (°C)	Shear rate (s^{-1})	Viscosity ($mNsm^{-2}$)	Temperature (°C)
1.17	0	23.2	379	22.5	23.2
38.1	22	23.2	416	22.6	23.2
76.4	22.9	23.2	455	22.4	23.2
115	22	23.1	492	22.5	23.2
152	22.6	23.2	531	22.5	23.2
190	22.4	23.2	568	22.6	23.2
228	22.5	23.2	606	22.5	23.2
265	22.5	23.2	644	22.4	23.2
303	22.3	23.2	682	22.5	23.2
341	22.3	23.1	720	22.5	23.2

50:50 water-in-dodecane emulsion (1 % Paranox 100). Homogenised at 8000 rpm for 3 minutes followed at 9500 rpm for 10 minutes

Shear rate (s^{-1})	Viscosity ($mNsm^{-2}$)	Temperature (°C)	Shear rate (s^{-1})	Viscosity ($mNsm^{-2}$)	Temperature (°C)
1.17	0	23.2	379	21.3	23.2
38.1	20.2	23.2	416	21.3	23.2
76.4	20.9	23.2	455	21.5	23.2
115	21.5	23.1	492	21.4	23.2
152	21.7	23.2	531	21.6	23.2
190	21.4	23.2	568	21.5	23.2
228	21.6	23.2	606	21.6	23.2
265	21.5	23.2	644	21.5	23.2
303	21.0	23.2	682	21.4	23.2
341	21.3	23.1	720	21.5	23.2

50:50 water-in-dodecane emulsion (1 % Paranox 100). Homogenised at 8000 rpm for 3 minutes followed at 8000 rpm for 10 minutes

Shear rate (s^{-1})	Viscosity ($mNsm^{-2}$)	Temperature (°C)	Shear rate (s^{-1})	Viscosity ($mNsm^{-2}$)	Temperature (°C)
1.17	0	23.1	379	7.90	23.0
38.1	3.98	23.1	416	8.67	23.0
76.4	4.5	23.1	455	9.28	23.0
115	4.03	23.1	492	10.8	22.9
152	5.05	23.1	531	10.4	22.9
190	5.26	23.1	568	11.5	22.9
228	7.09	23.0	606	11.4	22.9
265	6.36	23.1	644	11.1	22.9
303	7.09	23.0	682	12.5	22.9
341	7.20	23.0	720	12.4	22.9

20:80 water-in-dodecane emulsion (0.5 % Paranox 100). Homogenised at 8000 rpm for 3 minutes followed at 8000 rpm for 10 minutes

Shear rate (s^{-1})	Viscosity ($mNsm^{-2}$)	Temperature (°C)	Shear rate (s^{-1})	Viscosity ($mNsm^{-2}$)	Temperature (°C)
1.17	0	23.1	379	15.0	23.0
38.1	11.8	23.1	416	17.0	23.0
76.4	10.6	23.1	455	18.1	23.0
115	10.8	23.1	492	19.3	22.9
152	11.1	23.1	531	19.4	22.9
190	10.5	23.1	568	19.9	22.9
228	10.8	23.0	606	21.9	22.9
265	11.8	23.1	644	22.7	22.9
303	12.9	23.0	682	23.8	22.9
341	14.6	23.0	720	25.5	22.9

A1.3 Emulsion droplet size distribution

50:50 water-in-dodecane emulsion (2 % Paranox 100). Homogenised at 8000 rpm for 3 minutes followed at 9500 rpm for 10 minutes

Drop diameter (μm)	Number frequency	Number frequency (%)	Drop diameter (μm)	Number frequency	Number frequency (%)
1	6	2	5	60	20
2	35	11.7	6	43	14.3
3	64	21.3	7	3	1
4	89	29.7			

50:50 water-in-dodecane emulsion (1 % Paranox 100). Homogenised at 8000 rpm for 3 minutes followed at 9500 rpm for 10 minutes

Drop diameter (μm)	Number frequency	Number frequency (%)	Drop diameter (μm)	Number frequency	Number frequency (%)
2	3	0.9	8	54	17
3	12	3.8	9	22	6.9
4	20	6.3	10	14	4.4
5	36	11.4	11	8	2.5
6	63	19.9	12	2	0.6
7	86	27.1			

50:50 water-in-dodecane emulsion (1 % Paranox 100). Homogenised at 8000 rpm for 3 minutes followed at 8000 rpm for 10 minutes

Drop diameter (μm)	Number frequency	Number frequency (%)	Drop diameter (μm)	Number frequency	Number frequency (%)
6	3	1	13	51	17
7	5	1.7	14	29	9.7
8	14	4.7	15	17	5.7
9	19	6.3	16	10	3.3
10	25	8.3	17	9	3
11	43	14.3	18	6	2
12	69	23			

20:80 water-in-dodecane emulsion (0.5 % Paranox 100). Homogenised at 8000 rpm for 3 minutes followed at 8000 rpm for 10 minutes

Drop diameter (μm)	Number frequency	Number frequency (%)	Drop diameter (μm)	Number frequency	Number frequency (%)
1	1	0.3	8	60	18.6
2	5	1.5	9	33	10.2
3	10	3.1	10	18	5.6
4	20	6.2	11	12	3.7
5	28	8.7	12	10	3.1
6	64	19.8	13	4	1.2
7	74	22.9			

Appendix 2

Sample Calculations

A2.1 Calculation of osmotic pressure

The osmotic pressure of the aqueous phase is calculated using the vant'Hoff equation (Chapter 3.2.3).

External phase

The external phase was just water and therefore the osmotic pressure is zero.

Internal phase

The solution consists of 0.5 M nickel (II) nitrate dissociates in water to give 3 ions each of which contributes to the osmotic pressure.

$$Ni(NO_3)_2 \rightarrow Ni^{2+} + 2NO_3^{-1} \qquad ...(A1.1)$$

Hence a 0.5 M solution is 1.5 OsM, which in 25 ml contributes to 0.0375 Osmol. The mols of water is 1.4 mol and the mol fraction of nickel (II) nitrate is:

$$x = \frac{0.0375}{0.0375 + 1.4} = 0.0261$$

Which gives an osmotic pressure of 35.3 atm

At the beginning of the stability testing experiments (Chapter 3.4.1) the osmotic pressure across the membrane phase is 35.3 atm in the direction of the internal phase.

A2.2 Calculation of surface and interfacial tension

Surface and interfacial tension is calculated using equation 3.10. The following example is for the surface tension of a 50:50 water-in-dodecane emulsion (1 % Paranox 100). Homogenised at 8000 rpm for 3 minutes followed at 9500 rpm for 10 minutes.

$$\gamma = \frac{\phi V \rho g}{2\pi r}$$

$V=20 \times 0.319 = 6.38 \times 10^{-9} m^3$ $\rho = 880\ kgm^{-3}$ $r = 0.00044$ m

$\phi = 1.32$ (from figure 3.2)

$$\gamma = \frac{1.32 \times 6.38 \times 10^{-9} \times 880 \times 9.81}{2 \times 3.142 \times 0.00044} = 26.3\ mNm^{-1}$$

A2.3 Calculation of nickel in the external water phase

The sample calculation is for 50 ml of a 50:50 water-in-dodecane emulsion (1 % Paranox 100). Homogenised at 8000 rpm for 3 minutes followed at 9500 rpm for 10 minutes dispersed in 100 ml of water.

By using equation 3.5 the moles of reacted EDTA is determined. EDTA combines with metal ions in a 1:1 ratio and therefore, the moles of reacted EDTA is the moles of nickel II nitrate in the sample.

The concentration of the zinc solution and EDTA solution was 0.009234 M and 0.009989 M respectively

$(c_{Ed} \times V_{Ed}) - (c_Z \times V_Z)$ = millimoles of EDTA

$(0.009989 \times 25.00) - (0.009234 \times 26.38) = 0.006132$ moles of EDTA

The 5 ml samples were diluted 10 fold therefore, the concentration of the nickel in the external water phase was:

number of moles = volume × molarity

molarity = 0.006132 / 5 = 0.001226 M

A2.4 Calculation of the percentage breakdown

The sample calculation is for 50 ml of a 50:50 water-in-dodecane emulsion (1 % Paranox 100). Homogenised at 8000 rpm for 3 minutes followed at 9500 rpm for 10 minutes dispersed in 100 ml of water.

Equation 3.7 gives the percentage breakdown (Time was 15 minutes)

$$B\% = \frac{V_e C_{et}}{V_i C_{i0}} 100\%$$

$V_e = 100 \times 10^{-6}$ m^3 $C_{io} = 0.50$ M

$V_i = 25 \times 10^{-6}$ m^3 $C_{et} = 0.001226$ M (see section A2.3)

B%= 0.98%

Appendix 3

Statistical Methods

For each emulsion breakage experiment 3 repeat experiments were carried out under the same conditions and the average of the three runs was recorded (Appendix 1).

50:50 water-in-dodecane emulsion (2 % Paranox 100). Homogenised at 8000 rpm for 3 minutes followed at 9500 rpm for 10 minutes

Supor 200 membrane at flowrate 0.6×10^{-6} m^3/min

Pressure run1 (bar)	Pressure run2 (bar)	Pressure run 3 (bar)	Mean Pressure (bar)	pmax-pmin (bar)	max error (%)	Standard deviation
0.090	0.090	0.090	0.090	0	0	0
0.092	0.092	0.092	0.092	0	0	0
0.13	0.125	0.135	0.130	- 0.005	- 3.8	0.005
0.514	0.455	0.442	0.470	- 0.059	- 11.5	0.04
1.753	1.69	1.722	1.722	- 0.063	- 3.6	0.03
2.63	2.551	2.71	2.630	- 0.079	- 3	0.08
3.46	3.582	3.521	3.521	0.122	3.5	0.06
4.745	4.368	4.264	4.459	- 0.377	- 7.9	0.3
4.923	4.807	4.690	4.807	- 0.166	- 2.4	0.1
5.598	5.455	5.264	5.439	- 0.143	- 2.6	0.2
5.921	5.688	5.470	5.693	- 0.233	- 3.9	0.2
5.89	5.997	5.989	5.959	- 0.107	- 1.8	0.06
5.943	6.057	5.829	5.943	0.114	1.9	0.1
6.137	6.136	6.137	6.137	- 0.001	- 0.02	0.0005
6.464	6.446	6.425	6.425	- 0.018	- 0.3	0.03

The absolute error was ± 0.007 bar and the maximum error (excluding two readings) between readings was ± 4 %. The standard deviation between the repeat experiments varied. It is clear that the accuracy is greater than the precision and therefore, the uncertainty in the results can only be quoted to the number of significant figures of the precision. As the precision varied for each reading it was considered that the pressure should be quoted to the number of significant figures for the standard deviation calculated. Hence, the mean pressure was rounded as follows:

Mean Pressure (bar)	Standard deviation	Mean Pressure (bar)	Standard deviation
0.090	0	4.8	0.1
0.092	0	5.4	0.2
0.130	0.005	5.7	0.2
0.47	0.04	5.96	0.06
1.72	0.03	5.94	0.1
2.63	0.08	6.137	0.0005
3.52	0.06	6.43	0.03
4.5	0.3		

All of the pressure measurements were treated in the same way and the mean values for each run is tabulated in Appendix 1.

A3.2 Precision and accuracy

A3.2.1 Precision (standard deviation)

Precision is degree of agreement between replicate measurements of the same quantity. However good precision does not assure good accuracy. Standard deviation was calculated for surface/interfacial tension measurements, density measurements using the following equation

$$\sqrt{\frac{\sum(x_i - x_m)^2}{N-1}} \qquad \text{...(A3.1)}$$

Where x_i is the individual measurement, x_m is the mean of N experiments, N is the number of experiments.

A3.2.2 Accuracy

Accuracy is the degree of agreement between the measured value and the true value. An absolute true value is seldom known and therefore accuracy is the agreement between a measured value and an accepted true value. By good analytical technique, such as making comparisons against a known standard sample of similar composition, we can arrive at a reasonable assumption about the accuracy.

Absolute error = measured value - accepted true value ...(A3.2)

A3.2.3Concentration of nickel in the external water phase

A standard solution was tested for a 0.002 M Nickel II nitrate

Nickel concentration (M) x_i	Deviation from the mean $\lvert x_i - x_m \rvert$	$(x_i - x_m)^2$
2.021×10^{-3}	0	0
1.928×10^{-3}	9.267×10^{-5}	8.588×10^{-9}
2.113×10^{-3}	9.2×10^{-5}	8.464×10^{-9}
$\Sigma x_i = 6.062 \times 10^{-3}$		$\Sigma(x_i - x_m)^2 = 1.705 \times 10^{-8}$

Mean = $x_m = 6.062 \times 10^{-3} / 3 = 2.021 \times 10^{-3}$ M

Standard deviation = $s = \sqrt{\frac{\sum(x_i - x_m)^2}{N-1}} = \sqrt{\frac{1.705 \times 10^{-8}}{3-1}} = 9.233 \times 10^{-5}$

$= 9.2 \times 10^{-5}$ M

Absolute error $=2.021 \times 10^{-3} - 2.000 \times 10^{-3} = 2.1 \times 10^{-5}$ M

Relative error $= (2.1 \times 10^{-5}/2.000 \times 10^{-3})100 = 1.05$ %

The standard solution contained 0.002 M of nickel

A3.3 Calculation of the percentage breakdown

The total uncertainty in a computation determines how accurately we can know an answer. The uncertainty sets the number of significant figures. For example when calculating the percentage breakdown during stability tests we need to consider the absolute uncertainties of all measurements involved.

$$B\% = \frac{100(\pm 0.08) \times 0.001226(\pm 0.000021)}{25(\pm 0.03) \times 0.5(\pm 0.0021)} 100$$

Here the relative uncertainties are additive and the most probable error is represented by the square root of the sum of the relative variances.

The individual variances are:

100 ml $\pm 0.08/100 = \pm 0.0008$

25 ml $\pm 0.03/25 = \pm 0.0012$

0.001226 $\pm 0.000021/0.001226 = \pm 0.017$

0.5 $\pm 0.0021/0.5 = \pm 0.0042$

relative uncertainty $= \sqrt{(\pm 0.0008)^2 + (\pm 0.0012)^2 + (\pm 0.017)^2 + (\pm 0.0042)^2}$

uncertanty = $\sqrt{\left(\pm 6.4 \times 10^{-7}\right) + \left(\pm 1.44 \times 10^{-6}\right) + \left(\pm 2.89 \times 10^{-4}\right) + \left(\pm 1.764 \times 10^{-5}\right)}$

relative uncertainty = ± 0.0175

Absolute uncertainty $0.9808 \times (\pm 0.0175) = \pm 0.017$

Therefore the value 0.9808 is, 0.98 ± 0.02, quoted to 2 significant figures.